



HAL
open science

The effect of dyes, pigments and ionic liquids on the properties of elastomer composites

Anna Marzec

► **To cite this version:**

Anna Marzec. The effect of dyes, pigments and ionic liquids on the properties of elastomer composites. Polymers. Université Claude Bernard - Lyon I, 2014. English. NNT: 2014LYO10285 . tel-01166530v1

HAL Id: tel-01166530

<https://theses.hal.science/tel-01166530v1>

Submitted on 23 Jun 2015 (v1), last revised 23 Jun 2015 (v2)

HAL is a multi-disciplinary open access archive for the deposit and dissemination of scientific research documents, whether they are published or not. The documents may come from teaching and research institutions in France or abroad, or from public or private research centers.

L'archive ouverte pluridisciplinaire **HAL**, est destinée au dépôt et à la diffusion de documents scientifiques de niveau recherche, publiés ou non, émanant des établissements d'enseignement et de recherche français ou étrangers, des laboratoires publics ou privés.



PH.D. THESIS COMPLETED IN “COTUTELLE”

**THE EFFECT OF DYES, PIGMENTS AND IONIC LIQUIDS ON
THE PROPERTIES OF ELASTOMER COMPOSITES**

presented by

MSc. ANNA MARZEC

between

TECHNICAL UNIVERSITY OF LODZ (POLAND)

and

UNIVERSITY CLAUDE BERNARD – LYON 1 (FRANCE)

For obtaining the degree of Doctor of Philosophy

Specialty: Polymers and Composites Materials

Defence of the thesis will be held in Lodz, 2 December 2014

Thesis supervisors : Professor MARIAN ZABORSKI (Poland)
Doctor GISÈLE BOITEUX (France)

JURY

ZABORSKI	Marian	Professor	Thesis supervisor
BOITEUX	Gisèle	Doctor	Thesis supervisor
BEYOU	Emmanuel	Professor	Examiner
JESIONOWSKI	Teofil	Professor	Reviewer
PIELICHOWSKI	Krzysztof	Professor	Reviewer
GAIN	Olivier	Doctor	Thesis co-supervisor



Thèse “COTUTELLE”

**L'EFFET DE COLORANTS, DE PIGMENTS ET LIQUIDES
IONIQUES SUR LES PROPRIETES DE COMPOSITES
ELASTOMERES**

présentée par

MSc. ANNA MARZEC

entre

UNIVERSITÉ POLYTECHNIQUE DE LODZ (POLOGNE)

et

UNIVERSITÉ CLAUDE BERNARD – LYON 1 LYON (FRANCE)

pour obtenir le grade de docteur

Spécialité: Matériaux Polymères et Composites

École doctorale: Matériaux Innovants

Soutenue le 2 décembre 2014 à l'Université Polytechnique de Lodz

Directeur de thèse: Professeur MARIAN ZABORSKI (Pologne)
Directeur de Recherche CNRS GISÈLE BOITEUX (France)

JURY

ZABORSKI	Marian	Professeur	Directeur de thèse
BOITEUX	Gisèle	Directeur de Recherche CNRS	Directeur de thèse
BEYOU	Emmanuel	Professeur	Examineur
JESIONOWSKI	Teofil	Professeur	Rapporteur
PIELICHOWSKI	Krzysztof	Professeur	Rapporteur
GAIN	Olivier	Ingénieur de Research CNRS	Co-directeur de thèse

UNIVERSITE CLAUDE BERNARD - LYON 1

Président de l'Université	M. François-Noël GILLY
Vice-président du Conseil d'Administration	M. le Professeur Hamda BEN HADID
Vice-président du Conseil des Etudes et de la Vie Universitaire	M. le Professeur Philippe LALLE
Vice-président du Conseil Scientifique	M. le Professeur Germain GILLET
Directeur Général des Services	M. Alain HELLEU

COMPOSANTES SANTE

Faculté de Médecine Lyon Est – Claude Bernard	Directeur : M. le Professeur J. ETIENNE
Faculté de Médecine et de Maïeutique Lyon Sud – Charles Mérieux	Directeur : Mme la Professeure C. BURILLON
Faculté d'Odontologie	Directeur : M. le Professeur D. BOURGEOIS
Institut des Sciences Pharmaceutiques et Biologiques	Directeur : Mme la Professeure C. VINCIGUERRA
Institut des Sciences et Techniques de la Réadaptation	Directeur : M. le Professeur Y. MATILLON
Département de formation et Centre de Recherche en Biologie Humaine	Directeur : Mme. la Professeure A-M. SCHOTT

COMPOSANTES ET DEPARTEMENTS DE SCIENCES ET TECHNOLOGIE

Faculté des Sciences et Technologies	Directeur : M. F. DE MARCHI
Département Biologie	Directeur : M. le Professeur F. FLEURY
Département Chimie Biochimie	Directeur : Mme Caroline FELIX
Département GEP	Directeur : M. Hassan HAMMOURI
Département Informatique	Directeur : M. le Professeur S. AKKOUICHE
Département Mathématiques	Directeur : M. le Professeur Georges TOMANOV
Département Mécanique	Directeur : M. le Professeur H. BEN HADID
Département Physique	Directeur : M. Jean-Claude PLENET
UFR Sciences et Techniques des Activités Physiques et Sportives	Directeur : M. Y. VANPOULLE
Observatoire des Sciences de l'Univers de Lyon	Directeur : M. B. GUIDERDONI
Polytech Lyon	Directeur : M. P. FOURNIER
Ecole Supérieure de Chimie Physique Electronique	Directeur : M. G. PIGNAULT
Institut Universitaire de Technologie de Lyon 1	Directeur : M. le Professeur C. VITON
Ecole Supérieure du Professorat et de l'Education	Directeur : M. le Professeur A. MOUGNIOTTE
Institut de Science Financière et d'Assurances	Directeur : M. N. LEBOISNE

Acknowledgements

I am heartily thankful to my supervisors, Prof. dr hab. Marian Zaborski and dr Gisèle Boiteux, whose encouragement, guidance and support from the initial to the final level enabled me to develop an understanding of the subject.

I would like to express my sincere appreciation to my reviewers Prof. Teofil Jesionowski and Prof. Krzysztof Pielichowski as well as member of the committee Prof. Emmanuel Beyou, who have accepted to evaluate this work. I would also like to extend my appreciation to all jury members.

I am also grateful to dr Ewa Chrześcijańska, dr Zygmunt Boruszczyk, dr Olivier Gain and dr Anatloi Serghei for all helpful discussions we have shared.

Lastly, I offer my regards to all of those, especially my family and my friends, who supported me in any respect during the completion of this thesis.

LIST OF CONTENTS

LIST OF ABBREVIATIONS	8
LIST OF SYMBOLS.....	9
CHAPTER 1. GENERAL INTRODUCTION	10
CHAPTER 2. LITERATURE REVIEW	13
2.1 DEGRADATION OF POLYMER.....	14
2.1.1 POLYMER DEGRADATION – INTRODUCTION.....	14
2.1.2 EFFECTS OF CHEMICAL STRUCTURES AND ADDITIVES ON THE POLYMER STABILITY	15
2.1.3 TYPES OF POLYMER DEGRADATION	18
2.1.4 COMMERCIAL STABILIZERS	25
2.2 SOLVENT DYES	32
2.2.1 STRUCTURES OF DYES AND CLASSIFICATION	32
2.2.2 SOLVENT DYES - GENERAL DISCUSSION.....	35
2.2.3 CHEMICAL CONSTITUTION AND CHARACTERISTICS OF SOLVENT DYES	37
2.2.4 THE CHEMISTRY OF ANTHRAQUINONE SOLVENT DYES.....	40
2.2.5 ORGANIC PIGMENTS	45
2.2.6 EFFECT OF AGING ON THE PROPERTIES OF DYED AND PIGMENTED POLYMERS	51
2.3 IONIC LIQUIDS.....	57
2.3.1 PROPERTIES AND APPLICATIONS OF IONIC LIQUIDS	57
2.3.2 APPLICATIONS OF IONIC LIQUIDS IN POLYMER MATERIALS	60
2.4 SUMMARY	66
2.5 AIM OF WORK.....	68
CHAPTER 3. MATERIALS AND METHODS.....	69
CHAPTER 4. STUDIES THE OF PROPERTIES AND CHARACTERISTICS OF SOLVENT DYES AND PIGMENTS	86
4.1 THERMAL STABILITY OF DYES AND PIGMENTS	87
4.2 MORPHOLOGY OF DYE AND PIGMENT POWDERS	90
4.3 SPECTROPHOTOMETRIC ANALYSIS OF DYES.....	93
4.4 ELECTROCHEMICAL METHODS - CYCLIC AND DIFFERENTIAL PULSE VOLTAMMETRY OF SOLVENT DYES	96
4.5 ANTIOXIDANT ACTIVITY OF SOLVENT DYES STUDIED WITH THE ABTS METHOD.....	103
4.6 SOLUBILITY PARAMETERS	104
4.7 DIFFUSION COEFFICIENTS	106

4.8 CONCLUSIONS	108
CHAPTER 5. EFFECT OF AGING ON THE PROPERTIES OF NBR AND EN COMPOSITES	110
5.1 EN COMPOSITES CONTAINING SOLVENT DYES UNDER UV AGING	111
5.1.1 MECHANICAL PROPERTIES	111
5.1.2 SURFACE ANALYSIS – FTIR.....	115
5.1.3 COLORIMETRIC STUDY OF EN/COMPOSITES UNDER UV AGING	117
5.2 EN COMPOSITES CONTAINING PIGMENTS UNDER UV AGING.....	119
5.3 EN COMPOSITES CONTAINING SOLVENT DYES SUBJECTED TO WEATHERING WITH A FULL SOLAR SPECTRUM	122
5.3.1 MECHANICAL PROPERTIES (STATIC AND DYNAMIC)	122
5.3.2 DIFFERENTIAL SCANNING ANALYSIS OF EN/COMPOSITES	126
5.3.3 SURFACE ANALYSIS – FTIR AND XPS	127
5.3.4 SEM AND COLORIMETRIC MEASUREMENTS OF EN COMPOSITES.....	128
5.4 NBR COMPOSITES CONTAINING SOLVENT DYES UNDER UV AGING....	131
5.4.1 MECHANICAL PROPERTIES OF NBR/SiO ₂ /SOLVENT DYE COMPOSITES.....	131
5.4.2 COLORIMETRIC MEASUREMENTS AND MICROSCOPY ANALYSIS (SEM) OF NBR/SiO ₂ /SOLVENT DYE COMPOSITES.....	132
5.5 NBR COMPOSITES CONTAINING PIGMENTS UNDER UV AGING	133
5.5.1 MECHANICAL PROPERTIES OF NBR/SiO ₂ /PIGMENT COMPOSITES.....	133
5.5.2 COLORIMETRIC MEASUREMENTS AND MICROSCOPY ANALYSIS (SEM) OF NBR/SiO ₂ /PIGMENTS COMPOSITES.....	134
5.6 CONCLUSIONS	137
CHAPTER 6. IMPACT OF THE IMIDAZOLIUM IONIC LIQUIDS ON THE PROPERTIES OF NBR COMPOSITES	140
6.1 CUREING CHARACTERISTICS AND CROSSLINK DENSITY OF NBR/SiO ₂ /IL COMPOSITES	141
6.2 TENSILE PROPERTIES OF NBR/SiO ₂ /ILs COMPOSITES.....	145
6.3 DMA AND GLASS TRANSITION OF NBR/SiO ₂ /IL COMPOSITES.....	146
6.4 MORPHOLOGY ANALYSIS OF NBR/SiO ₂ /IL COMPOSITES.	149
6.5 IONIC CONDUCTIVITY OF NBR/SiO ₂ /IL COMPOSITES.....	153
6.6 EFFECT OF WEATHERING ON THE TENSILE PROPERTIES AND CROSSLINK DENSITY.....	156
6.7 DMA ANALYSIS AND IONIC CONDUCTIVITY AFTER WEATHERING	157
6.8 SURFACE STUDY AFTER WEATHERING	161
6.9 CONCLUSIONS	163
CHAPTER 7. GENERAL CONCLUSIONS	165

LIST OF CONTENTS

SUMMARY	169
PUBLICATIONS AND PATENTS	170
APPENDIX – TENSILE PROPERTIES.....	172

LIST OF ABBERIVATION

- ABTS – 2,2'-azino-bis(3-ethylbenzothiazoline-6-sulphonic acid)
- AMIM TFSI – 1-Allyl-3-methylimidazolium bis(trifluoromethylsulfonyl)imide
- ATR-IR – Attenuated total reflectance infrared spectroscopy
- BDS – Broadband dielectric spectroscopy
- BMIM TFSI – 1-butyl-3-methylimidazolium bis(trifluoromethylsulfonyl)imide
- CRI – Cure rate index
- CV – Cyclic voltammetry
- DMA – Dynamic mechanical analysis
- DSC – Differential scanning calorimetry
- DPV– Differential pulse voltammetry
- EMIM SCN – 1-Ethyl-3-methylimidazolium thiocyanate
- EMIM TFSI – 1-Ethyl-3-methylimidazolium bis(trifluoromethylsulfonyl)imide
- EN – Ethylene-norbornene random copolymer (Topaz)
- FTIR – Fourier transform infrared spectroscopy
- HALS – Hindered light amine stabilizer
- HMIM TFSI – 1-Hexyl-3-methylimidazolium bis(trifluoromethylsulfonyl)imide
- IL – Ionic liquid
- MBT – Mercaptobenzothiazole
- NBR – Acrylonitrile-butadiene rubber
- phr – Parts per hundred rubber
- rpm – Revolutions per minute
- SEM – Scanning electron microscopy
- TEAC - Trolox equivalent antioxidant capacity
- TGA – Thermogravimetric analysis
- UV – Ultraviolet
- XPS – X-ray diffraction roentgenography

LIST OF SYMBOLS

- A – Absorbance
- c – Molar concentration
- D – Diffusion parameter
- E' - Storage modulus
- $E_{1/2}$ – Half-wave potential
- E_b – Elongation at break
- E_{HOMO} – Highest occupied molecular orbital
- E_{LUMO} – Lowest unoccupied molecular orbital
- E_{pa} – Anodic peak potential
- E_{pc} – Cathodic peak potential
- H – Shore hardness
- L*, a*, b* - Color coordinates
- M_H – Maximum torque
- M_L – Minimum torque
- S – Aging coefficient
- SE_{100, 200, 300} – Stress at 100 %, 200 % and 300 % deformation
- t₂ – Scorch time
- T₂, T₁₀, T₅₀ – Temperature corresponding to the 2, 10 and 50 % weight loss
- t₉₀ – Optimal cure time
- T_g – Glass transition temperature
- TS – Tensile strength
- tanδ – Loss factor
- ΔE – Total color difference
- ΔH – Enthalpy
- ΔM – torque increment
- δ_d – Dispersive component
- δ_h – Hydrogen bonds component
- δ_p – Polar component
- ε - Molar extinction coefficient
- λ_{max} - Wavelength of maximum absorbance
- v_T – Crosslink density
- σ_{AC} – Alternating current conductivity

CHAPTER 1
GENERAL INTRODUCTION

1. GENERAL INTRODUCTION

The stability of polymer materials is an important issue for both the polymer industry and the potential user. Polymers and polymer composites are increasingly being used in a wide range of applications where long-term service in hostile environments is required. As a consequence, new specialized additive formulations and chemistries are developed on a current basis and have become the drivers to meet future challenges of polymer materials. One of the disadvantages of polymers is that they undergo the aging process when used in high temperatures or in outdoor conditions. The aging process of polymers is mainly induced by environmental factors like oxygen, ozone, light or high temperature and leads to undesired changes in their physico-chemical properties, such as discoloration and loss of mechanical properties ¹. Apart from the environmental factors, other parameters, such as the polymer itself, and the use of additives such as plasticizers, fillers etc. affect the rate of degradation. Many polymers are difficult to process without additives, certain vital polymer properties need to be enhanced, and undesirable properties need to be mitigated or even eliminated to meet different final application requirements. In many cases, additives open new application fields for polymers as they overcome weaknesses such as for example retardation against flammability and allow to obtain a product with the desired properties such as flexibility - plasticizers, strength - fillers, ionic liquids - conductivity, color - dyes or pigments and so on. Nevertheless, some additives may affect the aging process and act as a stabilizer or prodegradants in polymer materials. Therefore, when selecting additives for polymer blends it is necessary to know the effect of the additive on both the polymer matrix and its other components. For example, anatase form of titanium dioxide (TiO₂) is markedly photosensitive in degrading polymers ². Another pigment, carbon black, performs as a reinforcing filler and can impart conductive properties to polymers, but additionally inhibit polymer degradation ³. Phthalocyanine pigments are used for coloring, but they also enhance thermal and light stability of polymer materials ⁴. Organic pigments and dyes are widely used in the coloration of polymer materials for many commercial applications. Although they are primarily used to impart color to the

¹ J. V. Gulmine, P. R. Janissek, H. M. Heise, L. Akcelrud, Degradation profile of polyethylene after artificial accelerated weathering, *Polym. Degrad. Stab.* 2003, **79**, 385–397.

² S. Singh, H. Mahalingam, P. K. Singh, Polymer-supported titanium dioxide photocatalysts for environmental remediation: A review, *Appl. Catal. A* 2013, **462**, 178–195.

³ X. Wen, N. Tian, J. Gong, Q. Chen, Y. Qi, Z. Liu, J. Liu, Z. Jiang, X. Chen, T. Tang, Effect of nanosized carbon black on thermal stability and flame retardancy of polypropylene/carbon nanotubes nanocomposites, *Polym. Adv. Technol.* 2013, **24**, 971–977.

⁴ P. Anna, Gy. Bertalan, Gy. Marosi, I. Ravadits, M. A. Maatoug, Effect of interface modification on the photo-stability of pigmented polyethylene films, *Polym. Degrad. Stab.* 2001, **73**, 463–466.

particular polymer and make it attractive to consumers, pigments and dyes can have a dramatic effect on photostability. For example, by absorbing and/or scattering UV, pigments can induce a marked protective effect. Dyes as opposed to pigments, are soluble and transmit light in the media being colored. Out of the wide variety of dyes only a small group of them is suitable for coloring such polymers as PP, PE or ABS. They must fulfill a number requirements such as good solubility in non-polar or slightly polar media, light resistance, resistance to chemicals and high thermal stability under processing. Some of the colorants which almost fully meet these requirements are solvent dyes being the subject of this study.

Other interesting polymer additives also include ionic liquids (ILs), due to their useful physicochemical properties, like non-flammability, low vapour pressure and high thermal stability ⁵. In polymers, ionic liquids are applied as plasticizers, antistatic additives, aids substances in curing processes, as well as filler dispersion agents ^{6, 7}. The most popular are highly conductive ionic liquids with bis(trifluoromethylsulfonyl)imide (TFSI) anion, which are characterized by high thermal and chemical stability, as well as a wide electrochemical window, which makes them perfect additives for polymer materials.

In this study solvent type dyes, high performance pigments, and conductive ionic liquids were employed to obtain elastomer composites characterized by enhanced aging resistance and good mechanical strength.

⁵ S. Zhang, N. Sun, X. He, X. Lu, X. Zhang, Physical Properties of Ionic Liquids: Database and Evaluation, *J. Phys. Chem. Ref. Data* 2006, **35**, 1475–1517.

⁶ J. Lu, F. Yan, J. Texter, Advanced applications of ionic liquids in polymer science, *Prog. Polym. Sci.* 2009, **34**, 431–448.

⁷ K. Subramaniam, A. Das, K. W. Stöckelhuber, G. Heinrich, Elastomer composites based on carbon nanotubes and ionic liquid, *Rubber Chem. Technol.* 2013, **86**, 367–400.

CHAPTER 2
LITERATURE REVIEW

2.1 DEGRADATION OF POLYMER

2.1.1 POLYMER DEGRADATION - INTRODUCTION

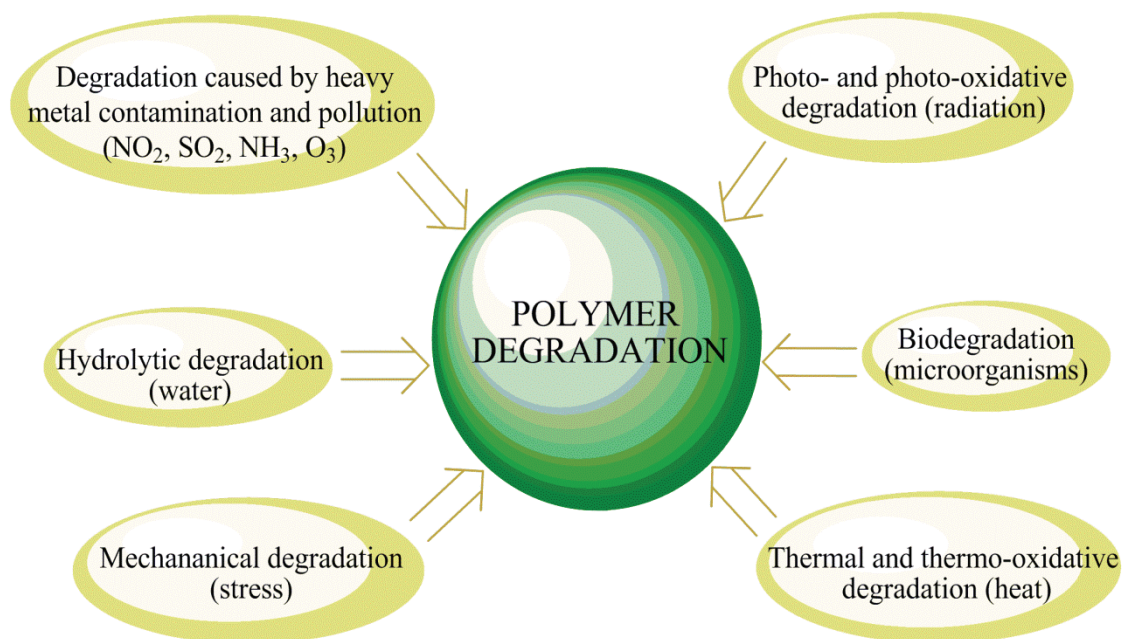
2.1.2 EFFECTS OF CHEMICAL STRUCTURES AND ADDITIVES ON THE POLYMER STABILITY

2.2.3 TYPES OF POLYMER DEGRADATION

2.2.4 COMMERCIAL STABILIZERS

2.1.1 POLYMER DEGRADATION - INTRODUCTION

Degradation of polymeric materials occurs in a wide variety of environments and service conditions, and very often limits the service lifetime. This process can be caused by light (photodegradation), heat (thermal degradation), mechanical action, heavy metal contamination or by fungi, bacteria, yeasts, algae, and their enzymes (biodegradation).



SCHEME 1. The physical, chemical and biological factors affecting the aging of polymer materials⁸.

Polymer degradation occurs result of environment-dependent chemical or physical attack, often caused by a combination of degradation agents, and may involve several chemical and mechanical mechanisms (Scheme 1)^{8, 9}. Degradation of polymer materials

⁸ J. R. White, A. Turnbull, Weathering of polymers: mechanisms of degradation and stabilization, testing strategies and modeling, *J. Mater. Sci.* 1994, **29**, 584–613.

⁹ C.-E. Wilen, R. Pfaendner, Improving weathering resistance of flame-retarded polymers, *J. Appl. Polym. Sci.* 2013, **129**, 925–944.

can be considered to be an irreversible change in some properties that is detrimental to their usefulness. For polymers, it is not just the loss of main properties (physical and mechanical), but also loss of some additives (such as plasticizers), fading of pigment, breakdown of the fiber–polymer matrix in polymer composites and changes in macrostructure^{10, 11}. The occurrence of polymer degradation is recognized by its effects on the appearance and properties. Common effects are discoloration, embrittlement, tackiness, loss of surface gloss, and crazing or chalking of the surface. Some indicators of polymer aging are also changes in mechanical properties (tensile strength, hardness), changes in weight and glass temperature T_g ¹². The irreversible nature of the oxidative processes to which industrial polymers are subjected during high temperature processing and under aggressive conditions during service intensified the search for improved stabilizing systems. This has resulted in the development of antioxidants, fire retardants, UV-stabilizers and antifatigue agents.

2.1.2 EFFECTS OF CHEMICAL STRUCTURES AND ADDITIVES ON THE POLYMER STABILITY

The chemical structure of polymers is of primary importance with respect to its stability^{13, 14}. The crucial factor is the chemical composition, e.g., types of chemical bonds and stereochemical organization. The dissociation energies of various bonds in the polymer determine the course of degradation: the process always begins with the scission of the weakest available bond or with an attack at this site, and the initiation step usually determines the further direction of the process. Polymers with low bond dissociation energies are more readily oxidized than polymers with higher bond dissociation energies (Table 1). Thermal stability of a polymer decreases as the number of substituents on polymer backbone increases. Phenyl group in styrene unit of PS makes C-C backbone labile for thermal degradation. Based on the same fact PE shows more thermal stability as compared to PP and polyisobutylene. A polymer with no hydrogen at all or with uncreative methyl and phenyl groups shows resistance to oxidation¹⁵.

¹⁰ G. Wypych, Handbook of material weathering (2008), Toronto, Chemtec Publishing.

¹¹ D. Feldman, Polymer weathering: photo-oxidation, *J. Polym. Environ.* 2002, **10**, 163–171.

¹² T. Gates (2008), Ageing of composites, R. Martin (Eds.), Cambridge, Woodhead Publishing Limited and CRC Press LLC, p. 3–33.

¹³ G. Y. Li, J. L. Koenig, A review of rubber oxidation, *Rubber Chem. Technol.* 2005, **78**, 355–390.

¹⁴ J. E. O’Gara, B. A. Alden, C. A. Gendreau, Dependence of cyano bonded phase hydrolytic stability on ligand structure and solution pH, *J. Chromatogr. A* 2000, **893**, 245–251.

¹⁵ F. A. Bovey, F. H. Winslow (1979), *Macromolecules - an introduction to polymer science*, London, Academic Press Inc Ltd., p. 423–430.

TABLE 1. Bond dissociation energies of various single bonds ¹³.

Bond Broken	Bond Dissociation Energies (kcal/mol)	Bond Broken	Bond Dissociation Energies (kcal/mol)
C ₂ H ₅ —H	99	C ₆ H ₅ —CH ₃	94
<i>n</i> -C ₃ H ₇ —H	98	C ₆ H ₅ CH ₂ —CH ₃	72
<i>t</i> -C ₄ H ₉ —H	91	CH ₃ —Cl	84
CH ₂ =CHCH ₂ —H	82	C ₂ H ₅ —Cl	81
C ₆ H ₅ —H	103	CH ₂ =CHCH ₂ —Cl	65
C ₆ H ₅ CH ₂ —H	83	CH ₃ —F	108
C ₂ H ₅ —CH ₃	83	C ₂ H ₅ —F	106

Presence of heteroatom in the polymer chain affects the strength of neighboring C-H bonds of the polymer and promotes carbanion formation in the presence of bases. Tertiary and allylic bonds are usually weaker than primary or secondary ones. Consequently, branching and unsaturation lower bond energies and increase the polymer's susceptibility to oxidation ¹⁶. The level of unsaturation present in a polymer is also important. The rubber with low level of unsaturation, such as ethylene propylene diene terpolymer (EPDM), is more resistant to oxidation than the highly unsaturated rubbers, such as styrene-butadiene rubber (SBR) and natural rubber (NR). A very effective degradation initiators are compounds containing carbonyl and hydroperoxide groups. The physical and morphological factors may also influence polymer stability. It is well known that oxidation is primarily initiated in the amorphous phase of semi-crystalline polymers and the propagation of the oxidation into the crystalline phase is a result of the destruction of the crystalline order ¹⁷. Amorphous regions in the polymer have been reported to be more labile to thermal oxidation as compared to crystalline areas because of their high permeability to molecular oxygen. The crystallinity depends on tacticity of the polymer, so tacticity also plays an important role in the degradation behavior ¹⁸. Atactic and isotactic polypropylene have very different oxidative stability - the isotactic one is much more stable. Increase in molecular weight of the polymer materials decreases the rate of polymer degradation ¹⁹. It has been reported that some microorganisms utilize polyolefins with low

¹⁶ J. M. Baldwin, D. R. Bauer, Rubber oxidation and tire aging - a review, *Rubber Chem. Technol.* 2008, **81**, 338–358.

¹⁷ M. Furukawa, Hydrolytic and thermal stability of novel polyurethane elastomers, *Angew. Makromol. Chem.* 1997, **252**, 33–43.

¹⁸ K. Endo, Synthesis and structure of poly(vinyl chloride), *Prog. Polym. Sci.* 2002, **27**, 2021–2054.

¹⁹ M. N. Kim, K. H. Kim, *Korean J. Environ. Biol.* 1997, **15**, 195–200.

molecular weight faster as compared to high molecular weight polyolefins²⁰. Linkage also affects the degree of degradation in polymer. In thermoplastic, head-to-head and tail-to-tail addition of monomer units during addition polymerization creates weak points which make the polymer susceptible for degradation, while head-to-head linkage in PMMA enhances thermal degradation of this polymer²¹.

Transition metal ions are widely reported as additives, which accelerate degradation in polymer materials. They possess ability to catalyse the decomposition of hydroperoxide into free radicals²². The most commonly used transition metals include iron, cobalt and manganese. Iron is highly effective in accelerating photodegradation while manganese and cobalt are sensitive to thermal degradation. The metal ions are generally introduced at trace levels in the form of an organic complex²³.

The additives intentionally added to the material, such as plasticizers or lubricants also influence the stability of the composite, especially if the oxidizability and biodegradability of such systems are higher than those of polymer components^{24, 25}. In special cases, additives are intentionally used to promote degradation of the composites (e.g. photosensitizers) which are specific culture media for bacteria in some rural and horticultural applications^{26, 27}. Titanium dioxide (anatase form)²⁸ is commonly used as pigment in polymer manufacture, but is also well-known as photosensitizer for polyamide and polyolefin degradation. The patent US 4360606 mentions organic dyes being employed as photosensitizers^{29, 30}. Examples given include Acridine Orange and Yellow,

²⁰ K. Yamada-Onodera, H. Mukumoto, Y. Katsuyaya, A. Saiganji, Y. Tani, Novel thermally stable and chiral poly(amide-imide)s bearing from N,N'-(4,4'-diphthaloyl)-bis-L-isoleucine diacid: Synthesis and characterization, *Polym. Degrad. Stab.* 2007, **72**, 323–327.

²¹ W. R. Zeng, S. F. Li, K. W. Chow, Review on chemical reactions of burning poly(methyl methacrylate) PMMA, *J. Fire Sci.* 2002, **20**, 401–433.

²² A. J. Chirinos-Padrón, P.H. Hernández, E. Chávez, N. S. Allen, C. Vasiliou, M. DePooor-tere, Influences of unsaturation and metal impurities on the oxidative degradation of high-density polyethylene *Eur. Polym. J.* 1987, **23**, 935–940.

²³ I. I. Eyenga, W. W. Focke, L. C. Prinsloo, A. T. Tolmay, Photodegradation: a solution for the shopping bag "visual pollution" problem ?, *Macromol. Symp.* 2002, **178**, 139–152.

²⁴ S. Rayne, M. G. Ikonou, Development of a multiple-class high-resolution gas chromatographic relative retention time model for halogenated environmental contaminants, *Anal. Chem.* 2003, **75**, 1049–1057.

²⁵ M. K. Mannisto, M. A. Tirola, J. A. Puhakka, Degradation of 2,3,4,6-tetrachlorophenol at low temperature and low dioxygen concentrations by phylogenetically different groundwater and bioreactor bacteria, *Biodegradation* 2001, **12**, 291–301.

²⁶ S. J. Chiu, W. H. Cheng, Promotional effect of copper(II) chloride on the thermal degradation of poly(ethylene terephthalate), *J. Anal. Appl. Pyrolysis.* 2000, **56**, 131–143.

²⁷ A. M. Gumel, M. S. Annuar, M. Suffian, T. Heidelberg, Current application of controlled degradation processes in polymer modification and functionalization, *J. Appl. Polym. Sci.* 2013, **129**, 3079–3088.

²⁸ N. S. Allen, M. Edge, G. Sandoval, A. Ortega, Ch. M. Liauw, J. Stratton, R. B. McIntyre, Interrelationship of spectroscopic properties with the thermal and photochemical behavior of titanium dioxide pigments in metallocene polyethylene and alkyd based paint films: micron versus nanoparticles, *Polym. Degrad. Stab.* 2002, **76**, 305–319.

²⁹ J. W. Tobias, L. J. Taylor (1982), Pat US4360606, Photodegradable polymer compositions.

Alizarin, Azure B, Brilliant Green, Bromothymol Blue, Crystal Violet and Methylene Blue. On the other hand, proper additives may also stabilize the polymer materials. In many cases the thermal and photochemical processes in polymers are dominated by the type of filler or pigment used.

Currently effective light absorbers such as benzotriazoles, benzophenones, and phenyl esters, as well as hindered amine light stabilizers are used in polymer formulations intended for outdoor use^{31, 32, 33}.

2.1.3 TYPES OF POLYMER DEGRADATION

Weathering is particularly severe for polymers because it combines the photophysical and photo-chemical effects of ultraviolet (UV) radiation with the oxidative effects of the atmospheric oxygen and hydrolytic effects of water. A common definition of weathering is “the undesirable change produced by outdoor exposure”. It has been stated that, the UV-radiation is one of the most important factors determining the polymers lifetime. However, other also parameters as the humidity, temperature, geographic location, mechanical stresses, abrasion and biological attack can affect the degradation rate. The combination of these factors produces an effect greater than the sum of the individual effects e.g., degradation due to radiation is accelerated when other elements operate at the same time. The mechanism describing oxidation and photo-oxidation of polymers is shown in Scheme 2. As the weather aging is an important issue to predict the polymer lifetime, in the next paragraphs the different types of polymer degradations and stabilization methods will be presented³⁴.

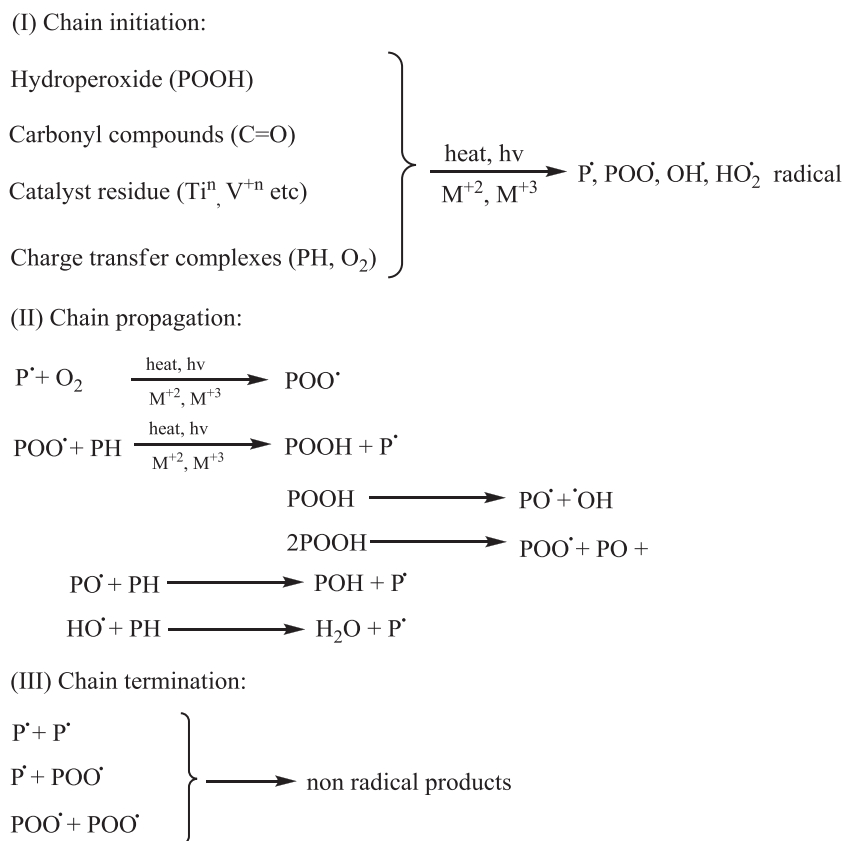
³⁰ A. Ammala, S. Bateman, K. Dean, E. Petinakis, P. Sangwan, S. Wong, Q. Yuan, L. Yu, C. Patrick, K. H. Leong, An overview of degradable and biodegradable polyolefins, *Prog. Polym. Sci.* 2011, **36**, 1015–1049.

³¹ J. Malik, Ch. Kroehnke, Polymer stabilization: present status and possible future trends, *C. R. Chim.* 2006, **9**, 1330–1337.

³² Y.-H. So, Photodegradation mechanism and stabilization of polyphenylene oxide and rigid-rod polymers, *Polym. Int.* 2006, **55**, 127–138.

³³ W. D. Habicher, I. Bauer, J. Pospisil, Organic phosphites as polymer stabilizers, *Macromol. Symp.* 2005, **225**, 147–164.

³⁴ J. F. Rabek (1994), Polymer degradation mechanisms and experimental methods, Stockholm, Springer.



Where P[·] is polymer radical, M⁺ is metal ion, and PH is polymer molecule

SCHEME 2. General oxidation and photo-oxidation in polymers³⁴.

2.1.3.1 PHOTO-OXIDATIVE DEGRADATION

Photo-oxidative degradation is the process of decomposition of the material by the action of light and oxygen. Solar radiation reaching the surface of the earth is characterized by wave lengths from approximately 295 up to 2500 nm. The energy from sunlight is mainly visible light (700–400 nm), infrared (760–2500 nm), manifested as heat and UV light (below 400 nm). Fortunately, the higher energetic part of UV-B; 280–295 nm (426 – 380 kJ·mol⁻¹) is filtered by the stratosphere and does not reach the earth's surface, UV-A (315–400 nm), has energy between 389 and 300 kJ·mol⁻¹ and is less harmful for organic materials than UV-B. Most of the synthetic polymers are susceptible to degradation initiated by UV and visible light. Normally the near-UV radiations (290-400 nm) in the sunlight determine the lifetime of polymeric materials in outdoor applications³⁵.

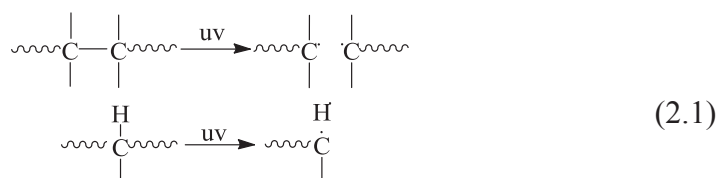
³⁵ B. C. Daglen, D. R. Tyler, Photodegradable plastics: end-of-life design principles, *Green Chem. Lett. Rev.* 2010, **3**, 69–82.

2.1.3.2.1 INITIATION OF PHOTO-OXIDATIVE DEGRADATION

The absorption of UV light that has sufficient energy to break the chemical bonds in the main polymer chain and leads to the initiation of mechanism responsible for polymer degradation. It involves a radical chain mechanism for the formation of initial radical. Different initiation steps under varied conditions have been undertaken in different polymers.

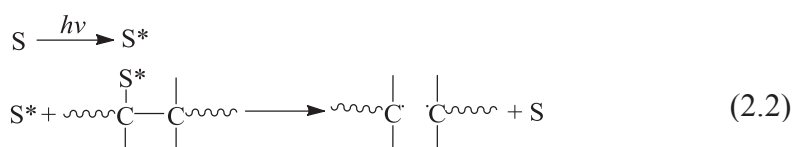
➤ Direct UV initiated photolysis of C-C and C-H bond

Bond dissociation energy of C-C bond (375 kJ/mol) and C-H bond (420 kJ/mol) is equivalent to UV radiation of 320 nm and 290 nm. Thus, direct photolysis of C-C and C-H bond is possible and the radical formed in these reactions become a source of initiation radicals as shown in the following reaction (2.1)³⁶.



➤ Photosensitized cleavage

Photosensitizers are highly photosensitive, readily get excited on exposure to light and are generally used to effective homolysis of the polymeric chains, which otherwise do not undergo sufficient photo-excitation at the frequency of light available to the system (2.2)³⁷.



S - sensitizer molecule

➤ Catalyst residues

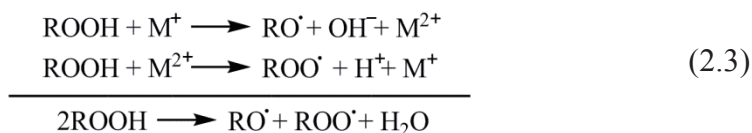
Catalyst residues are source of generation of radicals. Some metal salts, ions and oxidation products of such residues added to the polymers act as catalysts to generate initiation radicals (2.3)^{38, 39}.

³⁶ Q. Yan, D. Han, Y. Zhao, Main-chain photoresponsive polymers with controlled location of light-cleavable units: from synthetic strategies to structural engineering, *Polym. Chem.* 2013, **301**, 5026–5037.

³⁷ A. Ammala, S. Bateman, K. Dean, E. Petinakisa, P. Sangwan, S. Wong, Q. Yuan, L. Yu, C. Patrick, K. H. Leong, An overview of degradable and biodegradable polyolefins, *Prog. Polym. Sci.* 2011, **36**, 1015–1049.

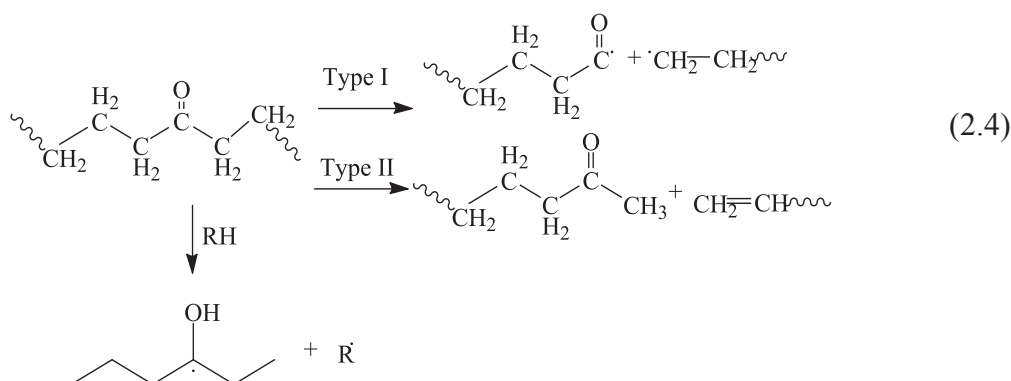
³⁸ A. C. Albertsson, S. Karlsson, Degradable polymers for the future, *Acta Polym.* 1995, **46**, 114–123.

³⁹ A. R. Freitas, G. J. Vidotti, A. F. Rubira, E. C. Muniz, Polychloroprene degradation by a Photo-Fenton process, *Polym. Degrad. Stab.* 2005, **87**, 425–432.



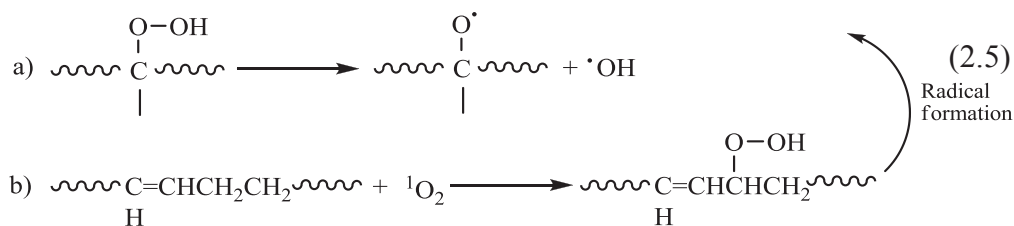
➤ Incorporation of carbonyl groups

Carbonyl groups formed by mild oxidation of polymer during synthesis or processing act as chromophores and become source of the initiation radicals. Carbonyl chromophore absorbs near-UV radiations and subsequently forms radicals following Norrish Type I, Norrish Type II and H-atom abstraction processes (2.4)^{40, 41}.



➤ Introduction of peroxides or sites of unsaturation

The peroxides or C=C sites become source of initiation radicals as shown in reaction (2.5 a, b)⁴². Chain oxidation occurs in most of the polymers because of the labile O-O bond present in the macrohydroperoxide -C-OOH, the macroalkoxyl and hydroxyl radicals thus formed may abstract hydrogen from the surrounding polymer matrix to generate alcohol, water and new macroalkyl radicals which can then take part in many cycles of the chain-initiation reactions (2.5 a)⁴³.



Singlet oxygen exhibits several specific reactions and the one that has been most often invoked in the photooxidation of polymers is the formation of a hydroperoxide by

⁴⁰ C. H. Bamford, R. G. W. Norrish, Primary photochemical reactions. VII. Photochemical decomposition of isovaleraldehyde and dipropyl ketone, *J. Chem. Soc.* 1935, 1504–1511.

⁴¹ G. H. Hartley, J. E. Guillet, Photochemistry of ketone polymers. I. Studies of ethylene-carbon monoxide copolymers, *Macromolecules* 1968, **1**, 165–170.

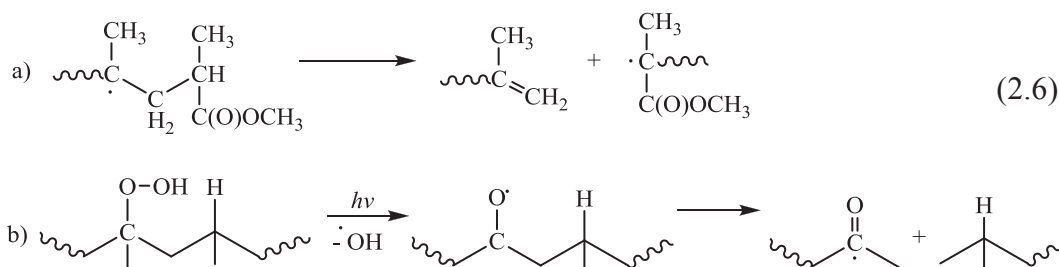
⁴² D. J. Carlsson, D. M. J. Wiles, The photooxidative degradation of polypropylene. Part I. Photooxidation and photoinitiation processes, *Macromol. Sci. Rev. Macromol. Chem.* 1976, **C14**, 65–106.

⁴³ T. Y. Soheir, J. N. Asaad, M. W. Sabaa, Thermal and mechanical behaviour of flexible poly(vinyl chloride) mixed with some saturated polyesters, *Polym. Degrad. Stab.* 2005, **91**, 385–392.

oxidation of an olefin containing an allylic hydrogen, and which could further decompose and lead to chain scission and formation of a terminal of carbonyl group (2.5 b) ⁴⁴.

2.1.3.1.2 PROPAGATION REACTION OF PHOTO-OXIDATIVE DEGRADATION

The propagating reactions of auto-oxidation cycle are common to all carbon backbone polymers. These reactions lead to generation of hydroperoxide species (2.6 a). Hydroperoxide species generated in propagating step lead to backbone degradation through cleavage of hydroperoxide O-O bond followed by β -scission (2.6 b). Polymer backbone cleavage occurs through Norrish Type I and II reactions of chromophores (carbonyl) following β -scission route, which is a prevailing route for photo-oxidative degradation. The scission process generates two chain ends that are free to restructure, and can often lead to increase in crystallinity as oxidative degradation proceeds ⁴⁵.



2.1.3.1.3 TERMINATION REACTION OF PHOTO-OXIDATIVE DEGRADATION

The termination of photodegradation occurs by combining free radicals or is assisted by using stabilizers in the polymer materials. Macroalkyl radicals may combine to give a crosslinked, branched or disproportionated product. Peroxyl radicals finally terminate by reaction with other radicals to give dialkyl peroxides, carbonyl species or alcohols ^{46, 47}.

2.1.3.2 THERMO-OXIDATIVE DEGRADATION

The thermal oxidation of the macromolecular substances is defined as their thermally initiated reaction with the molecular oxygen. Under normal conditions, photochemical and thermal degradations are similar and are classified as oxidative degradation. The main difference between the two is the sequence of initiation steps leading to auto-oxidation cycle. Other difference includes that thermal reactions occur throughout the bulk of the polymer sample, whereas photochemical reactions take place only on the surface.

⁴⁴ C. Fritscher, Degradable polymers, *Int. J. Mater. Prod. Technol.* 1994, **9**, 482–495.

⁴⁵ N. Grassie, G. Scott, (1985) Polymer degradation and stabilization, London, Cambridge University Press, Ch. 3.

⁴⁶ S. I. Kuzina, A. I. Mikhailov, Chain and photochain mechanisms of photooxidation of polymers, *High Energ. Chem.* 2010, **44**, 37–51.

⁴⁷ G. Wypych (2011), Handbook of UV degradation and stabilisation, Toronto, Chemtec, p. 14–30.

Thermal degradation of polymers occurs through random and chain end degradation (depolymerization reaction) initiated by temperature and UV light. The chain end degradation starts from the end of the chain and successively releases the monomer units^{48, 49, 50}. This type of degradation route is also known as depolymerization reaction, which involves successive release of monomer units from the chain ends. In general, a substituted vinyl polymers degrade mostly through the process of depolymerization, for example, poly(methyl methacrylate) (PMMA) depolymerized at elevated temperature has been converted almost quantitatively back to the monomer⁵¹. Random degradation occurs at any random point along the polymer chain. The oxidation of hydrocarbons is a free radical-initiated autocatalytic chain reaction. The reaction is slow at the start and accelerates with increasing concentration of the resulting hydroperoxides. The process can be regarded as proceeding in three distinct steps: chain initiation, chain propagation, and chain termination. The primary alkyl radical (R^{\bullet}) can be formed as an effect of heat, shear, catalyst residues, radical initiators, and/or impurities in the monomer. Especially polyolefins are known to be sensitive to thermal oxidation, due to the impurities generated during their manufacture at high temperatures⁵².

2.1.3.3 OZONE INDUCTED DEGRADATION

The presence of ozone in the air, even in very small concentrations, markedly accelerates the aging of polymeric materials. Ozone mainly affects vulcanized rubbers with unsaturation in the main polymer chain and causes cracking in stretched form in rubber. Ozone normally attacks the unsaturation in unsaturated polymers and this reaction generally occurs in three principal steps (2.7)^{53, 54}. The first step is a cycloaddition of ozone to the olefin double bond to form ozone-olefin adduct referred to as the “primary ozonide” which is an unstable species because it contains two very weak O-O bonds. The

⁴⁸ D. R. Tyler, Mechanistic aspects of the effects of stress on the rates of photochemical degradation reactions in polymers, *J. Macromol. Sci. Polym. Rev.* 2004, **C44**, 351–388.

⁴⁹ L. Halasz, K. Belina, A. Szucs, Thermal degradation of poly(olefin- α olefin) copolymers, *AIP Conf. Proc.* 2014, **1539**, 222–226.

⁵⁰ E. F. Abadir, Mechanism and kinetics of the non-isothermal degradation of ethylenepropylene diene monomer (EPDM), *J. Therm Anal. Calorim.* 2013, **114**, 1409–1413.

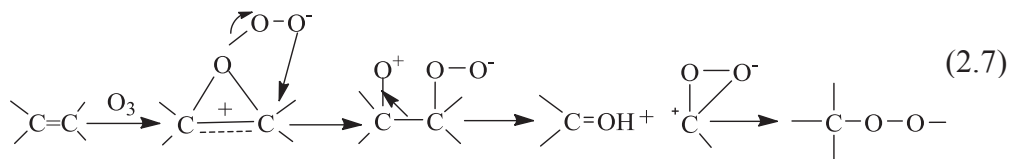
⁵¹ S. Bywater, P. E. Black, Thermal depolymerization of poly(methyl methacrylate) and poly(α -methylstyrene) in solution in various solvents, *J. Phys. Chem.* 1965, **69**, 2967–2970.

⁵² N. S. Allen, M. Edge (1992), Fundamentals of polymer degradation and stabilisation, London, Elsevier, Ch. 1.

⁵³ R. Lee, M. L. Coote, New insights into 1,2,4-trioxolane stability and the crucial role of ozone in promoting polymer degradation, *Phys. Chem. Phys.* 2013, **15**, 16428–16431.

⁵⁴ F. Cataldo, G. Angelini, Some aspects of the ozone degradation of poly(vinyl alcohol), *Polym. Deg. Stab.* 2006, **91**, 2793–2800.

second step in the ozonolysis mechanism is the decomposition of the primary ozonide to carbonyl compounds and a carbonyl oxide.



The carbonyl oxide is considered to be the key intermediate in the C=C bond ozonolysis mechanism. The third step is the fate of the carbonyl oxide, which depends on its source, as well as on its environment. The carbonyl oxide flips over with the nucleophilic oxyanion attacking the carbon atom of the carbonyl group^{55, 56}.

2.1.3.4 MECHANOCHEMICAL DEGRADATION

Mechanochemical degradation is defined as changes in physical properties caused by chemical reactions initiated by provide of mechanical energy to polymer^{57, 58}. Causes of changes in physical properties of polymer might be either bond scissions or cross-links, which are the results of chemical reactions inducted by input of energy. When excessive stress is applied, the molecular chain breaks and produces a pair of free radicals, which can take part in subsequent reactions. In the presence of oxygen, the first reaction results in the formation of peroxy radicals. The most important application of this type of reaction is the mastication of natural rubber to make it processable. Mechanically generated radicals are believed to result from the cleavage of the main backbone segments of polymer chains in the stressed amorphous regions connecting crystallites. High intensity ultrasounds can also induce mechanochemical degradation in polymer materials. As ultrasonic waves pass through the solution, the localized shear gradient produces tear off molecules leading to chain scission and decrease in molecular weight⁵⁹.

2.1.3.5 BIOGRADATION

Biodegradation is a biochemical transformation of compounds in mineralization by microorganisms. Mineralization of organic compounds yields carbon dioxide and water

⁵⁵ M. P. Anachkov, S. K. Rakovski, R. V. Stefanova, Ozonolysis of 1,4-cispolysoprene and 1,4-trans-polysoprene in solution, *Polym. Degrad. Stab.* 2000, **67**, 355–363.

⁵⁶ B. F. Ozen, L. J. Mauer, J. D. Floros, Effects of ozone exposure on the structural, mechanical and barrier properties of select plastic packaging films, *Pack. Technol. Sci.* 2003, **15**, 301–311.

⁵⁷ Y. Li, G. Chen, S. Guo, H. Li, Studies on rheological behavior and structure development of high-density polyethylene in the presence of ultrasonic oscillations during extrusion, *J. Macromol. Sci. B Phys.* 2006, **45**, 39–52.

⁵⁸ A. M. Striegel, Influence of chain architecture on the mechanochemical degradation of macromolecules, *J. Biochem. Biophys. Methods* 2003, **56**, 117–139.

⁵⁹ G. Schmidt-Naake, M. Drache, M. Weber, Combination of mechanochemical degradation of polymers with controlled free-radical polymerization, *Macromol. Chem. Phys.* 2002, **203**, 2232–2238.

under aerobic conditions, and methane and carbon dioxide under biodegradation can take place at different structural levels, i.e. molecular, macromolecular, microscopic and macroscopic depending upon the mechanism. Biodegradation of polymers occurs through four different mechanisms: solubilization, ionization, hydrolysis and enzyme-catalyzed hydrolysis^{60, 61}.

2.1.4 COMMERCIAL STABILIZERS

When polymers oxidize, they lose mechanical properties may, become rough or cracked on the surface. Aging and degradation process can be retarded or inhibited by chemical substances called antioxidants or stabilizers. The type and amount of antioxidant used depend on the type of polymer and application. Typical level is 0.05-1 % by weight on the weight of the polymer. The present formation of macroalkyls, hyperoxide-decomposing antioxidants (HD AO) and UV absorbers (UV abs.) are used during processing and outdoor exposure, respectively (Scheme 3)⁶². Radical scavengers (chain-breaking antioxidants, CB AO) are used to deactivate the formed macroalkyls and alkylperoxyl radicals. Homolysis of hyperperoxides is prevented by HD AO, photoantioxidants (hindered amine stabilizers, HAS), UV absorbers, and in special case, by metal deactivators (MD). The UV absorbers prevent formation of excited chromophores. Light stabilizers with properties of quenchers (Q) are able to deactivate excited chromophores⁶³.

There are a number of properties that antioxidants must possess besides good stabilizer activity if they are to be widely used in polymer applications. They should be highly effective, non-toxic, stable, compatible with the polymer as well as cost-effective. Service requirements placed on finished polymer products demand improved polymer stabilization. However, many reasons may cause stabilizer to not perform or to have reduce performance in real formations^{64, 65}.

⁶⁰ X. Gao, X. Shi, X. Yang, Dynamic behaviour of stationary pronuclei during their positioning in *Paramecium caudatum*, *Eur. J. Protistol.* 2011, **47**, 235–237.

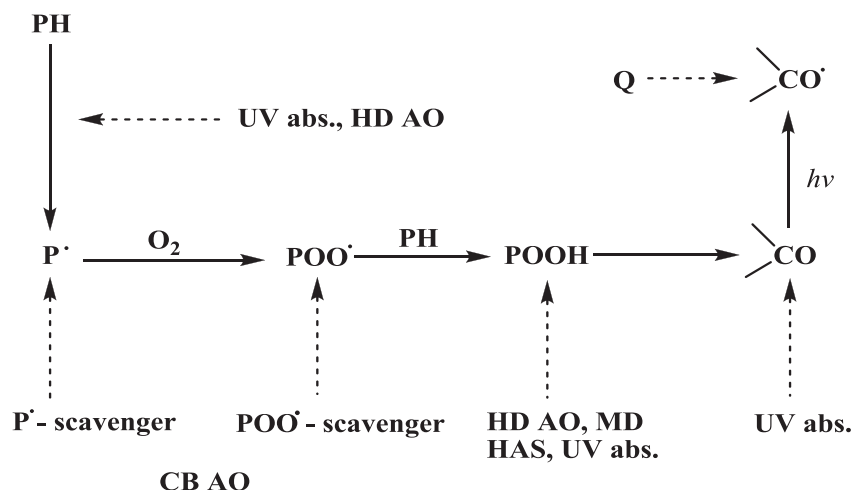
⁶¹ A. A. Kumar, K. Karthick, K. P. Arumugam, Properties of biodegradable polymers and degradation for sustainable development, *Int. J. Chem. Eng. Appl.* 2011, **2**, 164–167.

⁶² J. G. Drobný (2007), *Handbook of thermoplastic elastomers*, Norwich, William Andrew Publishing, p.13–14.

⁶³ K. Schwarzenbach (2001), *Plastic additive handbook*, Munich, Hanser Publishers, p. 1-12.

⁶⁴ M. Lundbäck, C. Strandberg, A.-C. Albertsson, M. S. Hedenqvist, U. W. Gedde, Loss of stability by migration and chemical reaction of Santonox R in branched polyethylene under anaerobic and aerobic conditions, *Polym. Deg. Stab.* 2006, **91**, 1071–1078.

⁶⁵ F. Ch.-Y. Wang, Polymer additive analysis by pyrolysis-gas chromatography. IV. Antioxidants, *J. Chromatogr.* 2000, **891**, 325–336.

SCHEME 3. Mechanism of autoxidation ⁶⁴.

The effectiveness of antioxidant depends on activity and permanence of the antioxidant in the polymer. The concentration of the antioxidant in a polymer decreases during long term use as a consequence of the chemical and physical process loss of antioxidant from the polymers. Chemical loss of antioxidant as a result of their mechanism of stabilization is summarised by Vink ⁶⁶. Physical loss of antioxidant mainly depends on compatibility and distribution of antioxidants in polymers, volatility of antioxidants, diffusion of antioxidants in polymers and extractability of antioxidants from polymers. Generally, the higher solubility and the lower diffusion coefficient of stabilizer, contribute to the lower potential of blooming and leaching in polymer materials ^{67, 68}.

1.1.4.1 BASIC CLASSIFICATION OF ANTIOXIDANTS

Classification of antioxidants is based on their mode of action. Two main groups of antioxidants are distinguished according to their mode of action: preventive and chain breaking antioxidants. The preventive antioxidants destroy hydroperoxides or otherwise neutralise their action and the chain-breaking antioxidants deactivate alkylperoxy radicals ⁶⁹.

⁶⁶ P. Vink (1980), *Developments in Polymer stabilisation*, G. Scott (Ed.), London, Applied Science Publishers, p. 117.

⁶⁷ M. Lundbäck, M. S. Hedenqvist, A. Mattozzi, U. W. Gedde, Migration of phenolic antioxidants from linear and branched polyethylene, *Polym. Deg. Stab.* 2006, **91**, 1571–1580.

⁶⁸ B. Neway, M. S. Hedenqvist, V. B. F. Mathot, U. W. Gedde, Free volume and transport properties of heterogeneous poly(ethylene-co-octene)s, *Polymer* 2001, **42**, 5307–5319.

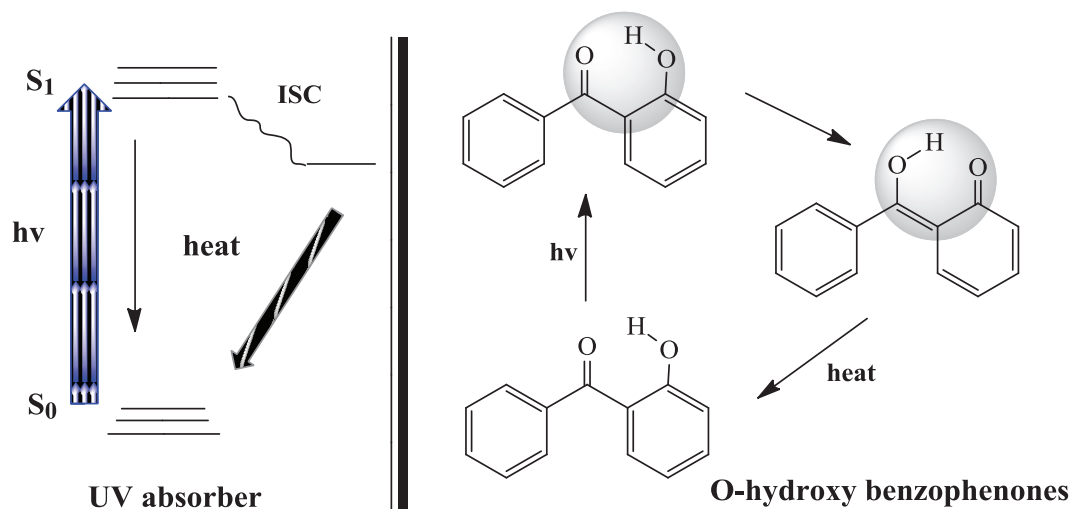
⁶⁹ G. Scott (1997), *Antioxidants in science, technology, medicine and nutrition*, Chichester, Albion Publishing, Ch 3–4.

A) Preventive antioxidants

Preventive antioxidants sometimes referred as secondary antioxidants, interrupt the second oxidative cycle by preventing or inhibiting the generation of free radicals.

➤ Light absorbers and UV screeners

The hydroperoxides can be reduced or eliminated by UV absorbers or screeners, which reflect UV radiation. Many of the inorganic (e.g. titanium dioxide - rutile form, zinc oxide)^{70, 71} and organic pigments screen the polymer from ultraviolet light. In general white pigments give better reflectance in the 300-400 nm range than colored pigments. The most effective screener is carbon black and here the efficiency depends on the type, concentration and particle size of the pigment⁷².



SCHEME 4. Energy dissipation by benzophenone UV absorber⁷⁶.

UV absorbers absorb ultraviolet light efficiently and convert the energy into relatively harmless thermal energy without themselves undergoing any irreversible chemical change, inducing any chemical change in the host molecules. Commonly used UV absorbers are derivatives of hydroxybenzophenone or benzotriazole⁷³. Scheme 6 shows mechanism of energy dissipation by benzophenone UV stabilizer. Absorption of a photon

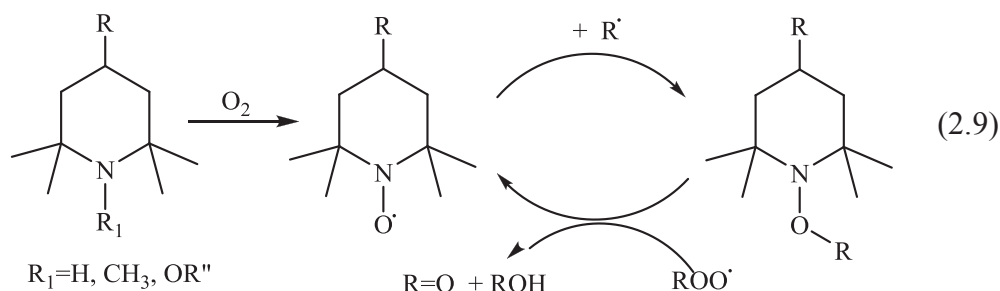
⁷⁰ N. S. Allen, M. Edge, A. Ortega, G. Sandoval, Ch. M. Liauw, J. Verran, J. Stratton, R. B. McIntyre, Degradation and stabilisation of polymers and coatings: nano versus pigmentary titania particles, *Polym. Degrad. Stab.* 2004, **85**, 927–946.

⁷¹ T. G. Smit, S. Pavel, Titanium dioxide and zinc oxide nanoparticles In sunscreens: focus on their safety and effectiveness, *Nanotechnol. Sci. Appl.* 2011, **4**, 95–112.

⁷² N. S. Allen, J. M. Pena, M. Edge, Ch. M. Liauw, Behaviour of carbon black pigments as excited state quenchers in LDPE, *Polym. Degrad. Stab.* 2000, **67**, 563–566.

⁷³ N. S. K. T. Gillen, R. Bernstein, R. L. Clough, M. Celina, Lifetime predictions for semi-crystalline cable insulation materials: I. Mechanical properties and oxygen consumption measurements on EPR materials, *Polym. Deg. Stab.* 2006, **91**, 2146-2156.

The initial inactive HALS molecule is activated through reacting with peroxy radicals or hydroperoxides and oxygen into a nitroxyl radical that will react with alkyl radical at a rate comparable to the reaction between oxygen and alkyl radicals.



The N–O bond of the substituted hydroxylamine is able to react further with peroxy and acyloxy radicals, to yield stable products and regenerate the nitroxyl radical. The effectiveness of this type of stabilizer at low concentrations is due to its cyclic mechanism where HALS is regenerated and not consumed during stabilization^{79, 80, 81}.

➤ *Metal deactivators*

The main function of metal deactivators (MD) is to retard efficiently the metal-catalysed oxidation of polymers. They are strong metal ion complexing agents that inhibit catalyzed initiation. The deactivators are normally polyfunctional chelating compounds with ligands containing atoms such as N, O, S and P that can chelate with metals and decrease their catalytic activity. The most effective groups are polydentate chelating agents able to form very stable chelates in which all the co-ordination sites are occupied. Examples are oxalyl bis(benzylidene) hydrazide, N,N'-di-naphthyl-p-phenylene, 2,2'-methylene-bis(4-methyl-6-tert-butylphenol) or ethylene diamine tetra acetic acid^{82, 83}.

➤ *Quenchers*

The main effect of quenchers is deactivation of excited states (singlet and/or triplet) of chromophoric groups (sensitizers) in polymers before bond scission⁸⁴. The excited state of chromophoric groups may react but it can also be made to transfer its excess electronic

⁷⁹ I. Rossi, A. Venturini, A. Zedda, Modeling hindered-amine light stabilizer-promoted polymer stabilization: computational insight into the mechanism for nitroxyl radical regeneration from aminoethers, *J. Am. Chem. Soc.* 1999, **121**, 7914–7917.

⁸⁰ P. Gijssman, New synergists for hindered amine light stabilizers, *Polymer* 2002, **43**, 1573–1579.

⁸¹ O. Haillant, Spectroscopic characterization of the stabilising activity of migrating HALS in a pigmented PP/EPR blend, *Polym. Deg. Stab.* 2008, **93**, 1973–1978.

⁸² N. Canter, Metal deactivators: inhibitors of metal interactions with lubricants, *Tribol. Lubr. Technol.* 2012, **68**, 11–22.

⁸³ Z. Osawa, Role of metals and metal-deactivators in polymer degradation, *Polym. Deg. Stab.* 1988, **20**, 203–236.

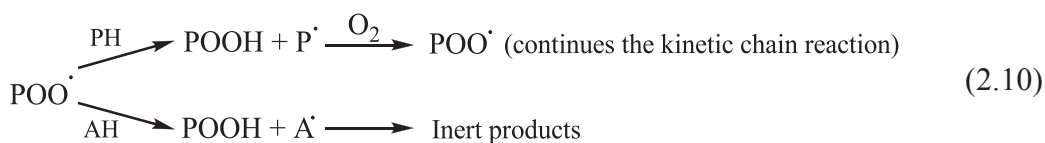
⁸⁴ J.-Q. Pan, C. Cao, Study on the photoprotecting behavior of a phenylformamidine light stabilizer 1992, **37**, 195–199.

energy to a quenching entity. Many different compounds can be sensitizers, including dyes, pigments, antioxidant products, carbonyl groups, a variety of impurities or pollutants such as polynuclear aromatic compounds, etc. Energy transfer can occur efficiently only if the energy level of the quencher is below that of the chromophore. The quenchers dissipate the excess energy harmlessly and the system is stabilized. In the solid state, transfer of energy occurs by conjugative or dipole-dipole interactions. Most widely used quenchers are organic nickel complexes such as 2,2'-thiobis(4-octylphenol)-n-butylamine nickel, nickel salts of thiocarbamate and nickel complexes with alkylated phenol phosphates^{85, 86}.

B) Chain-breaking antioxidants

Chain breaking antioxidants interfere with the chain propagation steps of polymer oxidation. Chain-breaking antioxidants can act by two complementary mechanisms.

➤ The **chain-breaking donor** (CB-D) antioxidants, depicted typically as AH, are generally phenols or arylamines. Both amine type and phenolic type antioxidants can donate hydrogen to an alkylperoxyl radicals. Transformation products of phenoxy and amino radical has been summarized by Pospisil^{87, 88}. A primary requirement is that the aryloxy or aminoxyl radical (A \cdot) produced should not continue the kinetic chain (2.10). This is normally achieved by delocalisation of the unpaired electron in the aromatic ring and/or by steric hindrance of a group formally containing the unpaired electron. CB-D antioxidants are widely distributed in biological systems to protect substrates that are susceptible to peroxidation from attack by atmospheric oxygen (e.g. α -tocopherol, lignin, tannic acids)⁸⁹.



⁸⁵ F. Gugumus, Mechanisms and kinetics of photostabilization of polyolefins with *N*-methylated HALS *Polym. Deg. Stab.* 1991, **34**, 205–241.

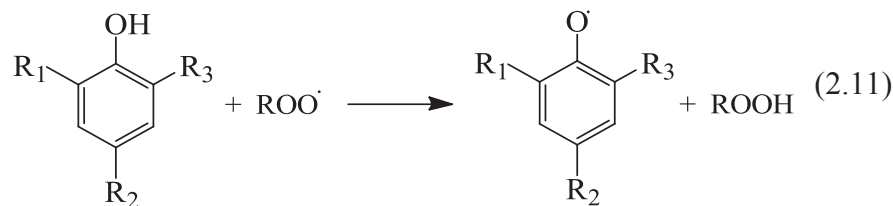
⁸⁶ E. Yousif, R. Haddad, Photodegradation and photostabilization of polymers, especially polystyrene: review, *Springerplus* 2013, **2**, 398–429.

⁸⁷ J. Pospisil (1979) *Developments in Polymer Stabilization 1*, London, Applied Science Publishers Ltd., Ch. 1.7.

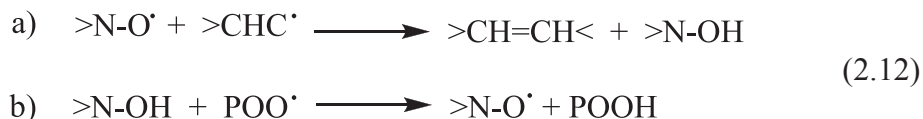
⁸⁸ J. Pospisil, Chemical and photochemical behaviour of phenolic antioxidants in polymer stabilization: a state of the art report, part II, *Polym. Degrad. Stab.* 1993, **39**, 103–115.

⁸⁹ D. M. Wiles, G. Scott, Polyolefins with controlled environmental degradability, *Polym. Degrad. Stab.* 2006, **91**, 1581–1592.

Phenolic antioxidants are the most widely used stabilizers for polymers⁹⁰. Hindered phenols act as free-radical scavengers and prevent or interrupt oxidation reactions. Steric hindrance of the phenolic moiety is one of the factors governing antioxidant efficiency. Most hindered phenols contain one tertiary butyl group combined with a methyl group or two tertiary butyls in positions 2 and 6. The key reaction is the formation of hydroperoxide by transfer of a hydrogen from the phenolic moiety to the peroxy radical and the formation of a phenoxyl radical according to reaction (2.11)⁹¹.



➤ The **chain-breaking acceptor** (CB-A) antioxidants are oxidizing agents. They are “stable” radicals such as aminoxyls $>\text{N}-\text{O}\cdot$ which remove an hydrogen from the propagating radical to give a stable molecule (2.12 a). Important commercial examples are the cycloaliphatic hindered aminoxyls that are reversibly reduced by carbon-centred radicals and continuously re-oxidized by peroxy radicals (2.12 b). This class includes quinines, nitro compounds and “stable” free radicals of which nitroxyls and phenoxyls have been most studied.



⁹⁰ E. Klein, V. Lukeš, Z. Cibulková, On the energetics of phenol antioxidants activity, *Petroleum Coal*. 2005, **47**, 33-39.

⁹¹ J. Pospisil, Chemical and photochemical behaviour of phenolic antioxidants in polymer stabilization: a state of the art report, Part I. *Polym. Degrad. Stab.* 1993, **40**, 217-232.

2.2 DYES AND PIGMENTS

2.2.1 STRUCTURES OF DYES AND THEIR CLASSIFICATION

2.2.2 SOLVENT DYES - GENERAL DISCUSSION

2.2.3 CHEMICAL CONSTITUTION AND CHARACTERISTICS OF SOLVENT DYES

2.2.4 THE CHEMISTRY OF ANTHRAQUINONE SOLVENT DYES

2.2.5 ORGANIC PIGMENTS

2.2.6 EFFECT OF AGING ON THE PROPERTIES OF DYED AND PIGMENTED POLYMERS

2.2.1 STRUCTURES OF DYES AND THEIR CLASSIFICATION

Colorants used in polymers are dyes or pigments. Dyes are organic compounds that are soluble in, or have an affinity for the media being colored. They produce bright, intense color, are transparent, easy to disperse and process. Dyes provide color in a polymer from selective absorption of visible light with wavelength ranging from 380 (violet) to 760 nm (red). The major structure element responsible for light absorption in dye molecules is the chromophore group, i.e. a delocalized electron system with conjugated double bonds. Usual chromophores are $-C=C-$, $-C=N-$, $-C=O$, $-N=N-$, $-NO_2$ and quinoid rings^{92, 93}. The absorption of UV/Vis radiation by an organic molecule and is associated with electronic transitions between molecular orbitals. The energy of the absorbed radiation is given by equation (2.13):

$$\Delta E = E_1 - E_0 = h\nu = hc / \lambda \quad (2.13)$$

where E_0 is the energy corresponding to the fundamental state of the molecule (J), E_1 is the excited state energy (J), h is the Planck's constant (6.626×10^{-34} Js), ν is the electromagnetic radiation frequency (Hz), c is the light velocity (3×10^8 m·s⁻¹) and λ is the wavelength (nm).

⁹² K. Ch. Kress, T. Fischer, J. Stumpe, W. Frey, M. Raith, O. Beiraghi, S. Holger Eichhorn, S. Tussetschläger, S. Laschat, Influence of chromophore length and acceptor groups on the optical properties of rigidified merocyanine dyes, *ChemPlusChem* 2014, **79**, 223–232.

⁹³ R. L. M. Allen, 1971, Colour chemistry, Bath, Pitman Press, p. 1–21.

TABLE 2. Classification and examples of dyes according to the chromophore present ¹⁰⁴.

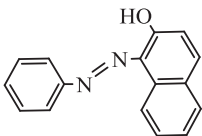
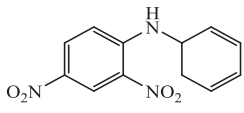
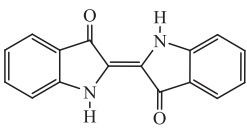
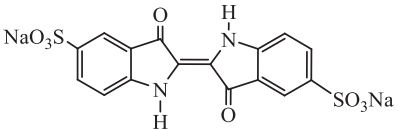
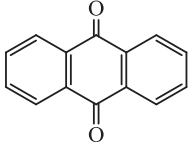
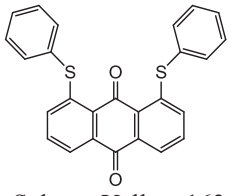
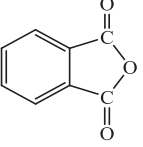
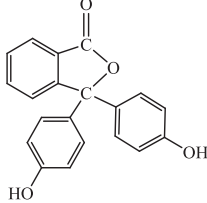
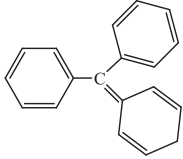
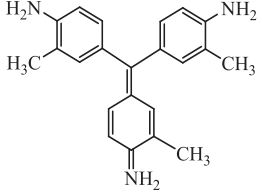
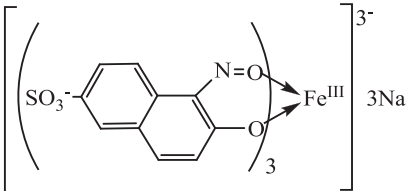
CLASS	CHROMOPHORE	EXAMPLE
Azo dyes	$-\text{N}=\text{N}-$	 Solvent Yellow 14
Nitro dyes	$-\text{N}=\text{O}$	 Disperse Yellow 14
Indigoid dyes		 Acid Blue 74
Anthraquinone dyes		 Solvent Yellow 163
Phthalein dyes		 Phenolphthalein
Triphenyl methyl dyes		 Basic Violet 2
Nitroso dyes	$-\text{N}=\text{O}$	

TABLE 3. The classification of dyes ⁹⁴.

TYPE OF DYE	CHARACTERISTICS	SUBSTRATES
Acid	When in solution are negatively charged; bind to the cationic NH_3^+ -groups present in fibres	Polyamide, wool, silk, paper, inks, leather, ink-jet printing, cosmetics
Reactive	Form covalent bonds with NH-, OH- or SH- groups	Cotton, wool, silk and polyamide
Direct	Large molecules bound by Van der Waals forces to the fibre	Cellulose fibres, cotton, viscose, paper, leather, polyamide
Basic	Cationic compounds that bind to the acid groups of the fibre	Synthetic fibers, paper, inks
Vat	Insoluble coloured dyes which on reduction give soluble colourless forms (leuco form) with affinity for the fibre; on exposure to air are reoxidised	Cellulose fibres, cotton, viscose, wool
Sulfur	Complex polymeric aromatics with heterocyclic S-containing rings	Cellulose fibers, cotton, viscose
Metal complex	Strong complexes of one metal ion (usually chromium, copper, cobalt or nickel) and one or two dye molecules (acid or reactive)	Silk, polyamide, wool
Azoic components and compositions	Insoluble products of a reaction between a coupling component and a diazotized aromatic amine that occurs in the fibre	Cotton, rayon, cellulose acetate, polyester
Mordant	These colorants require the addition of a chemical that combines with the dye and the fibre, like tannic acid, alum, chrome alum, and other salts of aluminium, chromium, iron, copper, tin and potassium	Wool, leather, silk
Fluorescence brightners	Mask the yellowish tint of the materials	Soaps and detergents, all fibres, oils, paints, plastic
Disperse	Scarcely soluble dyes that penetrate the fibre through fibres swelling	Polyester, polyamide, plastic
Solvent	Non-ionic dyes that dissolve the substrate to which they bind	Plastic, gasoline, varnish, lacquer, stains, inks, oils, waxes, fats

The more extended the electronic delocalisation, the lower is the transition energy and the higher is the wavelength. ⁹⁵. To allow delocalization of the electrons double bonds must alternate with single bonds. In case of synthetic dyes, delocalization is also promoted by naphthalene or benzene rings. Chromophores often contain heteroatoms with non-bonding electrons as N, S and O. By incorporating these non-bonding electrons into the delocalised

⁹⁴ K. Hunger (2003), *Industrial Dyes: Chemistry, Properties, Applications*, Weinheim, WILEY-VCH Verlag GmbH & Co. KGaA, p. 4–5.

⁹⁵ R. W. G. Hunt, M. R. Pointer (2011), *Measuring Colour*, West Sussex, John Wiley & Sons Ltd., Ch. 1.

system in the aryl rings, the energy of the electron cloud is modified, the wavelength of the absorbed radiation will shift towards the visible range, and the compound will be colored^{96, 97}. Most dyes also contain auxochromes, electron-withdrawing or electron donating substituents that cause or intensify the color of the chromophore by altering the overall energy of the electron system. Typical auxochromes are -NH₂, -COOH, -SO₃H and -OH. Auxochromes are often used to influence dye solubility and to increase the dye affinity for the fibre (natural or synthetic)^{98, 99}. Different attractive forces have the potential of binding dyes to fibres, and frequently more than one type of chemical bonding can operate with the same dye-fiber combination. The dominant force depends on the chemical groups in the dye molecule and the chemical character of the fiber. The types of bonds established between the dye and the fibre, by increasing relative strength of the bond, can be: Van der Waals, hydrogen, ionic or covalent^{100, 101}.

The vast array of commercial colorants is classified in terms of color, structure and application method in the Color Index (C.I.) which is edited since 1924 by the Society of Dyers and Colourists and the American Association of Textile Chemists and Colorists. The understanding of chemical structure of dye helps to assign the five digit C.I number. Common classes of dyes, based on the chromophore present and the application categories, are shown in Table 2 and Table 3. One category among them, solvent dyes used for dyeing substrates in which they can dissolve, e.g., polymers, varnish, waxes etc., are especially relevant to this research work.

2.2.2 SOLVENT DYES - GENERAL DISCUSSION

Drawn from a large number of chemical groups, the solvent dyes, disperse dyes and pigments have in common the property of being water insoluble¹⁰². Chemically there are

⁹⁶ R. J. D. Tilley (2011), Colour and the optical properties of materials: An exploration of the relationship between light, the optical properties of materials and colour, R. J. D. Tilley (Ed.), West Sussex, John Wiley & Sons Ltd., Ch. 1.

⁹⁷ R. S. H. Liu, A. E. Asato, Tuning the color and excited state properties of the azulenic chromophore: NIR absorbing pigments and materials, *Photochem. Photobiol. C* 2003, **4**,197–194.

⁹⁸ E. N. Abrahart (1977), Dyes and their intermediates, New York, Chemical Publishing, p. 1–12.

⁹⁹ A. D. Broadbent (2001), Basic principles of textile coloration, West Yorkshire, Society of Dyers and Colourist, Ch. 1.

¹⁰⁰ W. Ingamells (1993), Colour for textiles: a user's handbook, West Yorkshire, Society of Dyers and Colourist, Ch. 1

¹⁰¹ R. G. Kuehni (2013), Color: an introduction to practice and principles, New Jersey, John Wiley & Sons, Inc., p.1–37.

¹⁰² S. K. Patel, K. K. Saurabh K, Patel, K. Kamlesh, M. D. Mali, Studies on synthesis of novel low molecular weight anthraquinone disperse dyes and their application on polyester and nylon, *J. Ind. Chem. Soc.* 2012, **89**, 789–795.

few differences between the disperse dyes and some of the solvent dyes. For example, the well known Disperse Yellow 3 is the same as Solvent Yellow 77. The difference between disperse dyes and solvent dyes is mainly in their use. Disperse dyes are designed so they are hydrophobic in nature. Such colorants are very sparingly soluble in water and derive their name from the fact that they are dispersed rather than fully dissolved in water to carry out the dyeing process^{103, 104, 105, 106}. These dyes are usually used in dispersed form in aqueous medium for synthetic fibers and have no affinity to hydrophilic polymers such as cellulose, which make them unsuitable for coloring cotton, cellophane, and but suitable for poly(ethylene terephthalate) and cellulose acetate. Solvent dyes during application process, lose their crystal or particulate structure and form a molecular solution in the media being colored. They cannot be classified according to a specific chemical type of dyes and are found among the azo, metal-complex, disperse, anthraquinone, triarylmethane or phthalocyanine dyes. They are basically insoluble in water, but soluble in the different types of solvents. Solvent dyes are used for dyeing substrates in which they can dissolve, e.g. polymers, varnish, ink, waxes and fats¹⁰⁷. The first solvent dyes were discovered over 100 years ago for example Solvent Violet 8 (1862, Fig. 1 a), Solvent Black 5, Solvent Black 7 (1867) or Solvent Yellow 1 (in 1986, Fig. 1 b).

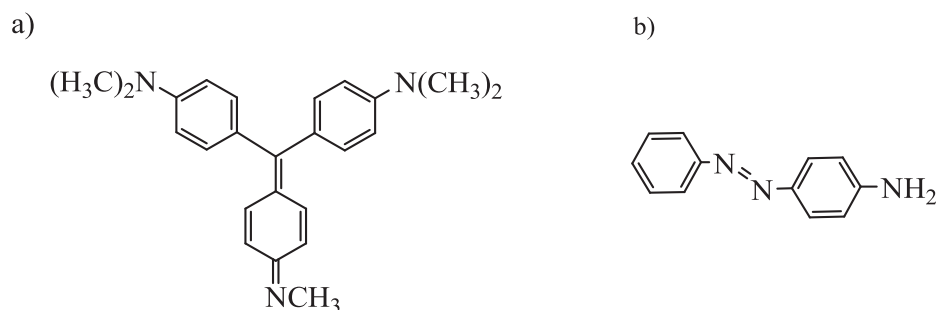


FIGURE 1. The chemical structure of Solvent Violet 8 (a) and Solvent Yellow 1 (b).

¹⁰³ D. G. Patel, N. K. Prajapati, M. K. Thakor, R. T. Patel, Formation of some novel disperse azo dyes: synthesis, characterization and printing properties, *Int. J. Pharm. Pharm. Sci.* 2012, **2**, 86–91.

¹⁰⁴ H. E. Gaffer, S. Shkra, Abbas, E. Dina, E. A. Allam, E. A. Synthesis and antimicrobial activity of some new sulphonamide disperse dyes and their applications to polyester fibres, *J. Appl. Sci. Res.* 2013, **9**, 4051–4058.

¹⁰⁵ L. Lu, L. He, S. Zhang, H. S. Freeman, Novel yellow azo-anthraquinone dyes for polylactide fibres: effects of alkyl chain length, *Color. Technol.* 2012, **128**, 121–126.

¹⁰⁶ Ch.- K. Dien (1978), *The Chemistry of Synthetic Dyes*, ed. K. Venkataraman, London, Academic Press, p. 81–131.

¹⁰⁷ R. M. Christie, Pigments, dyes and fluorescent brightening agents for plastics: An overview, *Polym. Int.* 1994, **34**, 351–361.

2.2.3 CHEMICAL CONSTITUTION AND APPLICATION PROPERTIES OF SOLVENT DYES

Since this type of colorants can be found among the different class of dyes, the different solubility can be used as a basis for a classification of solvent dyes ^{108, 109}.

A) Alcohol- and ester-soluble dyes

There is no precise delineation between alcohol- and ester-soluble dyes, nor between these two groups and the fat- and oil-soluble dyes. Mainly azo dyes and the blue copper phthalocyanine derivatives are soluble in polar solvents such as alcohols, glycols, esters, glycol ethers, and ketones. Dyes soluble in alcohols and esters are used in protective lacquers for the transparent coating of metal foils and other materials, such as wood, in flexographic inks for the printing of metal foils, cellophane and paper. They can be also used for the coloration of cellulose esters, celluloid and poly(vinyl acetate) ¹¹⁰. Alcohol- and ester -soluble azo dyes can be divided into three groups:

- 1:2 metal complexes of (mainly mono-) azo dyes, without sulfonic or carboxylic acid groups, and trivalent metals. The metals are preferably chromium and cobalt, less important are: nickel, manganese, iron, or aluminum. Diazo components are mainly chloro- and nitro aminophenols or aminophenol sulfonamides; coupling components are β -naphthol, resorcinol, and 1-phenyl- 3-methyl-5-pyrazolone. Formation of a complex from an azo dye and a metal salt generally takes place in the presence of organic solvents, such as alcohols, pyridine, or formamide (e.g. Solvent Red 8).
- 1:1 metal-complex azo dyes that contain sulfonic acid or carboxylic acid groups and are present in the form of internal salts (e.g. Solvent Yellow 32). Other 1:1 metal complex dyes are Solvent Orange 56 and Solvent Yellow 82.
- reaction products of acid azo dyes, acid 1:1 metal-complex azo dyes, or 1:2 metal complex azo dyes without acid groups, with organic bases or cationic dyes. For instance: C.I. Solvent Red 109 is composed of Solvent Yellow 19, and Solvent Red 49. These dyes are salts like compounds of a metal-complex azo dye acid and a base ^{111, 112}.

¹⁰⁸ K. Hunger (2003), *Industrial Dyes: Chemistry, Properties, Applications*, Weinheim, WILEY-VCH Verlag GmbH & Co. KGaA, p. 295-301.

¹⁰⁹ R. L. M. Allen, 1971, *Colour chemistry*, Bath, Pitman Press, p. 260–265.

¹¹⁰ M. S. Zakerhamidi, Sh. Golghasemi Sorkhabi, A. N. Shamkhali, Polar and low polar solvents media effect on dipole moments of some diazo Sudan dyes, *Spectrochim. Acta A* 2014, **127**, 340–348.

¹¹¹ N. Sekar, S. N. Shelar, V. Chaugule, Colorants for solvents- recent developments, *Colourage*, 2007, **54**, 70–77.

¹¹² J. M. Smith (2005), Organic solvent-soluble metal complex azo dyes, WO 2005030875 A2.

B) Fat- and oil-soluble dyes

Fat- and oil-soluble dyes are soluble in waxes, resins, lacquers, hydrocarbons, halogenated hydrocarbons, ethers, and alcohols, but not in water. They are used on a large scale in a wide variety of industrial sectors. Depending on the type of product being dyed, these colorants can be divided into two main fields of application: dyes for coloration mineral oil and wax products and for polymers.

➤ Dyes for coloration mineral oil and wax products

Mainly azo and some anthraquinone dyes are used for coloring this type of products. Azo dyes provide many yellow, orange and generally do not have a water-solubilizing group. Although they are cheap, they generally have poor fastness and heat stability. Solubility of these dyes is very high and this allows them to disperse easily. The main fields of application are the coloration of products in the mineral oil wax products (e.g., candles, shoe polishes, floor polishes). Mineral oil products (lubricating oils, fuels, fuel oil, and greases) are colored as a means of distinguishing between different grades (e.g., of gasoline) or for compulsory identification, e.g., of fuel oils and diesel, for duty purposes. The anthraquinone dyes with relatively simple structures like for example bis(alkylamino)anthraquinones are suitable additives for coloring gasoline¹¹³.

It is worth to note that, the lightfastness of fat- and oil-soluble dyes is highly dependent on the medium colored. Whereas colorations of the dye Solvent Yellow 56 in candle materials possess only moderate lightfastness, transparent colorations in polystyrene are distinguished by outstanding lightfastness. Other fields of application are the lacquers industry (especially coloration of transparent lacquers on aluminum foil), the office supplies industry (inks for felt-tip pens) and the cosmetics industry¹¹⁴.

Mainly due to their extreme brightness and low cost they are sometimes use in polymer applications for example Solvent Red 210 is used in polypropylene holiday ribbon for many years. Migration can occur at elevated loading, and use in plasticized polymers is not suggested. Also they are not suggested for dyeing olefin materials. In recent years, legislation in some countries has restricted the manufacture and use of azo dyes because of the possible toxicity of the intermediates and the potentially hazardous degradation

¹¹³ P. Bamfield (2001), *Chromic Phenomena: Technological Applications of Colour Chemistry*, Cornwall, Printed by MPB Books Ltd, p.131-132.

¹¹⁴ A. Whitaker, Crystal structures of azo colorants derived from pyrazolone: a review, *J. Soc. Dyers.Colour.* 1995, **111**, 66–72.

products. The most typically used azo dyes are: Solvent Yellow 14, Solvent Red 1 (Fig. 2 a), Solvent Black 3, Solvent Yellow 16 (Fig. 2 b), Solvent Red 23, Solvent Yellow 18, Solvent Red 26, Solvent Orange 7 ¹¹⁵.

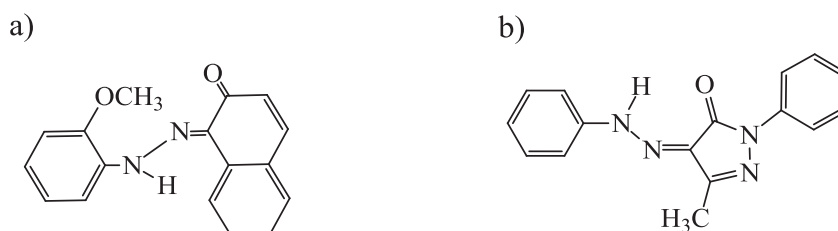


FIGURE 2. The chemical structure of Solvent Red 1 (a) and Solvent Yellow 16 (b).

➤ Dyes for polymers

The polymer industry values the fat- and oil-soluble dyes for the good lightfastness, that are obtainable with them. According to their degree of solubility they usually contain hydroxyl and/or amino groups, but not sulfonic acid and carboxylic acid groups.

Two major classes of dyes in coloring polymeric materials anthraquinones and perinones, however some quinophthalone and methine dyes can be also suitable for this purpose. Anthraquinones provide important blues and greens. Many dyes based on this group are used in mass coloration of polymer compositions.

Perinone dyes belong to group of colorants which show fluorescent characteristics. Perinone class is small in number compared with the others, but shows excellent light and heat stability in most polymers ^{116, 117}.

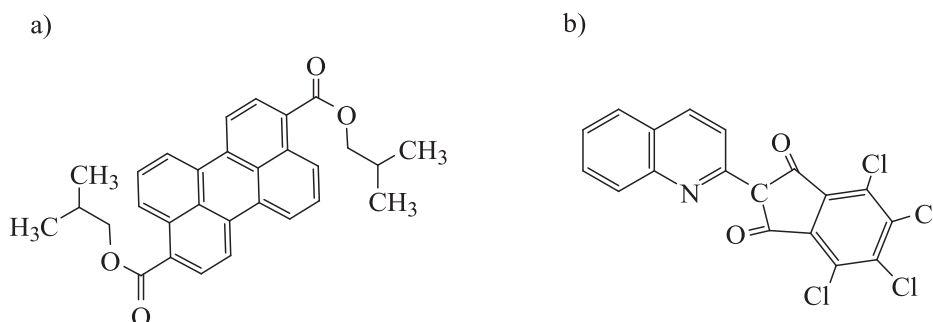


FIGURE 3. The chemical structure of Solvent Green 5 (a) and Solvent Yellow 157 (b).

¹¹⁵ H. Pan, J. Feng, G.-X. He, C. E. Cerniglia, H. Chen, Evaluation of impact of exposure of Sudan azo dyes and their metabolites on human intestinal bacteria, *Anaerobe* 2012, **18**, 445–453.

¹¹⁶ K. I. Kobrakov, N. S. Zubkova, G. S. Stankevich, Yu. S. Shestakova, V. S. Stroganov, O. I. Adrov, New aroyleneimidazoles as dyes for thermoplastic polymeric materials, *Fibre Chem.* 2006, **38**, 183–187.

¹¹⁷ Y. Yang, L. Yang, W. Wu, D. Huang, W. Ni, W. S. Wei (2009), A Method for preparation of Solvent Orange 60, CN 101565556.

The most commonly used in the plastics industry are: Solvent Orange 60, Solvent Red 135, Solvent Red 179, Solvent Green 5 (Fig. 3 a), Solvent Red 180, Solvent Orange 60, is best known for application in amber tail light lenses of acrylic, styrene or polycarbonate. Solvent Green 5, despite its names, has been found to be a bright fluorescent yellow in thermoplastics materials with good light and heat stability. Some solvents Greens listed in C.I. have greenish fluorescence in mineral oils and petroleum products.

Quinophthalone dyes are a group of important solvents yellow. The simplest is Solvent Yellow 33, made by condensing quinaldine with phthalic anhydrate ^{118, 119}. Some commercially available dyes belonging to the quinophthalone class are follows: Solvent Yellow 33, Solvent Yellow 114, Solvent Yellow 105, Solvent Yellow 157 (Fig. 3 b).

Methine and polymethine dyes are another family of colorants. Typical commercial example of these dyes is the Solvent Yellow 133, which provides shade yellow color and is applied in polyester materials. Methine and polymethine dyes are known for their brightness as well as good light stability ^{120, 121, 122}.

2.2.4 THE CHEMISTRY OF ANTHRAQUINONE SOLVENT DYES

2.2.4.1 THE CHEMISTRY OF ANTHRAQUINONE

A common arrangement of the carbonyl groups in colored molecules gives rise to a group of compounds known as quinones i.e., compounds containing two ketone carbonyl groups and two double bonds in a six-membered ring. Anthraquinones contain a characteristic system of three linear fused six-membered rings in which the carbonyl groups are in the central ring and the two outer rings are fully aromatic (Fig. 4) ¹²³. There is a wide variety of chemical structures of anthraquinone colorants. In contrast to the azo dyes, which have no natural counterparts, all the important natural red dyes were anthraquinones, for example alizarin (1, 2-dihydroxyanthraquinone), the principal constituent of madder.

¹¹⁸ N. Kuramoto, K. Asao, The syntheses and crystal structures of some bis(1,2-diaryl-1,2-ethylenedithiolato) nickel complexes and their photostabilizing efficiency to organic dyes, *Dyes Pigments* 1990, **12**, 65–76.

¹¹⁹ N. Sekar, Quinophthalone colorants, *Paintindia*, 2002, **52**, 63-64.

¹²⁰ A. M. Asiri, Synthesis and characterization of methine dyes derived from condensation of 4 nitrophenyl-acetonitrile with aromatic aldehydes, *Pigm. Resin Technol.* 2004, **33**, 370–374.

¹²¹ D. Keil, R. Flaig, A. Schroeder, H. Hartmann, Synthesis and characterization of methine dyes derived from N,N-disubstituted 2-aminoselenazoles and some of their heterocyclic sulfur analogues, *Dyes Pigments* 2001, **50**, 67–76.

¹²² A. M. Asiri, Synthesis, characterizations and absorption spectral properties of new styryl dyes derived from 1-dicyanomethyleneindane, *J. Saudi Chem. Soc.* 2000, **4**, 61–66.

¹²³ R. M. Christie (2001), *Colour Chemistry*, Manchester, Bookcraft Ltd, Ch. 4.

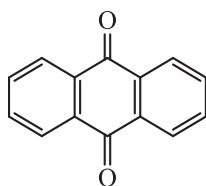


FIGURE 4. The chemical structure of 9,10-anthraquinone.

However, natural anthraquinone dyes are no longer of significant commercial importance. The range of the anthraquinone colorants includes also the anthraquinone pigments like some of the longest-established vat dyes, indanthrone (Pigment Blue 60) together with some of its halogenated derivatives, and flavanthrone (Pigment Yellow 24)¹²⁴. Anthraquinone dyes are based on 9,10-anthraquinone, which is weakly colored. To produce commercially useful dyes, strongly electron donating groups such as amino or hydroxyl are introduced.

TABLE 4. Absorption maxima for some substituted anthraquinones¹²³.

Compound	Substituent	λ (nm)*
4a	1-OH	420
4b	2-OH	368
4c	1-NH ₂	475
4d	2-NH ₂	440
4e	1-NHPh	500
4f	1,4-diNH ₂	590
4g	1,4,5,8-tetraNH ₂	610
4h	1,4-diNHPh	620

*methanol

The UV/Vis spectral data for a series of substituted anthraquinones (4a–h) and effects of the substituent pattern on the color are given in Table 4. The introduction of simple electron-releasing groups (hydroxyl or amino) into the anthraquinone nucleus gives rise to a bathochromic shift which is dependent on the number and position of the electron releasing groups and their relative strengths. The strength of electron-donor groups increases in the order: OH < NH₂ < NHR < HNPh^{125, 126, 127}. They are thus typical donor-acceptor systems, with the auxochromes (electron-releasing) as the donors and the carbonyl groups as the acceptors.

¹²⁴ J. Park, Y. Park, J. Park, Synthesis and physical property measurement of new red pigment based on anthraquinone derivatives for color filter pigments, *Mol. Cryst. Liquid. Cryst.* 2011, **551**, 116–122.

¹²⁵ N. Sekar, Developments in anthraquinone dyes - an update, *Colourage* 2000, **47**, 48–50.

¹²⁶ M. Hattori (2005), Kirk-Othmer Encyclopedia of Chemical Technology, A. Seidel (Ed.), New Jersey, John Wiley&Sons Inc., p. 300–349.

¹²⁷ M. S. Zakerhamidi, A. Ghanadzadeh, M. Moghadam, Intramolecular and intermolecular hydrogen-bonding effects on the dipole moments and photophysical properties of some anthraquinone dyes, *Spectrochim. Acta A* 2011, **79**, 74–81.

From the data, it is clear that the electron-releasing groups exert their maximum bathochromic effect in the α -positions (1, 4, 5, 8) rather than the β -positions (2, 3, 6, 7). The most common substitution patterns are 1, 4; 1, 2, 4, and 1, 4, 5, 8. Tetra substituted anthraquinones (1, 4, 5, 8) are more bathochromic than di- (1, 4) or trisubstituted (1, 2, 4) anthraquinones. Thus, by an appropriate selection of donor groups and substitution patterns, a wide variety of colors can be achieved. By choice of suitable pattern, dyes are obtained which may absorb in any desired region of the visible spectrum. To optimize the properties, primary and secondary amino groups (not tertiary) and hydroxyl groups are employed. In addition, α -substituents give dyes with higher molar extinction coefficients and enhance technical performance, especially lightfastness because of strong intramolecular hydrogen bonding with the carbonyl groups, with minimum steric hindrance.

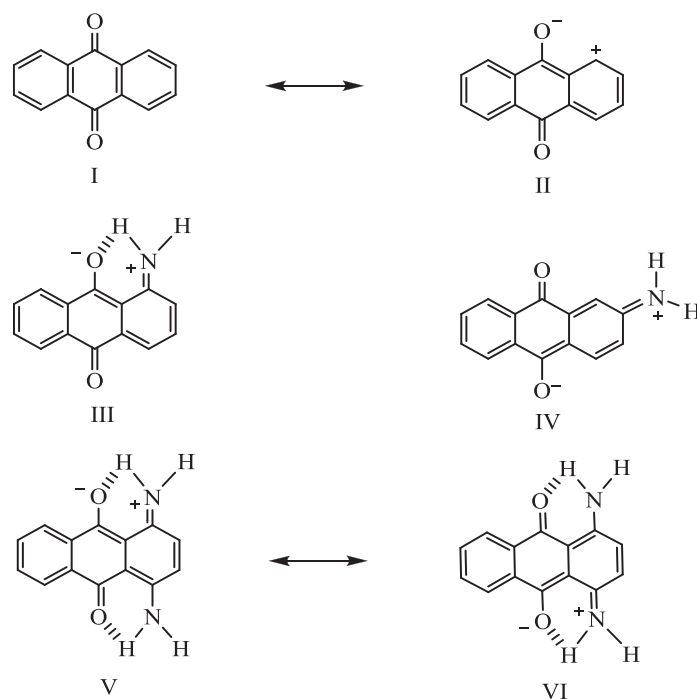


FIGURE 5. Some relevant resonance forms for anthraquinones 4 (I, II), 4 c (III), 4 d (IV) and 4 f (V, VI) ¹²³.

The effect of substituents on color in substituted anthraquinones can be explained using the valence-bond (resonance) approach. Some relevant resonance forms for anthraquinones 4, 4 c, 4 d and f are illustrated in Figure 5. The ground state of the parent compound (4) is assumed to resemble closely structures such as I, while charge-separated forms, such as structure II, are assumed to make a major contribution to the first excited state. Structure II is clearly unstable due to the carbocationic centre. In the case of aminoanthraquinones 4 c and 4 d, donation of the lone pair from the amino nitrogen atom markedly stabilises the

first excited states, represented respectively by structures III and IV, lowering their energy and leading, as a consequence of the inverse relationship between the difference in energy and the absorption wavelength, to a pronounced bathochromic shift. The 1, 4-diamino compound 4 f is particularly bathochromic because of an extensively resonance-stabilised first excited state, involving structures V and VI ^{128, 129}.

2.2.4.2 ANTHRAQUINONE SOLVENT DYES FOR POLYMERS

The one major classes of solvent dyes used in melt coloring polymer materials are the anthraquinones. Anthraquinone dyes have become the workhorses of the plastic colorant industry. They are relatively inexpensive, have very good solubility, excellent color strength, transparency as well as high heat and light stability. Because solvent dyes dissolve during melting processing and form a molecular solution into the polymer matrix, dispersion is not an issue. Another advantage with the anthraquinone solvent dyes is that a full range of colors, with similar solubilities and stabilities, can be developed by changing the pendants on the anthraquinone molecule ¹³⁰. Photo, heat and chemical stability vary considerably as the pendants on the base anthraquinone structure are substituted. Awareness of these differences is very important in color formulating ¹³¹. This is especially true of α -alkyl- or arylaminoanthraquinone in which the amino hydrogen is strongly bonded with a quinone carbonyl. When both 1- and 4- positions of anthraquinone are substituted with alkyl or arylamino groups, the shade shifts to the blue green range. The fastness properties of 1, 4-bisalkylaminoanthraquinones are generally not adequate for some thermoplastic materials and improved color substituent by arylalkylamines such as 2-phenylethylamine and alkoxybenzylamine are recommended. Also, when one or two alkylamino is replaced by an aryloamino group, the fastness often improved. The simple solvent dyes like 1, 4-bisalkylaminoanthraquinones are used for coloring oils, waxes, petroleum products, etc. The requirements for lightfastness, thermal and chemical resistance for dyes used to color plastics materials are more demanding ^{132, 133}.

¹²⁸ P. Dahiya, M. Kumbhakar, T. Mukherjee, H. Pal, Effect of the amino and hydroxy substituents on the photophysical properties of 1,4-disubstituted-9,10-anthraquinone dyes, *J. Mol. Struct.* 2006, **798**, 40–48.

¹²⁹ P. Dahiya, D. K. Maity, S. K. Nayak, T. Mukherjee, H. Pal, Solvent polarity and intramolecular hydrogen bonding effects on the photophysical properties of 1-amino-9,10-anthraquinone dye, *J. Photochem. Photobiol. A* 2007, **186**, 218–228.

¹³⁰ L. A. Bente (1998), *Plastics Additives*, G. Pritchard (Ed.), Bristol, Chapman & Hall, p. 219–225.

¹³¹ M. Matsui, A. Sedyohutomo, M. Satoh, Y. Abe, K. Funabiki, H. Muramatsu, K. Shibata, Solubility and decomposition temperature of 1,4-bis(aryl-amino)-anthraquinone dyes, *Dyes Pigments* 1998, **40**, 21–26.

¹³² N. Sekar, Solvent soluble anthraquinone dyes, *Colourage* 2005, **52**, 97–98.

¹³³ D. Li, G. Sun, Kinetics of thermo-fixation of solvent dyes and pigments in polyester fibres, *Color. Technol.* 2006, **122**, 194–200.

Anthraquinone solvent dyes are used for a broader spectrum of plastics than that of the azo dyes. As compared with azo dyes, anthraquinone solvent colorants are less bright but their light fastness and chemical resistance are generally superior of these of azo colors. On the other hand, like most dye, they can have also tend to migrate from the polymer and adverse effects on the plastic materials themselves e.g. acting as plasticizer ¹³⁴. Anthraquinone dyes are often applied in polystyrenes, polycarbonates, polymethacrylates, polyesters, ABS or SAN. Most these types of colorants are not recommended for polyamide applications as these material react with amine pendants and can remove the color. Similar behavior we can also observe in high butadiene ABS materials. It seems that the butadiene forms a highly reactive peroxide and this then may react with particular chromophores.

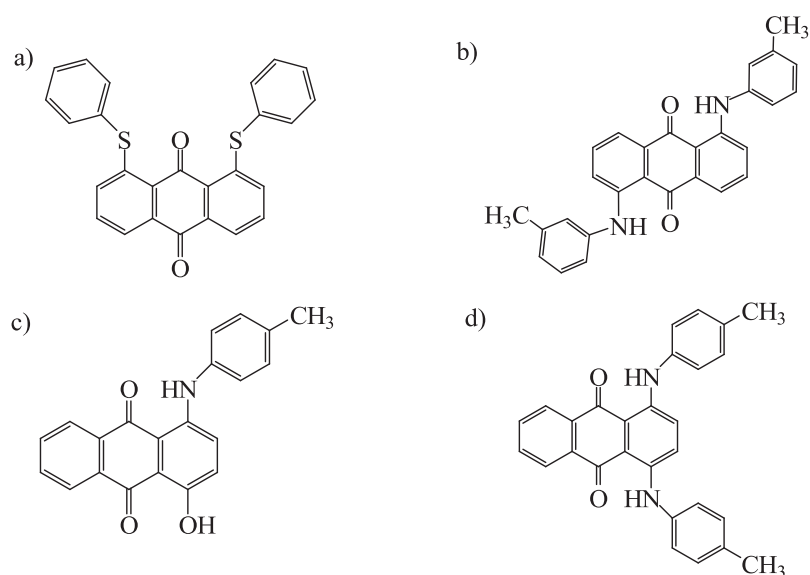


FIGURE 6. The chemical structure of Solvent Yellow 163 (a), Solvent Red 207 (b), Solvent Violet 13 (c) and Solvent Green 3 (d).

Solvent Yellow 163 and 167 are beginning to find applications in the coloration of polyamide 6,6. This non-reactive nature appears as a result of the replacement of the amine bridge with a sulfur atom. Many anthraquinone solvent dyes can be used in peroxide curing systems. Dyes such as Solvent Yellow 163 and 167 (Fig. 6 a), Red 168, 169, 172 and 207 (Fig. 6 b) and Solvent Violet 38 have all been found to be peroxide resistant. A typical commercially available anthraquinone solvents dyes are: Solvent Yellow 163, Solvent Violet 13 (Fig. 6 c), Solvent Yellow 167, Solvent Violet 36, Solvent Red 111,

¹³⁴ Q. Meng, D. Huang, S. Wei, L. Chen, The influence of crystal structure on the dyeing property of 1,4-diamino-2,3-diphenoxyanthraquinone, *Dyes Pigments* 2002, **53**, 15–20.

Solvent Red 168, Solvent Red 169, Solvent Red 172, Solvent Red 207, Solvent Green 28, Solvent Green 3 (Fig. 6 d), Solvent Blue 35, Solvent Blue 59, Solvent Blue 36, Solvent Blue 97, Solvent Blue 58, Solvent Blue 104, Solvent Red 149, Solvent Violet 14, Solvent Red 52^{135, 136}.

2.2.5 ORGANIC PIGMENTS

Pigments are colored, white or black materials, which are practically insoluble in the medium in which they are applied. Pigment is incorporated into the polymer by a dispersion process and form in material a separate phase. They are conveniently classified as either inorganic or organic types. Nevertheless in white reduction, many inorganic pigments have much less strength than organic pigments. Inorganic pigments not only exhibit coloristic limitations but also frequently present application problems¹³⁷. Organic pigments are characterized in general by high brightness and good color strength however they offer different fastness properties. The properties of a pigment are primarily dependent on its chemical structure, i.e., the way in which the molecules pack in their crystal lattice¹³⁸. Certain pigments like copper phthalocyanine, exist in different polymorphic forms with significantly different optical and stability properties. Other important factors, especially in influencing the strength or intensity of color of pigments, are particle shape and size.

Organic pigments generally show an increase in color strength as the particle size is reduced, while with many inorganic pigments there is an optimum particle size at which the color strength reaches a maximum. As opposed to dyes, crystal pigment particles in a polymer matrix cannot only absorb but also scatter and reflect light (Scheme 5)¹³⁹.

The main reason for incorporating pigments into polymers is to introduce color, either for aesthetic reasons and market appeal or because of functional demands. They are widely used for the coloration of polymers mainly because of their superior fastness properties, especially migration resistance.

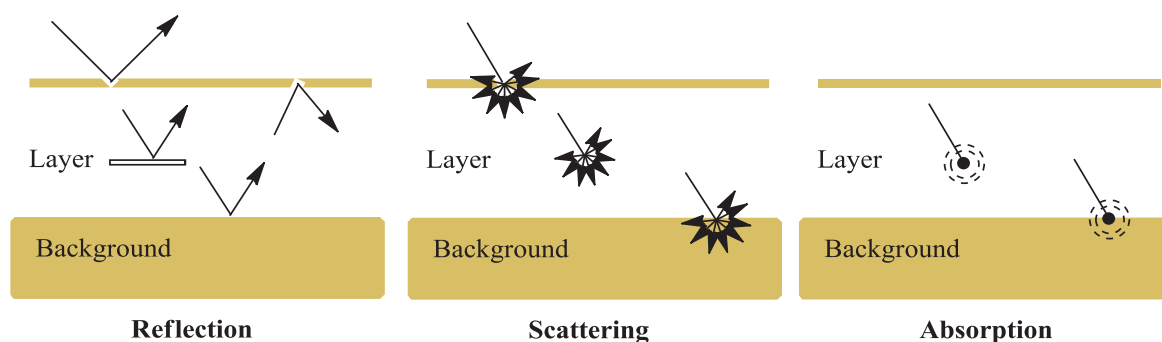
¹³⁵ D. Li, G. Sun, Diffusion of solvent dyes and pigments in polyester fibers, *PMSE Preprints*, 2004, **90**, 557–558.

¹³⁶ R. Rosen, Colours for a brighter future, *Polym. Paint Col. J.* 1994, **184**, 344–348.

¹³⁷ P. A. Lewis (2004), *Coloring of Plastics: Fundamentals*, R. A. Charvat (Ed.), New Jersey, John Wiley & Sons Inc., Ch. 8.

¹³⁸ T. Brock, M. Groteklaes, P. Mischke, Organic coloured pigments, *Europ. Coat. J.* 2002, **6**, 64–66.

¹³⁹ M. U. Schmidt, Crystal engineering and polymorphism of organic pigments, *Adv. Colour Sci. Technol.* 2003, **6**, 59–61.



SCHEME 5. Reflection, scattering and absorption of light in pigmented coatings ¹³⁷.

Pigments may often perform useful functions that are more wide-ranging than their optical role, for example mechanical reinforcement or the inhibition of polymer degradation. Some pigments can act as nucleating agents, changing the mechanical properties and improving the clarity of the resin. On occasions, the incorporation of pigments can also produce problems in polymers, such as the warping of polyolefins as a result of uncontrolled nucleation ^{140, 141, 142}.

Pigments must be adequately dispersed in the polymer for optimum scattering. The presence of specks and uneven coloration can result from incomplete dispersion. If agglomerates are present they may adversely impact the mechanical properties of the resulting product, mainly tensile strength, impact strength, and flex fatigue ^{143, 144}. The important factor which influence the dispersion properties is the degree of aggregation of pigment particles and the nature of the particle surfaces. Pigments may be introduced into polymers by different methods. Direct coloring, in which the pigment is incorporated into the molten polymer often along with other additives using high-shear dispersing equipment, may be used. However, high temperature during processing can destroy or damage the pigment causing loss of color or changes in shade. Many manufacturers of polymers articles find it more convenient to make use of pre-dispersed concentrates or masterbatches of pigment in a liquid additive such as a plasticizer or in a compatible resin ¹⁴⁵.

¹⁴⁰ B. L. Kaul, Coloration of Plastics using Organic Pigments, *Rev. Prog. Coloration* 1993, **23**, 19–35.

¹⁴¹ R. M. Christie (1993), *Pigments: Structures and Synthetic Procedures*, London, Oil and Colour Chemists Association.

¹⁴² P. A. Lewis (2006), *Coatings Technology Handbook*, A. A. Tracton (Ed.), Boca Raton, Taylor & Francis Group, Ch.78.

¹⁴³ G. Skillas, N. Agashe, D. J. Kohls, J. Ilavsky, P. Jemian, L. Clapp, R. J. Schwartz, G. Beaucage, Relation of the fractal structure of organic pigments to their performance, *J. Appl. Phys.* 2002, **91**, 6120–6124.

¹⁴⁴ A. Marcincin, A. Ujhelyiova, M. Hricova, Processing of the organic pigment dispersion in polypropylene and polypropylene fibers, *Vlakna Textil* 2002, **9**, 3–11.

¹⁴⁵ S.-H. Fu, Ch.-H. Xu, Ch. He, Effects of process conditions on properties of nanoscale organic pigment encapsulated by poly(styrene-maleic acid) dispersion, *J. Disper. Sci. Technol.* 2010, **31**, 617–624.

Some pigments may be partially soluble in the resin and may migrate through the polymer to the surface, where they rub off. The insolubility for pigments can be achieved by avoiding solubilizing groups in the molecule or by forming insoluble organic structures. Carboxylic and sulfonic acid functional groups lend themselves to the formation of insoluble metal salts, formation of metal complex compounds without solubilizing groups and finally suitable substitution may decrease the solubility of the parent structure (e.g., carbonamide groups)¹⁴⁶.

2.2.5.1 CLASSIFICATION OF ORGANIC PIGMENTS

The inorganic class contains a small number of pigments used in polymers and includes compounds like titanium dioxides, ultramarine blue, iron oxides, cadmium yellow, cadmium red, chromium oxide or molybdate yellow. The common classes of organic pigments for polymers are carbon black, phthalocyanine blue and green, quinacridones, isoindolinones, perylenes, anthraquinones, flavanthrones, dioxazines, thioindigos, dyarylides, quinophthalones, azocondensation and azomethine metal complex.

➤ **Copper phthalocyanines**

An important event in the development of the organic pigment industry was the discovery in the 1920s of copper phthalocyanine blue, the first product to offer outstanding coloristic properties combined with a range of excellent fastness properties. Copper phthalocyanine is the single most important organic pigment. It finds wide use in most plastics applications because of its excellent resistance to heat, light, acids and alkalis, migration and its brilliant blue color. In addition, in spite of its structural complexity, copper phthalocyanine is a relatively cheap pigment as it is produced in high yield from low cost starting materials¹⁴⁷.

There are two commercially important crystal modifications of the copper phthalocyanine blue: α - and β -type. The Pigment Blue 15 (α -form) is not stabilized towards phase-transfer, and may convert to the β -modification if is treated in insufficiently cooled dispersion units. This process is associated with a color change to a greener blue as well as with loss of cleanness and tinctorial strength. Compared to the other blue pigments, Pigment Blue 15 types are reddish blue in shade, tinctorial strong, and provide high color

¹⁴⁶ G. Lincke, Molecular stacks as a common characteristic in the crystal lattice of organic pigment dyes. A contribution to the “soluble–insoluble” dichotomy of dyes and pigments from the technological point of view, *Dyes Pigments* 2003, **59**, 1–24.

¹⁴⁷ W. Herbst, K. Hunger (1997), *Industrial Organic Pigments: Production, Properties, Applications*, Weinheim, WILEY-VCH Verlag GmbH & Co. KGaA, Ch. 1–5.

in yield and economy in use. Nonstabilized α -Copper Phthalocyanine Blue 15 is utilized in the printing industry, to a certain extent in oil-based binder system, such as offset printing inks for packaging and metal deco printing. However, the fact that unstable P. Blue 15 types tolerate less than 200 °C is a disadvantage in the coloration plastics. For plastics the α -form of copper phthalocyanine (P. Blue 15:1) stabilized by the presence of a single ring chlorine substituent is preferred. The phase-stabilized α -Copper Phthalocyanine Blue 15:1 (Fig. 7 a) has gained great commercial importance in almost all areas. Stabilization usually causes loss of tinctorial strength and cleanness as well as a color shift towards a greener blue. Despite this disadvantage P. Blue 15:1 types reign supreme among Copper Phthalocyanine Blue types as colorants for coating and paints, packaging printing inks, and plastics. They show good resistance to organic solvents. Excellent lightfastness and weather fastness high heat stability and superior migration fastness, along with a reasonable price make these pigments attractive products^{148, 149, 150}.

A number of α -Copper Phthalocyanine Blue types which are stabilized towards flocculation and change of modification are registered in the Colour Index as 15:2. Their main area of application are paints. Additionally, they are employed wherever P. Blue 15:1 types show too much tendency to flocculate or where economical consideration make P. Blue 15:2 more attractive. In printing inks, P. Blue 15:2 is employed mostly in special gravure and flexographic inks, because in this area lack of fastness to overcoating is frequently of no consequence. The β -modification of Copper Phthalocyanine Blue 15:3 is used primarily in graphical printing, rubber and plastics as well as in textile printing. The β -modification demonstrates excellent heat stability and they are therefore entirely suitable candidates for the pigmentation of plastics. Nevertheless, this form often presents dispersion problems, especially in polyolefins. Moreover, β -Copper Phthalocyanine Blue, like α -types, tends to nucleate in polyolefin, a problem which may lead to distortion and stress cracking in injection-molded parts. This type of modification is available in form stabilized toward flocculation, known as P. Blue 15:4. Copper phthalocyanine green pigments are products in which most of the sixteen outer ring hydrogen atoms are replaced

¹⁴⁸ F. H. Moser (1973), *Pigment Handbook*, T. C. Patton (Ed.), New York, John Wiley & Sons Inc., p. 679–695.

¹⁴⁹ K. E. Fagelman, J. T. Guthrie, The effect of pigmentation on the mechanical properties and the crystallisation behaviour of polymer blends (Xenoy), *Dyes Pigments* 2006, **69**, 62–73.

¹⁵⁰ Z. Tianyong, Z. Chunlong, Properties of Copper Phthalocyanine Blue (C.I. Pigment Blue 15:3) Treated with Poly(ethylene glycol)s, *Dyes Pigments* 1997, **35**, 123–130.

by halogens, and include polychloro, polybromo and polybromochloro derivatives, the shade of the pigments becoming progressively yellower with increasing bromine content.

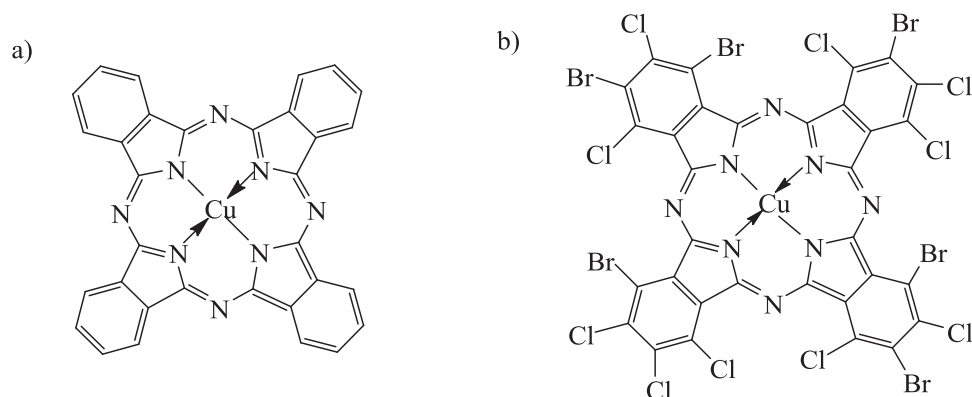


FIGURE 7. The chemical structure of Pigment Blue 15:1 (a) and Pigment Green 36 (b).

The copper phthalocyanine greens (P. Green 7, Pigment Green 36, Fig. 7 b), which exhibit properties comparable to the blues, are also excellent pigments for plastics. Pigment Green 36 is more yellow in comparison to Pigment Green 7, because more chlorine atoms are replaced by bromine atoms. Copper phthalocyanine green pigments are used in all types of paints, including high grade original automotive finishes^{151, 152, 153}.

➤ Azo pigments

The most important commodity yellow, orange and red organic pigments currently in use in polymers are long-established series of azo pigments. Azo colorants are generally described as structures containing one or more azo (-N=N-) groups. Simple classical monoazo pigments find little general use in polymer as they are too soluble and hence liable to migration. This type of compounds is recommended for use in polypropylene, polystyrene and rigid PVC. The disazoacetoacetanilides (Diarylide or Benzidine Yellows) due to good color strength and migration resistance are the most important yellow azo pigments, used in polyethylene, polypropylene and flexible PVC due. There are two main types of high performance azo pigments¹⁵⁴. The benzimidazolone group provide colors in from yellow to bluish-red and browns and exhibit excellent fastness properties. Their insolubility and their good stability to light and heat is attributed to strong intermolecular

¹⁵¹ R. Y. Ting (2012), Wiley Encyclopedia of Composites, L. Nicolais, A. Borzacchiello (Eds.), New Jersey, John Wiley & Sons, Inc., Hoboken, N. J., p. 2068–2073.

¹⁵² H.-T. Wu, H.-M. Lin, M.-J. Lee, Ultra-fine particles formation of C.I. Pigment Green 36 in different phase regions via a supercritical anti-solvent process, *Dyes Pigments* 2007, **75**, 328–334.

¹⁵³ G. Wilker, Shades of green: the impact of pigments on the weathering resistance of coating formulations *Europ. Coat. J.* 2007, **5**, 196–198.

¹⁵⁴ Ch.-H. Chang, R. M. Christie, G. M. Rosair, The crystal structures of three azonaphtharylamide pigments, *Dyes Pigments* 2009, **82**, 147–155.

hydrogen-bonding and dipolar forces involving the benzimidazolone group in the crystal lattice ¹⁵⁵.

➤ **Miscellaneous high-performance organic pigments**

High performance organic pigments exhibit excellent solvent stability, good to very good migration stability in plastics, high chemical inertness, and superior light and thermal stability ¹⁵⁶. Many of this group of products owe their good stability to light and heat and their extreme insolubility to extensive intermolecular association as a result of hydrogen-bonding and dipolar forces in the crystal lattice. A notable example is provided by quinacridones (Fig. 8 a), which are used widely in plastics offering red and violet colors and heat stability to 400 °C ¹⁵⁷. Other high performance pigments used in plastic include, the yellow to red tetrachloroisoindolinones, the dioxazine violet and the perylenes (Fig. 8 b). Perylene pigments offer high tinctorial strength, and they are frequently found to be appreciably stronger than quinacrydone pigments. Moreover, perylene pigments provide excellent light and weatherfastness.

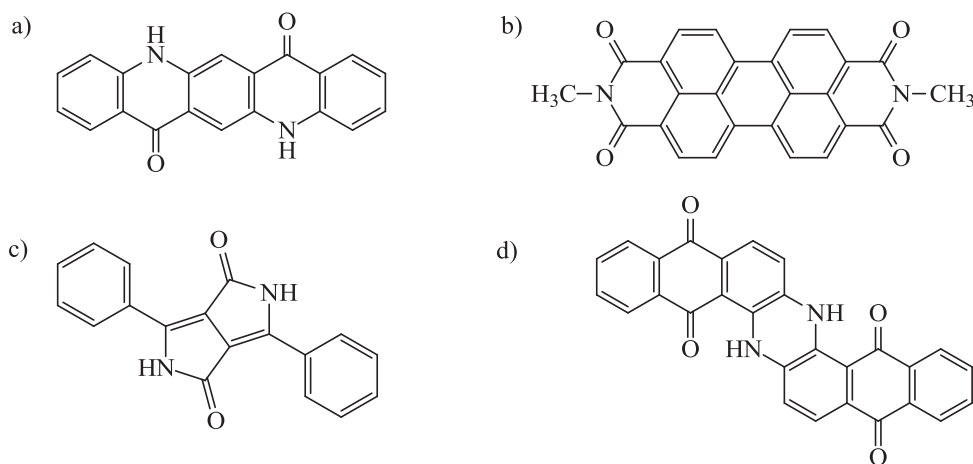


FIGURE 8. The chemical structure of Pigment Violet 19 (a), Pigment Red 179 (b), Pigment Red 255 (c) and Pigment Blue 60 (d).

Another significant organic pigments are diketopyrrolopyrrole (DPP) pigments and its derivatives (Fig. 8 c). These pigments providing brilliant red shades with outstanding durability and excellent thermal stability. It is worth to note that, a number of vat dyes developed originally for textile industry after conversion to an appropriate pigmentary structure, are suitable for use in plastics applications. Examples of these so-called vat

¹⁵⁵ R. M. Christie, J. L. Mackay, Metal salt azo pigments, *Color. Technol.* 2008, **124**, 133–144.

¹⁵⁶ R. M. Christie, C. H. Chang, H. Y. Huang, M. Vincent, Colour and constitution relationships in organic pigments: Part 6. Azonaphtharylamide pigments, *Surf. Coat. Int. Part B: Coat. Transact.* 2006, **89**, 77–85.

¹⁵⁷ R. M. Christie (1998), *Plastics Additives*, G. Pritchard (Ed.), Bristol, Chapman & Hall, p. 485–498.

pigments include the anthraquinones, indanthrone (Fig. 8 d) and flavanthrone, red to violet thioindigo derivatives as well as the orange perinone¹⁵⁸.

2.2.6 EFFECT OF AGING ON THE PROPERTIES OF DYED AND PIGMENTED POLYMERS

Organic pigments and dyes are widely used in the coloration of polymer materials for many commercial application. However, the presence of dyes and pigments can dramatically influence the chemistry of the oxidation, degradation and stabilization process involved in a polymer and will quite often dominate the stability of the end-product. For example, by absorbing and/or scattering UV light, pigments can induce a marked protective effect. Nevertheless, a number of dyes and pigments may be also photoactive and can therefore catalyze or accelerate the photochemical break down of the polymer materials. It is well known that the photostability of dyed and pigmented materials is influenced by several external factors, such as light source, humidity, atmosphere, temperature and aggregation, as well as by the chemical structure both of the colorant and of the substrate^{159, 160, 161, 162}.

The absorption of light by organic dyes and pigments, is followed by various chemical and physical interactions which result from the dye or pigment molecules being promoted to an excited state which is more reactive than the ground state. In certain conditions environments the energy is dissipated as heat because of radiationless transitions between the energy states. There is also the possibility of release of the excitation energy as phosphorescence or fluorescence. The excitation energy can also be converted into chemical energy by dissociation, redox processes, intramolecular rearrangement, or other photochemical reactions^{163, 164, 165}.

¹⁵⁸ T. Zhang, X. Fei, S. Wang, Ch. Zhou, Pigmentation of Vat Blue RS by ball milling in solvents, *Dyes Pigments* 2000, **45**, 15–21.

¹⁵⁹ N. S. Allen, Effects of dyes and pigments, *Comprehensive Polymer Science and Supplements* 1989, **6**, 579–595.

¹⁶⁰ K. A. Wood, S. R. Gaboury, Service life prediction of colour retention for PVDF architectural coatings with organic pigments, *Surf. Coat. Int. Part B: Coat. Transact.* 2006, **88**, 285–298.

¹⁶¹ M. Wijdekop, J. C. Arnold, M. Evans, V. John, A. Lloyd, Monitoring with reflectance spectroscopy the color change of PVC plastisol coated strip steel due to weathering, *Mater. Sci. Tech.* 2005, **21**, 791-797.

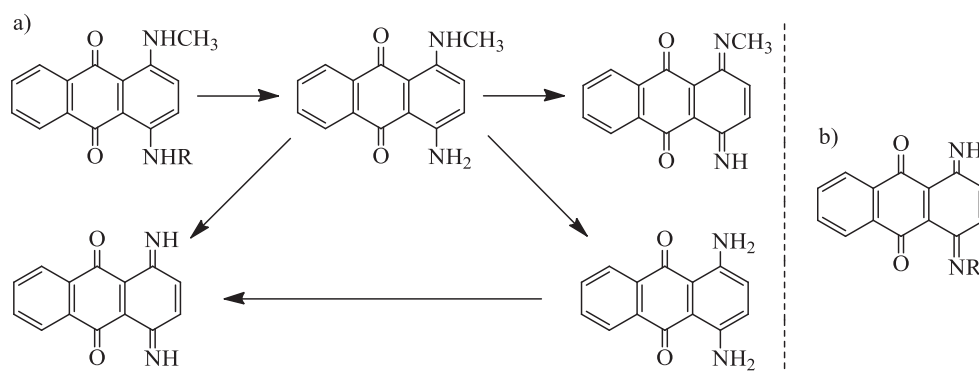
¹⁶² D. Ruch, J. Exposito, C. Becker, F. Aubriet, Surface characterization of photodegraded dyed styrene butadiene and natural rubbers, *Surf. Interface Anal.* 2008, **40**, 668–672.

¹⁶³ N. S. Allen, Polymer photochemistry, *Photochemistry* 2007, **36**, 232–297.

¹⁶⁴ O. Haillant, Photofading of coloured materials, *PPCJ* 2009, **199**, 48–50.

¹⁶⁵ Y. Okada, T. Hihara, Z. Morita, Analysis of photofading of phenylazo-indole and phenylazo-N-ethanolaniline disperse dyes on poly(ethylene terephthalate) fabric using the PM5 method, *Dyes Pigments* 2009, **83**, 237–248.

Many of investigations have been carried out on the mechanism of dye photodegradation based on specific chemical reactions. Anthraquinone dyes are generally characterized by high fastness to light in comparison with those of many other dye classes. The photochemical reactions of anthraquinone acid^{166, 167}, disperse^{168, 169} and vat dyes¹⁷⁰ have been extensively studied both in solution and in polymer substrates. In some cases, a similarity was found between the photochemical reaction of the dye in solution and on the polymer film. From the results of earlier studies, the photochemistry of *N*-alkylaminoanthraquinone compounds can be summarized as involving the following reactions: (a) *N*-dealkylation, (b) nuclear hydroxylation, (c) substitution of amino by hydroxy groups, (d) introduction of an oxygen function at the C-atom adjacent to the *N*-atom in *N*-alkyl amino groups, and (e) formylation of amino groups^{171, 172}.



SCHEME 6. Scheme of the photodecomposition of *N*-alkylaminoanthraquinone dye (a) and l-amino-4-formimidoanthraquinone as one of the final photofading product, R= H, CH₃ (b)¹⁷³.

On the basis of reported data the oxidative aspect of the photodecomposition of *N*-alkylaminoanthraquinone dyes is illustrated in the Scheme 6 a. The *N*-dealkylation occurs by cleavage of the C-N or by dehydrogenation to form imine. Further investigation

¹⁶⁶ N. S. Allen, J. M. Mckellar and B. M. Moghaddam, Lightfastness and spectroscopic properties of aminocarboxyanthraquinones, *J. Photochem.* 1979, **10**, 193–197.

¹⁶⁷ Y. Yang, Q. Y. Guo, Ch. Hu, E. Wang, Efficient degradation of dye pollutants on nanoporous polyoxotungstate–anatase composite under visible-light irradiation, *J. Mol. Catal. A: Chem.* 2005, **225**, 203–212.

¹⁶⁸ N. Katsuda, T. Omura, T. Takagishi, Photodegradation behavior of disperse dyes in solution, *Dyes Pigments* 1998, **36**, 231–241.

¹⁶⁹ B. V. Rao, V. Choudhary, K. Varma, Synthesis and properties of some anthraquinone dyes, *J. Soc. Dyers Colour.* 1990, **106**, 388–394.

¹⁷⁰ S. Shakra, N. F. Ali, Vat and vat/disperse anthraquinone dyes: Part I. Light and sublimation fastness, *Text. Chem. Color. Am. Dyest. Rep.* 1995, **84**, 25–30.

¹⁷¹ N. S Allen, Photofading and light stability of dyed and pigmented polymers, *Polym. Degrad. Stab.* 1994, **44**, 357–374.

¹⁷² R. P. Ponomareva, O. P. Studzinskii, L. M. Borisova, Photodegradation of aminoanthraquinones and dyes derived from them in the presence of complexones, *Russ. J. Gen. Chem.* 2002, **72**, 11043–1106.

reported that one the final products of fading was a 1-amino-4-formimidoanthraquinone (Scheme 6 b) ^{173, 174}.

The fading behavior of some *N*-alkylaminoanthraquinone dyes on polyamide fibers, cellulose acetate and poly(ethylene terephthalate) (PET) ^{175, 176, 177, 178, 179} have been also extensively studied. Thanki and Singh ¹⁸⁰ investigated photo-oxidative stability of polyamide (Nylon 66) in the presence of three different anthraquinone dyes (Acid Blue 25, Acid Blue 40 and Acid Blue 129) with different substituents. The studied dyes have provided higher photostability than the one of the control sample. However, the substitution on the pendant phenyl ring (outside the anthraquinone moiety) does not have any significant effect of photo stabilizing property of the dyes.

Some anthraquinone structures were found to be phototendering dyes. Phototendering occurs when a dye sensitizes or accelerates the break down in molecular structure of a polymer substrate. Egerton ¹⁸¹ in their work reported, various phototendering results obtained with different fibers (viscose, silk, nylon and cotton) dyed with a series of anthraquinone vat dyes (e.g., Vat Yellow 46, Vat Brown 25, Vat Yellow 2). Nevertheless the nature of the polymer was important. Fibers from viscose, cotton and nylon were the most affected by such dyes, while degradation of wool and cellulose esters was much less extended. The phototendering effects of conducted vat dyes, especially red and yellow dyes, were attributed to facile hydrogen abstraction from the substrate by photoexcited carbonyl groups. Some yellow and red anthraquinone dyes were recognized to sensitize the oxidation of underlining substrates through a complex series of reaction initiated by the absorption of the light. Other dyes and pigments with aromatic ketone functionalities may

¹⁷³ C. H. Giles, R. S. Sinclair, S. Roy, Photodecomposition of aminoanthraquinone disperse dyes on poly(ethylene terephthalate), *J. Soc. Dyers Colour.* 1973, **89**, 54–56.

¹⁷⁴ N. Kuramoto (1996), Physico-chemical principles of color chemistry, A. T. Peters, H. S. Freeman (Eds.), Glasgow, Blackie Academic & Professional, p.197–253.

¹⁷⁵ T. Hihara, Y. Okada, Z. Morita, Photo-oxidation and -reduction of vat dyes on water-swollen cellulose and their lightfastness on dry cellulose, *Dyes Pigments* 2002, **53**, 153–177.

¹⁷⁶ Q. Meng, D. Huang, L. Chen, S. Wei, Melting-reactive dyes for mass coloration of synthetic fibres (II)—1,4-dihydroxyanthraquinone diglycidylether in nylon, *Dyes Pigments* 2001, **50**, 127–131.

¹⁷⁷ Y. Okada, A. Sugane, A. Watanabe Z. Morita, Color variations of anthraquinone and azo reactive dyes on cellulose caused by nitrogen oxides under wet conditions, *Dyes Pigments* 2008, **65**, 53–63.

¹⁷⁸ N. Katsuda, S. Yabushita, K. Otake, T. Omura, T. Takagishi, Photodegradation of a disperse dye on polyester fiber and in solution, *Dyes Pigments* 1996, **31**, 291–300.

¹⁷⁹ K. Miyazaki, I. Tabata, T. Hori, Effects of molecular structure on dyeing performance and colour fastness of yellow dyestuffs applied to polypropylene fibres in supercritical carbon dioxide, *Color. Technol.* 2012, **128**, 51–59.

¹⁸⁰ P. N. Thanki, R. P. Singh, Photostabilization of Nylon 66 in presence of acid blue dyes, *Polym. Degrad. Stab.* 2002, **75**, 423–430.

¹⁸¹ G. S. Egerton, The mechanism of the photochemical degradation of textile materials, *J. Soc. Dyers Colour.* 1949, **65**, 764–780.

operate by similar mechanism¹⁸². However, not all anthraquinone dyes are harmful to polymers. In some cases, substituents on the rings influence the photoexcitation path.

Chang and Miller¹⁸³ have demonstrated the effects of various ring substituents on photostability in *N*-ethylacetamide. They concluded that, unsubstituted anthraquinone, 2-methyl-, 2-chloro-, 1-nitro- and 2-sulphono-substituted anthraquinone derivatives, are strong sensitizers and exhibited high reactivity in *N*-ethylacetamide especially in absence of oxygen. The anthraquinone derivatives containing electron donating substituents such as NH₂ were found to be weak sensitizers. The photostability of substituted derivatives was found to increase with the electron donation power of the substituents in the order: methyl < methoxy < hydroxyl < amino. Such anthraquinone structures with electron-donating groups can be found among Disperse and Solvent Dyes classes, for example Disperse Violet 4, Disperse Blue 19 or Solvent Blue 97. In the literature, it was already reported that, the application of disperse dyes to polyester materials improves the photostability of these fibers during weathering conditions^{184, 185, 186}. Saron et al.¹⁸⁷ have been reported the effects of bismuth vanadate and anthraquinone dye on the photodegradation of polycarbonate. Bismuth vanadate accelerated the photodegradation of polycarbonate, what caused a faster drop in the mechanical properties and an increase in the hydroperoxide concentration during the aging process, whereas solvent dye protected the polycarbonate against photodegradation.

Organic pigments can significantly influence, both favorably and unfavorably, the thermal and light stability of the polymer materials. Light absorbing characteristics, photochemical behavior and the nature of pigment fading product determine whether a pigment will provide stability through absorption and/or scattering harmful radiation or whether it will provide sensitize the degradation of the polymer materials, for example by generating singlet oxygen or by hydrogen-abstraction by photoexcited pigment molecules. All organic pigments are structurally complex, generally achieving light absorption by

¹⁸² I. H. Leaver (1980), Photochemistry of dyed and pigmented polymers, N. S. Allen, J. F. McKellar (Eds.), London, Applied Science, p. 180.

¹⁸³ I. Y. Chang, I. K. Miller, Photostability of anthraquinone and azo dyes in *N*-Ethylacetamide (nylon model), *J. Soc. Dyers Colour.* 1986, **102**, 46–53.

¹⁸⁴ G. A. Horsfall, Factors influencing the daylight photodegradation of nylon 66, nylon 6, and polyester in commercial fabrics, *Text. Res. J.* 1982, **52**, 197–205.

¹⁸⁵ V. G. Kulkarni, Color, functional and multi-attribute solutions for polyester fibers, *Chem. Fibers Int.* 2003, **53**, 452–454.

¹⁸⁶ N. Katsuda, S. Yabushita, K. Otake, T. Omura, T. Takagishi, Photodegradation of a disperse dye on polyester fiber and in solution, *Dyes Pigments* 1996, **31**, 291–300.

¹⁸⁷ C. Saron, M. I. Felisberti, F. Zulli, M. Giordano, Effects of bismuth vanadate and anthraquinone dye on the photodegradation of polycarbonate, *J. Braz. Chem. Soc.* 2007, **18**, 900–910.

means of conjugated aromatic system. Some of the aromatic system absorb ultra-violet as well as visible light but it is not clear how significant is the absorption to polymer stability. Numerous studies have provided considerable knowledge on pigment - polymer interrelations^{188, 189, 190, 191}.

The effect of different types aging on the polypropylene materials containing organic and inorganic pigments, have been also extensively studied. Uzelmeier¹⁹² reported that Pigment Red 177, Phthalocyanine Blue and Green, Quinacridone Magenta, Carbon Black, Cadmium Yellow, Mercadmium Red, Ultramarine Blue contributed to the heat (except P. Red 177) and light stability of polypropylene films. However, they noticed negative influence of studied pigments on the heat stability of polypropylene containing additional stabilizers. Chijioke *et al.*¹⁹³ have investigated the oxidative photodegradation of colored linear low density polyethylene (LLDPE). In this study pigment masterbatches had been incorporated into the colored films by means of an effective masterbatching process. The photooxidized films were analyzed with respect to the pigment effects. They have found that, the extent of colored LLDPE deterioration depends to a large scale on the chemical composition of the respective coloring pigment masterbatches used. A study of the cadmium yellow, ultramarine blue, phthalocyanine green and blue pigments in LDPE films showed that all colorants contributed to improved stability of these materials, however, only phthalocyanine green and chrome green, contributed to light stability in the presence of UV absorber¹⁹⁴.

Steinlin and Saar¹⁹⁵ studied the influence of pigments on the light stability of stabilized (Tinuvin 770) polypropylene fibre and found that a significant number of the pigments had a negative effect on light stability. Most of those are yellows, red and orange (e.g., P. Yellow 94, P. Yellow 83, P. Red 224, P. Yellow 109, P. Orange 31, P. Yellow 110).

¹⁸⁸ P. P. Klemchuk, Influence of pigments on the light stability of polymers: A critical review, *Polym. Photochem.* 1982, **3**, 1–27.

¹⁸⁹ J. C. V. P. Moura, A. M. F. Oliveira-Campos, J. Griffiths, The effect of additives on the photostability of dyed polymers, *Dyes Pigments* 1997, **3**, 173–196.

¹⁹⁰ H. Schmidt, K. Twarowska-Schmidt, Effect of pigments on the photooxidative degradation of polypropylene fibers, *Fibres Text. East. Eur.* 1997, **5**, 51–52.

¹⁹¹ I. F. M. Major, G. M. McNally, A. Clarke, H. Ross, Effect of phthalocyanine blue pigment on mechanical and thermal properties of polypropylene copolymers, *Dev. Chem. Eng. Mineral Process.* 2004, **12**, 91–105.

¹⁹² C. Uzelmeier, How heat and light affect pigmented polypropylene, *SPE* 1970, **26**, 69–74.

¹⁹³ I. F. Chijioke O. M. Egbuhuzor, Oxidative photodegradation of colored LLDPE, *ANTEC* 2004, **3**, 3559–3563.

¹⁹⁴ M. Mlinac, J. Rolich, M. Bravar, Photodegradation of colored polyethylene films, *J. Polym. Sci. C. Polym. Symp.* 1976, **57**, 161–169.

¹⁹⁵ F. Steinlin, W. Saar, Influence of pigments on the degradation of polypropylene fibers on exposure to light and weather, *Melliand Textilberichte* 1980, **61**, 941–945.

Greens, blues and black pigments (P. Black 7, P. Blue 60, P. Violet 37, P. Blue 16, P. Red 177, P. Red 220, P. Blue 15:3, P. Green 7) improved the light stability of the fiber, despite the presence of stabilizer Tinuvin 770. Carbon black and phthalocyanines pigments in many polymer are highly effective and induce a marked protective effect. The reason of negative influence of so many yellow and red pigments, as in the case of some red and yellow dyes, may reside in the photochemical behavior of the excited dye or pigment molecules. Gilroy and Chan ¹⁹⁶ noticed favorable effect of some organic pigments (e.g., P. Blue 15, P. Red 220, P. Green 7, P. Green 36, P. Yellow 14) on the thermal stability polyolefin wires and cables.

Most studies on pigment - polymer stability interactions have been carried out with polyolefins but there are a few limited studies which indicate that the pigments can influence the light stability of other polymers as well. Black, brown and red pigments, were recommended to improve color and physical properties of ABS under weather aging. In rigid PVC, most pigments contributed to improved light stability on outdoor exposure. It was found that surfaces degraded much faster than the bulk of the polymer with only minor differences in surface protection by the various organic and inorganic pigments (phthalocyanine blue, iron oxide red, channel black, P. Red 48, P. Yellow 83) ^{197, 198}.

¹⁹⁶ H. M. Gilroy, M. G. Chan, Effect of pigments on the aging characteristics of polyolefins, *Org. Coat. Appl. Polym. Sci. Proc.* 1981, **46**, 293–298.

¹⁹⁷ M. Wijdekop, J. C. Arnold, M. Evans, V. John, A. Lloyd, Monitoring with reflectance spectroscopy the color change of PVC plastisol coated strip steel due to weathering, *Mater. Sci. Tech.* 2005, **21**, 791–797.

¹⁹⁸ G. Iannuzzi, B. Mattsson, M. Rigdahl, Color changes due to thermal ageing and artificial weathering of pigmented and textured ABS, *Polym. Eng. Sci.* 2013, **53**, 1687–1695.

2.3 IONIC LIQUIDS

2.3.1 PROPERTIES AND APPLICATIONS OF IONIC LIQUIDS

2.3.2 APPLICATIONS OF IONIC LIQUIDS IN POLYMER MATERIALS

2.3.1 PROPERTIES AND APPLICATIONS OF IONIC LIQUIDS

Room temperature ionic liquids (ILs) which usually consist of organic cations and various anions have attracted increasing interests due to their potential applications in various areas. Ionic liquids are understood as liquids consisting entirely of ions and having melting points below 100 °C. Their excellent properties, such as very low vapor pressures and wide temperature ranges of liquid phase, have attracted the attention of a large number of researchers in many fields. One of the promising applications of ionic liquids is the potential to be ideal nonvolatile solvents, making them replacements for volatile organic solvents^{199, 200}. Common IL cations include imidazolium, pyrrolidinium, guanidinium, pyridinium, alkylammonium, alkylphosphonium and alkylpyrrolidinium. IL anions can be selected from a broad range of inorganic anions including, Cl⁻, Br⁻, I⁻, PF₆⁻, BF₄⁻, or from organic anions such as NO₃⁻, TFSI⁻ and Tf⁻. The structures of common IL anions and cations are shown in Figure 9^{201, 202, 203}.

Millions of possible cation and anion combinations offer their widely tunable properties with regard to polarity, hydrophobicity melting point, viscosity and solvent miscibility behavior. ILs can be also defined as aprotic or protic (depending on the nature of cation), with their liquid character being determined by the judicious choice of ionic structures²⁰⁴. The properties of ILs result from the cation and anion nature and include those that are, water miscible - hydrophilic and water immiscible - hydrophobic.

¹⁹⁹ K. R. Seddon, Ionic liquids for clean technology, *J. Chem. Technol. Biotechnol.* 1997, **68**, 351–356.

²⁰⁰ T. Welton, Room-temperature ionic liquids. solvents for synthesis and catalysis, *Chem. Rev.* 1999, **99**, 2071–2084.

²⁰¹ G. Laus, G. Bentivoglio, H. Schottenberger, V. Kahlenberg, H. Kopacka, T. Röder, H. Sixta, Ionic liquids: current developments, potential and drawbacks for industrial applications, *Lenzinger Ber.* 2005, **84**, 71–85.

²⁰² M. J. Earle, K. R. Seddon, Ionic liquids. Green solvents for the future, *Pure Appl. Chem.* 2000, **72**, 1391–1398.

²⁰³ Y.-S. Ye, J. Rick, B.-J. Hwang, Ionic liquid polymer electrolytes, *J. Mater. Chem. A* 2013, **1**, 2719–2743.

²⁰⁴ Ch. P. Fredlake, J. M. Crosthwaite, D. G. Hert, S. N. V. K. Aki, J. F. Brennecke, Thermophysical properties of imidazolium-based ionic liquids, *J. Chem. Eng. Data.* 2004, **49**, 954–964.

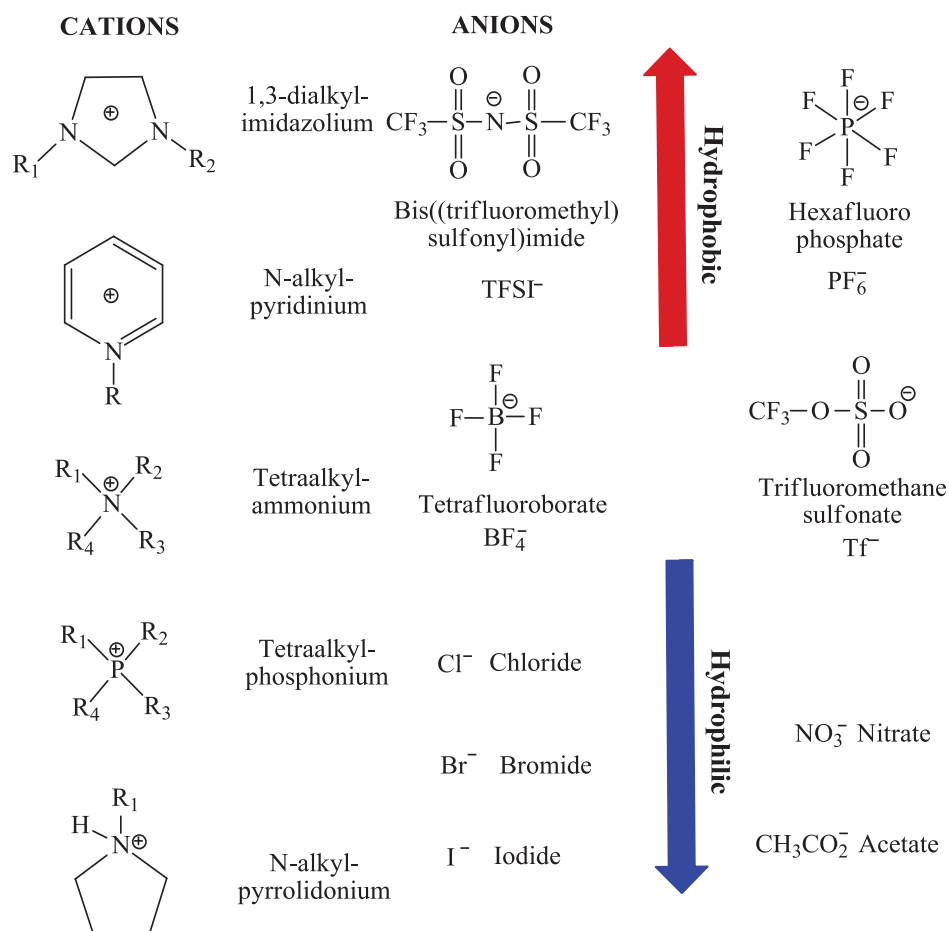


FIGURE 9 Examples of cations and anions used in the formation of ILs, together with changes in hydrophilic–hydrophobic properties associated with anion type²⁰³.

Generally, the anion is used to control the water miscibility, hydrophobicity or hydrogen bonding ability^{205, 206}. The properties of ionic liquids can be also modified by altering the substitutive group on the cation. For example, the melting points of 1-alkyl-3-methylimidazolium tetrafluoroborates and hexafluorophosphates are a function of the length of the 1-alkyl group, which forms a liquid crystalline phase for alkyl chain length over 12 carbon atoms. Another property that varies with structure is the miscibility of water in these ionic liquids. For example, 1-alkyl-3-methylimidazolium tetrafluoroborate salts are miscible with water at 25 °C where the alkyl chain length is less than six, but at or above six carbon atoms, they form a separate phase when mixed with water²⁰⁷.

²⁰⁵ J. G. Huddleston, A. E. Visser, W. M. Reichert, H. D. Willauer, G. A. Broker, R. D. Rogers, Characterization and comparison of hydrophilic and hydrophobic room temperature ionic liquids incorporating the imidazolium cation, *Green Chem.* 2001, **3**, 156–164.

²⁰⁶ J. M. Pringle, J. Golding, C. M. Forsyth, G. B. Deacon, M. Forsyth, D. R. MacFarlane, Physical trends and structural features in organic salts of the thiocyanate anion, *J. Mater. Chem.* 2002, **12**, 3475–3480.

²⁰⁷ S. Sowmiah, V. Srinivasadesikan, M.-Ch. Tseng, Y.-H. Chu, On the chemical stabilities of ionic liquids, *Molecules* 2009, **14**, 3780–3813.

Another chemical property that imparts a variety of physical characteristics to the ionic liquids is the relative acidity or basicity of the component ions. The simplest examples of slightly acidic ionic liquids are those based on the protic ammonium, pyrrolidinium and imidazolium ions^{208, 209}. There are also a number of ionic liquids forming anions that can class as basic e.g., the lactate, formate, acetate and the dicyanamide anion²¹⁰.

Typical ionic liquid anions are those that can be described as neutral in the acid/base sense or very weakly basic. They exhibit only weak electrostatic interactions with the cation and thus impart advantageously low melting points and viscosities. To this class belong such anions as bis(trifluoromethanesulfonyl)amide (TFSI), hexafluorophosphate, tetrafluoroborate, thiocyanate, tricyanomethide, methanesulfonate and *p*-toluenesulfonate. Ionic liquids formed from these anions typically exhibit good electrochemical and thermal stability and thus are often utilized as inert solvents in a wide range of applications^{211, 212, 213}.

The high ion conductivity, high electrochemical and thermal stability, a wide liquid temperature range, large potential windows (ESW) and very low vapor pressure of ionic liquids provide potentially increased safety compared to current organic electrolytes. The ESW limits are roughly determined by the ions composing the ILs, the cation influences the negative potential limit, the anion affects the positive potential limit of the ESW. The ILs mainly studied for electrochemical application are imidazolium and pyrrolidinium salts with asymmetric anions like tetrafluoroborate (BF_4^-), trifluoromethanesulfonate (Tf), bis(trifluoromethanesulfonyl) imide (TFSI), bis(fluorosulfonyl)imide (FSI) or hexafluorophosphate (PF_6^-)¹⁶⁸. The series of ionic liquids based on the thiocyanate (SCN^-) anion has also been investigated. Incorporation of this anion with an imidazolium, tetraalkylammonium or pyrrolidinium cation produces ionic liquids with advantageously low melting points, high ionic conductivity and thermal stability what makes them good additives not only for electrochemical devices.

²⁰⁸ M. A. P. Martins, C. P. Frizzo, D. N. Moreira, N. Zanatta, H. G. Bonaccorso, Ionic liquids in heterocyclic synthesis, *Chem. Rev.* 2008, **108**, 2015–2050.

²⁰⁹ Q. Wu, H. Chen, M. Han, D. Wang, J. Wang, Transesterification of cottonseed oil catalyzed by bronsted acidic ionic liquids, *Ind. Eng. Chem. Res.* 2007, **46**, 7955–7960.

²¹⁰ D. R. MacFarlane, J. M. Pringle, K. M. Johansson, S. A. Forsyth, M. Forsyth, Lewis base ionic liquids, *Chem. Commun.* 2006, **14**, 1905–1917.

²¹¹ A. R. Hajipour, F. Rafiee, Basic ionic liquids, a short review, *J. Iran. Chem. Soc.* 2009, **6**, 647-678.

²¹² D. R. MacFarlane, P. Meakin, J. Sun, N. Amini, M. Forsyth, Pyrrolidinium imides: A New Family of Molten Salts and Conductive Plastic Crystal Phases, *J. Phys. Chem. B.* 1999, **103**, 4164–4170.

²¹³ J. Golding, S. Forsyth, D. R. MacFarlane, M. Forsyth, G. B. Deacon, Methanesulfonate and *p*-toluenesulfonate salts of the *N*-methyl-*N*-alkylpyrrolidinium and quaternary ammonium cations: novel low cost ionic liquids, *Green Chem.* 2002, **4**, 223–229.

2.3.2 APPLICATION OF IONIC LIQUIDS IN POLYMER MATERIALS

The applications of ILs that have attracted most attention are as green chemistry substitutes of volatile organic solvents in organic and organometallic synthesis, including alkylation reactions, Diels-Alder cyclization as well as dimerization, oligomerization and polymerization of olefins^{214, 215}. However, the functions of ionic liquids are not limited to their applications as solvents. Given their unique properties and designable characteristics, ILs have been investigated as potential electrolytes for application in electrochemical devices including lithium ion batteries²¹⁶, solar batteries²¹⁷ or fuel cells²¹⁸. ILs have also found use in polymers as lubricant, components of polymer electrolytes, plasticizers²¹⁹, antistatic and antimicrobial additives^{220, 221}.

The combination of elastic polymers and ILs provided semiconductive elastomer materials with excellent mechanical properties used to produce specialty materials such as solid-state polymer electrolytes or electroactive polymers²²². Marwanta *et al.*²²³ obtained polymer electrolytes with high ionic conductivity and good elasticity prepared by mixing nitrile rubber (NBR) with ionic liquid, *N*-ethylimidazolium bis(trifluoromethanesulfonyl) imide (EMIM TFSI). In their investigations, NBR rubber with ionic liquid content of 50 wt% showed the ionic conductivity of $1.21 \times 10^{-5} \text{ S} \cdot \text{cm}^{-1}$ at 30 °C. Marwanta reported also the Raman study of NBR/EMIM TFSI composites and detected the existence of interaction between the TFSI anion and the –CN group, what may be responsible for better compatibility of this type of ionic liquid with polar matrix.

²¹⁴ S. Carda-Broch, A. Berthod, D. W. Armstrong, Solvent properties of the 1-butyl-3-methylimidazolium hexafluorophosphate ionic liquid, *Anal. Bioanal. Chem.* 2003, **375**, 191–199.

²¹⁵ J. Holbrey, K. R. Seddon, Ionic liquids for catalysis, *Clean Prod. Proc.* 1999, **1**, 223–236.

²¹⁶ M. Park, X. Zhang, M. Chung, G. B. Less, A. M. Sastry, A review of conduction phenomena in Li-ion batteries *J. Power Sources* 2010, **195**, 7904–7929.

²¹⁷ P. Wang, S. M. Zakeeruddin, I. Exnar, M. Gratzel, High efficiency dye-sensitized nanocrystalline solar cells based on ionic liquid polymer gel electrolyte, *Chem. Commun.* 2002, 2972–273.

²¹⁸ J. Sun, D. R. MacFarlane, M. Forsyth, Novel alkaline polymer electrolytes based on tetramethyl ammonium hydroxide, *Electrochim. Acta* 2003, **48**, 1971–1976.

²¹⁹ S. Wang, L. Hou, Application of four ionic liquids as plasticizers for PVC paste resin, *Iran. Polym. J.* 2011, **20**, 989–997.

²²⁰ J. Pernak, A. Czepukowicz, R. Prozniak, New ionic liquids and their antielectrostatic properties, *Ind. Eng. Chem. Res.* 2001, **40**, 2379–2383.

²²¹ K. M. Docherty, C. F. Kulpa, Toxicity and antimicrobial activity of imidazolium and pyridinium ionic liquids, *Green Chem.* 2005, **7**, 185–189.

²²² W.-J. Lee, H.-R. Jung, M. S. Lee, J.-H. Kim, K. S. Yang, Preparation and ionic conductivity of sulfonated-SEBS/SiO₂/plasticizer composite polymer electrolyte for polymer battery, *Solid State Ionics* 2003, **164**, 65–72.

²²³ E. Marwanta, T. Mizumo, N. Nakamura, H. Ohno, Improved ionic conductivity of nitrile rubber/ionic liquid composites, *Polymer* 2005, **46**, 3795–3800.

Cho *et al.*²²⁴ employed NBR and ionic liquid for preparation of electroactive polymers (EAP). Nitrile rubber (NBR) containing ionic liquid, 1-butyl-3-methyl imidazolium bis(trifluoromethylsulfonyl)imide (BMIM TFSI), was utilized as the solid polymer electrolyte exhibiting high ionic conductivity as well as electrical stability. They obtained a maximum conductivity of $2.54 \times 10^{-4} \text{ S} \cdot \text{cm}^{-1}$ at 20 °C in the NBR sample containing 40 mol% ACN groups and activated in BMIM TFSI ionic liquid.

In the field of elastomers ionic liquids are used for the enhancement of the ionic conductivity, mechanical and thermal properties of polymer composites as well as the improvement of ionic conductivity²²⁵. The most common reason for the use of ILs in elastomers is the improvement of filler dispersion e.g., carbon nanotubes, carbon black, halloysite nanotubes or silica (Table 5). ILs have been demonstrated to be interactive towards numerous fillers such as single-walled carbon nanotubes, silica and clays through interaction mechanisms such as π - π stacking, cation- π interactions, hydrogen bonding, van der Waals and electrostatic forces. The combination of elastic polymers and ILs was expected to provide semiconductive elastomer materials with excellent mechanical properties. Likozar²²⁶ described properties of HNBR polymer films containing different ionic liquids. Samples were prepared by pressing the compounds reinforced with functionalized MWCNT-OH between steel plates (180 °C) to obtain cross-linked structure, then HNBR composites were immersed in to the excessive amount of ionic liquids. He found that 1-ethyl-3- methylimidazolium, 1-butyl-3-methylimidazolium, and 1-butyl-1-methylpyrrolidinium tetrafluoroborate (EMImBF₄, BMImBF₄, and BMPyBF₄), hexafluorophosphate (EMImPF₆, BMImPF₆, and BMPyPF₆), and bis(trifluoromethylsulfonyl)imide (EMImTFSI, BMImTFSI, and BMPyTFSI) in hydroxy-functionalized multi-walled carbon nanotubes (MWCNT-OH) reinforced HNBR composites. Sekitani *et al.*²²⁷ dispersed CNTs uniformly in a fluorinated polymer matrix with the aid of an IL (BMIM TFSI), by grinding the CNTs with the IL. In this way, they could increase the CNT content in the composite up to 20 % and fabricate an elastic conductor without impairing the mechanical properties of the matrix.

²²⁴ M. S. Cho, H. Seo, J. Nam, H. Choi, J. Koo, Y. Lee, High ionic conductivity and mechanical strength of solid polymer electrolytes based on NBR/ionic liquid and its application to an electrochemical actuator, *Sens. Actuators, B* 2007, **128**, 70–74.

²²⁵ K. Subramaniam, A. Das, G. Heinrich, Development of conducting polychloroprene rubber using imidazolium based ionic liquid modified multi-walled carbon nanotubes, *Compos. Sci. Technol.* 2011, **71**, 1441–1449.

²²⁶ B. Likozar, The effect of ionic liquid type on the properties of hydrogenated nitrile elastomer/hydroxyl – functionalized multi-walled carbon nanotube/ionic liquid composites, *Soft Matter*, 2011, **7**, 970–977.

²²⁷ T. Sekitani, Y. Noguchi, K. Hata, T. Fukushima, T. Aida, T. Someya, A rubberlike stretchable active matrix using elastic conductors, *Science* 2008, **321**, 1468–1472.

Kreyenschulte *et al.*²²⁸ investigated the interactions of the ionic liquid 1-allyl-3-methylimidazolium chloride (AMIMCl) with different grades of carbon black in styrene-butadiene rubber (S-SBR), butadiene rubber (BR), and ethylene-propylene-diene rubber (EPDM). A surface treatment of carbon black with AMIMCl led to significant changes of the mechanical and electrical properties of different rubber compounds filled with carbon black, which can be attributed to a decreased filler–polymer interaction and a local plasticizing effect of the AMIMCl at the carbon black surface.

The researchers reported plasticizing effect of ionic liquids, in many elastomer composites, containing ILs in order to improve of filler dispersion. They found that with the increase in the proportions of ionic liquids, the glass transition temperature (T_g) of the composites rubber/ILs decreases²²⁵. The plasticizing effect of TFSI⁻ containing ionic liquids on NBR rubber was also described by Marwanta and Cho^{223, 224}.

The plasticizing effect of ionic liquids on polymers was also investigated by Scott *et al.*^{229, 230}. They employed 1-ethyl-3-methylimidazolium tetrafluoroborate (EMIm BF₄) as a plasticizer for poly-(methyl methacrylate) and reported that ionic liquids are better than conventional plasticizers. There are some articles reporting the performances of some ILs as plasticizers in polymer materials including PLLA²³¹ and suspension polymerized PVC^{232, 233}. These works show that ILs offer several potential advantages as plasticizers, for example, high-temperature stability and low volatility with minimum loss in mechanical properties.

²²⁸ H. Kreyenschulte, S. Richter, T. Gotze, D. Fischer, D. Steinhauser, M. Kluppel, Interaction of 1-allyl-3-methylimidazolium chloride and carbon black and its influence on carbon black filled rubbers, *Carbon* 2012, **50**, 3649–3658.

²²⁹ M. P. Scott, C. S. Brazel, M. G. Benton, J. W. Mays, J. D. Holbrey, R. D. Rogers, Application of ionic liquids as plasticizers for poly(methyl methacrylate), *Chem. Commun.* 2002, **7**, 1370–1371.

²³⁰ M. P. Scott, M. Rahman, V. S. Brazil, “Application of Ionic Liquids as Low Volatility Plasticizers for PMMA, *Eur. Polym. J.* 2003, **39**, 1947–1953.

²³¹ M. Rahman, C. S. Brazel, Ionic liquids: new generation stable plasticizers for poly(vinylchloride), *Polym. Degrad. Stab.* 2006, **91**, 3371–3382.

²³² X. H. Lin, S. Wang, Study on ionic liquid [bmim]PF₆ and [hmim]PF₆ as plasticizer for PVC paste resin, *Polym. Bull.* 2011, **67**, 1273–1283.

²³³ S. Wang, L. Hou, Application of four ionic liquids as plasticizers for PVC paste resin, *Iran Polym. J.* 2011, **20**, 989–997.

TABLE 5. Effect of ionic liquids on the properties of polymer composites.

Author	Type of ionic liquid	Polymer and filler	Results
K. Subramani <i>et al.</i> ²³⁴	1-butyl 3-methyl imidazolium bis (trifluoromethylsulphonyl) imide (BMIM TFSI)	polychloroprene rubber, multi-walled carbon nanotubes (MWCNTs)	The presence of IL improved conductivity (10^{-2} S/cm), filler dispersion and thermal stability of the polychloroprene composites.
A. Das <i>et al.</i> ²³⁵	1-allyl-3-methyl imidazolium chloride, 1-ethyl-3-methyl imidazolium thiocyanate, 1-methyl-3-octylimidazolium chloride, trihexyl tetradecyl phosphonium decanoate	solution-styrene-butadiene rubber (S-SBR) polybutadiene rubber (BR), MWCNTs	Multi-walled carbon nanotubes along with an ionic liquid 1-allyl-3-methyl imidazolium chloride provide a strong level of reinforcement to an S-SBR/BR rubber matrix.
Y. D. Lei <i>et al.</i> ²³⁶	thiol ionic liquids, 1-methylimidazolium mercaptopropionate, bis(1-methylimidazolium) mercaptosuccinate	styrene butadiene rubber (SBR), halloysite nanotubes (HNT)	Significant improvement in mechanical properties and HNTs dispersion.
K. Subramani <i>et al.</i> ²³⁷	1-butyl 3-methyl imidazolium bis (trifluoromethylsulphonyl) imide (BMIM TFSI)	solution-styrene-butadiene rubber (S-SBR), multi-walled carbon nanotubes (MWCNTs)	The reinforcing effect of m-CNTs was not profound in the composites due to the plasticizing nature of IL in non-polar SSBR. However the maximum electrical conductivity of the investigated samples was found to be around 0.01 S/cm.
A. Kim <i>et al.</i> ²³⁸	1-butyl-3-methylimidazolium bis(trifluoromethylsulfonyl)imide (BMIM TFSI)	silicone rubber, single-walled carbon nanotube (SWCNTs)	Ionic liquid provided the enhanced dispersibility of the SWCNTs and higher conductivity (63 S/cm) in the polymer matrix.
Y. D. Lei <i>et al.</i> ²³⁹	1-methylimidazolium methacrylate (MimMa)	styrene-butadiene rubber (SBR), precipitated silica	The addition of MimMa effectively improved silica dispersion and mechanical properties of the rubber composites.

²³⁴ K. Subramaniam, A. Das, D. Steinhäuser, M. Klüppel, G. Heinrich, Effect of ionic liquid on dielectric, mechanical and dynamic mechanical properties of multi-walled carbon nanotubes/polychloroprene rubber composites, *Eur. Polym. J.* 2011, **47**, 2234–2243.

²³⁵ A. Das, K. W. Stockelhuber, R. Jurk, J. Fritzsche, M. Klüppel, G. Heinrich, Coupling activity of ionic liquids between diene elastomers and multi-walled carbon nanotubes, *Carbon* 2009, **47**, 3313–3321.

²³⁶ Y. D. Lei, Z. Tang, L. Zhu, B. Guo, D. Jia, Functional thiol ionic liquids as novel interfacial modifiers in SBR/HNTs composites, *Polymer* 2011, **52**, 1337–1344.

²³⁷ K. Subramaniam, A. Das, F. Simon, G. Heinrich, Networking of ionic liquid modified CNTs in SSBR, *Eur. Polym. J.* 2013, **49**, 345–352.

²³⁸ A. Kim, H. S. Kim, S. S. Lee, M. Park, Single-walled carbon nanotube/silicone rubber composites for compliant electrodes *Carbon* 2012, **50**, 444–449.

²³⁹ Y. D. Lei, Z. H. Tang, B. C. Guo, L. X. Zhu, D. Jia, Synthesis of novel functional liquid and its application as a modifier in SBR/silica composites *Express Polym. Lett.* 2010, **4**, 692–703.

As it is known from the literature, imidazolium ILs may affect the crosslinking behavior of rubber composites^{233, 240}. It has already been found that some types of ILs play a role as vulcanization accelerators by catalyzing the interface crosslinking reactions. As a consequence, the vulcanization time of rubber compounds significantly decreases. The efficacy of ILs for vulcanization acceleration is mainly dependent on the anion type. For instance, higher cure rate of NBR vulcanized with sulfur was exhibited by rubber compounds containing alkylimidazolium chlorides and bromides, whereas the longest vulcanization times were observed for rubber compounds with alkylimidazolium hexafluorophosphates²⁴¹.

Ionic liquids have been also reported to be effective anti-electrostatic agents on plastics²⁴², floors²⁴³ and wood²⁴⁴. Most polymers are electric insulators, and therefore are easily charged by static electricity, which may generate discharges and even create the danger of explosions. Antistatic agents are added to materials which possess high resistivity in order to reduce or eliminate buildup of static electricity. Ohno *et al.*²⁴⁵ studied a series of bis(trifluoromethanesulfonyl)imide-type ILs containing such cations as 1-butyl-3-methylimidazolium, 1-(2-hydroxyethyl)-3-methylimidazolium, tris(2-hydroxyethyl)-methylammonium, 1-ethylpyridinium, *N,N*-diethyl-*N*-methyl-*N*-(2-methoxyethyl)-ammonium, 1-butyl-1-methylpyrrolidinium, tributyl-*N*-octylphosphonium, and 1-butyl-2,3-dimethylimidazolium, as well as 1-butyl-3-methylimidazolium and tributyl-*N*-octylphosphonium type ILs with bromide anion as antistatic additives for polyurethanes. The effect of 1-butyl-3-methylimidazolium bis(trifluoromethanesulfonyl)imide addition on the antistatic properties of the PU films was much larger than that of 1-butyl-3-methylimidazolium bromide addition. They concluded that bis(trifluoromethanesulfonyl)-imide-type ILs are excellent antistatic agents for polyurethanes films. Wang *et al.*²⁴⁶ prepared an ionic-liquid antistatic/photostabilization additive and studied its effects on polypropylene. The volume resistance, tensile strength and impact strength of neat PP and

²⁴⁰ M. Przybyszewska, M. Zaborski, Effect of ionic liquids and surfactants on zinc oxide nanoparticle activity in crosslinking of acrylonitrile butadiene elastomer, *J. Appl. Polym. Sci.* 2010, **116**, 155–164.

²⁴¹ J. Pernak, F. Walkiewicz, M. Maciejewska, M. Zaborski, Ionic liquids as vulcanization accelerators, *Ind. Eng. Chem. Res.* 2010, **49**, 5012–5017.

²⁴² C. Gibon, H. Herbst, E. Minder (2011), WO2011069960, Antistatic thermoplastic compositions.

²⁴³ Ch. Krausche Ch., Wai Man Wong, Stefanie Sand, Michael Hiller, Pedro Cavaleiro (2007), US 20090068435 A1, Thick floor coating having antistatic properties.

²⁴⁴ A. Roessler, H. Schottenberger, Antistatic coatings for wood-floorings by imidazolium salt-based ionic liquids, *Prog. Org. Coat.* 2014, **77**, 579–582.

²⁴⁵ T. Iwata, A. Tsurumaki, S. Tajima, H. Ohno, Bis(trifluoromethanesulfonyl)imide-type ionic liquids as excellent antistatic agents for polyurethanes, *Macromol. Mater. Eng.* 2013, DOI: 10.1002/mame.201300333.

²⁴⁶ X. Wang, L. Liu, J. Tan, Preparation of an ionic-liquid antistatic/photostabilization additive and its effects on polypropylene, *J. Vinyl. Addit. Techn.* 2010, **16**, 58–63.

PP/IL blends indicated that the synthesized IL had excellent antistatic properties as well as good light stability. Ding *et al.*²⁴⁷ tested 1-*n*-tetradecyl-3-methylimidazolium bromide ([C₁₄mim]Br) ionic liquid in polypropylene film (PP) and found the best antistatic ability, when the weight ratio of [C₁₄mim]Br to PP reached 3/100.

The literature reported the use of alkyimidazolium-based ionic liquids as potential UV-stabilizing agents for wood^{248, 249} and cellulose materials²⁵⁰. Subramaniam *et al.*^{251, 252} described the thermal degradation of polychloroprene rubber (CR) composites based on unmodified and ionic liquid (1-butyl-3-methylimidazolium bis(trifluoromethylsulfonyl) imide) modified multi-walled carbon nanotubes (MWCNTs). The authors concluded that the composites with modified MWCNTs exhibited higher mechanical properties (tensile modulus, hardness) and thermal stability than the composites with unmodified MWCNTs. In the studied composites IL and CNTs acted as accelerators for crosslinking during aging thereby improving the thermal stability of the composites as crosslinked specimens require more energy to degrade. ILs were also found to have multifunctional roles (as antioxidants, as coupling agents) in the composites.

²⁴⁷ Y. Ding, H. Tang, X. Zhang, S. Wu, R. Xiong, Antistatic ability of 1-*n*-tetradecyl-3-methylimidazolium bromide and its effects on the structure and properties of polypropylene, *Eur. Polym. J.* 2008, **44**, 1247–1251.

²⁴⁸ S. Patachia, C. Croitoru, Ch. Friedrich, Effect of UV exposure on the surface chemistry of wood veneers treated with ionic liquids, *Appl. Surf. Sci.* 2012, **258**, 6723–6729.

²⁴⁹ T.-Q. Yuan, L.-M. Zhang, F. Xu, R.-C. Sun, Enhanced photostability and thermal stability of wood by benzoylation in an ionic liquid system, *Ind. Crop. Prod.* 2013, **45**, 36–43.

²⁵⁰ Effect of alkyimidazolium based ionic liquids on the structure of UV-irradiated cellulose, *Cellulose* 2011, **18**, 1469–1479.

²⁵¹ K. Subramaniam, A. Das, L. Häußler, Ch. Harnisch, K. W. Stöckelhuber, G. Heinrich, Enhanced thermal stability of polychloroprene rubber composites with ionic liquid modified MWCNTs, *Polym. Degrad. Stab.* 2012, **97**, 776–785.

²⁵² K. Subramaniam, A. Das, G. Heinrich, Improved oxidation resistance of conducting polychloroprene composites, *Compos. Sci. Technol.* 2013, **74**, 14–19.

2.4 SUMMARY OF THE LITERATURE

Over the past decades the production of polymer materials increased rapidly. Polymers, due to their versatility, have become the essential ingredients to provide a better quality of life. Many polymers are used for outdoor applications, which usually cause more intensive aging process of these materials. Numerous literature sources prove that considerable work has been done on the degradation and stabilization of polymers. The researchers and the technologists have developed techniques to stabilize polymers e.g., by adding different types of stabilizers. However the degradation process of polymers during their service life depends not only on the polymer structure and environmental impacts but also on the type of processing aids and additives such as plasticizers, fillers, dyes or pigments. These additives can either accelerate or retard the aging process of polymer products. Due to their complex effects on the degradation process, almost each polymer system should be individually examined.

Literature data showed that, pigments generally have positive effect on the light and weathering stability of polymers. Favorable pigment influences on polymer light stability is most likely due to screening or selective absorption of harmful radiation, and deactivation of polymer photoexcited species. Phthalocyanine blue and green pigments were identified as the most useful in this regard, because they exhibit strong absorption in UV range.

Photodecomposition and light stability behavior of *N*-alkylaminoanthraquinone dyes on cellulose acetate, polyamides and poly(ethylene terephthalate) (PET) have been also investigated. It was found that, the application of disperse dyes with anthraquinone chromophore with electron donating substituents, to polyester fibers improved their photostability during outdoor exposure. These substituents play role of color helpers (auxochromes) and influence dye solubility. Although solvent dyes are commercially available, there are no complete studies describing their impact on the polymer composites stability in various weather conditions and under UV radiation.

Recently, much work has been carried out on the ionic liquids as additives for polymer materials. The use of ionic liquids (ILs) as performance additives in rubber compound formulations is increasing due to their chemical stability, thermal stability, low vapor pressure and high ionic conductivity as well as their designable characteristics. Antielectrostatic properties, lubricant properties and activity in crosslinking reactions of ILs have also been reported. The most common reason for the use of ILs in elastomers was

CHAPTER 2.4 SUMMARY OF THE LITERATURE

the improvement of filler dispersion (e.g., carbon nanotubes, carbon black, halloysite nanotubes, silica) in hydrophobic matrices as well as the enhancement of the ionic conductivity, thermal and mechanical properties of polymer composites.

The most popular are highly conductive ionic liquids with bis(trifluoromethylsulfonyl) imide (TFSI) anion, which exhibit high thermal and chemical stability as well as wide electrochemical window. Although quite a lot of works has been published work on the degradation of elastomers there are still no studies on the impact of this type of ionic liquids on the mechanical and conductive properties of acrylonitrile-butadiene rubber composites exposed to outdoor weather conditions.

2.5 THE AIM OF WORK

This study examined the effects of several polymer additives on the aging properties of elastomer composites. Solvent-type dyes, high-performance pigments and conductive ionic liquids (ILs) were employed as polymer additives to obtain elastomer composites that were characterized by enhanced weather aging resistance and good mechanical strength.

Commercially available solvent dyes, mainly including anthraquinone derivatives that exhibited high light and temperature resistance, were selected for study. The organic pigments studied, including phthalocyanines, thiazines and pyrroles, were also characterized by similar resistance criteria.

The properties of the weathering composites that contained the solvent dyes and pigments were compared with the properties of samples that contained commercial stabilizers, such as benzophenones, benzotriazoles, triazines and hindered amines, that are commonly used in polymer technology. The application of coloring agents as insoluble pigments and soluble dyes allowed the determination of the impact of dispersion or a molecular solution on the aging processes in two polymers with different polarities: ethylene-norbornene cyclic olefin (non-polar) and acrylonitrile butadiene rubber (polar).

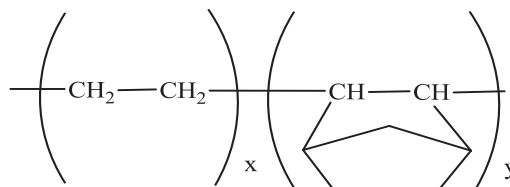
The next part of this study investigated the effects of ILs on the properties of nitrile rubber/IL composites that were exposed to outdoor weathering conditions. The ILs were used to obtain improved conductivity and good mechanical properties in the elastomer composites. Hydrophilic 1-ethyl-3-methylimidazolium thiocyanate and hydrophobic 1-ethyl-3-methylimidazolium, 1-butyl-3-methylimidazolium, 1-hexyl-3-methylimidazolium and 1-allyl-3-methylimidazolium bis(trifluoromethylsulfonyl)imide were chosen as ILs based on their high ionic conductivity, wide electrochemical window and high thermal stability. This study also investigated the influence of hydrophilic and hydrophobic imidazolium ILs on the curing kinetic, mechanical, morphological and ionic conductivity properties as well as the resistance to outdoor weathering conditions of nitrile rubber composites.

CHAPTER 3
MATERIALS AND METHODS

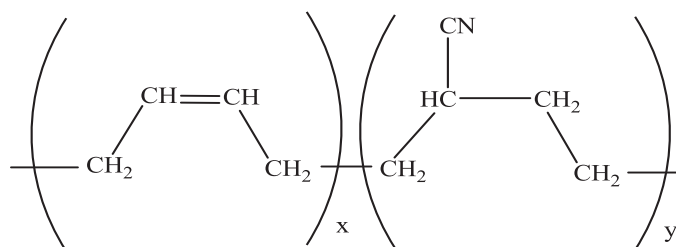
3.1 MATERIALS

3.1.1 POLYMERS

1. Ethylene norbornene random copolymers (EN) - Topas Elastomer 140 (norbornene content 40 wt%), TOPAS Advanced Polymers, Germany.



2. Acrylonitrile butadiene rubber (NBR) – Perbunan 28-45 (28 wt% acrylonitrile content) Lanxess, Germany.



3.1.2 ADDITIVES

TABLE 3.1 Chemical composition of the dyes studied.

NR	COLOR INDEX, NAME	CHEMICAL STRUCTURE	SUPPLIER
1.	Solvent Blue 97 1,4-bis[2,6-diethyl-4-methylphenylamino]anthracene-9,10-dione		Keystone, USA
2.	Solvent Blue 104 1,4-bis[2,4,6-trimethylphenylamino]anthracene-9,10-dione		Keystone, USA

TABLE 3.1 Chemical composition of the dyes studied (cont.).

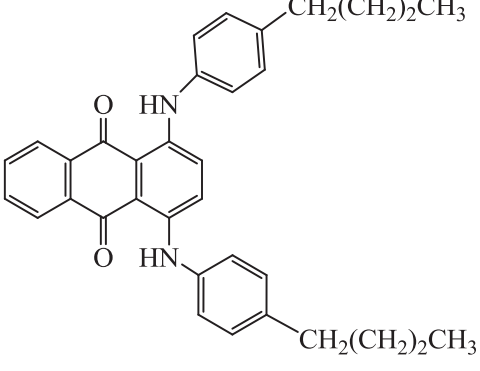
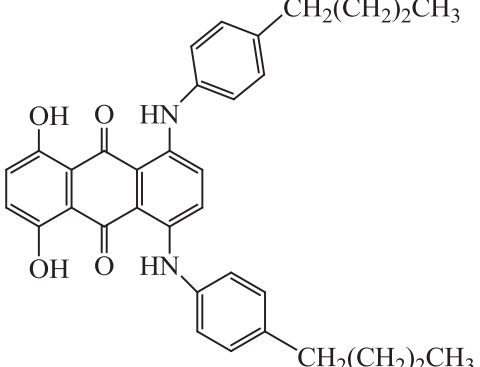
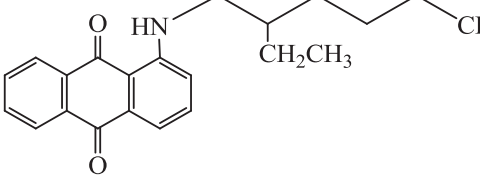
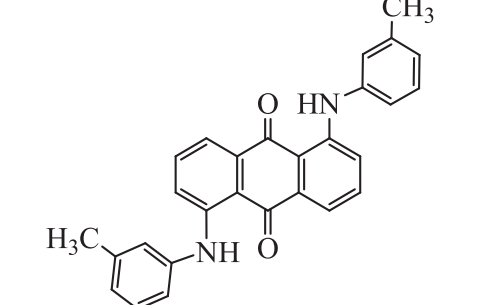
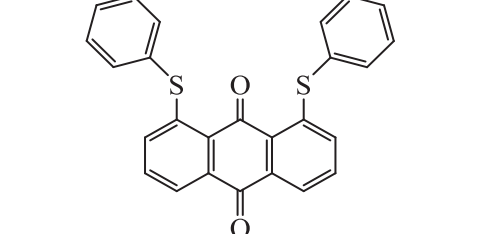
3.	<p>Solvent Blue</p> <p>1,4-bis[(4-n-butylphenyl)amino]anthracene-9,10-dione</p>		Synthesized in IPDT/
4.	<p>Solvent Green 28</p> <p>1,4-bis[(4-n-butylphenyl)amino-5,8-dihydroxy]anthracene-9,10-dione</p>		Keystone, USA
5.	<p>Solvent Red</p> <p>1-[N-(2-ethylhexyl)amino]anthracene-9,10-dione</p>		Synthesized in IPDT
6.	<p>Solvent Red 207</p> <p>1,5-bis[(3-methylphenyl)amino]anthracene-9,10-dione</p>		Keystone, USA
7.	<p>Solvent Yellow 163</p> <p>1,8- bis(phenylthio)anthracene-9,10-dione</p>		Keystone, USA

TABLE 3.1 Chemical composition of the dyes studied (cont.).

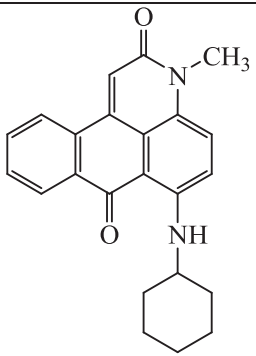
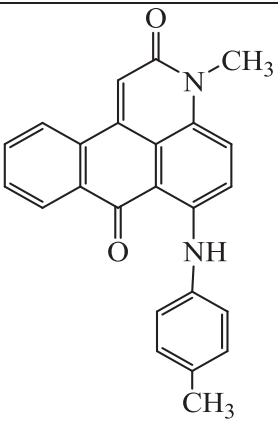
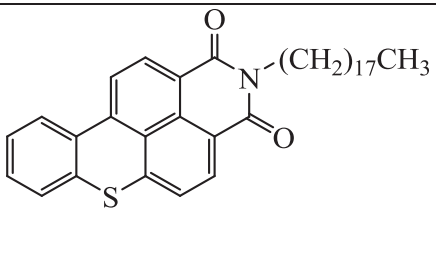
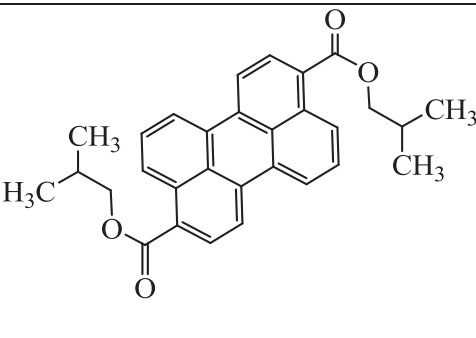
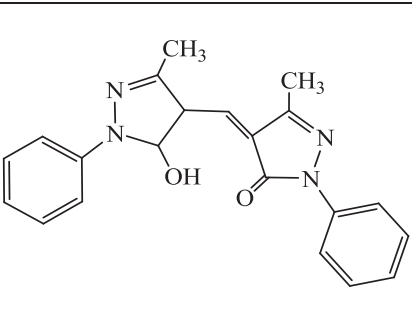
8.	Solvent Red 149 6-(cyclohexylamino)-3-N-methylantrapyridone		Keystone, USA
9.	Solvent Red 52 3H-naphtho[1,2,3-de]quinoline-2,7-dione, 3-methyl-6-[(4-methylphenyl) amino]		Keystone, USA
10.	Solvent Yellow 98 2-octadecyl-1H-thioxantheno[2,1,9-def]isoquinoline-1,3(2H)-dione		Keystone, USA
11.	Solvent Green 5 3,9-perylenedicarboxylic acid, bis(2-methylpropyl)ester		Keystone, USA
12.	Solvent Yellow 93 3H-pyrazol-3-one, 4-[(1,5-dihydro-3-methyl-5-oxo-1-phenyl-4H-pyrazol-4-ylidene)methyl]-2,4-dihydro-5-methyl-2-phenyl		Keystone, USA

TABLE 3.2 Chemical composition of the pigments studied.

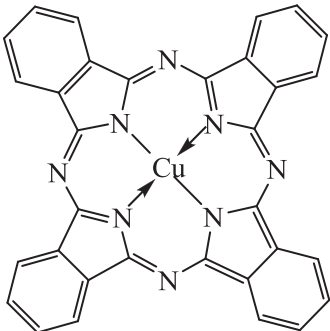
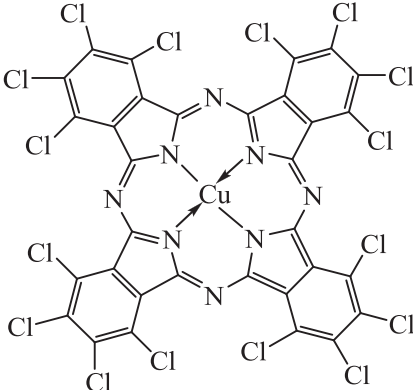
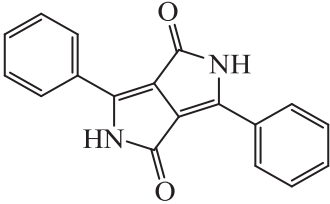
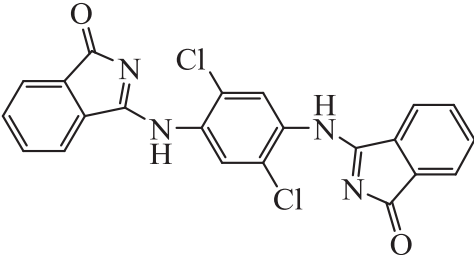
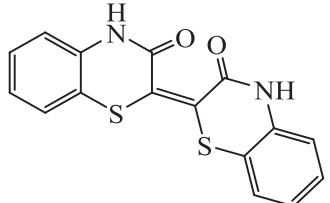
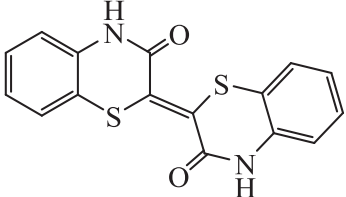
	COLOR INDEX, NAME	CHEMICAL STRUCTURE	SUPPLIER
1.	Pigment Blue 15:1 Copper, [C-chloro-29H, 31H-phthalocyaninato(2-)-N29,N30,N31,N32]-0.5-1 – number of chlorine atom		Synthesia, Czech Republic
2.	Pigment Green 7 Copper, [1,2,3,4,8,9,10,11,15,16,17,18,22,23,24,25-hexadecachloro-29H,31H-14-15 – number of chlorine atom		Synthesia, Czech Republic
3.	Pigment Red 254 3,6-bis(4-chlorophenyl)pyrrolo[3,4-c]pyrrole-1,4(2H,5H)-dione		Synthesia, Czech Republic
4.	Pigment Yellow 173 3-[2,5-dichloro-4-[(3-oxoisoindol-1-yl)amino]anilino]isoindol-1-one		Clariant, Germany
5.	cis-Indigothiazine <i>cis</i> -([2,2']-bi(1,4-benzothiazynylidene)-3,3'-(4H, 4'H)-dione		Synthesized in IPDT
6.	trans-Indigothiazine <i>trans</i> -([2,2']-bi(1,4-benzothiazynylidene)-3,3'-(4H, 4'H)-dione		Synthesized in IPDT

TABLE 3.3 Chemical composition of the commercial stabilizers studied.

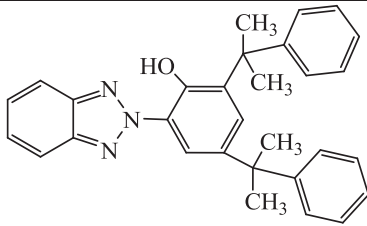
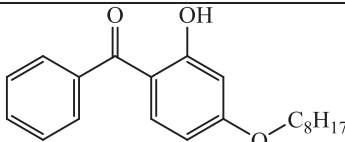
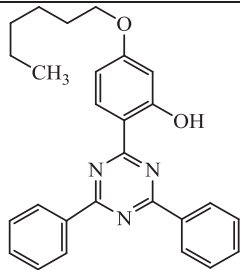
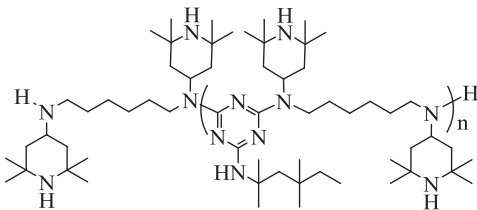
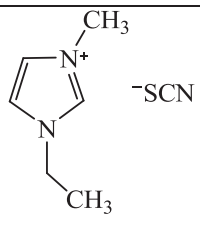
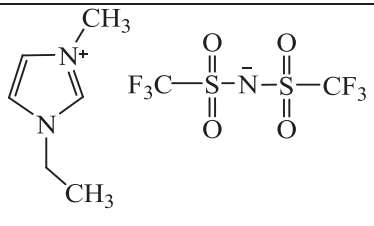
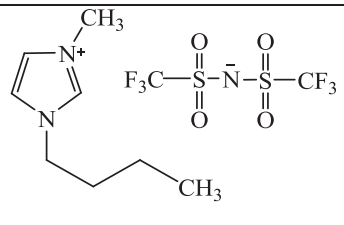
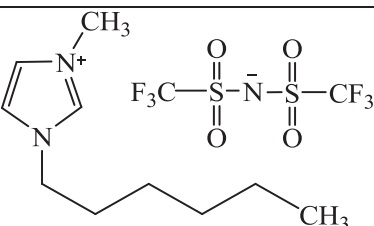
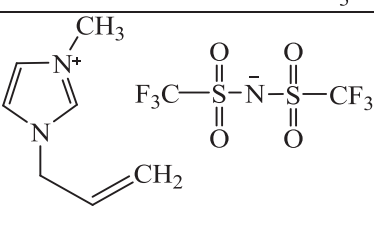
	NAME	CHEMICAL STRUCTURE	SUPPLIER
1.	Tinuvin 234 phenol, 2-(2H-benzotriazol-2-yl)-4,6-bis(1-methyl-1-phenylethyl)		Ciba, Switzerland
2.	Chimassorb 81 methanone, [2-hydroxy-4-(octyloxy)phenyl]phenyl		Ciba, Switzerland
3.	Tinuvin 1577 2-(4,6-diphenyl-1,3,5-triazin-2-yl)-5-[(hexyl)oxy]-phenol		Ciba, Switzerland
4.	Chimassorb 944 (HALS) poly[[6-[(1,1,3,3-tetramethylbutyl)amino]-1,3,5-triazine-2,4-diyl][(2,2,6,6-tetramethyl-4-piperidiny)imino]-1,6-hexanediyl][(2,2,6,6-tetramethyl-4-piperidiny)imino]]		Ciba, Switzerland

TABLE 3.4 Chemical composition of the ionic liquids studied.

NR	NAME/ ABBREVIATION	CHEMICAL STRUCTURE	SUPPLIER/ CONDUCTIVITY (mS/cm)
1.	EMIM SCN 1-ethyl-3-methylimidazolium thiocyanate hydrophilic		Fluka, Germany 27 mS/cm
2.	EMIM TFSI 1-ethyl-3-methylimidazolium bis(trifluoromethyl- sulfonyl)imide hydrophobic		IoLiTec, Germany 8.6 mS/cm
3.	BMIM TFSI 1-butyl-3-methylimidazolium bis(trifluoromethyl- sulfonyl)imide hydrophobic		IoLiTec, Germany 3.5 mS/cm
4.	HMIM TFSI 1-hexyl-3-methylimidazolium bis(trifluoromethyl sulfonyl)imide hydrophobic		IoLiTec, Germany 1.9 mS/cm
5.	AMIM TFSI 1-allyl-3-methylimidazolium bis(trifluoromethyl sulfonyl)imide hydrophobic		IoLiTec, Germany 2.8 mS/cm

3.1.3 OTHER MATERIALS AND SOLVENTS

- Sulfur - curing substance, Siarkpol, Poland,
- Mercaptobenzothiazole (MBT) - accelerator in the sulfur vulcanization, Lanxess, Germany,
- Zinc oxide (ZnO) - activator in the sulfur vulcanization, Lanxess, Germany,
- Stearic acid - activator in the sulfur vulcanization, Sigma Aldrich, Germany,

- Silica Aerosil 380 - reinforcing filler, hydrophilic fumed silica, Evonik Degussa, Germany,
- 1-Methyl-2-pyrrolidinone 99.8%, Sigma Aldrich, Germany,
- Chloroform - 99.8%, Sigma Aldrich, Germany,
- Acetone - 99.5%, Sigma Aldrich, Germany,
- Toluene - 99.5%, Sigma Aldrich, Germany,
- 2,2'-Azino-bis(3-ethylbenzothiazoline-6-sulfonic acid) (ABTS), Sigma Aldrich, Germany,
- Tetrabutylammonium perchlorate ($C_4H_9)_4NClO_4$) - supporting electrolyte, Fluka, Germany
- 6-hydroxy-2,5,7,8-tetramethylchroman-2-carboxylic acid (Trolox), Sigma Aldrich, Germany,
- potassium persulfate, Sigma Aldrich, Germany.

3.2 METHODS

3.2.1 SAMPLE PREPARATION

❖ Ethylene-norbornene (EN) composites with dyes and pigments

The ethylene-norbornene EN mixtures were prepared by homogenization of the EN copolymer and dyes, pigments or stabilizers in an internal mixer (Brabender Measuring Mixer N50). The formulations of the EN compounds are given in Table 3.5.

The polymer mixtures were processed at a rotor speed of 50 rpm and an initial temperature of 80 °C. Samples with a thickness of 1 mm were obtained by pressing the compounds between steel plates at 100 °C for 10 min.

TABLE 3.5 Composition of the ethylene-norbornene-based compounds.

	phr	phr	phr	phr
EN	100	100	100	100
Dyes	-	0.2	-	-
Pigments	-	-	0.2	-
Stabilizers	-	-	-	0.2

❖ **Acrylonitrile butadiene rubber (NBR) composites with dyes and pigments**

The materials used to prepare the NBR composites are tabulated in Table 3.6. The composites that contained solvent dyes, pigment or stabilizers were prepared using a laboratory two-roll mill (roller dimensions: D = 200 mm, L = 450 mm). Vulcanization of the nitrile rubber compounds was performed in a compression-type laboratory press at a temperature of 160 °C with an optimum curing time $t_{90} = 30$ min, which was determined in a moving die rheometer (see paragraph 3.2.10).

TABLE 3.6 Composition of the NBR-based rubber compounds.

	phr	phr	phr
NBR	100	100	100
Sulfur	2	2	2
Mercaptobenzothiazole	2	2	2
Zinc oxide	5	5	5
Stearic acid	1	1	1
Silica	30	30	30
Dyes	1	-	-
Pigments	-	1	-
Stabilizers	-	-	1

❖ **Acrylonitrile butadiene rubber (NBR) composites with ionic liquids (ILs)**

The preparation of the rubber mixtures was performed by following a two-step procedure. Homogenization of the rubber and silica SiO₂ filler mixed with the ionic liquid was performed in an internal mixer (Brabender Measuring Mixer N50). The rubber compounds were processed at a rotor speed of 50 rpm and an initial temperature of 50 °C. Subsequently, the compounded rubbers were then milled with sulfur, mercaptobenzothiazole, zinc oxide and stearic acid in a laboratory rolling mill (roll dimensions: D = 200 mm, L = 450 mm). The formulations of the acrylonitrile-butadiene rubber compounds are summarized in Table 3.7.

TABLE 3.7 Composition of the NBR-based rubber compounds.

	phr	phr
NBR	100	100
Sulfur	2	2
Mercaptobenzothiazole	2	2
Zinc oxide	5	5
Stearic acid	1	1
Silica	30	30
Ionic liquids	-	2.5; 5; 10; 15

The optimum curing time (t_{90}) was determined in a moving dye rheometer (see paragraph 3.2.10). Vulcanization of the nitrile rubber compounds was carried out in compression type laboratory-press under pressure of 3 MPa and temperature of 160 °C in line with the curing time specifications (See paragraph 6.1).

3.2.2 ELECTROCHEMICAL METHODS

To assess the electrochemical oxidation mechanism and the kinetics for the compound under investigation, cyclic voltammetry (CV) and differential pulse voltammetry (DPV) were used with an Autolab analytical unit (EcoChemie, Holland). A three-electrode system was used for the measurements. Platinum was used as the anode and auxiliary electrode. The electrode potential was measured against a ferricinium/ferrocene reference electrode (Fc^+/Fc), whose standard potential is defined as zero, independent of the solvent used. Prior to taking the measurements, all solutions were degassed with argon. During the measurements, an argon atmosphere was maintained over the solution. The effect of the scan rate on the electrooxidation and electroreduction of solvent dyes in an anhydrous medium was assessed. All of the experiments were performed at room temperature and measurement error was in range ± 0.01 - 0.02 ²⁵³.

Cyclic voltammetry (CV)

This technique is based on varying the applied potential at a working electrode in both forward and reverse directions (at some scan rate) while monitoring the current. For example, the initial scan could be in the negative direction to the switching potential. At that point the scan would be reversed and run in the positive direction. Depending on the analysis, one full cycle, a partial cycle, or a series of cycles can be performed ^{254, 255}.

Differential Pulse Voltammetry (DPV)

This technique is scanned with a series of pulses and each potential pulse is fixed, of small amplitude (10 to 100 mV), and is superimposed on a slowly changing base potential. Current is measured at two points for each pulse, the first point just before the application of the pulse and the second at the end of the pulse.

²⁵³ A. Masek, M. Zaborski, E. Chrzescijańska, Electrooxidation of flavonoids at platinum electrode studied by cyclic voltammetry, *Food Chem.* 2011, **127**, 699–704.

²⁵⁴ B. R. Horrocks (2003), Encyclopedia of Electrochemistry, A. J. Bard, M. Stratmann, P. R. Unwin (Eds.), Weinheim, Wiley-VCH Verlag GmbH&Co, KGaA, Vol. 3.

²⁵⁵ Z. Galus (1994), Fundamentals of electrochemical analysis, E. Horwood (Ed.), New York, John Wiley & Sons.

The difference between current measurements at these points for each pulse is determined and plotted against the base potential ²⁵⁶.

Electrochemical studies were performed in the Institute of General and Ecological Chemistry, Faculty of Chemistry at Technical University of Lodz.

3.2.3 HOMO-LUMO CALCULATIONS

The energies of the highest occupied molecular orbital (E_{HOMO}) and the lowest unoccupied molecular orbital (E_{LUMO}) were calculated using the AM1 method with the HyperChem software.

3.2.4 ABSORPTION SPECTROSCOPY

The UV–Visible absorption measurement were studied with a Jasco V-670 spectrophotometer (Japan), using standard quartz cuvettes. The absorption spectra were recorded over a wavelength range of 200–800 nm. The dyes concentrations were chosen to be 1×10^{-5} M for all the samples.

The molar extinction coefficients of the studied compounds were calculated according to the Beer-Lambert law (3.1).

$$\epsilon = \frac{A}{d c} \quad (3.1)$$

A – absorbance

ϵ - molar extinction coefficient [$\text{dm}^3 \cdot \text{cm}^{-1} \cdot \text{mol}^{-1}$]

d – pathlength [cm]

c – molar concentration [$\text{mol} \cdot \text{dm}^{-3}$]

3.2.5 ANTIOXIDANT ACTIVITY - ABTS METHOD

The activities of the solvent dyes were estimated spectrophotometrically using the 2,2'-azinobis-(3-ethylbenzothiazoline-6-sulfonic acid) (ABTS) method as described by Yu and Ong ²⁵⁷ with slight modifications.

ABTS and potassium persulfate were dissolved in distilled chloroform to final concentrations of 7 mM and 2.45 mM, respectively. These two solutions were mixed, and the

²⁵⁶ S. P. Kounaves (1997), Handbook of Instrumental Techniques for Analytical Chemistry, F. Settle (Ed.), New Jersey, Prentice Hall PTR, Ch. 37.

²⁵⁷ T.-W. Yu, C.-N. Ong, Lag-time measurement of antioxidant capacity using myoglobin and 2,2'-azinobis(3-ethylbenzothiazoline-6-sulfonic acid): rationale, application, and limitation, *Anal. Biochem.* 1999, **275**, 217–223.

mixture was allowed to stand in the dark at room temperature for 16 h before use in the production of the radical monocation of ABTS (ABTS^{•+}). The pre-formed ABTS^{•+} exhibits absorbance at 734 nm (blue color) and is reduced in the presence of hydrogen-donating compounds. During this reaction, the blue ABTS^{•+} radical cations are converted back to their colorless neutral form. Solvent dyes or Trolox (vitamin E analogue) standards were added to the diluted ABTS^{•+} solution, and the absorbance reading was taken 2 min after mixing using a Macherey-Nagel Nanocolor UV/Vis spectrophotometer (Germany). All of the determinations were performed at least three times. The results were expressed relative to standard amounts of the synthetic antioxidant Trolox to yield the Trolox equivalent antioxidant capacity (TEAC).

3.2.6 THE SOLUBILITY PARAMETERS

The solubility parameters of the solvent dyes and stabilizers were predicted according to Krevelen's method from the group contributions (dispersion forces δ_d , polar forces δ_p , hydrogen-bonding forces δ_h) using the following equations:²⁵⁸:

$$\delta_d = \frac{\sum F_{di}}{V} \quad (3.2)$$

$$\delta_p = \frac{\sqrt{\sum F_{pi}^2}}{V} \quad (3.3)$$

$$\delta_h = \sqrt{\frac{\sum E_{hi}}{V}} \quad (3.4)$$

The differences in the solubility parameters ($\Delta\delta$) between the polymer and additives (solvent dyes, stabilizers) were calculated using equation 3.5.

$$\Delta\delta = \left[(\delta_{d,P} - \delta_{d,D})^2 + (\delta_{p,P} - \delta_{p,D})^2 + (\delta_{h,P} - \delta_{h,D})^2 \right]^{\frac{1}{2}} \quad (3.5)$$

For good solubility, $\Delta\delta$ must generally be small ($\Delta\delta \leq 5 \text{ (MJ/m}^3\text{)}^{\frac{1}{2}}$).

3.2.7 SCANNING ELECTRON MICROSCOPY (SEM)

The morphology of the powders particles (dyes, pigments), the surface of composites aging process as well as the silica dispersion in the elastomer matrix silica was estimated using scanning electron microscopy with a ZEISS SEM microscope. The nitrile rubber vulcanisates were broken down in liquid nitrogen, and the fracture surfaces of the

²⁵⁸ D. W. Krevelen, K. Nijenhuis (2009), Properties of polymers, Amsterdam, Elsevier, p. 211–227.

composites were examined. Prior to the measurements, the samples were coated with carbon.

3.2.8 THERMOGRAVIMETRIC ANALYSIS (TGA)

The thermal stability of the powders was studied using a TGA/DSC1 (Mettler Toledo, Italy) analyzer. The samples were heated from 25 °C to 500 °C in an argon atmosphere (60 ml/min) with a heating rate of 10 °C/min.

3.2.9 DIFFUSION COEFFICIENT

The diffusion coefficients (D) of the solvent dyes and stabilizers were estimated using the method of Hayduk and Laudie (3.6)²⁵⁹.

$$D_w = \frac{13,26 \cdot 10^{-5}}{0,001 \cdot 10 \eta_w^{1,4} \cdot V_a^{0,589}} \quad (3.6)$$

Where: η - viscosity of the solvent [Pa·s], V_a - molar volume [$\text{cm}^3 \cdot \text{g}^{-1} \cdot \text{mole}^{-1}$]. The coefficient D represents the weight of the organic substance that diffuses through an area of 1 cm^2 in 1 s.

3.2.10 CURING CHARACTERISTICS

The curing characteristics of the rubber composites were determined using a MonTech Moving Die Rheometer MDR 3000 (Germany) at 160 °C for 120 minutes. A sinusoidal strain of 7 % was applied at a frequency of 1.67 Hz. The optimum cure time (t_{90}), scorch time (t_2), minimum torque (M_L), maximum torque (M_H), and delta torque (ΔM) were determined from the curing curves. The mixed stocks were cured in a standard hot press at 160 °C for t_{90} . The difference between M_H and M_L of the vulcanization curve was defined as the ultimate rheometric torque ΔM . The time required to reach 90 % of ΔM was termed t_{90} – optimal curing time; t_2 – (scorch time) the time at which the torque rises above M_L by 2.0 dNm.

5.11. X-RAY PHOTOELECTRON SPECTROSCOPY ANALYSIS (XPS)

The surface elemental compositions of the ethylene-norbornene composites were determined by X-ray photoelectron spectroscopy (XPS) analysis. The XPS spectra were

²⁵⁹ J. A. Schramke, S. F. Murphy, W. J. Doucette, W. D. Hintze, Prediction of aqueous diffusion coefficients for organic compounds at 25 °C, *Chemosphere* 1999, **38**, 2381–2406.

recorded on a Prevac X-ray photoelectron spectrometer (Rogow, Poland) equipped with a SES 2002 VG Scienta hemispheric electron energy analyzer (Sweden) and an aluminum (mono) K_{α} source (1486.6 eV). The aluminum K_{α} source was operated at 15 kV and 25 mA. The spectrometer was calibrated using Ag 3D BE=368.27 eV core-level photoemission spectra. A high-resolution survey (pass energy 50 eV) of the samples was performed in the appropriate spectral regions. All of the core-level spectra were referenced to the C 1s neutral carbon peak at 284.6 eV.

3.2.12 FOURIER-TRANSMISSION INFRARED SPECTRAL ANALYSIS (FTIR)

Attenuated total reflection Fourier transform infrared (ATR-FTIR) spectra were recorded on a Thermo Scientific Nicolet 6700 FT-IR spectrometer (USA), equipped with a diamond crystal, at room temperature with a resolution of 4 cm^{-1} and a 32-scan signal from $600\text{-}4000\text{ cm}^{-1}$ in absorbance mode. The each result were taken from 3 different places of sample and averaged.

3.2.13 DYNAMIC MECHANICAL ANALYSIS (DMA)

Dynamic mechanical analysis (DMA) was performed on a TA Instruments Q 800 Dynamic Mechanical Analyzer (USA) operating in tension mode at a frequency of 10 Hz. Testing was conducted over the temperature range of -80 to $100\text{ }^{\circ}\text{C}$ with a heating rate of $2\text{ }^{\circ}\text{C}/\text{min}$.

3.2.14 DIFFERENTIAL SCANNING CALORIMETRY (DSC)

DSC measurements (Q 200 DSC, TA Instrument, USA) of samples were performed at a heating rate of $10\text{ }^{\circ}\text{C min}^{-1}$ in the temperature range -80 to $180\text{ }^{\circ}\text{C}$ under a nitrogen atmosphere. The glass transition temperatures (T_g) were determined at the midpoint of the step.

3.2.15 CROSSLINK DENSITY MEASUREMENTS

The crosslink density of the rubber composites was determined by equilibrium swelling in toluene, using the Flory-Rehner equation 3.7, and the Huggins parameter for elastomer-solvent interaction given by equation 3.8:

$$\nu_T = -\frac{\ln(1-V_p) + V_p + \chi \cdot V_p^2}{V_s \left(V_p^{\frac{1}{3}} - \frac{V_p}{2} \right)} \quad (3.7)$$

$$\chi = 0.381 + 0.671 \cdot V_p \quad (3.8)$$

where v_T is crosslink density, V_p is the volume fraction of elastomer in the swollen gel, and V_S is the molar volume of solvent ($\text{mol}\cdot\text{cm}^{-3}$)²⁶⁰.

3.2.16 BROADBAND DIELECTRIC SPECTROSCOPY (BDS)

Dielectric measurements were conducted with broadband dielectric spectroscopy (Novocontrol alpha analyser, Germany) in the frequency range from 10^{-1} to 10^7 Hz at room temperature. The samples were placed between two copper electrodes with diameters of 20 mm.

3.2.17 TENSILE TESTING

Tensile properties were characterized on a ZWICK 1435 tensile testing machine from the Zwick Roell Group (Germany). The modulus at 100 % and 300 % elongation (SE_{100} , SE_{200} , SE_{300}) tensile strength (TS) and elongation at break (Eb) were measured at room temperature with a crosshead speed of 500 mm/min. For testing, type 2 dumb-bell specimens were prepared according to the ISO-37-2005 standard. Five different dumbbell-shaped specimens were tested, and the average value for each formulation was reported.

3.2.18 HARDNESS SHORE A

The Shore A hardness (H) of the vulcanizates was determined according to the standard PN-EN ISO 868:2005P by use durometer Zwick Roell Group (Germany). The result reported is the average of three measurements taken from different areas of the sample (measurement error ± 0.1).

3.2.19 COLORIMETRIC STUDIES

The color of the obtained composites was measured using a CM-3600d spectrophotometer from Konica Minolta Sensing, Inc. (Japan). The instrument provided the color in the terms of the CIE $L^*a^*b^*$ color space system. In this color space, L represented the lightness (or brightness), a and b were color coordinates, where $+a^*$ was the red direction, $-a^*$ was the green direction, $+b^*$ was the yellow direction, and $-b^*$ was the blue direction (Fig. 3.1).

²⁶⁰ P. J. Flory, J. Rehner, Statistical mechanics of cross-linked polymer networks II. Swelling, *J. Chem. Phys.* 1943, **11**, 521–526.

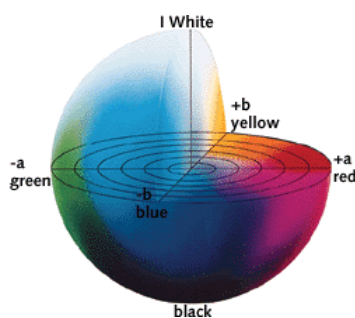


FIGURE 3.1 Characterization of the colors in CIELab system.

Moreover, changes in individual components allowed to estimate the total change of color E . The spectral range of the apparatus was 360–740 nm, where the change of color ΔE was calculated by the equation below (3.9):

$$\Delta E = \sqrt{(\Delta L)^2 + (\Delta a)^2 + (\Delta b)^2} \quad (3.9)$$

ΔL corresponds to the difference in the brightness intensity between light and dark, Δa corresponds to the difference of intensity between green and red, Δb corresponds to the difference of intensity between blue and yellow, and the Δ symbol implies the difference in the colors of the samples before and after aging.

3.2.20 UV AGING STUDIES – COMPOSITES WITH DYES AND PIGMENTS

Accelerated UV aging studies were carried out for rubber composites using a UV 2000 Atlas solar simulation chamber (Germany) ($\lambda = 343$ nm). The test was based on two variable periods that simulated day and night conditions. The test timeline had the following parameters: day period: UV irradiation, temperature 60 °C, duration 8 h; night period: temperature 50 °C, duration 4 h.

3.2.21 WEATHER AGING STUDIES (SOLAR IRRADIATION) - COMPOSITES WITH DYES AND PIGMENTS

Weather aging of samples that contained dyes, pigments and stabilizers was performed with light radiation of $\lambda = 280$ -3000 nm using a Solar Climatic 340 instrument. The test was based on two variable periods that simulated day and night conditions. The test timeline had the following parameters: day period: solar irradiation, temperature 70 °C, humidity 50 %, duration 8 h; night period: temperature -20 °C, humidity 60 %, duration 4 h.

3.2.22 WEATHER AGING STUDIES - COMPOSITES WITH IONIC LIQUIDS

Weather aging was carried out using a Weather-Ometer (Atlas; Ci4000) with light radiation of $\lambda = 300\text{-}400$ nm. The measurement lasted for 216 h and consisted of two alternately repeating periods with the following parameters: day period: UV irradiation temperature 60 °C, humidity 60 %, duration 4 h; night period: temperature 50 °C, humidity 50 % duration 3 h. The samples were controlled every 24 h.

CHAPTER 4

**STUDIES OF THE PROPERTIES AND
CHARACTERISTICS OF SOLVENT DYES AND
PIGMENTS**

INTRODUCTION

The properties of dyes and pigments can have a significant impact on the behavior of composites during use. For this reason, it is important to estimate the properties of dyes and pigments before they are applied in the polymer composite. The thermal stability of dyes and pigments was estimated by thermogravimetric analysis (TGA) and differential scanning calorimetry (DSC) methods. The morphology of the studied powders was determined by scanning electron microscopy (SEM). The oxidation and reduction potentials of the solvent dyes were measured by cyclic voltammetry (CV) and differential pulse voltammetry (DPV). The activities of the solvent dyes toward free radicals and the absorption ranges were examined by ABTS and spectrophotometric methods, respectively. The solubility parameters and diffusion coefficients were also evaluated theoretically.

4.1 THERMAL STABILITY OF DYES AND PIGMENTS

Thermal analysis plays an important role in the study of the structure and stability of polymer additives. Elevated processing temperatures restrict the number of applicable additives, such as dyes and pigments, for a variety of polymer materials. To be suitable for application, the dyes and pigments must be able to withstand the polymer processing conditions and the subsequent environmental conditions.

Table 4.1 shows the thermal stability data of the dyes, pigments and stabilizers as determined by thermogravimetric analysis (TGA). The nature and position of the substituents in the anthraquinone dyes influence the color and other properties. The heat and chemical stabilities vary considerably for different substituted pendants on the base anthraquinone chromophore. It is known that α -substituents increase the molar extinction coefficients and enhance the technical performance, especially the lightfastness, of dyes because of their participation in intramolecular hydrogen bonding with the carbonyl groups. Solvent Green 28 has the highest heat resistance of the anthraquinone dyes with different substituents (S. Green 28, S. Blue, S. Blue 97, S. Blue 104, S. Red, S. Red 207, S. Yellow 163). The presence of hydroxyl groups in the 5- and 8-positions in the molecule of Solvent Green 28 not only provides a bathochromic shift but also increases its thermal stability compared to Solvent Blue. The order of stability of the anthraquinone dyes is as follows: Solvent Green 28 > Solvent Blue > Solvent Yellow 163 > Solvent Blue 104 > Solvent Blue 97 > Solvent Red 207 > Solvent Red. Generally, the heat stability of 1,4-disubstituted anthraquinone dyes increases with the polarity of the substituent group.

CHAPTER 4 STUDIES OF THE PROPERTIES AND CHARACTERISTICS OF SOLVENT DYES AND PIGMENTS

However, the alkyl butyl chain attached to the aromatic ring in Solvent Blue provided better heat stability than the methyl or ethyl groups in the ortho, meta and para positions (S. Blue 97, S. Blue 104). This effect is most likely related to the tendency to creation intramolecular hydrogen bonds between the quinoid oxygens and amino groups.

TABLE 4.1 The results from thermogravimetric analysis of dyes, pigments and commercial stabilizers.

Dyes					
Sample	Start of degradation	T (2%)	T (10%)	T (50%)	Char residue at 500 °C (%)
Solvent Blue 97	335	345	368	409	9.27
Solvent Blue 104	350	357	377	420	15.34
Solvent Blue	382	390	405	434	37.70
Solvent Green 28	407	415	433	462	44.00
Solvent Red	259	272	300	342	6.40
Solvent Red 207	329	338	360	402	19.14
Solvent Yellow 163	357	368	388	437	25.85
Solvent Red 149	341	353	376	429	24.62
Solvent Red 52	379	386	407	450	40.65
Solvent Yellow 98	414	420	437	472	8.86
Solvent Green 5	368	375	392	424	25.47
Solvent Yellow 93	286	294	312	347	28.39
Pigments					
Pigment Blue 15:1		Resistance above 500 °C			
Pigment Green 7		Resistance above 500 °C			
Pigment Red 254	390	393	408	Further decomposition above 500°C	
Pigment Yellow 173	367	369	373	Further decomposition above 500°C	
Indigothiazine <i>cis</i>	238	248	355	428	24.18
Indigothiazine <i>trans</i>	327	338	389	426	27.48
Commercial stabilizers					
Tinuvin 234	306	315	336	375	3.46
Chimassorb 81	246	256	276	376	3.39
Tinuvin 1577	336	345	368	410	3.75
Chimassorb 944L	397	410	435	468	4.77

Based on the obtained values, the decomposition point of Solvent Red 149, which contains a cyclo-hexyl ring, is considerably lower (38 °C) from that of Solvent Red 52, in which a cyclo-hexyl ring is replaced by the polar benzene ring with a methyl group. The other solvent dyes are stable from 286 °C (Solvent Yellow 93) to 314 °C (Solvent Yellow 98). Of the studied pigments, copper phthalocyanine, including blue (P. Blue 15:1) and green (P. Green 7), had the best thermal stability. The excellent resistance of these pigments is the result of their crystalline structure.

CHAPTER 4 STUDIES OF THE PROPERTIES AND CHARACTERISTICS OF SOLVENT DYES AND PIGMENTS

Differences in thermal stability were observed for the *cis* and *trans* forms of Indigothiazine pigment. The thermal properties of *cis*- and *trans*-Indigothiazine were measured using the DSC method (Fig. 4.1). The resulting diagram shows that the melting bands of the pigment's crystalline phase are located at approximately 440 °C for both forms.

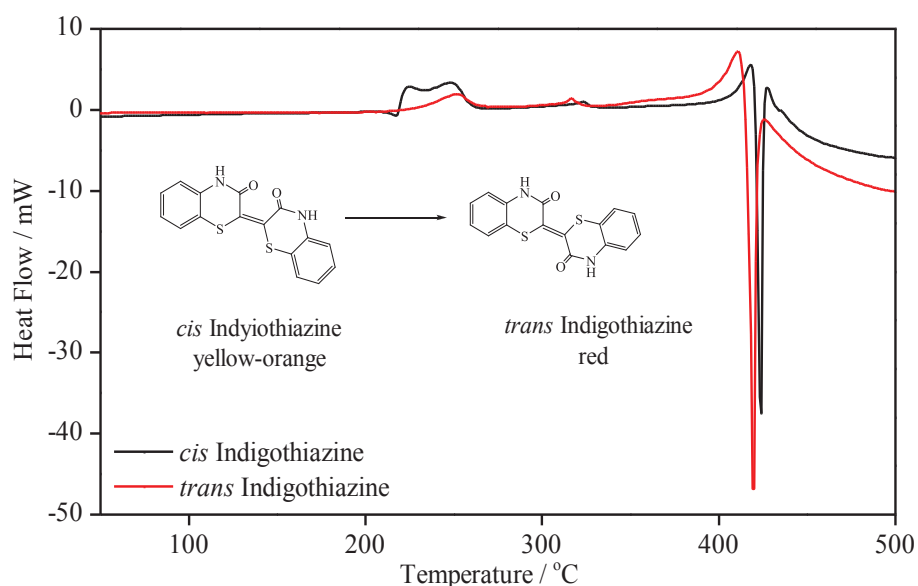


FIGURE 4.1 DSC curves of Indigothiazine pigments, including the *cis* and *trans* forms.

The exothermic peak on the *cis*-Indigothiazine curve is in the regime in which the *cis*-to-*trans* conversion occurred. Below 180 °C, the *cis* form of this pigment was yellow-orange in color, and it transforms into the highly durable red *trans* form above this temperature. This change can be seen on the DSC diagram as the exothermic peak at 200-240 °C.

Of the commercial stabilizers, the thermal resistance was highest for the hindered amine light stabilizer (HALS) Chimassorb 994, at approximately 400 °C, and lowest for stabilizers of the benzophenone group Chimassorb 81, at 246 °C

4.2 MORPHOLOGY OF DYE AND PIGMENT POWDERS

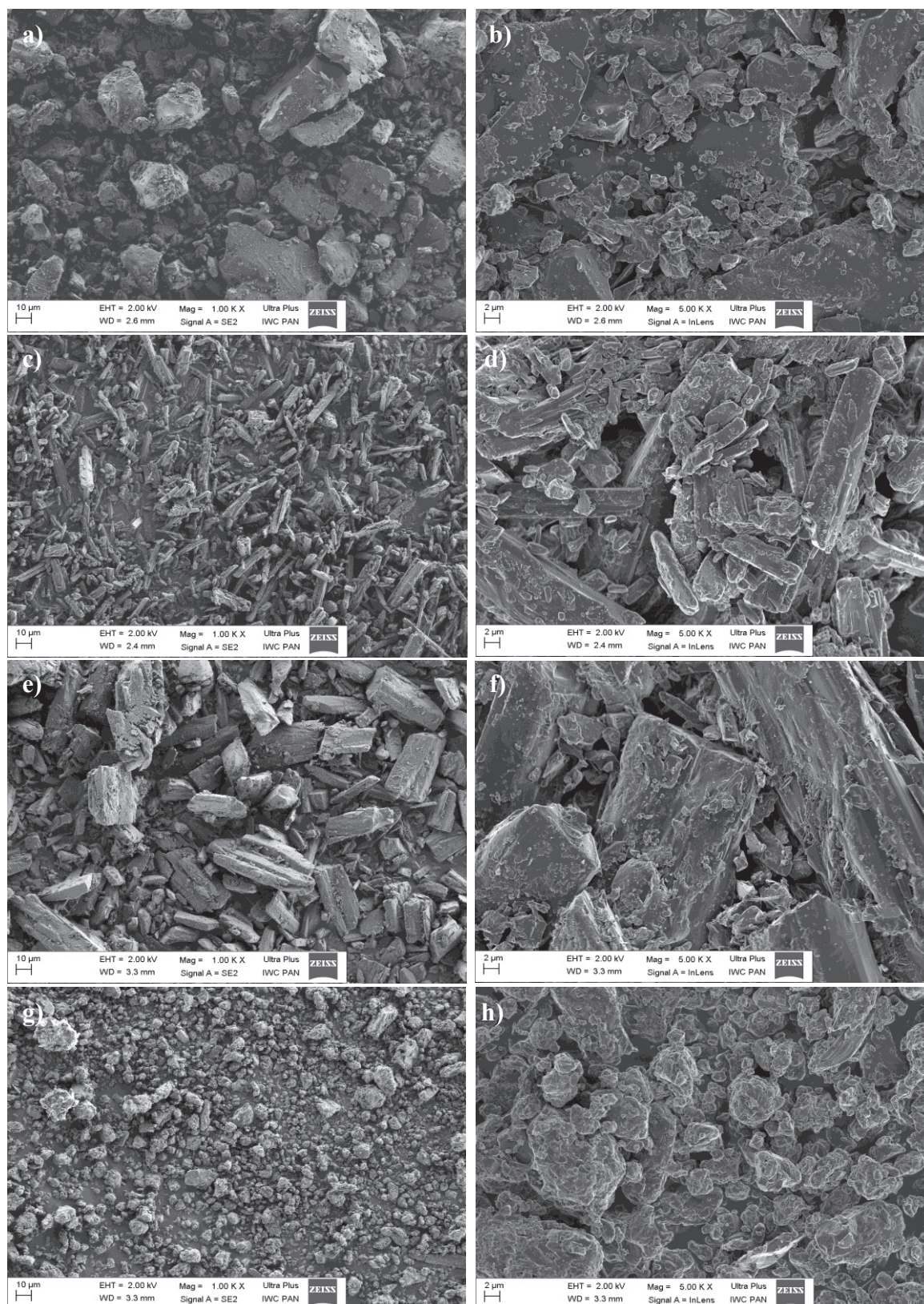


FIGURE 4.2 SEM micrographs of powder dyes: Solvent Blue 97 (a, b), Solvent Green 28 (c, d), Solvent Red 207 (e, f), Solvent Yellow 163 (g, h).

CHAPTER 4 STUDIES OF THE PROPERTIES AND CHARACTERISTICS OF SOLVENT DYES AND PIGMENTS

The tiny crystals of dyes and pigments are often amenable to examination by electron microscopy and have been observed to vary in shape from bricks to rods to plates. The scanning electron microscopy SEM was used to determine the morphology of the selected dyes and pigments (Fig. 4.2 and Fig. 4.3). Dye molecules are usually characterized by a crystalline structure; however, during the application process, they lose their crystalline or particulate structure and form a molecular solution in the medium being colored. Figure 4.2 shows microscopic images of the representative solvent dye powders at several magnifications. Some plate structures can be observed in Solvent Blue 97 and Solvent Yellow 163, where the minor dimensions of the particle aggregates and agglomerates range from 2 to 20 μm . Needle-shaped crystals approximately 10-30 μm in length were observed in Solvent Green 28, while Solvent Red 207 contained rod- and brick-shaped particle structures. Whereas the properties of the dyes are controlled almost exclusively by their chemical compositions, the overall pigmentary performance of a colored particulate depends on not only its intrinsic molecular properties but also its molecular interactions within the solid state (crystal) lattice and at the interface with the medium. In general, the color properties of pigments are strongly influenced by their particle shape ²⁶¹. Copper phthalocyanine (P. Blue 15:1) had plate-shaped crystals with particle dimensions between approximately 200 nm and 300 nm. Morphological studies of green phthalocyanine (P. Green 7) and isoindoline pigment (P. Yellow 173) demonstrated that these particles were spherical, ranging in size from 150 to 200 nm, and tended to aggregate or agglomerate. Figure 4.2 g, h shows irregular flake-shaped crystals of *trans*-Indigothiazine pigment with crystal sizes of 1-3 μm .

²⁶¹ A. Iqbal, B. Medinger, R. B. McKay (1996), *Physico-chemical principles of color chemistry*, A. T. Peters, H. S. Freeman (Eds.), Glasgow, Blackie Academic & Professional, p.107–143.

CHAPTER 4 STUDIES OF THE PROPERTIES AND CHARACTERISTICS OF SOLVENT DYES AND PIGMENTS

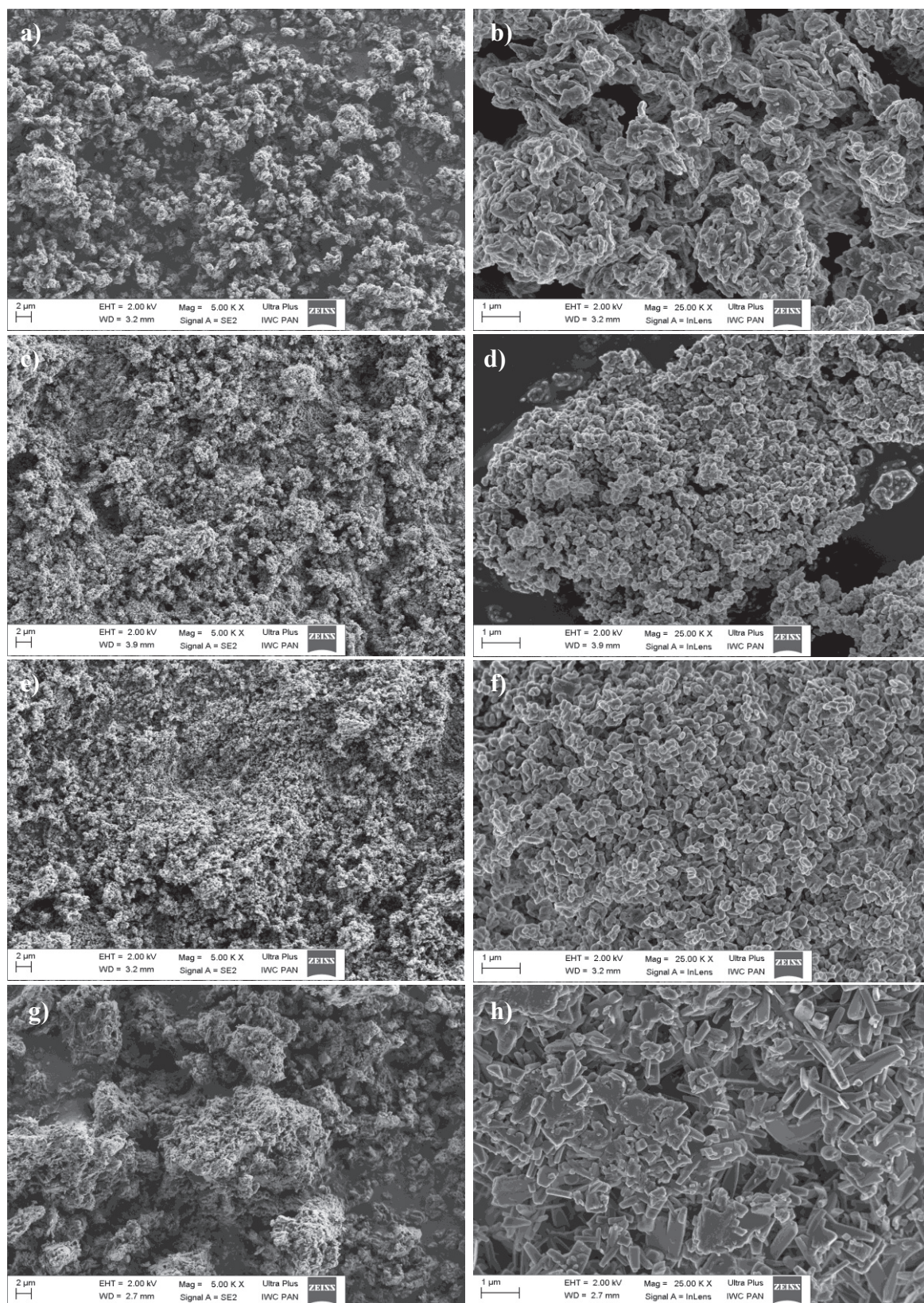


FIGURE 4.3 SEM micrographs of powder pigments: Pigment Blue 15:1 (a, b), Pigment Green 7 (c, d), Pigment Yellow 173 (e, f), *trans*-Indiothiazine (g, h).

4.3 SPECTROPHOTOMETRIC ANALYSIS OF DYES

The optical properties of the solvent dyes and commercial stabilizers were investigated by UV/Vis spectroscopy in the range of 200-800 nm. The absorption spectra of the studied compounds are shown in Figure 4.4-4.6, and the optical data are presented in Table 4.3. The UV/visible spectral data for a series of anthraquinone dyes, which are given in Figure 4.4-4.6, illustrate the effect of the substituent pattern on the color. The introduction of simple electron-donating groups into the anthraquinone dyes causes a bathochromic shift that is dependent on the number and position of the electron-donating groups and their relative strengths. As was already mentioned, the electron-donating groups exert stronger bathochromic effects in the α -positions (1-, 4-, 5-, 8-) than the β -positions (2-, 3-, 6-, 7-)^{95, 96}.

As indicated in Figure 4.4 (a, b), the green and blue dyes exhibited absorbance in the UV (200–300 nm) and visible (600–700 nm) regions. As shown in Figure 4.4 a, the ethyl group (-CH₂CH₃) that is attached to the phenyl ring of the Solvent Blue 97 dye endows it with higher UV absorbance than Solvent Blue 104. The presence of hydroxyl auxochromes (-OH; 5, 8 position) in Solvent Green 28 molecules results in a bathochromic shift in the near-infrared (NIR) region ($\lambda_{\max} = 688$ nm, $\epsilon = 12859$ dm³·mol⁻¹·cm⁻¹) and greater absorbance (hyperchromic shift) than the 1,4-disubstituted derivative of Solvent Blue (Fig. 4.4 b). The strongest absorption bands of the red dye compounds are found from 280 to 330 nm, whereas the visible region exhibits significant absorption between 450 and 600 nm (Fig. 4.5 a, b). Of the yellow dyes, Solvent Yellow 93 had the highest absorption maxima above 300 nm, and the molar extinction for $\lambda_{\max} = 400$ nm was 11173 dm³·mol⁻¹·cm⁻¹ (Fig. 4.6 a).

The commercial UV absorbers considered in this study (Tinuvin 234, Chimassorb 81, Tinuvin 1577) exhibit absorption maxima in the UV A (315–400 nm) and UV B (280–315 nm) regions (Fig. 4.6 b). Exposure to ultraviolet radiation in this range may cause significant degradation of the polymer materials; thus, stabilizers are used to preferentially absorb harmful UV radiation and dissipate it as thermal energy⁷⁶. Another studied commercial stabilizer, the hindered amine light stabilizer (HALS) Chimassorb 994, does not absorb radiation. Instead, it protects materials by neutralizing free radicals, which hinders chemical degradation.

**CHAPTER 4 STUDIES OF THE PROPERTIES AND CHARACTERISTICS OF
SOLVENT DYES AND PIGMENTS**

TABLE 4.2 Measured wavelengths and absorbance values of the absorbance maxima of dyes and commercial stabilizers.

		Dyes						
Solvent Blue 97	Wavelength	635	589	280	229	-	-	-
	Absorbance	0.112	0.10	0.381	0.818	-	-	-
Solvent Blue 104	Wavelength	634	589	278	253	236	227	-
	Absorbance	0.130	0.11	0.271	0.369	0.500	0.678	-
Solvent Blue	Wavelength	647	611	410	284	227	-	-
	Absorbance	0.119	0.11	0.061	0.324	0.734	-	-
Solvent Green 28	Wavelength	688	640	417	366	286	239	227
	Absorbance	0.202	0.16	0.078	0.051	0.355	0.547	0.70
Solvent Red	Wavelength	515	278	245	227	-	-	-
	Absorbance	0.072	0.29	0.615	0.903	-	-	-
Solvent Red 207	Wavelength	532	346	281	238	224	-	-
	Absorbance	0.116	0.10	0.323	0.519	0.684	-	-
Solvent Red 149	Wavelength	534	516	346	257	235	226	-
	Absorbance	0.131	0.11	0.110	0.414	0.472	0.583	-
Solvent Red 52	Wavelength	539	346	281	238	224	-	-
	Absorbance	0.116	0.10	0.323	0.519	0.684	-	-
Solvent Yellow 98	Wavelength	460	379	345	257	-	-	-
	Absorbance	0.230	0.06	0.110	0.710	-	-	-
Solvent Yellow 163	Wavelength	459	382	274	239	224	-	-
	Absorbance	0.088	0.10	0.406	0.821	1.208	-	-
Solvent Green 5	Wavelength	467	441	261	227	-	-	-
	Absorbance	0.241	0.20	0.294	0.389	-	-	-
Solvent Yellow 93	Wavelength	400	282	230	-	-	-	-
	Absorbance	0.342	0.34	1.580	-	-	-	-
		Commercial stabilizers						
Tinuvin 234	Wavelength	346	287	239	227	221	-	-
	Absorbance	0.147	0.30	0.557	0.639	0.600	-	-
Chimassorb 81	Wavelength	328	291	239	-	-	-	-
	Absorbance	0.138	0.14	0.204	-	-	-	-
Tinuvin 1577	Wavelength	344	277	227	223	-	-	-
	Absorbance	0.174	0.34	0.490	0.495	-	-	-

Solvent – chloroform

CHAPTER 4 STUDIES OF THE PROPERTIES AND CHARACTERISTICS OF SOLVENT DYES AND PIGMENTS

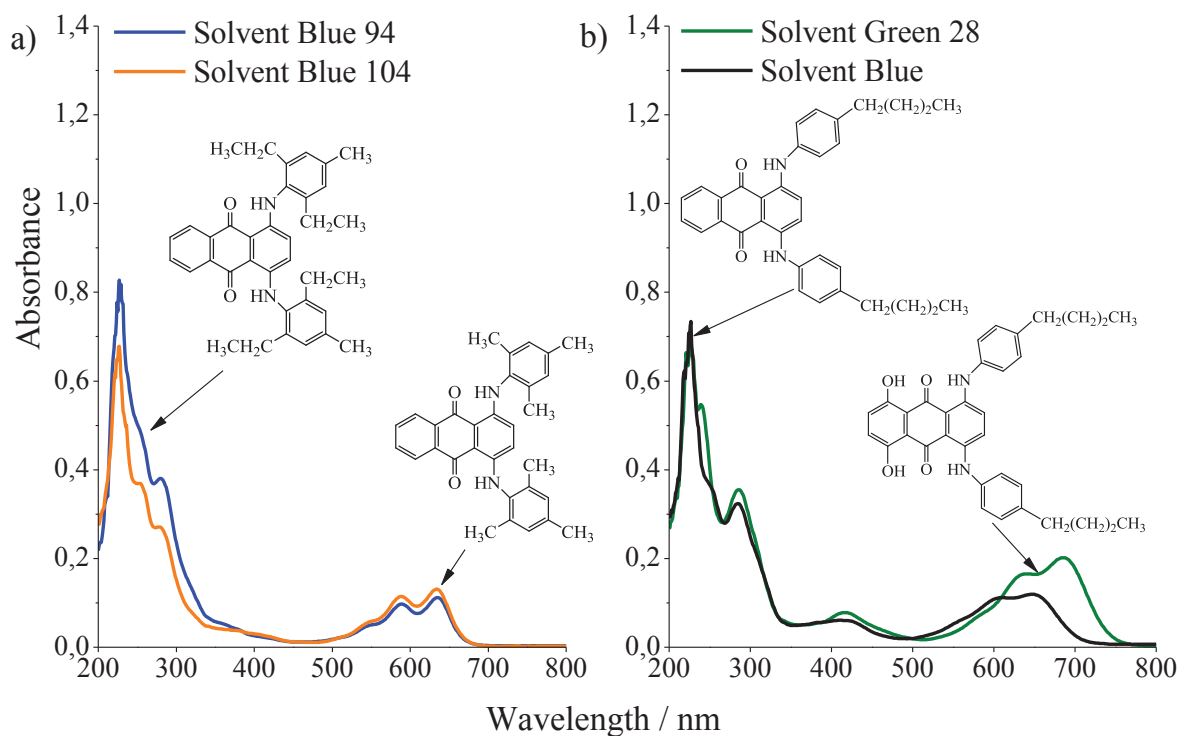


FIGURE 4.4 Absorption spectra of Solvent Blue 97 (a), Solvent Blue 104 (a), Solvent Green 28 (b) and Solvent Blue (b) in chloroform ($c = 1 \times 10^{-5}$ M).

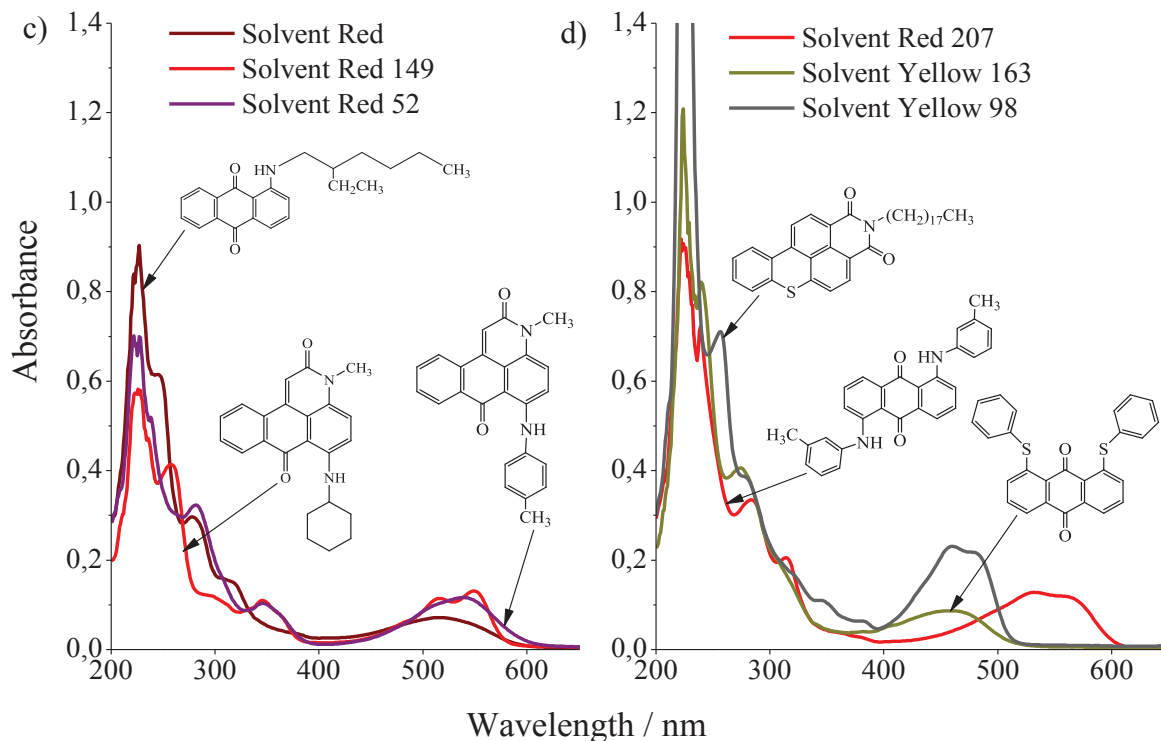


FIGURE 4.5 Absorption spectra of Solvent Red (a), Solvent Red 149 (a), Solvent Red 52 (a), Solvent Red 207 (b), Solvent Yellow 163 (b) and Solvent Yellow 98 (b) in chloroform ($c = 1 \times 10^{-5}$ M).

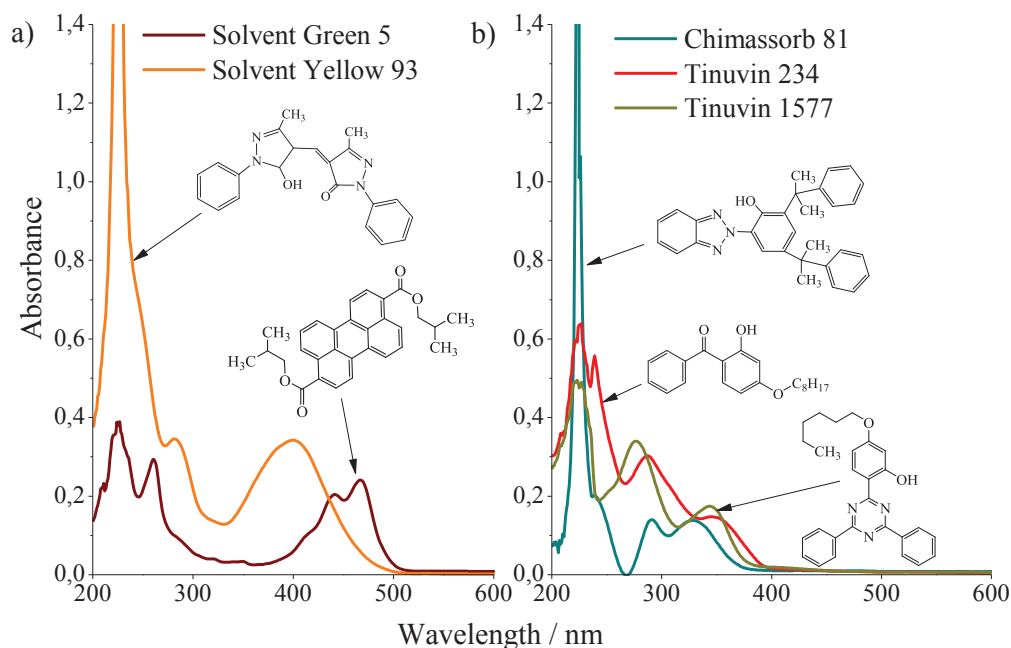


FIGURE 4.6 Absorption spectra of Solvent Green 5 (a), Solvent Yellow 93 (a), Chimassorb 81 (b), Tinuvin 234 (b) and Tinuvin 1577 (b) in chloroform ($c = 1 \times 10^{-5}$ M).

4.4 ELECTROCHEMICAL METHODS - CYCLIC AND DIFFERENTIAL PULSE VOLTAMMETRY OF SOLVENT DYES

Cyclic voltammetry (CV) and differential pulse voltammetry (DPV) are important electroanalytical methods used to analyze electronically activated molecules and their corresponding chemical reactions. They are also used to characterize the electrochemical properties of anthraquinones and may provide important information about the kinetics and identify the side and final products of different electrochemical reactions^{262, 263}.

This section examines the ability of solvent dyes and commercial stabilizers to participate in redox reactions (i.e., their potential to donate and accept electrons). Due to their limited solubility, these studies were not performed on pigments. The electrochemical properties of solvent dyes were measured by cyclic voltammetry (CV) and differential

²⁶² M. Shamsipur, A. Sirouinejad, B. Hemmateenejad, A. Abbaspour, H. Sharghi, K. Alizadeh, S. Arshadi, Cyclic voltammetric, computational, and quantitative structure–electrochemistry relationship studies of the reduction of several 9,10-anthraquinone derivatives, *J. Electroanal. Chem.* 2007, **600**, 345–358.

²⁶³ A. Doménech-Carbó, M. T. Doménech-Carbó, M. C. Sauri-Peris, J. V. Gimeno-Adelantado, F. Bosch-Reig, Electrochemical identification of anthraquinone-based dyes in solid microsamples by square wave voltammetry using graphite/polyester composite electrodes, *Anal. Bioanal. Chem.* 2003, **375**, 1169–1175.

CHAPTER 4 STUDIES OF THE PROPERTIES AND CHARACTERISTICS OF SOLVENT DYES AND PIGMENTS

pulse voltammetry (DPV) in a solution of 1-methyl-2-pyrrolidinone at room temperature under the protection of argon.

The voltammograms recorded by CV showed that the oxidation of S. Blue, S. Green 28, S. Red 207, S. Yellow 98, S. Green 5, Chimassorb 81, Tinuvin 1577 and Chimassorb 994 on a platinum electrode proceeds in at least one electrode step below the oxidation potential of the electrolyte. Other dyes, such as S. Blue 97, S. Blue 104, S. Red, S. Red 149, S. Red 52, S. Yellow 93 and Tinuvin 234, were electrooxidized in at least two electrode steps, and two peaks can be observed in the cyclic and differential pulse voltammograms (Fig. 4.7 a, Fig. 4.8 a).

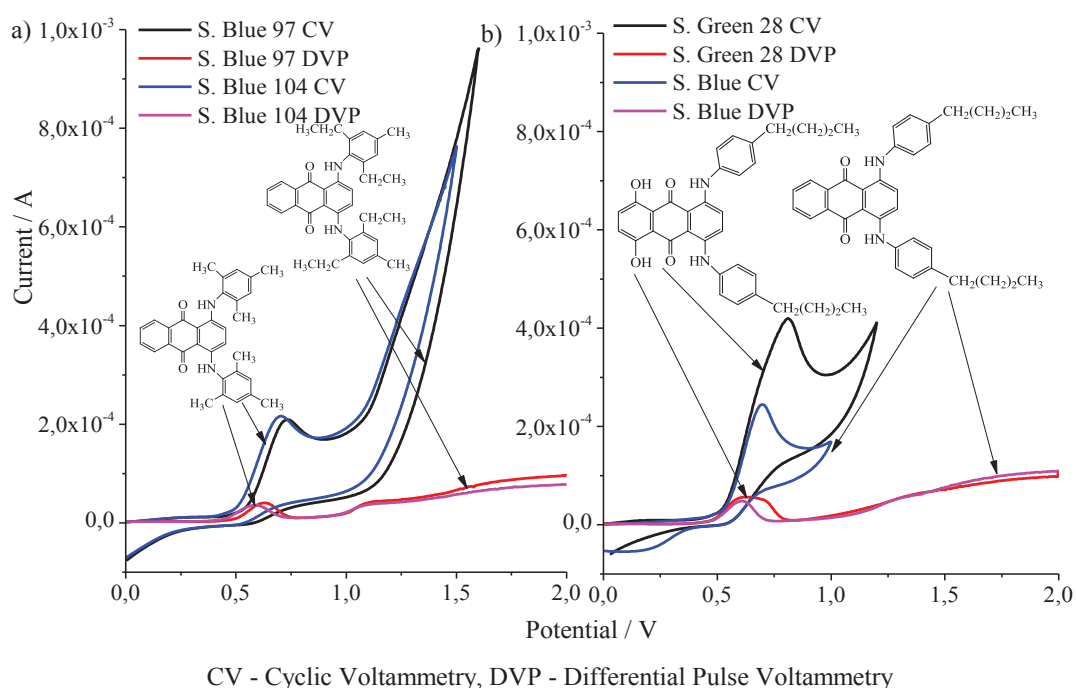


FIGURE 4.7 Cyclic voltammograms and differential pulse voltammograms of solvent dye electrooxidation at the platinum electrode recorded in the supporting electrolyte; $c = 2 \times 10^{-3}$ M in 0.1 M $(C_4H_9)_4NClO_4$ in 1-methyl-2-pyrrolidinone, $\nu = 100$ V \cdot s $^{-1}$.

Moreover, all of the studied dyes and stabilizers were irreversibly oxidized, as demonstrated by the lack of peaks in the reverse scan. Although S. Yellow 163, similarly to other dyes, has an anthraquinone chromophore, the electrooxidation peak did not appear in the voltammograms in the studied potential range, i.e., lower than that of electrolyte decomposition. Different substituents, such as the replacement of the $-NHR$ group by $-SR$, and their positions in the dye molecule (1, 8-) may cause this behavior during the electrooxidation process.

CHAPTER 4 STUDIES OF THE PROPERTIES AND CHARACTERISTICS OF SOLVENT DYES AND PIGMENTS

Within the potential range in which the oxidation peaks of the solvent dyes appear, the supporting electrolyte (tetrabutylammonium perchlorate in 1-methyl-2-pyrrolidinone, $0.1 \text{ mol}\cdot\text{L}^{-1}$) shows no characteristic peaks other than charging the electrical double layer. DPV is a higher-resolution method that enables the better separation of peaks that characterize the subsequent electrooxidation and reduction steps. The half-wave potential of the peaks in a cyclic voltammogram corresponds to the potential of a peak in a differential pulse curve and is characteristic of each of the subsequent steps of the investigated electrode reactions. Selected cyclic and differential pulse voltammograms recorded in the solvent dye solutions are presented in Figures 4.7 (a, b) and 4.8 (a, b).

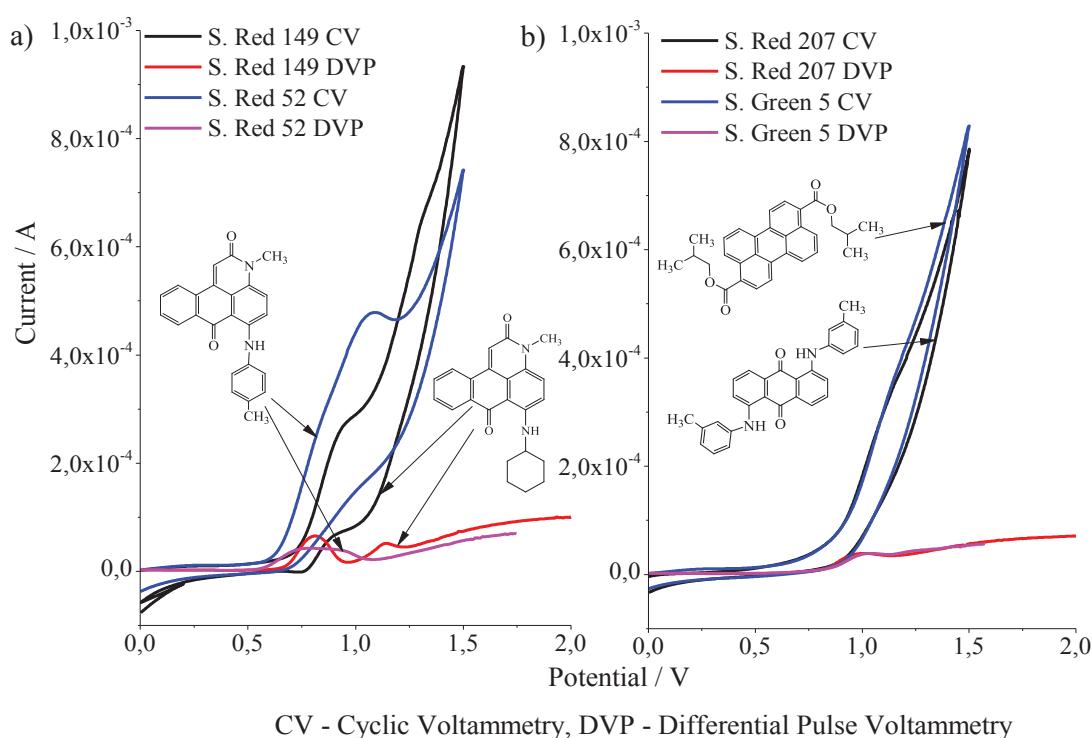


FIGURE 4.8 Cyclic voltammograms and differential pulse voltammograms of solvent dyes electrooxidation at Pt electrode, recorded in the supporting electrolyte; $c = 2 \times 10^{-3} \text{ M}$ in $0.1 \text{ M } (\text{C}_4\text{H}_9)_4\text{NClO}_4$ in 1-methyl-2-pyrrolidinone, $\nu = 100 \text{ V}\cdot\text{s}^{-1}$.

The effects of the substituents on the electrochemical properties of solvent dyes and stabilizers were evaluated on the basis of determinate physic-chemical parameters like the peak potential (E_{pa}) and half-wave potential ($E_{1/2}$), which are summarized in Table 4.3. Low values of the oxidation potentials E_{pa} and $E_{1/2}$ generally indicate higher electron-donating ability (easier oxidation). The shifts of the half-wave potential ($E_{1/2}$) are in the order S. Red (1.05) > S. Red 207 (0.98 V) > S. Green 28 (0.65 V) > S. Blue 97 (0.62 V) > S. Blue (0.59 V) > S. Blue 104 (0.58 V). The anthraquinone dyes with stronger electron-donating groups (Solvent Green 28, Solvent Blue, Solvent Blue 104 or Solvent Blue 97)

CHAPTER 4 STUDIES OF THE PROPERTIES AND CHARACTERISTICS OF SOLVENT DYES AND PIGMENTS

clearly had a greater tendency for electrooxidation than those with weaker electron-donating substituents (Solvent Red, Solvent Red 207).

TABLE 4.3 Peak potential (E_{pa}) and half-wave potential ($E_{1/2}$) of the studied dyes for the half-wave potential of the first electrode step during electrooxidation of the dyes at the platinum electrode; $c = 2 \times 10^{-3}$ M in 0.1 M $(C_4H_9)_4NClO_4$ in 1-methyl-2-pyrrolidinone, $\nu = 10$ m·V·s⁻¹ (cyclic and differential pulse voltammetry).

Dye	Cyclic Voltammetry (CV)			Differential Pulse Voltammetry (DPV)		E_{HOMO} (eV)
	Oxidation peaks			Oxidation peaks		
	I		II	I	II	
	E_{pa} , V	$E_{1/2}$, V	E_{pa} , V	E_{pa} , V	E_{pa} , V	
Solvent Blue 97	0.65	0.62	1.18	0.63	1.13	-8.50
Solvent Blue 104	0.61	0.58	1.17	0.57	1.23	-8.22
Solvent Blue	0.62	0.59	-	0.61	-	-8.60
Solvent Green 28	0.70	0.65	-	0.63	-	-8.61
Solvent Red	1.08	1.05	1.25	1.08	1.24	-8.72
Solvent Red 207	1.02	0.98	-	1.00	-	-8.38
Solvent Yellow 163	-	-	-	-	-	-8.13
Solvent Red 149	0.89	0.85	1.15	0.81	1.14	-8.03
Solvent Red 52	0.76	0.73	0.91	0.76	0.91	-8.13
Solvent Yellow 98	1.20	1.17	-	1.16	-	-8.20
Solvent Green 5	1.06	1.00	-	1.03	-	-8.24
Solvent Yellow 93	0.34	0.32	1.05	0.32	0.41	-8.47
Tinuvin 234	1.23	1.20	1.95	1.11	-	-8.80
Chimassorb 81	1.56	1.49	-	1.44	-	-9.16
Tinuvin 1577	1.42	1.38	-	1.34	-	-8.97
Chimassorb 994	1.92	1.87	-	1.87	-	-8.81

Although the presence of hydrogen atoms in S. Green 28 at the 5,8- positions of two hydroxyl groups increases intramolecular hydrogen bonding, the electrooxidation potential is lower than in S. Blue. The lack of a good correlation can be explained by the different steric, mesomeric or inductive effects of the presence of additional electron-donating

CHAPTER 4 STUDIES OF THE PROPERTIES AND CHARACTERISTICS OF SOLVENT DYES AND PIGMENTS

substituents in anthraquinones, which was also observed in the results of the electroreduction study²⁶⁴.

Of the other solvent dyes, Solvent Yellow 93 had the lowest half-wave potential ($E_{1/2} = 0.32$ V), or electron-donating ability, whereas Solvent Yellow 98 oxidized at a potential of 1.17 V. The most difficult stabilizer to oxidize was Chimassorb 994.

The calculated energies of the highest occupied molecular orbital (E_{HOMO}) of solvents dyes are demonstrated in Table 4.3. A molecule with low values of E_{HOMO} energy (more negative) has a weak electron donating ability. Otherwise, a high E_{HOMO} energy implies that the molecule is a good electron-donor^{265, 266}. Nevertheless, for studied dyes with anthraquinone chromophores (S. Blue 97, S. Blue 104, S. Blue, S. Green 28, S. Red, S. Red 207) not showed correlation between E_{HOMO} energy values and half-wave potentials ($E_{1/2}$) values determined from the electrochemical study. The relationship between the electrooxidation potentials and the calculated energy E_{HOMO} for other solvent dyes and stabilizers, was also not found, most likely due to the large differences in the structure between these compounds.

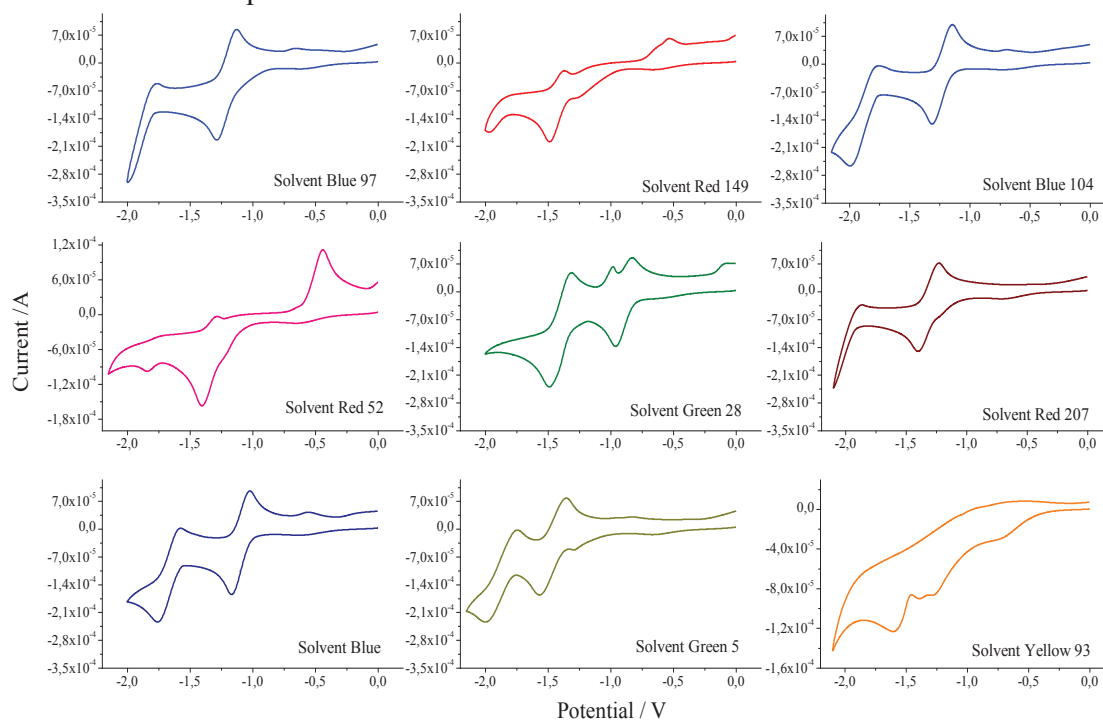


FIGURE 4.9 Cyclic voltammograms of solvent dyes at the Pt electrode; $c = 2 \times 10^{-3}$ M in 0.1 M $(\text{C}_4\text{H}_9)_4\text{NClO}_4$ in 1-methyl-2-pyrrolidinone, $\nu = 100 \text{ mV} \cdot \text{s}^{-1}$.

²⁶⁴ A. Salimi, H. Eshghi, H. Sharghi, S. M. Golabi, M. Shamsipur, Electrocatalytic reduction of dioxygen at the surface of glassy carbon electrodes modified by some anthraquinone substituted podands, *Electroanal.* 1999, **11**, 114–119.

²⁶⁵ K. M. Honório, A. B. F. da Silva, An AM1 study on the electron-donating and electron-accepting character of biomolecules, *Int. J. Quant. Chem.* 2003, **95**, 126–132.

²⁶⁶ A. N. Queiroz, B. A. Q. Gomes, W. M. Jr. Moraes, R. S. Borges, A theoretical antioxidant pharmacophore for resveratrol, *Eur. J. Med. Chem.* 2009, **44**, 1644–1649.

CHAPTER 4 STUDIES OF THE PROPERTIES AND CHARACTERISTICS OF SOLVENT DYES AND PIGMENTS

TABLE 4.4 Peak potential (E_{pc}) and half-wave potential ($E_{1/2}$) of the studied dyes for the half-wave potential of the first electrode step during electroreduction of the dyes at the platinum electrode; $c = 2 \times 10^{-3}$ M in 0.1 M $(C_4H_9)_4NClO_4$ in 1-methyl-2-pyrrolidinone, $\nu = 10$ mV·s⁻¹ (cyclic and differential pulse voltammetry).

Dye	Cyclic Voltammetry (CV)				Differential Pulse Voltammetry (DPV)		E_{LUMO} (eV)
	Reduction peaks				Reduction peaks		
	I		II		I	II	
	E_{pc} , V	$E_{1/2}$, V	E_{pc} , V	$E_{1/2}$, V	E_{pc} , V	E_{pc} , V	
Solvent Blue 97	-1.28	-1.25	-2.01	-	-1.20	-1.88	-1.02
Solvent Blue 104	-1.31	-1.27	-1.98	-	-1.23	-1.86	-1.06
Solvent Blue	-1.17	-1.13	-1.76	-	-1.10	-1.65	-1.38
Solvent Green 28	-0.96	-0.92	-1.49	-	-0.89	-1.40	-1.56
Solvent Red	-1.24	-1.20	-2.03	-	-1.15	-1.89	-1.11
Solvent Red 207	-1.41	-1.37	-	-1.22*	-1.31	-1.99	-1.18
Solvent Yellow 163	-1.13	-1.08	-1.94	-	-1.04	-1.78	-1.25
Solvent Red 149	-1.27	-1.23	-1.48	-1.46	-1.27	-1.41	-0.95
Solvent Red 52	-1.41	-1.38	-1.83	1.22*	-1.17	-1.32	-1.40
Solvent Yellow 98	-1.19	-1.13	-1.45	-1.43*	-1.38	-	-1.52
Solvent Green 5	-1.56	-1.52	-1.99	1.29*	-1.46	-1.85	-1.67
Solvent Yellow 93	-1.28	-1.23	-1.60	0.73*	-0.69	-1.20**	-1.15
Tinuvin 234	-1.24	-1.17	-1.63	-	-1.10	-	-0.46
Chimassorb 81	-1.27	-1.13	-	-	-1.15	-	-0.27
Tinuvin 1577	-1.32	-1.24	-	-	-1.11	-	-0.57
Chimassorb 994	-1.27	-1.16	-	-	-1.12	-	0.70

*Pre-wave, ** III Reduction peak -1.31 V

As in electrooxidation processes, the recorded voltammograms (CV and DVP) of the first reduction step under linear diffusion were used to determine E_{pc} and $E_{1/2}$. Table 4.4 summarizes the peak potential data for the studied systems. The cyclic voltammograms recorded in almost all of the dyes showed quasi-reversible reactions that characterizes at least one or two steps of the electroreduction of the dyes in the potential range above the potential at which electrolyte decomposition begins (Fig. 4.9). The S. Red 149 and S. Red 52 dyes were also reduced during at least two electrode reactions; however, they were found to be irreversible. Solvent Yellow 93 was the exception, reducing irreversibly in at least three electrode steps.

CHAPTER 4 STUDIES OF THE PROPERTIES AND CHARACTERISTICS OF SOLVENT DYES AND PIGMENTS

The $E_{1/2}$ of a peak in a cyclic voltammogram corresponded to the potential of a peak in the corresponding differential pulse curve and was characteristic of each of the subsequent steps of the investigated electrode reductions. Within the potential range in which the compound reduction peaks appear, the supporting electrolyte $(C_4H_9)_4NClO_4$ in 1-methyl-2-pyrrolidinone showed no characteristic peaks and was characterized by only a small capacitive current. The reduction potentials ($E_{1/2}$) of anthraquinones are in the order S. Red 207 (-1.37 V) < S. Blue 104 (-1.27 V) < S. Blue 97 (-1.25 V) < S. Red (-1.20 V) < S. Blue (-1.13 V) < S. Yellow 163 (-1.08 V) < S. Green 28 (-0.92 V).

As shown in Table 4.4, the redox potentials of dyes with anthraquinone chromophores strongly depend on the nature, position and number of the substituting groups on the anthraquinone dyes. The reduction potentials can be shifted positively or negatively by electron-donating moieties. The presence of 5, 8-dihydroxyl groups in S. Green 28 results in a smaller shift towards a less negative reduction potential than S. Blue and other anthraquinone chromophore dyes. This may be related to steric hindrance of the side arms as well as resonance or inductive effects of different groups that substitute at various positions of the anthraquinone dyes, some of which have been discussed in previous reports²⁶⁷. The most easily reduced stabilizers were Chimassorb 81 and Chimassorb 994; they had the lowest reduction values of -1.13 and -1.16, respectively.

The calculated E_{LUMO} values of the solvent dyes are shown in Table 4.4. Generally, the E_{LUMO} determines the electron acceptance ability of a molecule. Lower (more negative) values of the calculated E_{LUMO} should correspond to greater (less negative) $E_{1/2}$ values obtained from the electroreduction voltammograms. Among the anthraquinone dyes, E_{LUMO} is consistent with the electroreduction potential for S. Green 28. Despite having similar structures, anthraquinone dyes do not show correlations between E_{LUMO} and $E_{1/2}$, which could be related to the different effects of the substituents as was described previously.

The most negative E_{LUMO} values, -1.67 eV and -1.52 eV among other solvent dyes, were found for Solvent Green 5 and Solvent Yellow 98, respectively.

²⁶⁷ M. Shamsipur, A. Salimi, S. M. Golabi, H. Sharghi, M. F. Mousavi, Electrochemical properties of modified carbon paste electrodes containing some amino derivatives of 9, 10-anthraquinone, *J. Solid State Electrochem.* 2001, **5**, 68-73.

4.5 ANTIOXIDANT ACTIVITY OF SOLVENT DYES STUDIED WITH THE ABTS METHOD

Free radicals can form as a result of the aging of polymer composites and may react with dye molecules. Thus, the activity of solvent dye powders toward ABTS^{•+} radical cations was investigated.

The generation of ABTS^{•+} involves the direct production of the blue/green ABTS^{•+} chromophore through the reaction between ABTS and potassium persulfate. The activity of solvent dyes was assessed by reacting them with ABTS radicals and monitoring the process by UV-Vis spectroscopy.

The ability of the solvent dyes to scavenge ABTS^{•+} radical cations was compared to the Trolox standard, and the obtained results were expressed in terms of the Trolox equivalent antioxidant capacity (TEAC), i.e., 100 mmol Trolox/100 g dry weight²⁶⁸. The total antioxidant activity of this mixture was calculated from the decolorization of ABTS^{•+}, which was measured spectrophotometrically at 734 nm²⁶⁹. The solvent dye solution was mixed with the ABTS^{•+} solution and measured after 2 minutes at 25 °C. Previous studies of these compounds showed that no further changes in the intensity of the absorption maxima at 734 nm occur after 2 minutes.

The characteristic ABTS^{•+} radical cation absorption maximum at 734 nm was significantly weakened upon reaction with several solvent dyes, which confirms the free radical scavenging ability of these compounds. Figure 4.9 shows that the anthraquinone dyes with the strongest electron-donor substituents (Solvent Green 28, Solvent Blue 97 and Solvent Blue) showed antioxidant activity against ABTS radicals. The most effective dye in the reactions with cation radicals ABTS was Solvent Green 28, which had the highest TEAC value of 195.4. Flavonoids and other polyphenols have been shown to have antioxidative properties due to the presence of various numbers of hydroxyl groups in different arrangements²⁷⁰. Thus, the high antioxidant efficiency in this dye is most likely caused by the presence of hydroxyl groups at positions 5, 8-, which may provide additional reaction sites for the generated radicals. Solvent Blue and Solvent Blue 97 show activities on a similar level; the TEAC values of the compounds were 137.3 and 105.3, respectively.

²⁶⁸ Y. Z. Cai, Q. Luo, M. Sun, H. Corke, Antioxidant activity and phenolic compounds of 112 traditional Chinese medicinal plants associated with anticancer, *Life Sci.* 2004, **74**, 2157–2184.

²⁶⁹ W.-Y. Huang, H.-Ch. Zhang, W.-X. Liu, Ch.-Y. Li, Survey of antioxidant capacity and phenolic composition of blueberry, blackberry, and strawberry in Nanjing, *J. Zhejiang. Univ.-Sci. B Biomed & Biotechnol.* 2012, **13**, 94–102.

²⁷⁰ S. Burda, W. Oleszek, Antioxidant and antiradical activities of flavonoids, *J. Agric. Food. Chem.* 2001, **49**, 2774–2779.

CHAPTER 4 STUDIES OF THE PROPERTIES AND CHARACTERISTICS OF SOLVENT DYES AND PIGMENTS

In this study, the activity of solvent dyes toward $\text{ABTS}^{+\cdot}$ radical cations was compared to the activity of morin and hesperidin, which are known for their antioxidant properties²⁷¹. Although flavones have better radical scavenging ability, the dyes also showed relatively high activities. Other dyes did not show any activity with $\text{ABTS}^{+\cdot}$ radical cations.

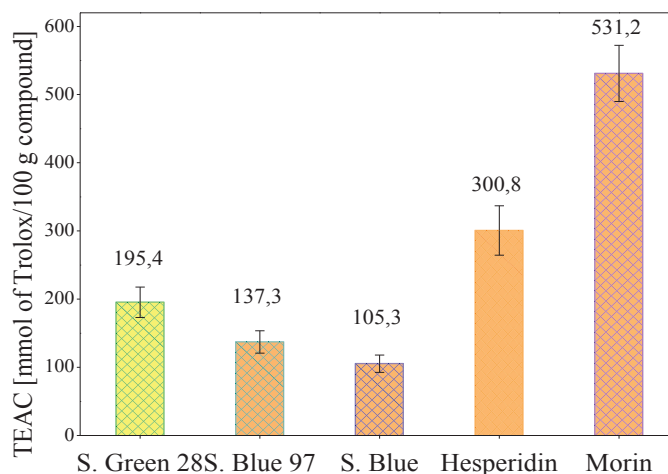


FIGURE 4.9 Results from the reaction of solvents with $\text{ABTS}^{+\cdot}$ radical cations.

Interestingly, despite the similar construction of the Solvent Blue 97 and Solvent Blue 104 dyes, only the former contributes to a reduction in the absorbance band of the test solution at 734 nm. The lower activity of Solvent Blue 104 with respect to $\text{ABTS}^{+\cdot}$ radical cations may reflect other substituents at the ortho and para positions or may indicate that a higher concentration of dye should be used. Other dyes did not exhibit activity with $\text{ABTS}^{+\cdot}$ radical cations under the studied conditions.

4.6 SOLUBILITY PARAMETERS

Dye solubility is an important parameter to the dye chemist. Knowledge of dye solubilities is useful for problems related to polymers, electronics, solvents, environmental exposure assessment, and many other products and applications²⁷². In this study, the solvent dye is expected to exhibit good solubility in the investigated polymer, which will result in an intense and uniform color of the material at a low dye concentrations.

The solubility parameter of a chemical characterizes the interactions between its molecules due to dispersion forces, polar forces, and hydrogen bonding. The total solubility can be expressed in terms of these components. The solubility parameters of

²⁷¹ A. Masek, E. Chrzescijańska, M. Zaborski, Electrooxidation of morin hydrate at a Pt electrode studied by cyclic voltammetry, *Food Chem.* 2014, **148**, 18–23.

²⁷² R. R. Bommu, T. Nakamura, B. V. Rao, Application of solubility parameter concept in dyeing studies of polyester and nylon 6, *Colourage* 2000, **47**, 59–64.

CHAPTER 4 STUDIES OF THE PROPERTIES AND CHARACTERISTICS OF SOLVENT DYES AND PIGMENTS

solvent dyes and stabilizers in ethylene-norbornene polymers were estimated using the group contribution method as described by Krevelen²⁵⁸. The calculated solubility parameters and their components for the dyes and commercial stabilizers are shown in Table 4.5 and Table 4.6, respectively.

TABLE 4.5 Estimated solubility parameters for solvent dyes.

Name	δ_d (MJ/m ³) ^{1/2}	δ_p (MJ/m ³) ^{1/2}	δ_h (MJ/m ³) ^{1/2}	δ (MJ/m ³) ^{1/2}	$\Delta\delta$ (MJ/m ³) ^{1/2}
Solvent Blue 97	20.49	2.46	4.67	21.16	5.45
Solvent Blue 104	21.08	2.85	5.03	21.86	6.11
Solvent Blue	17.59	2.44	4.61	18.35	5.43
Solvent Green 28	17.52	2.70	9.96	20.33	10.44
Solvent Red	16.79	4.55	13.61	22.08	14.53
Solvent Red 207	19.47	3.06	5.16	20.37	6.01
Solvent Yellow 163	46.04	5.11	4.29	46.52	27.76
Solvent Red 149	35.04	10.96	8.69	37.73	21.21
Solvent Red 52	22.81	7.09	6.97	24.88	10.61
Solvent Yellow 98	21.06	4.02	4.56	21.91	6.38
Solvent Green 5	16.30	2.37	5.75	17.45	6.81
Solvent Yellow 93	19.47	13.61	9.58	25.62	16.65

The analysis of the calculated solubility parameters of the solvent dyes indicated that high solubility in ethylene-norbornene EN polymer can be expected for Solvent Blue 97 (5.45 (MJ/m³)^{1/2}), Solvent Blue 104 (6.11 (MJ/m³)^{1/2}), Solvent Blue (5.43 (MJ/m³)^{1/2}), Solvent Red 207 (6.01 (MJ/m³)^{1/2}), Solvent Yellow 98 (6.38 (MJ/m³)^{1/2}), and Solvent Green 5 (6.81 (MJ/m³)^{1/2}) because the $\Delta\delta$ values for these solvents were the lowest. Good solubility can also be anticipated for Solvent Green 28 and Solvent Red 52, which have $\Delta\delta$ values of 10.44 (MJ/m³)^{1/2} and 10.61 (MJ/m³)^{1/2}, respectively.

The solubilities of the dyes depend on both the nature of the groups and their location in the molecule²⁷³. Generally, the presence of aliphatic groups contributes to decreases in the values of the calculated parameters. For example, the substitution of methyl groups in the dye Solvent Blue 104 with the ethyl groups (Solvent Blue 97) resulted in a lower $\Delta\delta$ value, which promotes better solubility of this dye in the polymer matrix. This observation is

²⁷³ D. W. Krevelen, K. Nijenhuis (2009), Properties of polymers, Amsterdam, Elsevier, p. 211–227.

CHAPTER 4 STUDIES OF THE PROPERTIES AND CHARACTERISTICS OF SOLVENT DYES AND PIGMENTS

consistent with previously reported results that polylactide (PLA) was more compatible with disperse dyes that contain longer aliphatic groups^{274, 275}.

TABLE 4.6 Estimated solubility parameters for commercial stabilizers calculated by Kraveln method.

Name	δ_d (MJ/m ³) ^{1/2}	δ_p (MJ/m ³) ^{1/2}	δ_h (MJ/m ³) ^{1/2}	δ (MJ/m ³) ^{1/2}	$\Delta\delta$ (MJ/m ³) ^{1/2}
Tinuvin 234	26.89	6.16	11.27	29.79	15.02
Chimassorb 81	19.68	5.587	9.49	22.55	10.02
Tinuvin 1577	20.62	7.72	10.84	24.54	13.39
Chimassorb 994	15.61	4.08	6.69	17.47	8.58
EN	19.01	0	0	19.01	-

Solvent Blue dye, with two butyl groups attached to the aromatic ring, has the best solubility (the lowest $\Delta\delta$ value), while the solubility ($\Delta\delta$) of Solvent Green 28, which has a similar molecular structure, is twice as high. This observation may explain why the hydroxyl groups in Solvent Green 28 increase the contribution of hydrogen bonding ($\delta_h = 9.96$ (MJ/m³)^{1/2}), thereby reducing the solubility of this dye in ethylene-norbornene polymer. These results reflect the influence of hydrogen bonding on the solubility properties of the studied dyes. Chimassorb 994 had the best solubility of the commercial stabilizers; its parameters as calculated by the Krevelen method are the lowest.

4.7 DIFFUSION COEFFICIENT

The diffusion coefficient (D) is an important parameter that describes diffusion mass transfer phenomena, such as those that occur in electrode processes or polymer materials. Many methods for predicting the diffusion coefficients of organic compounds are based on correlations between D and indicators of molecular size, such as the alkyl chain length²⁷⁶.

In this study, the diffusion coefficients D of solvent dyes and commercial stabilizers in non-aqueous media were calculated using the Hayduk and Laudie equation²⁵⁹. The results are shown in Figure 4.10 and Figure 4.11 and demonstrate that the diffusion ability of the

²⁷⁴ D. Karst, Y. Yang, Using the solubility parameter to explain disperse dye sorption on polylactide, *J. Appl. Polym. Sci.* 2005, **96**, 416–422.

²⁷⁵ A. F. M. Barton (1983), Handbook of solubility parameters and other cohesion parameters, Florida, CRC Press.

²⁷⁶ J. M. P. Q. Delgado, Molecular diffusion coefficients of organic compounds in water at different temperatures, *J. Phase. Equilib. Diff.* 2007, **28**, 427–432.

CHAPTER 4 STUDIES OF THE PROPERTIES AND CHARACTERISTICS OF SOLVENT DYES AND PIGMENTS

investigated compounds is strictly related to their structure^{277, 278}. The lowest D are for Solvent Blue 97 ($3.44 \times 10^{-6} \text{ cm}^2 \cdot \text{s}^{-1}$), Solvent Blue 104 ($3.65 \times 10^{-6} \text{ cm}^2 \cdot \text{s}^{-1}$), Solvent Blue ($3.42 \times 10^{-6} \text{ cm}^2 \cdot \text{s}^{-1}$), Solvent Green 28 ($3.54 \times 10^{-6} \text{ cm}^2 \cdot \text{s}^{-1}$) and Solvent Yellow 98 ($3.30 \times 10^{-6} \text{ cm}^2 \cdot \text{s}^{-1}$), which indicates their weak diffusion ability (Fig. 4.10).

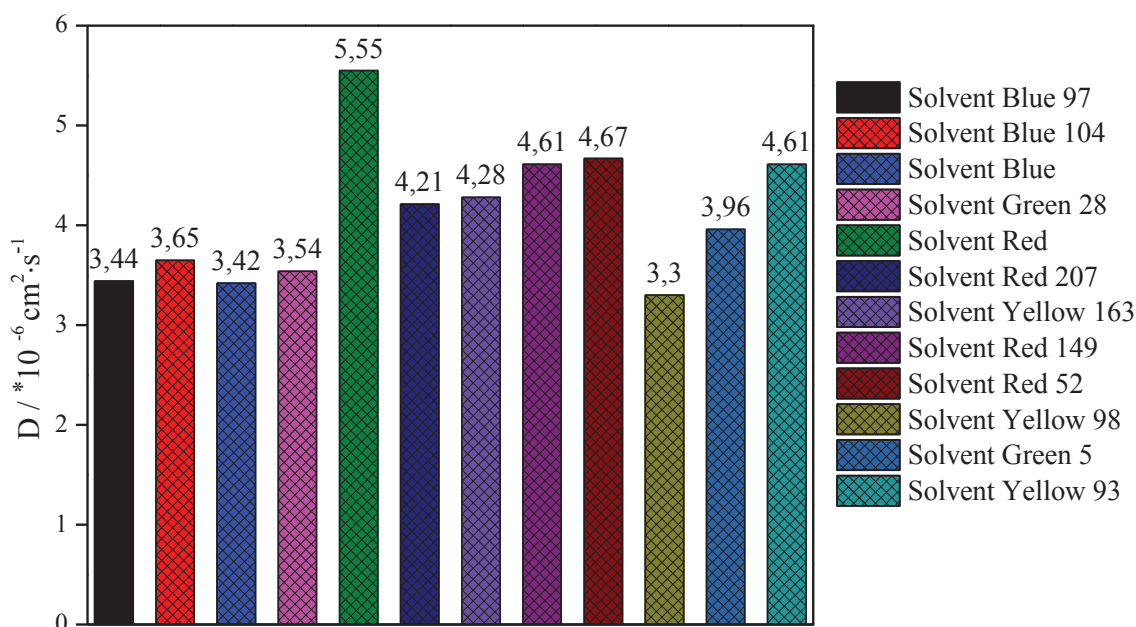


FIGURE 4.10 Diffusion coefficients of solvent dyes.

The common features of these dyes are their branched structure and aliphatic chains. Although the Solvent Yellow 98 dye had a relatively simple, non-branched structure, it had the lowest D of the studied dyes, most likely due to its long alkyl chain structure and high molecular weight. Long alkyl chains can significantly decrease the diffusion ability of molecules²⁷⁹. Diffusion occurs when molecules travel from an area of higher concentration to an area of lower concentration. For antioxidants, high diffusion coefficients are preferred. However, in the case of colorants, high mobility of the dye particles in the material can lead to non-uniform color and migration. Solvent Red, Solvent Red 52 and Solvent Yellow 93 had the highest diffusion ability, most likely because of their relatively low molecular weights. Of the studied stabilizers, Chimassorb 994 had the

²⁷⁷ D. P. Valencia, F. J. González, Understanding the linear correlation between diffusion coefficient and molecular weight. A model to estimate diffusion coefficients in acetonitrile solutions, *Electrochem. Commun.* 2011, **13**, 129–132.

²⁷⁸ S. A. Volyniyuk, V. I. Bezrodnyi, E. A. Tikhonov, Determination of the diffusion coefficients of dyes in polymer media by the absorption method with a high spatial resolution, *J. Appl. Spectrosc.* 2000, **67**, 623–628.

²⁷⁹ N. Dahmen, A. Kordikowski, G. M. Schneider, Determination of binary diffusion coefficients of organic compounds in supercritical carbon dioxide by supercritical fluid chromatography, *J. Chromatogr.* 1990, **505**, 169–178.

lowest diffusion ability ($D = 3.01 \text{ cm}^2\text{s}^{-1}$) because its bulky structure. Due to its relatively low molecular weight and low degree of branching, Chimassorb 81 had the highest diffusion coefficient ($4.51 \text{ cm}^2\text{s}^{-1}$) and thus the greatest tendency to move in an anhydrous environment among the stabilizers studied.

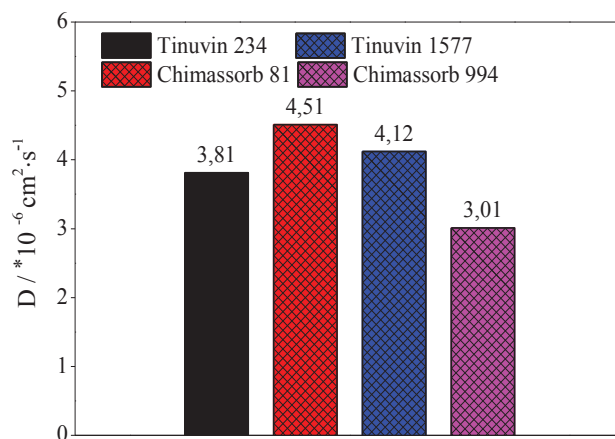


FIGURE 4.11 Diffusion coefficients of commercial stabilizers.

4.8 CONCLUSIONS

This chapter examined selected properties of polymer additives, such as dyes, pigments and stabilizers. These properties may determine their behavior in composites during use and aging. Nearly all of the tested dyes are able to withstand the processing conditions of the polymers at temperatures greater than $300 \text{ }^\circ\text{C}$. A thermal study of anthraquinone dyes showed that their heat stability increases with the polarity of the substituent group. Solvent Green 28 has the highest heat resistance due to the presence of hydroxyl auxochromes, which result in stronger intramolecular bonds. Thus, the stability is strongly related to the type and position of the substituent in the dye molecule, particularly in dyes with anthraquinone chromophores. Copper phthalocyanine (blue and green) and the HALS Chimassorb 994 also have high stabilities, with thermal resistances up to approximately $400 \text{ }^\circ\text{C}$. A spectrophotometric study showed that commercial stabilizers absorb most intensively in the UV region, whereas the strong electron-donating groups in anthraquinone dyes, especially Solvent Blue 97, Solvent Blue 104, Solvent Blue and Solvent Green 28, have maxima in the NIR region.

Anthraquinone dyes with stronger electron-releasing groups generally exhibited lower potentials of electrooxidation than other dyes and stabilizers. The highest antioxidant activity against $\text{ABTS}^{+\cdot}$ radical cations occurred in the anthraquinone dyes with the most strongly electron-donating groups, such as Solvent Green 28, Solvent Blue 97 or Solvent

CHAPTER 4 STUDIES OF THE PROPERTIES AND CHARACTERISTICS OF SOLVENT DYES AND PIGMENTS

Blue. Due to the presence of additional hydroxyl groups, the most effective was Solvent Green 28, which had the highest TEAC value of 195.4. Moreover, the theoretically calculated solubility parameters showed that the anthraquinone dyes with electron-releasing groups should have good solubility in the ethylene-norbornene polymer and low diffusion coefficients.

CHAPTER 5
EFFECT OF AGING ON THE PROPERTIES
OF NBR AND EN COMPOSITES

INTRODUCTION

The aim of this research was to investigate the effects of dyes, pigments and stabilizers on the properties of ethylene-norbornene (EN) and acrylonitrile-butadiene rubber (NBR) composites under weathering with UV irradiation ($\lambda = 343$ nm) and the full solar spectrum ($\lambda = 280$ -3000 nm) for various time periods. Moreover, during irradiation, the mechanical properties were measured by low and high degrees of deformation using dynamic mechanical analysis (DMA) and tensile tests until break, respectively.

Fourier transform infrared (FTIR) spectroscopy and XPS studies confirmed the presence of hydroxyl and carbonyl groups in the aged samples. However, the amounts of these groups depend on the type of additive in the composite. Changes in the color and surface defects in the investigated composites were evaluated using spectrophotometry and scanning electron microscopy (SEM). The effects of dyes and pigments on the properties of the tested composites were compared to a reference sample and stabilizer-based composites of ethylene-norbornene EN, which are commonly used in polymer technology.

5.1 EN COMPOSITES CONTAINING SOLVENT DYES UNDER UV AGING

5.1.1 MECHANICAL PROPERTIES

Polymer composites lose their mechanical properties during aging. Small changes in the physical or chemical structures can cause intense variations in the mechanical properties of the composites. Thus, the estimation of mechanical properties, such as tensile strength (TS) and elongation at break (Eb) during the aging process is important for evaluating polymer behavior during aging process.

Solvent dyes and stabilizer-based composites of EN were subjected to artificial UV aging ($\lambda = 343$ nm), and the changes in the mechanical properties of the samples were monitored over 1600 h of exposure.

Figure 5.1 (a-d) presents the TS and modulus at 300 % elongation as a function of irradiation time for EN composites that contain solvent dyes and commercial stabilizers. The reference sample (Topaz), EN/solvent dyes and EN/stabilizer composites had similar mechanical properties before UV irradiation. In general, the mechanical properties of all of the EN composites changed considerably during exposure. It is worth mentioning that two parallel processes occur during the aging of a polymer: crosslinking and chain scission²⁸⁰. In all of the samples, the modulus at 300 % elongation, which is related to the crosslink

²⁸⁰ N. S. Tomer, F. Delor-Jestin, R. P. Singh, J. Lacoste, Cross-linking assessment after accelerated ageing of ethylene propylene diene monomer rubber, *Polym. Degrad. Stabil.* 2007, **92**, 457–463.

CHAPTER 5 EFFECT OF AGING ON THE PROPERTIES OF NBR AND EN COMPOSITES

density, was found to increase with exposure time, which indicates crosslink formation during aging.

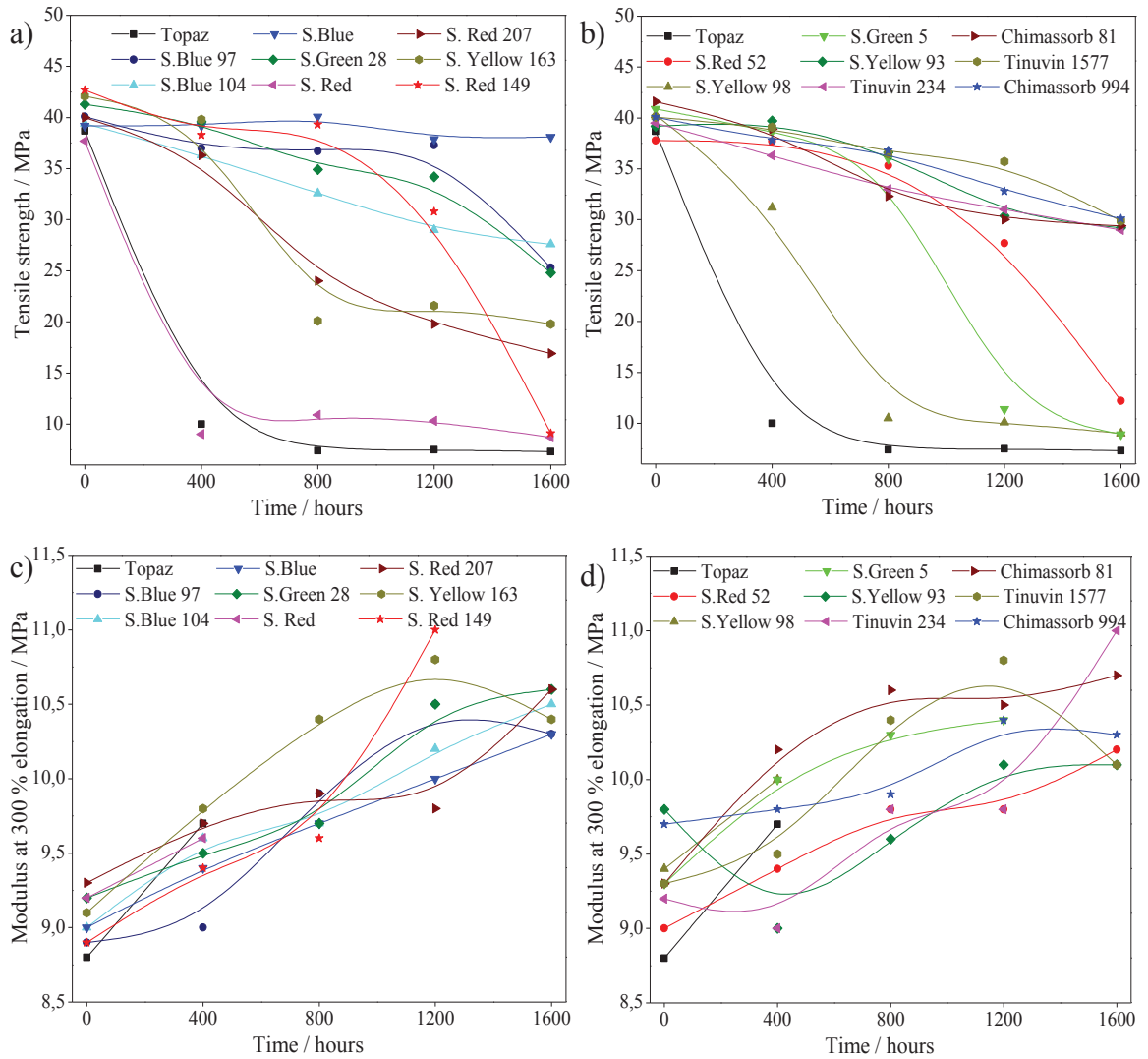


FIGURE 5.1 Tensile strength (a, b) and modulus at 300 % elongation at break (c, d) as a function of the UV aging time of EN composites that contain dyes and stabilizers.

Before aging, the reference sample had a tensile strength TS of 39.1 MPa. However, degradation develops rapidly under unfavorable aging conditions and leads to a marked decrease in TS of approximately 70 % after 400 h of UV radiation. With an increase in the aging time of the reference sample, an increase in the modulus and decreases in the TS as well as aging coefficient (S) were observed.

Moreover the aging factor (S) was much lower than 1 (after 400 h), what confirms the considerable degree of degradation of this sample. The ageing coefficient S was calculated from the ratio of the sample deformation energy and is combination of tensile strength and elasticity before and after aging (Fig. 5.2).

CHAPTER 5 EFFECT OF AGING ON THE PROPERTIES OF NBR AND EN COMPOSITES

Composites containing dyes and stabilizers exhibited similar trends to the reference sample (EN) but had better resistance to aging. The mechanical properties decreased rapidly with UV exposure duration only in the EN/Solvent Red composite; after 400 h of irradiation, it had a TS (9.1 MPa) and S (0.1) that were similar to or slightly lower than those of pure EN. The photostability and thermostability of substituted anthraquinone derivatives have been found to increase with the electron-donating power of the substituents in the α -positions. It appears that the 1-amino substituent that is present in the Solvent Red dye have poor stability, which leads to dye degradation. Thus, Solvent Red is more vulnerable to aging²⁸¹.

All of the studied EN composites that contain solvent dyes, except S. Red, exhibited better resistance to aging than the reference sample. As indicated by the aging coefficients (S), the use of Solvent Blue 97, Solvent Blue 104, Solvent Blue, Solvent Green 28 and Solvent Yellow 93 is most effective in increasing the durability of ethylene-norbornene films. This observation might be related to the UV absorption capability of the dyes, as previously determined by spectroscopic measurements (section 4.3). Nevertheless, such dyes as Solvent Red 52 and Solvent Red 207, which exhibited absorption bands near the UV region (343 nm), were less effective in protecting EN composites than anthraquinone dyes with strong electron-donating moieties. These results suggest that the greatest improvement in the durability of EN/solvent dye composites is related to not only the absorption of irradiation but also the ability of the dye to react with the radicals that form during the aging process.

The antioxidant activity of solvent dyes was assessed in a previous chapter (Chapter 4.4) by reacting them with ABTS^{•+} cation radicals. The characteristic ABTS absorption maximum at 734 nm was significantly weakened upon reaction with Solvent Blue 97, Solvent Blue and Solvent Green 28, which confirms the free radical scavenging ability of these dyes. These results agree with data obtained from mechanical tests, as these dyes effectively improve the durability of EN composites. Although the activity of the Solvent Blue 104 dye toward ABTS^{•+} cation radicals was not detected, it had a good protective effect during aging and has a similar chemical structure to Solvent Blue 97, which suggests a similar protective mechanism in the EN composite.

²⁸¹ O. P. Sharma, T. K. Bhat, Antioxidant and antibacterial activity of *Hippophae rhamnoides* methanolic leaf extracts from dry temperate agro-climatic region of Himachal Pradesh, *Food Chem.* 2009, **113**, 1202–1205.

CHAPTER 5 EFFECT OF AGING ON THE PROPERTIES OF NBR AND EN COMPOSITES

Figure 5.1 (b, d) and Figure 5.2 (b) show the response of the mechanical properties (tensile strength and aging coefficient) of stabilizer-based EN composites under accelerated aging. The EN/stabilizers showed high tensile strengths and aging coefficients after 1600 h of aging. The most significant reductions in the tensile strength and aging coefficient were observed in the EN/Chimassorb 81 composite, decreasing to 31.1 MPa and 0.63, respectively, after 800 h.

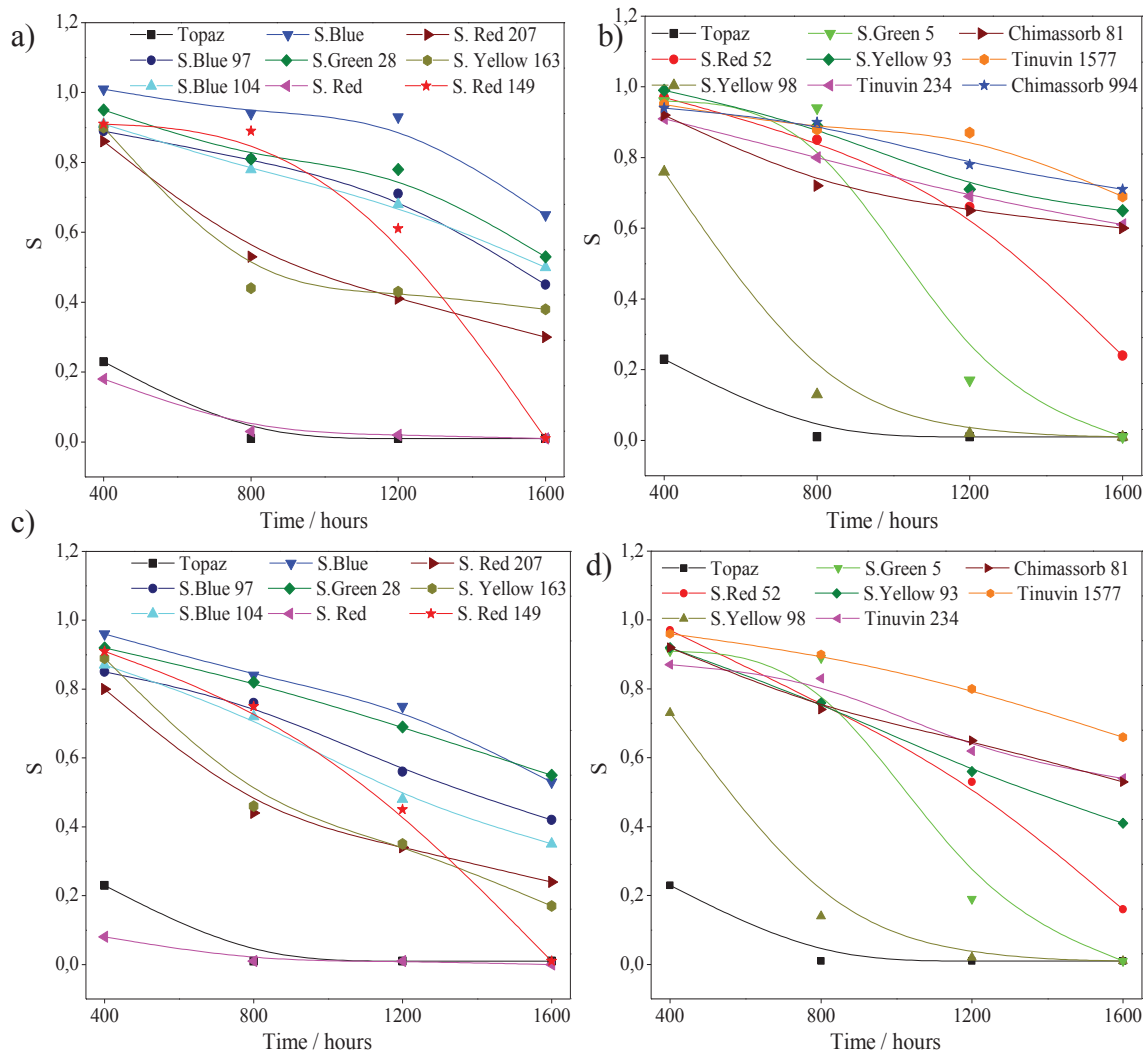


FIGURE 5.2 Aging coefficient S (a, b) as a function of the UV aging time of EN composites that contain dyes and stabilizers at different concentrations: 0.2 phr (a, b) and 3.5×10^{-4} M (c, d).

The best protection against UV aging after 1600 h was provided by Tinuvin 1577 and Chimassorb 994, as indicated by their aging coefficients of 0.69 and 0.71, respectively. The introduction of stabilizers markedly enhanced the EN resistance to UV aging and gave better results than solvent dyes. The difference in the mechanical properties becomes more significant after 1600 h of UV exposure.

CHAPTER 5 EFFECT OF AGING ON THE PROPERTIES OF NBR AND EN COMPOSITES

The concentrations of dyes and stabilizers in the studied composites were calculated by weight (0.2 phr). To better estimate the effects of these additives on EN materials, the influence of the number of dye particles and stabilizer molecules on the EN composite was investigated. Composites that contained 3.5×10^{-4} M of dyes and stabilizers were also subjected to aging for the same durations and conditions. The results are shown as the aging factor in Figure 5.2 d, e. EN composites that contain 0.2 phr and 3.5×10^{-4} M showed only slight differences in their S values and similar aging profiles. These investigations demonstrate that the number of particles in the composites has no significant impact on the final result of aging.

However, the aging coefficient of the EN composite with 3.5×10^{-4} M S. Yellow 93 was lower than that in the sample with 0.2 phr of this dye because the latter contained more dye particles, as its molecular weight is much lower than that of the other dyes. Because Chimassorb 994 has a very high molecular weight, it was not considered in this comparison.

5.1.2 SURFACE ANALYSIS – FTIR

Hydroxyl groups are formed in the ethylene-norbornene chains and composites during aging. IR spectroscopic measurements allowed the carbonyl index to be determined based on the ratio of the band intensity for the carbonyl group to the band intensity for the C-H group²⁸². The photooxidation behavior of EN/composites was monitored by FTIR spectra, revealing notable changes (Fig. 5.3 a, b). To determine the aging progress and assess the effective lifetime of the materials, components, or products, FTIR spectra were recorded before, during, and after aging.

The highest values of the carbonyl index after 400 h of UV exposure were observed for the EN composites that contained Solvent Red, Solvent Yellow 163, and Solvent Yellow 98 as well as the reference sample. These results are consistent with previous results (tensile strength and aging coefficient) that showed that the mechanical performance of pure EN samples decreases as the amount of carbonyl increases.

The analysis of solvent dye-based composites showed that the lowest carbonyl indexes were detected in anthraquinone dyes with strong electron-donor groups (S. Blue 97, S. Blue 104, S. Blue and S. Green 28) as well as in S. Yellow 93. These results are in agreement with the mechanical properties of these samples and confirm their effectiveness

²⁸² J. V. Gulminea, P. R. Janissekb, H. M. Heiseck, L. Akcelrudd, The effect of accelerated aging on the surface mechanical properties of polyethylene, *Polym. Degrad. Stab.* 2003, **81**, 367–373.

CHAPTER 5 EFFECT OF AGING ON THE PROPERTIES OF NBR AND EN COMPOSITES

in prolonging the lifetime of EN composites. Of the stabilizers, Tinuvin 1577 and Chimassorb 994 provided the best protection to EN/composite (Fig. 5.2 b).

The surfaces of EN samples that contained 3.5×10^{-4} M of dyes and stabilizers were also examined. It appears that the number of dye and stabilizer particles exert a stronger influence on the concentration of carbonyl groups in EN composites than the mechanical properties do. The surfaces of EN/S. Green 5 and EN/Tinuvin 235 were particularly affected by the aging process. Nevertheless, the aging of most samples was similar to that in the samples that contain dyes and stabilizers added by weight. Solvent Red caused an increase in the carbonyl index, despite lower amount of particles which suggests that it accelerates the aging of the polymer (Fig. 5.3 c).

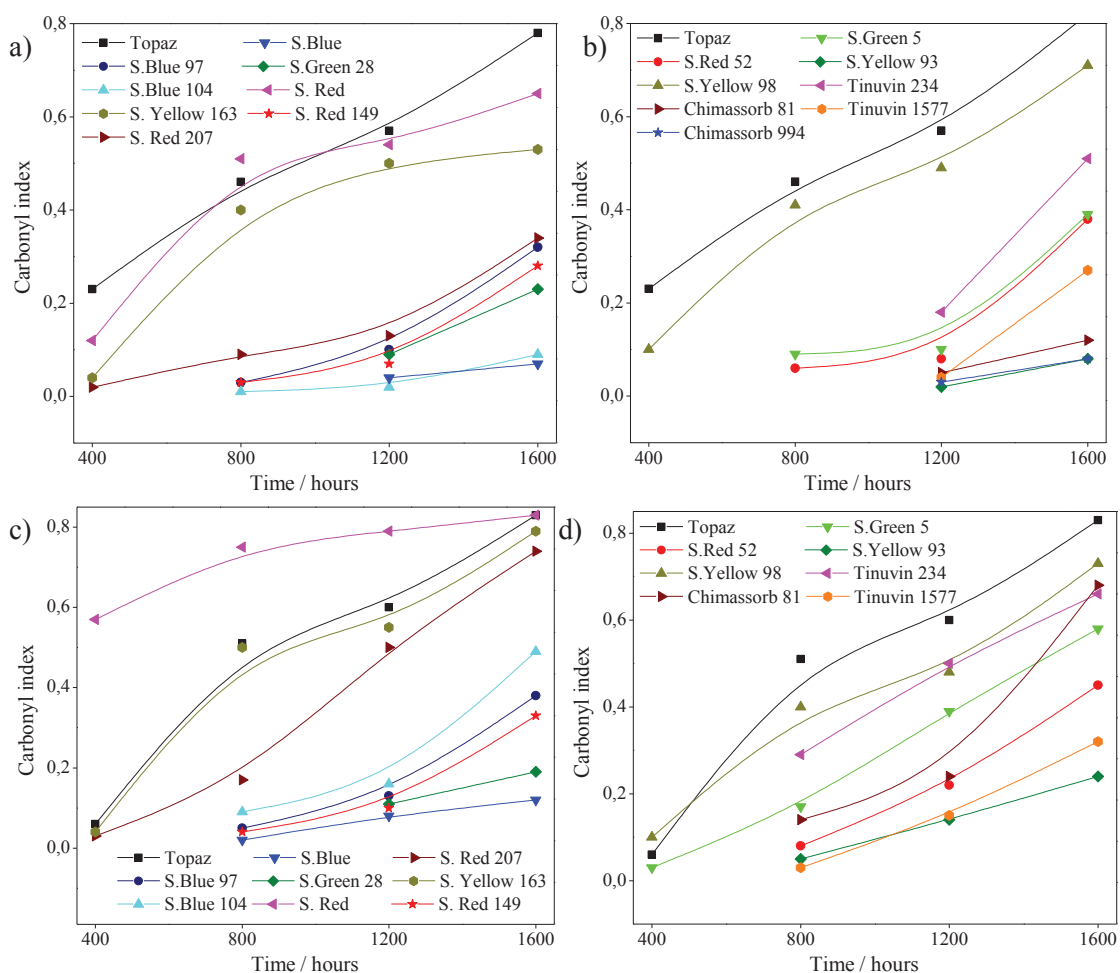


FIGURE 5.3 Carbonyl index (a, b) as a function of the UV aging time of EN composites that contain dyes and stabilizers at different concentrations: 0.2 phr (a, b) and 3.5×10^{-4} M (c, d).

5.1.3 COLORIMETRIC STUDY OF EN COMPOSITES UNDER UV AGING

This section examines the color stability of solvent dye-based composites of ethylene-norbornene during UV aging. Colorimetric analysis provides important data about color changes in materials, which can be related to the formation of oxidizing groups in the polymeric chains and/or the decomposition of colorants that are incorporated in the polymer. A spectrophotometric method that is based on calculating color differences from visible spectra in the CIELab color space was used to monitor the discoloration process. Table 5.1 shows the results of the color variation studies of the EN/solvent dye composites that were the most sensitive to the aging processes. The obtained color results are expressed in terms of the total color difference (ΔE) and the differences in the color parameters (ΔL^* , Δa^* , Δb^*). Despite degradation during aging, as in the case of colorless samples, such as EN and EN/stabilizer composites, the color variations are only slightly noticeable compared to the dyed materials.

TABLE 5.1 Color parameters of the ethylene–norbornene composites containing solvent dyes as a function of the UV aging time.

EN/composites	Aging time [hours]	ΔE	ΔL^*	Δa^*	Δb^*
Solvent Red	200	8.99	6.3	-8.78	2.01
	400	19.56	10.7	-7.97	3.93
	800	22.05	11.28	-12.19	-5.33
	1200	25.02	12.14	-13.03	-5.26
Solvent Red 207	800	19.15	7.85	-8.03	-5.13
	1200	23.11	9.23	-10.12	-7.40
Solvent Red 149	400	6.12	9.28	-18.24	-3.28
	800	17.18	10.15	-18.24	-3.28
	1200	22.13	11.42	-20.17	-5.02
Solvent Yellow 98	800	20.85	-12.04	7.29	-10.02
	1200	24.16	-18.52	8.99	-14.12
Solvent Yellow 163	800	13.09	-4.43	-2.48	-8.01
	1200	20.16	-6.58	-1.96	-10.15
Solvent Green 5	800	12.03	-15.38	-10.26	-12.77
	1200	19.08	-16.09	-13.62	-16.57

The EN composite that contained Solvent Red was the most affected most by UV aging in terms of color change. The total color difference ΔE was as high as 10.99 after 200 h of UV aging. Further aging treatments of EN/S. Red composite resulted in discoloration (400 h), which was reflected in increases in the ΔE and Δa^* parameters of the CIELab color coordinates. The discoloration effect was most likely the result of the destruction of the

CHAPTER 5 EFFECT OF AGING ON THE PROPERTIES OF NBR AND EN COMPOSITES

chromophore ring structures in the dye molecules by UV exposure. For that reason, the values of the color coordinates were significantly lower after 800 h and 1200 h of exposure (Fig. 5.4). Moreover, color changes after aging may be correlated with other factors, such as polymer degradation or stain accumulation ²⁸³.

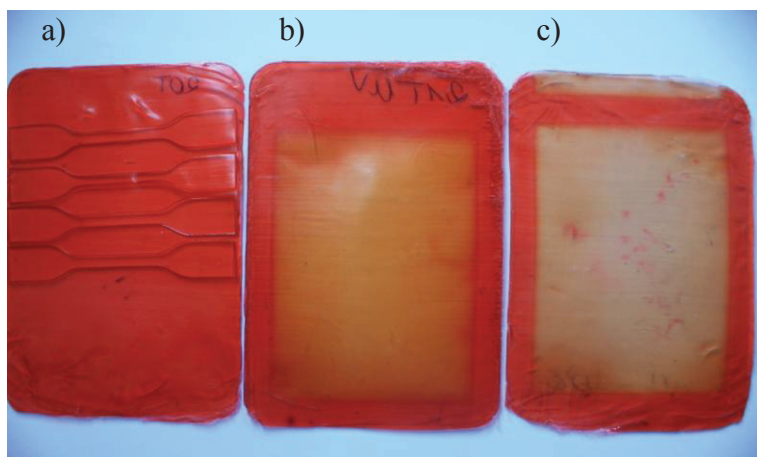


FIGURE 5.4 Images of EN composites that contain Solvent Red dye: before UV aging (a), after 200 h of UV aging (b) and after 400 h of UV aging (c).

The results obtained for EN/S. Red 149 and EN/S. Red 207 composites showed increases in ΔE^* and substantial decreases in Δa^* over time. The coordinate a^* exhibits increases in the red hue along the long positive axis and the green hue along the long negative axis. In contrast, progressive decreases in the b^* values of EN/S. Yellow 98, EN/S. Yellow 163 and EN/S. Green 5 composites indicate the degradation of yellow chromophores in the samples, as the coordinate b^* indicates an increase in the yellow hue along the long positive axis and the blue hue along the long negative axis ²⁸⁴.

Figure 5.5 shows the changes in the reflectance spectra as a result of the aging process for EN composites colored by S. Red 149 (Fig. 5.5 a) and S. Green 5 (Fig. 5.5 b) dyes. Comparison of the reflectance values of the EN/S. Red 149 sample at the start time (green line) with the respective values after 400 h of UV aging (blue line) confirms a marked decrease in red and a slight increase in blue with exposure time. An intense color variation was noted for the EN/S. Green 5 sample, where the decreases in green and yellow after 800 h of irradiation were caused by the slow degradation of the Solvent Green 5 dye chromophore. The discoloration of all of the dye composites was generally preceded by the appearance of carbonyl groups on the surface.

²⁸³ Y. K. Lee, B. S. Lim, S. H. Rhee, H. C. Yang, J. M. Powers, Changes of optical properties of dental nano-filled resin composites after curing and thermocycling, *J. Biomed. Mat. Res. B. Appl. Biomater.* 2004, **71**, 16–21.

²⁸⁴ R. G. Kuehni (1997), *Color: An Introduction to Practice and Principle*, New York, John Wiley & Sons.

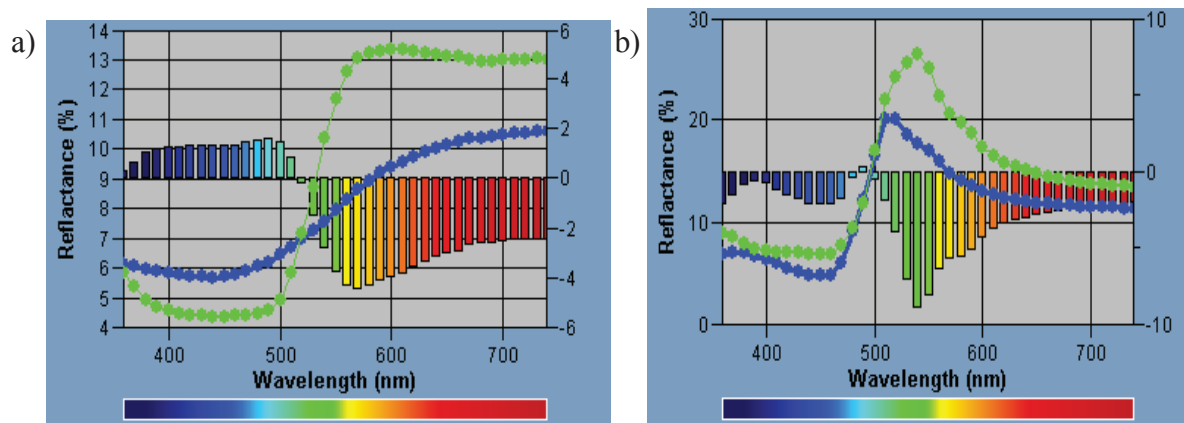


FIGURE 5.5 Color variations in EN composites that contain Solvent Red 149 after 400 h of UV aging (a) and Solvent Green 5 after 800 h of UV aging (b); green line – before aging; blue line – after aging.

5.2 EN COMPOSITES CONTAINING PIGMENTS UNDER UV AGING

The effects of Pigment Blue 15:1, Pigment Green 7, Pigment Yellow 173 and *trans*-indigothiazine on the properties of EN composites during the aging process are discussed in this section and compared with previous results obtained from EN/solvent dye composites. Moreover, the behavior of dyes and pigment mixtures in EN composites under UV exposure was also examined. Figure 5.6 a–c depicts the changes in the mechanical properties (aging coefficient, S) and the carbonyl index of aged EN/pigment and EN/pigment/dye composites for different time periods.

As expected, the most significant decrease in the mechanical properties with increasing aging time was found for the reference sample. The addition of pigment at 0.2 phr loading improved the durability of the composites, and the decrease of the properties in these samples was reduced to different degrees depending on the type of pigment applied (Fig. 5.6 a, b). The analysis of S and the carbonyl index showed that phthalocyanine blue (P. B. 15:1) provided the best protective effect and exhibited a strong absorption band in the UV region and very high thermal resistance. Even after 1200 h of exposure, composite EN/P. Blue 15:1 showed minor changes in S ($S = 0.92$) and a low concentration of carbonyl groups on the surface (0.08). A weak anti-aging potential of Pigment Green 7 in the EN polymer ($S = 0.73$, carbonyl index = 0.23 after 1200 h) can be explained by a low number of particles because the molar mass of this compound is much greater than that of the other pigments.

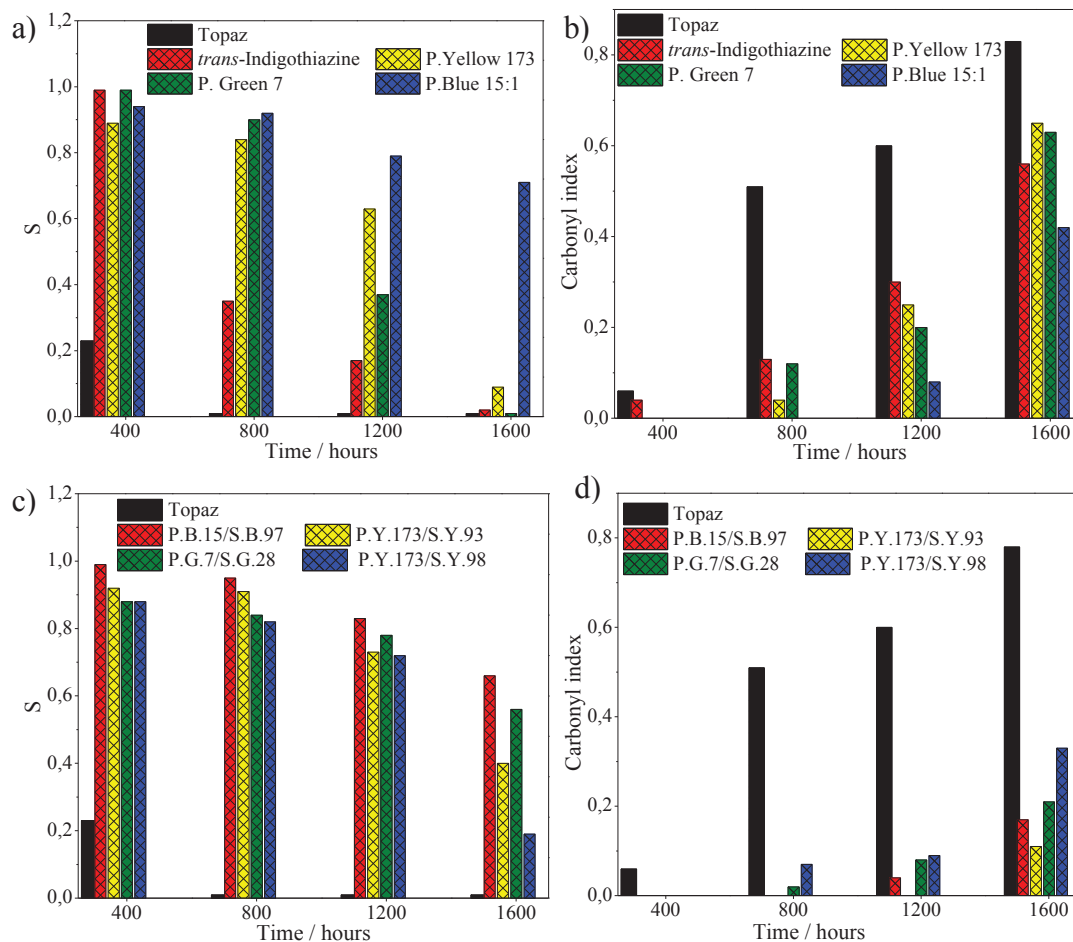


FIGURE 5.6 Aging coefficient S (a, c) and carbonyl index (b, d) as a function of the UV aging time of EN composites that contain pigments and mixtures pigments/dyes in ratio 0.1 phr/0.1 phr.

The S and carbonyl index values of EN/pigment and EN/dye (section 5.1) composites after 800 h of irradiation show that the samples that contain the Solvent Blue, Solvent Blue 104 and Solvent Green 28 dyes showed better resistance to UV exposure than composites with pigments (*trans*-Indigothiazine, Pigment Green 7, Pigment Yellow 173).

The exception was the composite EN/P. Blue 15, which had a higher S factor ($S = 0.71$) than that of the samples that contained solvent dyes after 1600 h of irradiation; however, it also had a higher carbonyl index (0.42). As previously mentioned, the loss of color in the samples that contained dyes was preceded by the appearance of carbonyl groups on their surfaces.

Interestingly, the colors of the composites with EN/pigments (e.g., EN/P. Yellow 173) remained nearly unchanged despite the extended degree of degradation, even after 1600 h (Fig 5.7). This effect occurs because the color in pigments is associated with not only the chemical structure but also the arrangement of molecules in the crystal lattice²⁶².

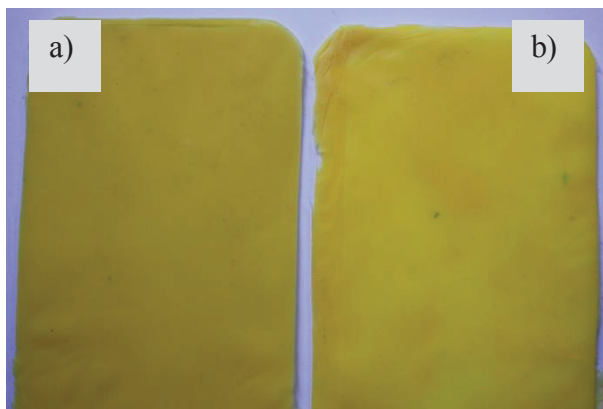


FIGURE 5.7 Images of EN composites that contain Pigment Yellow 173 (0.2 phr) before (a) and after (b) 1600 h of UV aging.

In polymer composites based on combinations of solvent dyes and pigments, the pigments create dispersion in which there are some distances between the pigment crystals (depending on the pigment concentration), while the dyes form a molecular solution which fills the composite-free spaces between the pigment particles. Figure 5.8 shows that the composites filled with mixtures of dye and pigment showed higher resistance to aging than composites that only contain pigments (or only dye for composite EN/P.Yellow 173/S.Yellow 98). The exception was EN/P. Blue 15:1, which showed better mechanical properties during UV exposure (Fig. 5.6 c, d). This effect may be the result of a synergistic effect of dispersed pigment crystals and the molecular solution that forms the dye in the composite. Additionally, the studies showed that dyes better protect the surfaces of the composites, while pigments protect the bulk composite despite having a higher carbonyl index.

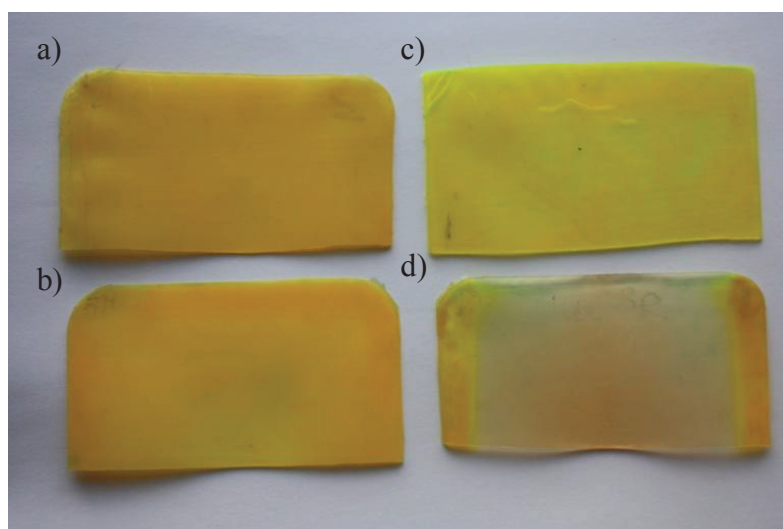


FIGURE 5.8 Images of EN composites that contain mixtures of Pigment Yellow 173 (0.1 phr) and Solvent Yellow 98 (0.1 phr) before (a) and after (b) 1600 h of UV aging and Solvent Yellow 98 (0.2 phr) before (c) and after (d) 1600 h of UV aging.

Generally, pigments have a favorable influence on the stability of polymer composites and selectively absorb and reflect radiation. Light that is reflected or scattered from the crystal grains of the pigment most likely contributes to the deterioration of surface composites. This effect of pigments will also be observed in acrylonitrile-rubber composites.

5.3 EN COMPOSITES CONTAINING SOLVENT DYES SUBJECTED TO WEATHERING WITH A FULL SOLAR SPECTRUM

5.3.1 MECHANICAL PROPERTIES (STATIC AND DYNAMIC)

This section discusses the effects of dyes and stabilizers on the weathering behavior of EN composites. As in the previous studies, EN composites that contain solvent dyes and stabilizers were subjected to aging. However, the aging conditions in this study include radiation with the full solar spectrum ($\lambda = 280\text{-}3000$ nm).

Figure 5.9 a–d illustrates the changes in the mechanical properties (tensile strength and 300 % modulus) of EN composites that contain dyes and stabilizers as a function of the aging time. The tensile strengths of all of the study samples decrease gradually with time, whereas the stress at 300 % elongation increases. As in UV aging, the type of applied solvent dye or stabilizer was an important factor that controlled the lifetimes of the EN materials. The general behavior of the EN composites is similar to the results obtained from UV aging; however, large differences in the durability of EN/solvent dye and EN/stabilizer composites were observed. Moreover, as a result of the extended aging process, decreases of the modulus were noted at 300 % elongation after 1050 h in the EN, EN/S. Red and EN/S. Red 149 composites.

The initial mechanical properties of the EN/stabilizer composites were similar, and the differences become more prominent after 700 h of weathering exposure. The TS values of the EN/Tinuvin 234 and EN/Chimassorb 81 composites decreased rapidly to 26.5 MPa and 25.4 MPa, respectively. Moreover Figure 5.9 b shows that the crosslinking process dominates in the EN/stabilizer samples, as revealed by the increase of the modulus²⁸⁵.

Figure 5.10 illustrates the aging of the investigated composites as a function of S, (Fig. 5.10 a, b). The S values of samples that contain dyes with anthraquinone chromophores demonstrate that the greatest improvements in the durability of EN were provided by the

²⁸⁵ T, Ha-Anh, T. Vu-Khanh, Prediction of mechanical properties of polychloroprene during thermo-oxidative aging, *Polym. Test.* 2005, **24**, 775–780.

CHAPTER 5 EFFECT OF AGING ON THE PROPERTIES OF NBR AND EN COMPOSITES

addition of S. Blue 97, S. Blue 104, S. Blue and S. Green 28. Of the other solvent dyes, the best retention of mechanical properties was observed in the EN/S. Yellow 93 composite. The results exhibited a similar trend to the aging study, in which the wavelength was $\lambda = 343$ nm. However, the addition of stabilizers to EN did not enhance the durability of the composites as effectively as under UV exposure. The S values indicate significant aging in composites with Tinuvin 234 and Chimassorb 81 after 700 h. The reduction in the mechanical properties of EN/Tinuvin 1577 was less prominent than the other stabilizers.

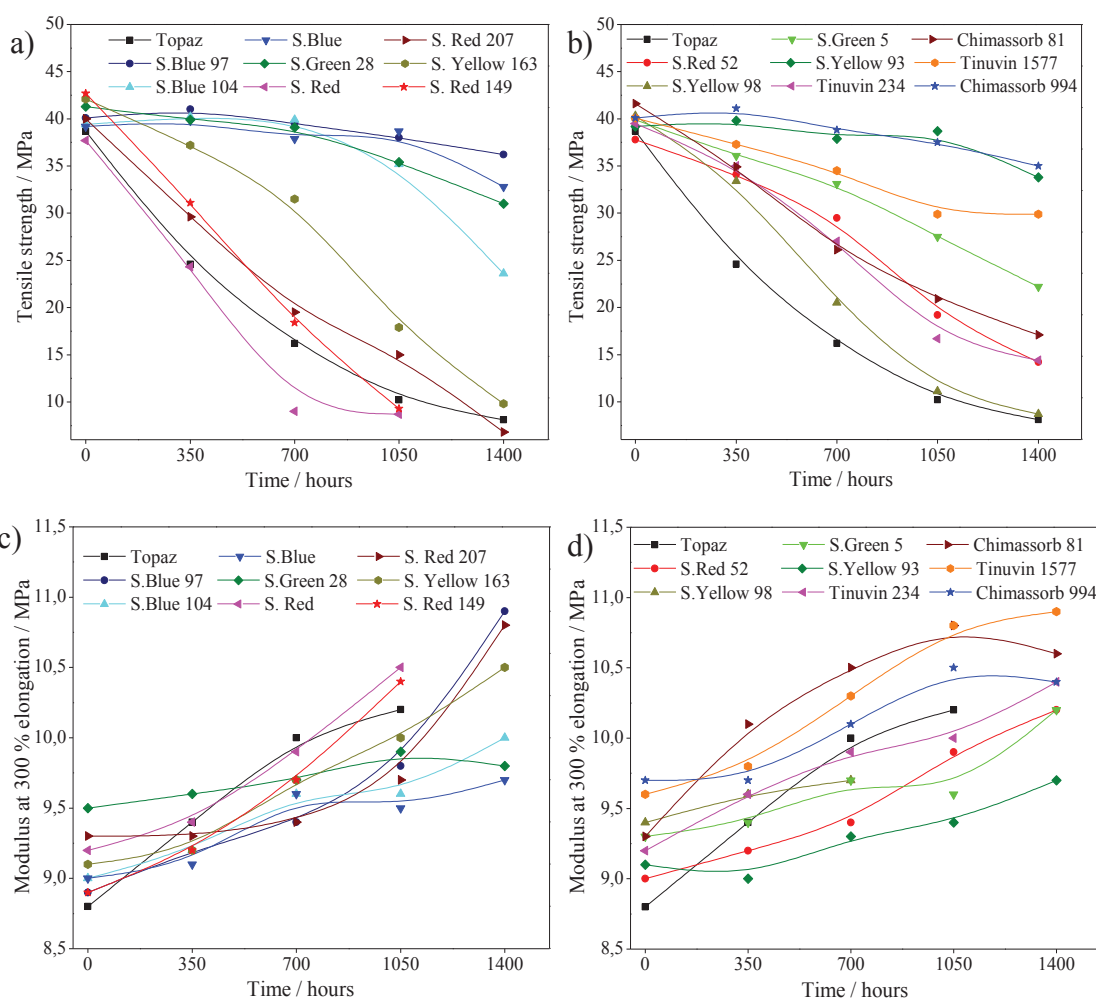


FIGURE 5.9 Tensile strength (a, b) and modulus at 300 % elongation at break (c, d) of EN composites that contain dyes and stabilizers as a function of the weathering time.

Nevertheless, the investigated stabilizers (Tinuvin 234, Chimassorb 81 and Tinuvin 1577) exhibited worse protection of the samples during weathering than some of the solvent dyes. Of the investigated additives, the best durability during both weathering and UV aging was found for composites that contain HALS (Chimassorb 994), which confirmed their high antioxidant efficiency.

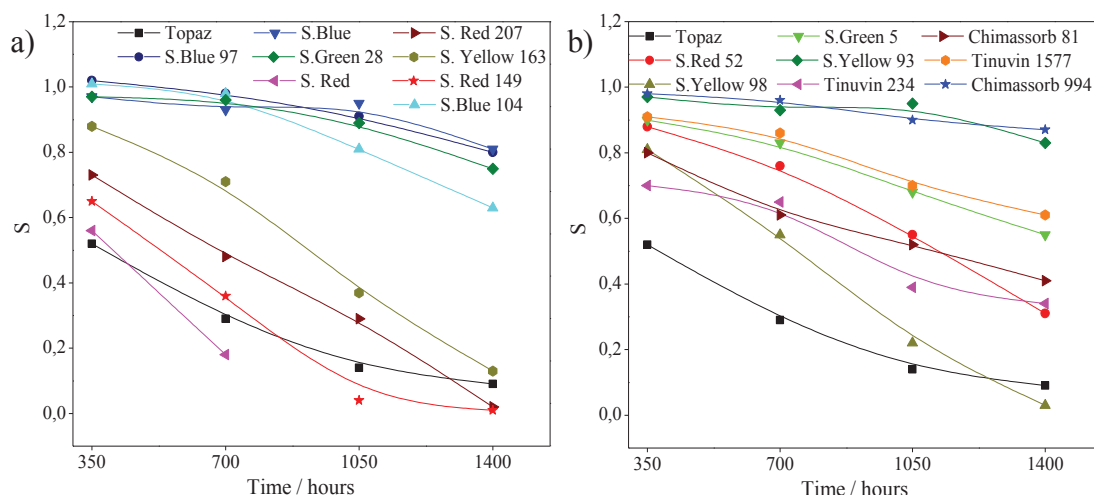


FIGURE 5.10 Aging coefficients S (a, b) of EN composites that contain dyes and stabilizers as a function of the weathering time.

The obtained results revealed that the application of anthraquinone dyes with strong electron-donating substituents significantly prolonged the lifetimes of the EN composites during aging. Based on the previous study, the common features of these dyes (S. Blue 97, S. Blue 104, S. Blue and S. Green 28) are high thermal stability, good ability to react with free radicals and absorption maxima in the near UV and infrared regions of the spectrum. The improvement in the durability of the EN/solvent dye composites might originate from ability of the dye to absorb light and react with radicals as well as the high thermal stability of their particles. Under UV exposure, commercial stabilizers provided better resistance of EN/composites against aging than stabilizers with solvent dyes.

It is interesting that, under weathering with the full solar spectrum, the protection efficiency of solvent dyes in EN composites was much greater than for most of the investigated stabilizers. This effect may be caused by several factors. The conditions in the weathering chamber affected the stabilizer particles and reduced their absorbance efficiency, and this type of stabilizer may not provide sufficient protection under these aging conditions. On the other hand, the four dyes with strong electron-donating substituents (S. Blue 97, S. Blue 104, S. Blue and S. Green 28) had absorption maxima in the near infrared region (approximately 700 nm). The absorbance of this irradiation may also affect the structure of dyes, and therefore may impact the aging process.

The good stability of EN/S. Yellow 93 composite may be related to the presence of intensive maxima in the near UV region and a greater number of molecules (as was discussed in section 5.1).

Figure 5.11 shows the change of E' and $\tan\delta$ in both materials before and after 1400 h of irradiation. The change of the damping properties of materials during aging is due to

changes in the polymer structure. The formation of a three-dimensional network by means of crosslinking leads to decreases of the chain mobility and the maximum loss factor ($\tan\delta_{\max}$)²⁸⁶.

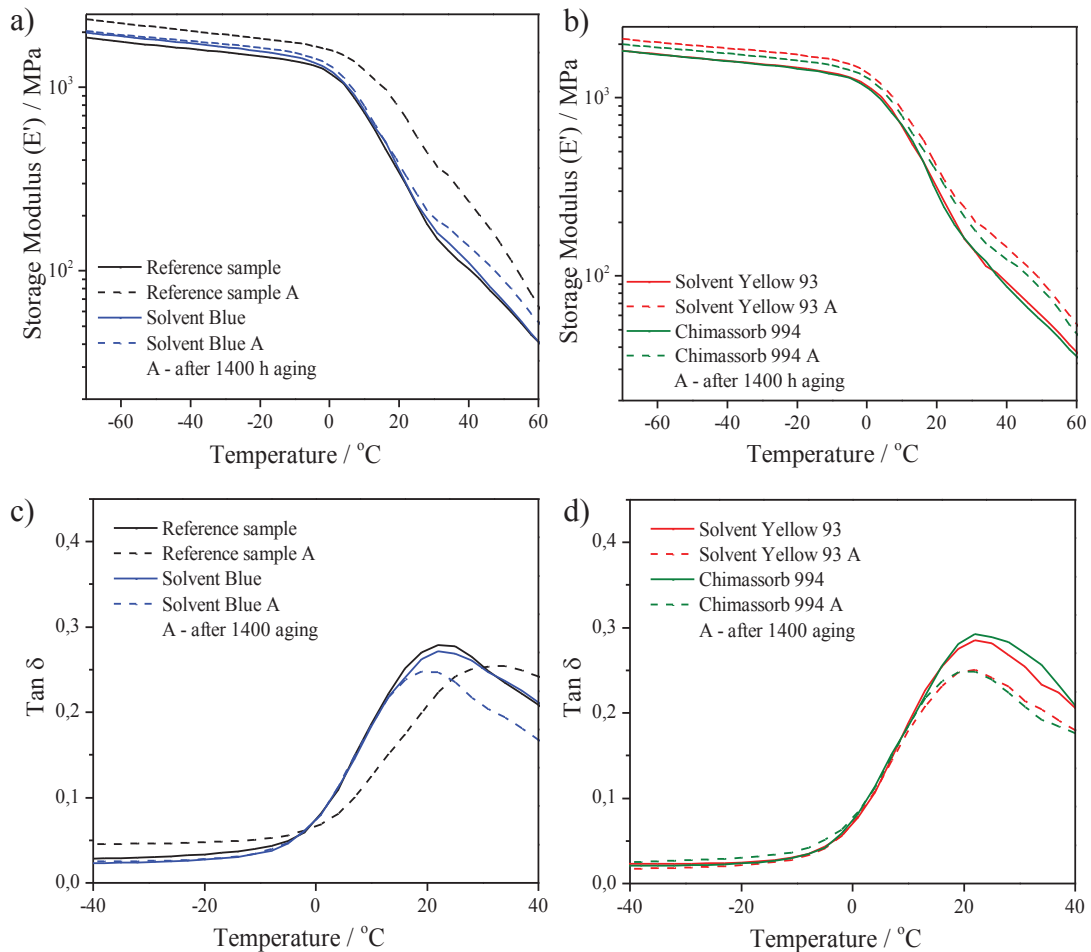


FIGURE 5.11 Temperature dependence of the storage modulus E' (a, b) and the decrease of the tangent $\tan\delta$ (c, d) at 10 Hz for EN composites before and after 1400 of aging.

All of the composites exhibited higher stiffnesses after aging, which is reflected in the higher values of the storage modulus (E'). The most significant increase in E' occurred in the reference sample EN after exposure to weathering. Moreover, the curve that corresponds to the maximum loss factor shifted to higher temperatures after aging, and a decrease in the maximum loss factor is noted. In this case, DMA showed the most significant variations in the visco-elastic properties during outdoor exposure for the reference sample. This observation is consistent with the results obtained from the static properties. Some of the variations in the glass transition temperature (T_g) of the composites can be related to the changes in the polymer structure as a result of aging.

²⁸⁶ M. C. S. Perera, U. S. Ishiaku, Z. A. M. Ishak, Thermal degradation of PVC/NBR and PVC/ENR50 binary blends and PVC/ENR50/NBR ternary blends studied by DMA and solid state NMR, *Polym. Degrad. Stab.* 2000, **68**, 393–402.

5.3.2 DIFFERENTIAL SCANNING ANALYSIS OF EN COMPOSITES

The effects of aging on EN composites that contain selected dyes (Solvent Blue, Solvent Green 28) and the stabilizer Tinuvin 234 were studied using differential scanning calorimetry (DSC). The values of T_g and heat flow (expressed as the enthalpy ΔH) of the samples before and after aging are shown in Table 5.2 and Figure 5.12 (a-d).

TABLE 5.2 Characteristic values obtained from the DSC analysis of EN composites before and after aging.

Sample	T_g from DSC / °C	ΔH J·g ⁻¹
EN	-1.8	-75.7
EN after 1400 h	2.5	-80.3
EN/Tinuvin 234	-2.0	-73.5
EN/Tinuvin 234 after 1400 h	4.8	-81.1
EN/Solvent Blue	-1.3	-74.4
EN/Solvent Blue after 1400 h	-1.7	-58.2
EN/Solvent Green 28	-1.2	-73.4
EN/Solvent Green 28 after 1400 h	-1.4	-58.6

The analysis of the EN composites before aging shows that the T_g values of the Tinuvin 234 and solvent dyes are only slightly different from those of the reference sample. The application of dyes and stabilizers did not affect the crystal phase; the enthalpies of the studied samples ranged from -73.4 J·g⁻¹ to -74.7 J·g⁻¹. However, significant difference in the glass transition temperatures and the content of the crystalline phase were present after 1400 h of aging.

The density and crystalline content of some of the polymers increase at the beginning of degradation^{287, 288}. After 1400 h of weathering, T_g increased in the EN composites and EN/Tinuvin 234, which was likely due to the increase in the crosslink density as well as some changes in the crystal structure of the samples. Moreover, both composites showed increases in the crystalline phase content, as the energies required for the phase transitions for EN and EN/Tinuvin 234 increased to -80.3 J·g⁻¹ and -81.1 J·g⁻¹, respectively.

The behavior of the composites that contain dyes was different after weathering. After 1400 h of exposure, the composites with solvent dyes (Solvent Blue and Solvent Green 28) showed slight decreases in the T_g values and reductions of the crystalline phase. It appears

²⁸⁷ M. Elvira, P. Tiemblo, J. M. Go´mez-Elvira, Changes in the crystalline phase during the thermo-oxidation of a metallocene isotactic polypropylene. A DSC study, *Polym. Degrad. Stab.* 2004, **83**, 509–518.

²⁸⁸ M. S. Rabello, J. R. White, Crystallization and melting behaviour of photodegraded polypropylene- II. Recrystallization of degraded molecules, *Polymer* 1997, **38**, 6389–6399.

that the presence of this type of dye hinders the crystallization and formation of crystals during the aging process.

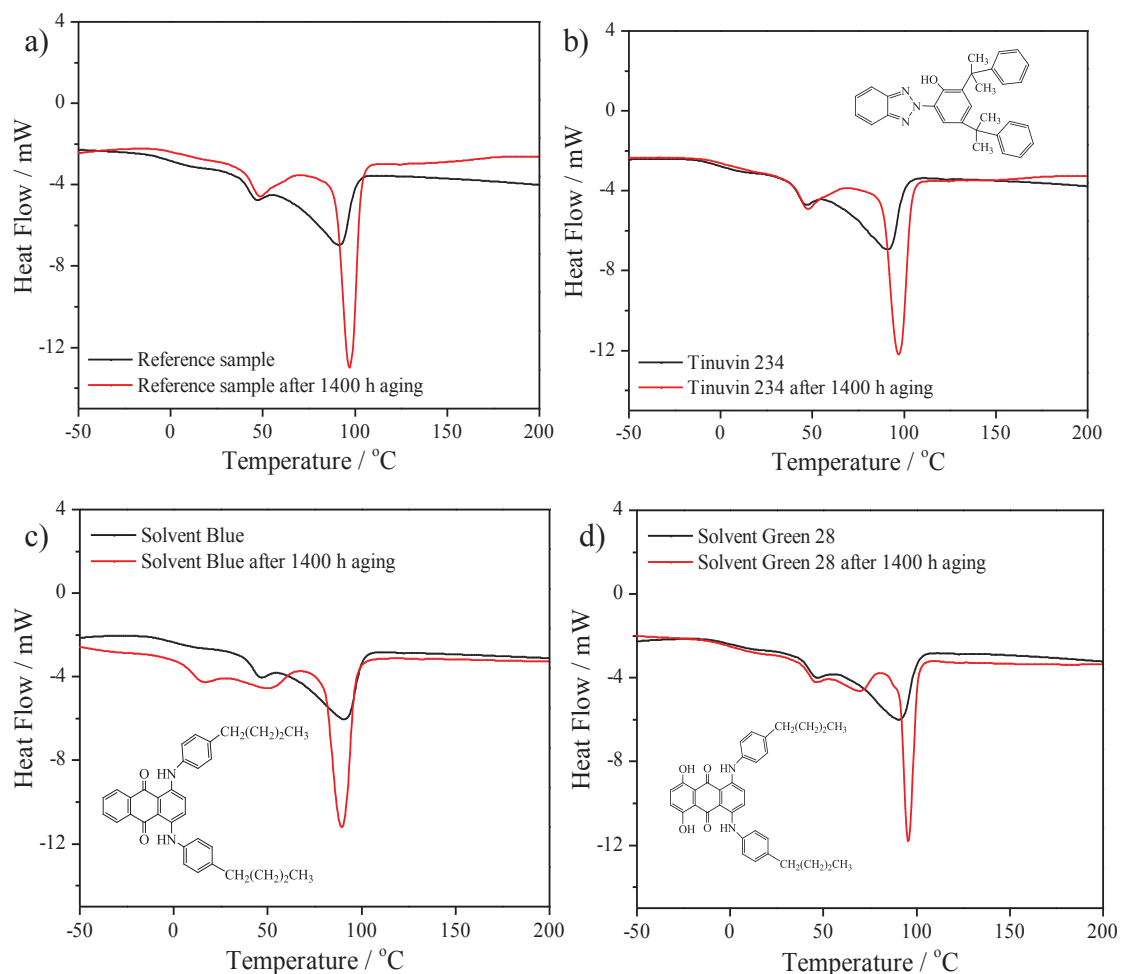


FIGURE 5.12 DSC curves of EN composites: pure EN (a), EN/Tinuvin 234 (b), EN/S. Blue (c), EN/S. Green 28 (d) before (black line) and after 1400 h of aging (red line).

5.3.3 SURFACE ANALYSIS – FTIR AND XPS

Figure 5.13 shows the changes in the carbonyl indexes of EN composites with different solvent dyes and stabilizers. The highest values of the index after 700 h were obtained in the EN composites that contained Solvent Red and Solvent Red 149 and in the reference sample. The lowest intensities of the carbonyl group after 1400 h of irradiation were detected in the EN samples with S. Blue 97, S. Blue 104, S. Blue, S. Green 28 and S. Yellow 93, which correlated with good mechanical properties. Nevertheless, the greatest improvement in durability was found in the Chimassorb 994-based composites (HALS).

CHAPTER 5 EFFECT OF AGING ON THE PROPERTIES OF NBR AND EN COMPOSITES

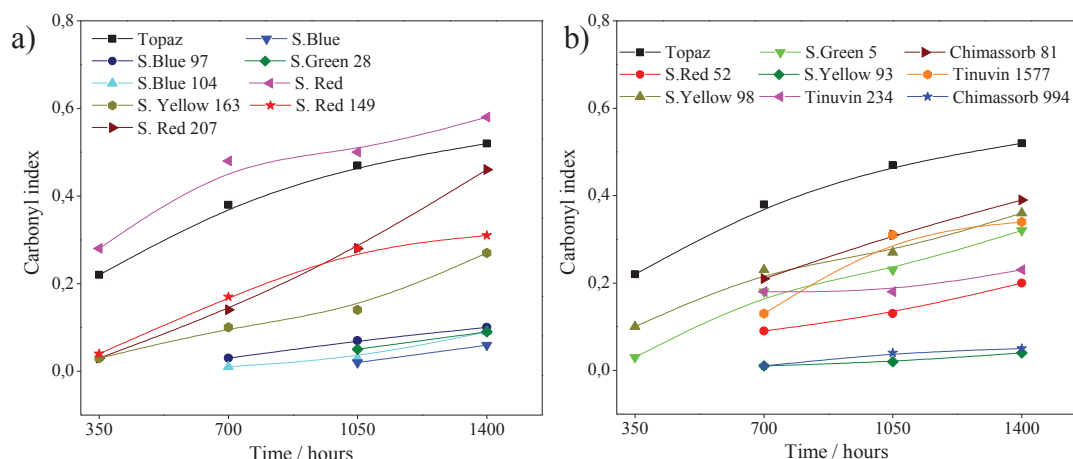


FIGURE 5.13 Carbonyl index (a, b) as a function of the weathering time of the EN composites that contain dyes and stabilizers.

Some of the results obtained from the FTIR analysis were also confirmed by XPS studies of the sample surfaces (Table 5.3). The polymer surfaces before and after aging and the concentrations of the different chemical bonds were studied in detail using the C1s peak of the XPS spectra. The results in Table 5.3 show the contribution of the different groups in the selected samples that are the result of the aging process. The best protection of the surface against aging was provided by Chimassorb 994; the composition of the groups on its surface changed the least.

TABLE 5.3 The percentage of individual components in the spectra of C 1s [%] of EN composites before and after 1400 h aging.

Sample	The percentage of individual components in the spectra of C 1s [%]			
	C-C	C-OH	C=O	COOH
EN	89.3	6.0	3.0	1.6
EN after 1400 h aging	83.9	10.5	2.4	3.2
EN/S. Blue	92.1	4.0	2.0	1.5
EN/S. Blue after 1400 h aging	85.5	10.0	2.4	1.4
EN/Chimassorb 994	86.8	9.5	1.9	2.0
EN/Chimassorb 994 after 1400 h aging	86.6	8.5	2.9	1.9

5.3.4 SEM AND COLORIMETRIC MEASUREMENTS OF EN COMPOSITES

Table 5.4 shows the differences in the ΔE , ΔL^* , Δa^* and Δb^* values of EN/solvent dye composites subjected to weather conditions that showed the most significant changes in color. As in the case of the UV tests, composites that contain S. Red, S. Red 207, S. Red

CHAPTER 5 EFFECT OF AGING ON THE PROPERTIES OF NBR AND EN COMPOSITES

149 and S. Yellow 98 dyes were very sensitive to aging; the greatest total color differences ΔE after 700 h of exposure were observed in these composites. Despite the increase in ΔE value after 700 h and 1400 h of irradiation, the composite EN/S. Green 5 still exhibited a yellow color. However, the shade of yellow was much less intense than before aging. As in UV aging, the dye concentrations in the composites decreased over time due to the destruction of the chromophore by solar radiation.

TABLE 5.4 Changes in the color parameters of EN composites that contain dyes after aging in the full solar spectrum.

EN/composites	Aging time [hours]	ΔE	ΔL^*	Δa^*	Δb^*
Solvent Red	700	24.05	12.26	-16.26	-5.33
	1400	25.93	12.89	-17.84	-4.98
Solvent Red 207	700	18.67	6.85	-11.18	-7.29
	1400	23.28	7.23	-13.03	-9.08
Solvent Red 149	700	18.39	9.45	-20.43	-6.36
	1400	24.78	11.23	-22.12	-7.25
Solvent Yellow 98	700	18.85	-9.79	8.77	-14.43
	1400	23.12	-9.92	9.86	-16.18
Solvent Yellow 163	700	14.49	-1.34	-3.41	-7.32
	1400	22.05	-3.03	-6.07	-10.21
Solvent Green 5	700	9.13	-11.36	-12.98	-13.62
	1400	20.78	-12.91	-15.47	-21.44

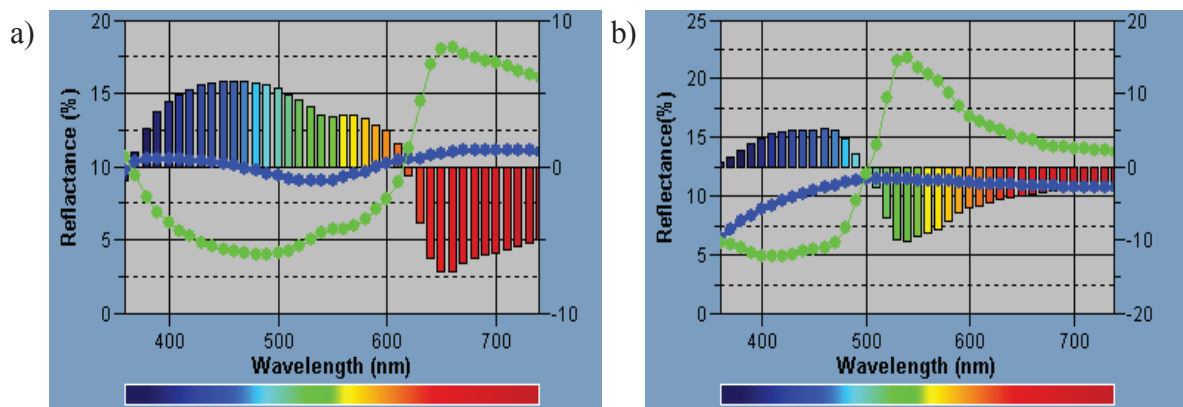


FIGURE 5.14 Change in reflectance in EN composites that contain Solvent Red 207 (a) and Solvent Yellow 98 (b) after 700 solar irradiation (b), green line – before aging, blue line – after aging.

The spectrophotometric measurements showed smaller changes in color after 1400 h in the EN composites that contained S. Blue 97, S. Blue 104, S. Blue, S. Green 28 and S. Yellow 93. The analysis of the mechanical properties and surfaces shows that these samples also exhibit the best resistance to aging. Figure 5.14 shows the variations in the

CHAPTER 5 EFFECT OF AGING ON THE PROPERTIES OF NBR AND EN COMPOSITES

reflectance spectra of EN/S. Red 207 (Fig. 5.14 a) and EN/S. Yellow 98 composites (Fig. 5.14 b) after 700 h of solar irradiation. As was expected for the EN/S. Red 207 sample, the most significant decrease was found for the red color. The analysis of the reflectance values showed that the EN/S. Yellow 98 composites were less yellow and green in color than before aging.

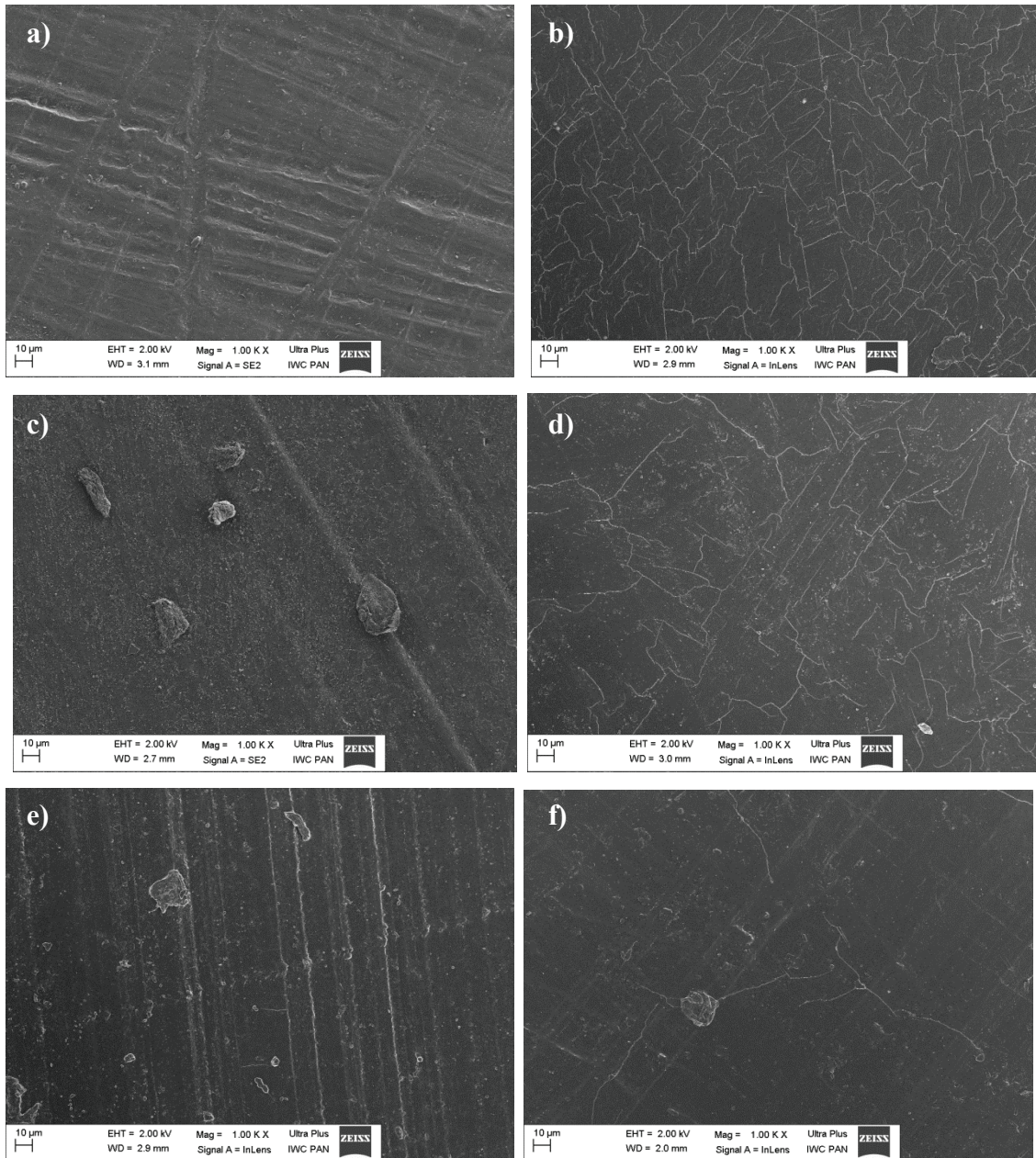


FIGURE 5.15 SEM micrographs of (a) EN before aging, (b) EN after 700 h aging, (c) EN/Tinuvin 234 before aging, (d) EN/Tinuvin 234 after 700 h aging, (e) EN/S. Blue 97 before aging, (f) EN/S. Blue 97 after 700 h aging.

SEM was used to evaluate the effect of weathering on the surfaces of samples of pure EN and EN composites with Tinuvin 234 stabilizer or Solvent Blue 97 dye. Figure 5.15 (a-

CHAPTER 5 EFFECT OF AGING ON THE PROPERTIES OF NBR AND EN COMPOSITES

f) shows micrographs of the studied sample surfaces. Before weathering, the surfaces of the composites did not show defects that would indicate any degradation. Numerous cracks were detected on the EN composites after 700 h of aging, and the images show several differences. Cracks and defects were observed mainly on the surfaces of the EN and EN/Tinuvin 234 samples. Only minor cracks were observed on the EN/S. Blue 97 surface after this amount of aging.

These data are in agreement with the mechanical properties that were obtained after 700 h. Less deterioration occurred in the EN/S. Blue 97 composite than in the EN and EN/Tinuvin 234 samples. The results show that the presence of Solvent Blue 97 makes EN less sensitive to degradation under solar conditions.

5.4 NBR COMPOSITES CONTAINING SOLVENT DYES UNDER UV AGING

5.4.1 MECHANICAL PROPERTIES NBR/SiO₂/SOLVENT DYES COMPOSITES

This work investigates the effect of UV exposure on the mechanical properties of NBR composites that contain solvent dyes. The influence of the solvent dyes on the aging properties of NBR/SiO₂/solvent dye samples is summarized in Table 5.5. Before irradiation, the NBR/SiO₂ and NBR/SiO₂/solvent dyes exhibit similar tensile properties. Previous studies have shown that differences in the NBR composites caused by exposure to UV irradiation can be observed after 120 h of aging.

TABLE 5.5 Results of the tensile properties of NBR composites that contain solvent dyes after 120 h of UV aging.

NBR composites	Aging time [hours]	SE ₁₀₀ [MPa]	SE ₃₀₀ [MPa]	TS [MPa]	Eb [%]	S
Without dye*	-	1.9±0.1	4.3±0.3	25.0±1.2	653±15	0.44
	120	2.7±0.2	5.5±0.2	13.8±1.1	532±9	
Solvent Blue 97	-	1.7±0.1	4.4±0.2	22.7±2.2	620±11	0.38
	120	2.5±0.2	4.8±0.3	10.1±1.4	530±13	
Solvent Green 28	-	1.6±0.1	4.1±0.1	22.7±1.6	616±12	0.45
	120	2.5±0.2	4.5±0.2	12.3±1.2	527±8	
Solvent Yellow 98	-	1.8±0.1	3.9±0.1	22.9±1.9	621±13	0.21
	120	2.8±0.1	5.6±0.3	7.3±0.9	405±9	

*Without dye – NBR/SiO₂

The obtained results clearly show that aging significantly contributed to the reduction of TS and Eb values. In all cases, the modulus increased after UV exposure, mainly as a result of increased crosslinking density and stiffness. The addition of solvent dyes into NBR did not enhance the durability of the films, and both NBR/SiO₂ and NBR/SiO₂/solvent dyes

were significantly deteriorated after 120 h, which can be observed from the S values. Moreover, composites that contain Solvent Yellow 98 dye (S = 0.21) appear to be affected more by aging than the reference sample (S = 0.44).

5.4.2 COLORIMETRIC MEASUREMENTS AND MICROSCOPY ANALYSIS (SEM) OF NBR/SiO₂/SOLVENT DYE COMPOSITES

Table 5.6 shows significant color changes in all of the samples after 120 h of irradiation. The NBR composites deteriorate much more easily due to the double bonds in the butadiene structure. Therefore, the total color change of the reference sample was found to be high ($\Delta E = 27.70$)²⁸⁹.

TABLE 5.6 Changes in the color parameters of NBR composites that contain solvent dyes after 120 h of UV aging.

NBR composites	Aging time [hours]	ΔE	ΔL^*	Δa^*	Δb^*
NBR/SiO ₂	120	27.70	9.26	9.05	-24.49
Solvent Blue 97	120	29.57	-8.51	-0.15	-3.97
Solvent Green 28	120	11.32	-3.19	10.4	7.47
Solvent Yellow 98	120	60.69	-8.88	2.09	-9.22

Irradiation modified the physical and chemical characteristics of the NBR/SiO₂/solvent dyes and resulted in rapid color changes. The greatest increase in the total color difference was observed for samples of NBR/SiO₂/S. Yellow 98 ($\Delta E = 60.69$). Moreover, the contributions of the chromaticity coordinates ΔL^* (lightness) and Δb^* (yellow hue), which were initially high, decrease progressively during aging. The greatest color changes correlate with the results of the tensile properties and confirmed their susceptibility to the aging process. Although the color changes evaluated by the ΔE parameter were the lowest for the NBR/SiO₂/S. Green 28 composite, the mechanical properties and aging coefficients were similar to those of the reference sample after 120 h of UV exposure. This behavior of solvent dyes in the NBR composites can be explained by their different light-fastnesses in opaque materials or possible interactions with the components of the sulfur-based system²⁹⁰.

²⁸⁹ R. D. Chai, J. Zhang, Synergistic effect of hindered amine light stabilizers/ultraviolet absorbers on the polyvinyl chloride/powder nitrile rubber blends during photodegradation, *Polym. Eng. Sci.* 2013, **53**, 1760–1769.

²⁹⁰ R. M. Harris (1999), *Coloring Technology for Plastics*, R. M. Harris (Ed.), Norwich, Plastics Design Library a division of William Andrew Inc., p. 1–13.

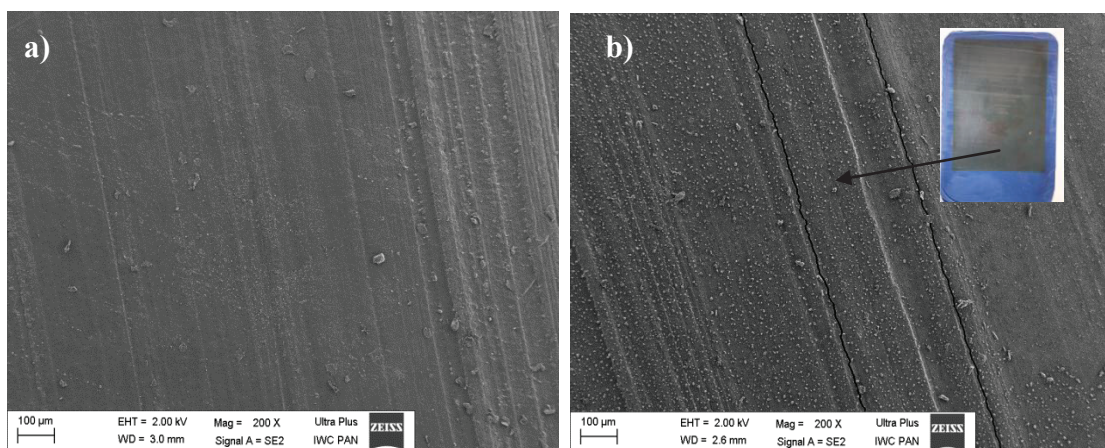


FIGURE 5.16 SEM micrographs of NBR/SiO₂/S. Blue 97 before UV aging (a), NBR/SiO₂/S. Blue 97 after 120 h UV aging (b).

Figure 5.16 compares the surface morphologies of the NBR/SiO₂/S. Blue 97 composite before and after accelerated aging. Before the UV test, the sample surfaces were relatively smooth except for some defects from the compression molding. After 120 h of UV irradiation, the reference sample shows the formation of slight cracks that span the entire surface. This is caused by significant chemical reactions, such as oxidation or chain scission during accelerated aging (Fig. 5.18 a). Although the surfaces of the reference sample and the solvent dye composite were not seriously damaged, the colors of both samples completely changed with radiation exposure. It appears that the change in color of NBR composites was most likely related to NBR surface oxidation under UV exposure.

5.5 NBR COMPOSITES CONTAINING PIGMENTS UNDER UV AGING

5.5.1 MECHANICAL PROPERTIES OF NBR/SiO₂/PIGMENT COMPOSITES

The effects of selected pigments on the aging properties of NBR composites was also investigated. Table 5.7 shows the changes in the mechanical properties of NBR composites that contain pigments and stabilizers after 120 hours of UV irradiation. The UV irradiation caused the deterioration of the exposed materials and increased the crosslink density, which was reflected in the elevated values of the modulus for 100 % and 300 % elongations. The greatest reduction in mechanical properties was observed for the NBR/SiO₂ and NBR/SiO₂/Chimassorb 81 samples.

CHAPTER 5 EFFECT OF AGING ON THE PROPERTIES OF NBR AND EN COMPOSITES

TABLE 5.7 Tensile properties of NBR composites that contain pigments and stabilizers after 120 h of UV aging.

Sample	Aging time [hours]	SE ₁₀₀ [MPa]	SE ₃₀₀ [MPa]	TS [MPa]	Eb [%]
NBR/SiO ₂	-	1.9±0.1	4.3±2	25.0±2.1	653±15
	120	2.7±0.2	5.5±0.3	13.8±1.3	532±14
Pigment Blue 15:1	-	1.9±0.2	4.2±0.2	22.3±1.9	640±18
	120	2.1±0.1	4.6±0.1	20.3±1.7	585±8
Pigment Green 7	-	1.6±0.1	4.0±0.3	25.6±2.1	635±16
	120	2.2±0.3	4.7±0.2	19.9±1.8	580±12
Pigment Yellow 173	-	1.7±0.1	4.3±0.3	24.0±2.1	607±19
	120	2.0±0.2	4.3±0.2	19.8±2.2	605±10
Pigment Red 254	-	2.0±0.1	4.8±0.2	25.2±1.8	671±18
	120	2.0±0.1	5.2±0.3	19.9±2.2	610±12
<i>cis</i> -Indigothiazine	-	2.5±0.2	4.2±0.3	24.6±2.3	660±15
	120	2.3±0.2	5.3±0.2	15.9±1.2	525±12
<i>trans</i> -Indigothiazine	-	1.8±0.1	4.0±0.1	25.8±2.1	642±8
	120	2.2±0.2	4.8±0.3	18.6±1.1	605±12
Tinuvin 234	-	2.1±0.1	4.4±0.1	24.6±1.9	690±13
	120	2.6±0.3	5.1±0.3	16.5±1.3	560±10
Chimassorb 81	-	1.9±0.1	3.8±0.1	23.7±2.1	658±15
	120	1.7±0.2	5.5±0.2	14.4±1.3	476±7
Tinuvin 1577	-	2.1±0.1	4.2±0.2	24.6±2.4	660±17
	120	2.3±0.3	5.3±0.3	15.9±1.3	525±12
Chimassorb 944	-	1.9±0.1	5.2±0.2	20.5±2.1	534±14
	120	2.7±0.3	6.0±0.3	18.7±1.7	527±11

Composites that contain a *cis*-Indigothiazine showed greater decreases in flexibility and strength than those with the *trans* form. The improved protection of the NBR composite by *trans*-Indigothiazine was most likely due to the higher stability of this pigment compared to *cis*-Indigothiazine. Figure 5.17 demonstrates that the greatest improvement in the durability of NBR composites was provided by HALS (Chimassorb 994) because its S value was the highest (S = 0.92).

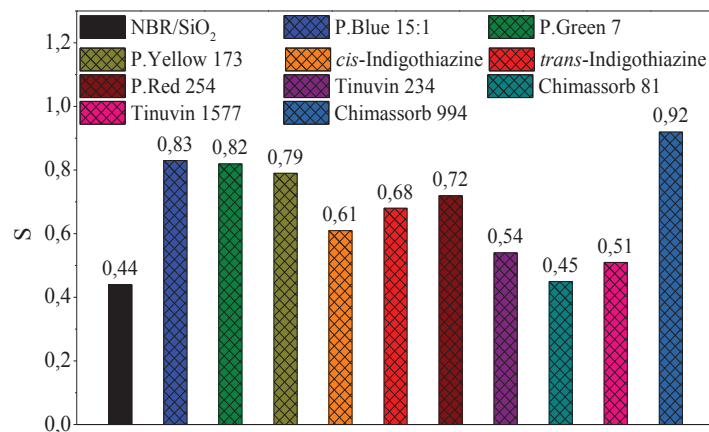


FIGURE 5.17 Aging coefficients of NBR composites that contain pigments and stabilizers after 120 h of UV aging.

CHAPTER 5 EFFECT OF AGING ON THE PROPERTIES OF NBR AND EN COMPOSITES

Generally, all of the investigated pigments protected NBR composites against unfavorable factors better than the considered UV absorbers. Of the pigments, the greatest S values were found for NBR/SiO₂/P. Blue 15:1 (S = 0.83) and NBR/SiO₂/P. Green 7 (S = 0.82) composites. These results showed that the addition of phthalocyanine blue (P. Blue 15:1) and green (P. Geen 7) into NBR most significantly enhanced the durability of the composites. The composites that contained commercial stabilizers were more vulnerable to UV exposure because their deformation ratios after and before aging varied between 0.45-0.54 and were similar to that of the reference sample (S = 0.44).

5.5.2 COLORIMETRIC MEASUREMENTS AND MICROSCOPY ANALYSIS (SEM) OF NBR/SiO₂/PIGMENTS

Table 5.8 shows the results of studies of the color variation parameters during the aging process. The surfaces of all of the tested materials changed color after aging. The value of the total color change (ΔE) was significant, even in the composites that exhibited good mechanical properties after aging, such as NBR/SiO₂/P.B.15:1 ($\Delta E = 28.91$) or NBR/SiO₂/Chimassorb 994 ($\Delta E = 21.01$). These results suggested that radiation affected the surfaces of the materials more than the bulk materials. The NBR/SiO₂/*cis*-indigothiazine composite changed color more than the sample with the *trans* form of indigothiazine. The intense color variation was most likely caused by the partial conversion of yellow (orange) *cis*-indigothiazine pigment into the red *trans* form during aging.

TABLE 5.8 Color parameters of NBR composites that contain pigments and stabilizers after 120 h of UV aging.

NBR composites	Aging time	ΔE^*	ΔL^*	Δa^*	Δb^*
Without pigment	120 h	27.70	9.26	9.05	-24.49
Pigment Blue 15:1	120 h	21.01	-4.18	-6.82	19.43
Pigment Green 7	120 h	11.92	-4.97	8.91	6.17
Pigment Yellow 173	120 h	17.63	-9.36	12.03	-8.9
<i>cis</i> -Indigothiazine	120 h	13.74	-5.87	-4.94	-2.36
<i>trans</i> -Indigothiazine	120 h	9.39	-3.19	-2.19	-1.26
Pigment Red 254	120 h	11.39	-5.23	-5.17	-2.18
Tinuvin 234	120 h	27.79	9.54	9.09	-23.82
Chimassorb 81	120 h	28.28	10.88	-9.22	-22.08
Tinuvin 1577	120 h	27.56	11.38	-9.37	-23.29
Chimassorb 944	120 h	28.91	11.03	-8.97	-22.56

CHAPTER 5 EFFECT OF AGING ON THE PROPERTIES OF NBR AND EN COMPOSITES

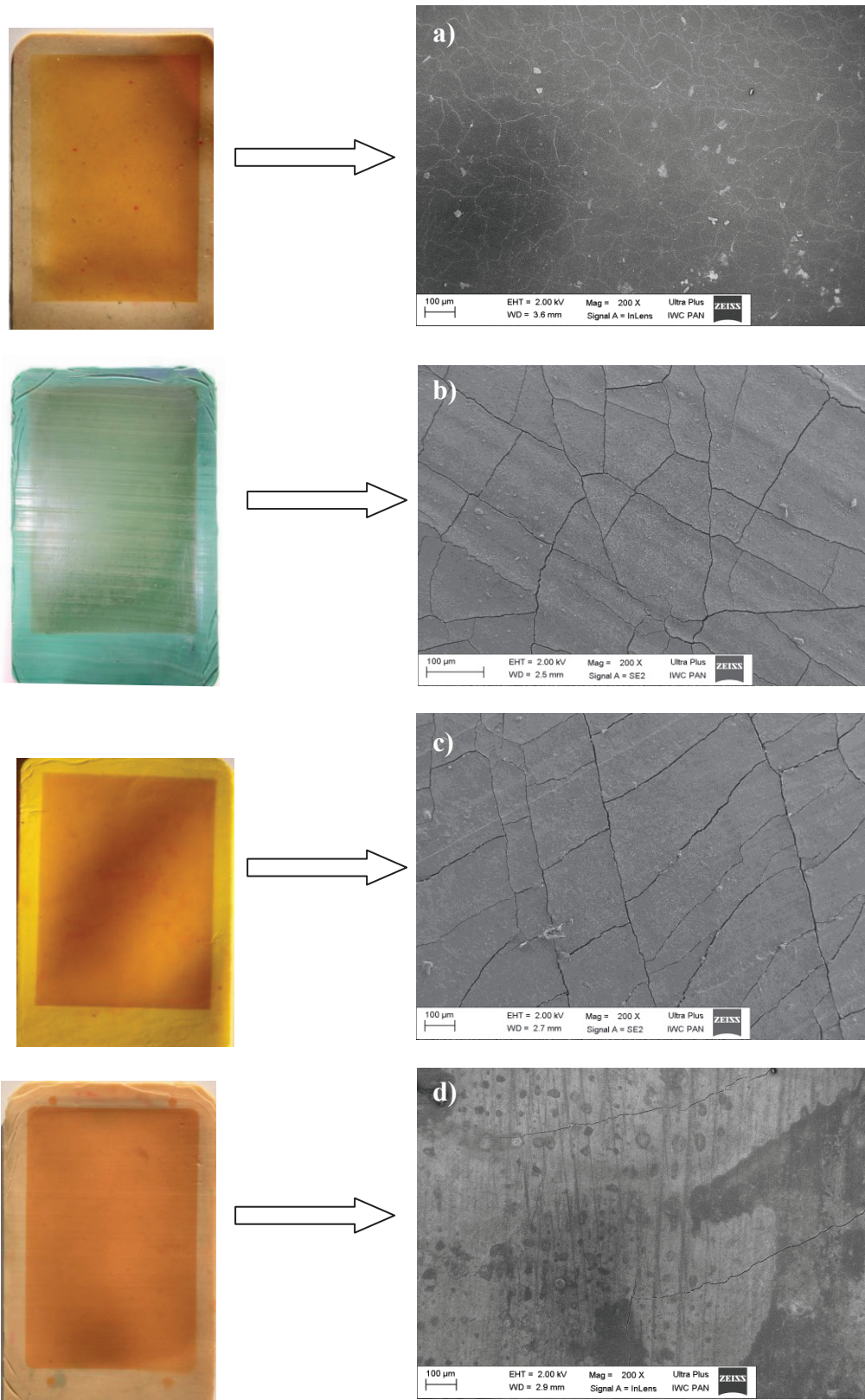


FIGURE 5.18 Pictures and SEM micrographs of NBR composites after 120 h of UV aging: NBR/SiO₂ (a), NBR/SiO₂/P. Green 7 173 (b), NBR/SiO₂/P. Yellow 173 and (c), NBR/SiO₂/Chimassorb 994 (d).

CHAPTER 5 EFFECT OF AGING ON THE PROPERTIES OF NBR AND EN COMPOSITES

SEM images showed the presence of cracks on the surfaces of all of the investigated NBR composites that were subjected to UV aging (Fig. 5.18 a-d). However, in case of NBR/SiO₂ (Fig. 5.18 a) and NBR/SiO₂/Chimassorb 994 (Fig. 5.18 d) composites, they were less regular and deeper than those with pigments. SEM images of the surfaces of composites colored with P. Yellow 173 (Fig. 15.8 b) and P. Green 7 (Fig. 15.8 c) exhibited numerous cracks and defects, which is interesting because the composites that contain phthalocyanine pigment exhibited especially good resistance to outdoor exposure. Several studies have shown that the presence of copper phthalocyanine increases the sensitivity of polycarbonate surfaces to photodegradation²⁹¹. This behavior was found in all of the pigments investigated in this study. This observation implies that, as in the case of ethylene-norbornene samples, pigments provide more effective protection to NBR composites in bulk, while their surfaces are more vulnerable to UV irradiation. The explanation may be a protective mechanism of composites by the pigments, which involves not only the absorbance of radiation, but also their reflection and scattering. Light that is reflected and scattered from the pigment crystals likely contributes to the destruction of the surface because the radiation is most intense in this area and takes part in the formation of an “oxidized skin”.

5.6 CONCLUSIONS

This research examined the effects of solvent dyes and pigments on the properties of ethylene-norbornene (EN) and acrylonitrile-butadiene rubber (NBR) composites that were exposed to weathering conditions with different amounts of irradiation with UV light ($\lambda = 343$ nm) and the full solar spectrum ($\lambda = 280$ -3000 nm).

The analysis of the properties of EN during UV aging showed that all of the studied dyes (except Solvent Red) prolonged the lifetime of EN composites. The best protective effect was found in samples that contain anthraquinone solvent dyes with strong electron-donating substituents, such as Solvent Blue 97, Solvent Blue 104, Solvent Blue, Solvent Green 28 and Solvent Yellow 93. In the dyes with anthraquinone chromophores, the protective effect may be related to the absorption of radiation and the ability of the dye to react with radicals that form during aging. The investigated stabilizers, especially Tinuvin 1577 and Chimassorb 994, improved the durability of EN composites for the range of UV irradiation at 343 nm and provided better protection than solvent dyes.

²⁹¹ C. Saron, F. Zulli, M. Giordano, M. I. Felisberti, Influence of copper-phthalocyanine on the photodegradation of polycarbonate, *Polym. Degrad. Stab.* 2006, **91**, 3301–3311.

CHAPTER 5 EFFECT OF AGING ON THE PROPERTIES OF NBR AND EN COMPOSITES

The number of particles has no significant impact on the final results of aging for the composites. The exception was EN/S. Yellow 93 composite with a dye concentration of 3.5×10^{-4} M, which demonstrated less ability to protect the material than EN/S. Yellow 93 composite that contained 0.2 phr of this dye. This is related to the relatively low molecular weight of S. Yellow 93 compared to the other studied dyes.

The results of weathering in the full solar spectrum exhibited a similar trend to the aging study, in which the wavelength was $\lambda = 343$ nm. However, the protection efficiencies of solvent dyes in EN composites under weathering in the full solar spectrum were much greater than those of most of the investigated stabilizers. The application of anthraquinone dyes with strong electron-donating substituents significantly prolonged the lifetimes of EN composites during aging. Nevertheless, the addition of stabilizers to EN did not enhance the durability of the composites as effectively under UV exposure (except for HALS). This effect may be caused by several factors. Solvent dyes with strong electron-donating substituents (S. Blue 97, S. Blue 104, S. Blue and S. Green 28) may prolong the lifetime of EN under weathering with full sun exposure more than commercial absorbers. On the other hand this type of stabilizer may not provide good protection under these aging conditions.

The impact of selected pigments on the aging behavior of EN composites exposed to UV irradiation ($\lambda = 343$ nm) was also investigated. The addition of the studied pigments at 0.2 phr loading resulted in improved durability of the composites, and decreases in the properties of these samples were reduced depending on the type of pigment. The EN composite with blue phthalocyanine pigment (Pigment Blue 15:1) had the best mechanical properties after 1600 h of UV irradiation; however, a high carbonyl index was detected. The study demonstrated that the pigments provided good protection to EN composites in bulk even when the surfaces deteriorated.

The accelerated UV aging test showed that some solvent dyes with strong electron-donating substituents improved the durability of EN composites better than the studied pigments and also provided good surface protection. As was previously described, the loss of color in the EN samples that contained solvent dyes was related to a significant decrease in mechanical properties. Interestingly, despite the extended degree of degradation and poor tensile properties, the color of the EN/pigment composites remained nearly unchanged.

The surface and mechanical properties demonstrate that the presence of EN composite mixtures with dyes and pigments, such as EN/P.Yellow 173/S.Yellow 93, EN/P.Yellow

CHAPTER 5 EFFECT OF AGING ON THE PROPERTIES OF NBR AND EN COMPOSITES

173/S.Yellow 98 and EN/P.Green 7/S.Green 28, improved the lifetime of the samples more than pigments or some dyes at the same concentration. This observation may be the result of a synergistic effect of the dispersed pigment crystals and molecular solution that form the dye in the composite.

Other studies were focused on the behavior of NBR composites that contained solvent dyes, pigments and stabilizers that were subjected to UV exposure. A protective effect of solvent dyes in NBR materials was not observed because the mechanical properties of the NBR/solvent dye composites and the reference sample were similar after UV exposure. The significant changes in color of the NBR and NBR/solvent dye composites were most likely related to NBR surface oxidation, which is very sensitive to UV irradiation. The investigated pigments generally improved the durability of NBR composites better than most of the applied stabilizers (Tinuvin 234, Chimassorb 81 and Tinuvin 1577). Of the pigments, the best protection against UV aging occurred in the NBR composites that contained phthalocyanine blue (P. Blue 15:1) and green (P. Green 7). As in the case of ethylene-norbornene, hindered amine light stabilizer HALS (Chimassorb 994) was most effective in prolonging the lifetime of the NBR composites. As in the previous test, intense color variations were observed in all of the NBR/pigment composites as a result of surface oxidation during the aging process. The surfaces of the studied NBR/pigment composites showed the formation of numerous cracks, voids and sinks after 120 h of UV aging. Only minor crack formation was observed on the NBR and NBR/Chimassorb 994 surfaces after this length of UV exposure. This investigation confirmed the results of the ethylene-norbornene EN study, in which pigments provided effective protection of polymer composites in bulk but may somehow contributed to faster surface degradation under UV irradiation.

CHAPTER 6

**IMPACT OF IMIDAZOLIUM IONIC LIQUIDS ON THE
PROPERTIES OF NITRILE RUBBER COMPOSITES**

INTRODUCTION

As reported in the literature, additives such as ionic liquids (ILs) have been found to have multifunctional roles in polymer composites, such as dispersing and coupling agents, plasticizers, and ion sources for electrochemical and antistatic applications. However, due to their complex effects on the polymer properties, polymer systems that contain ILs should be examined individually. In this chapter, hydrophilic and hydrophobic imidazolium ions of different concentrations were applied to acrylonitrile-butadiene rubber (NBR) to obtain composites that were characterized by good mechanical properties and improved ionic conductivity. The NBR compounds were vulcanized with a conventional sulfur-based crosslinking system and reinforced by silica filler Aerosil 380. The influence of thiocyanate (SCN) and bis(trifluoromethylsulfonyl)imide, TFSI anion types and the length of the alkyl chain (from ethyl to hexyl) of imidazolium ILs on the curing kinetic, mechanical, morphological and ionic conductivity properties of nitrile rubber composites was investigated. The effects of ILs on the properties of the nitrile rubber/IL composites exposed to outdoor weathering conditions were estimated for selected samples.

6.1 CUREING CHARACTERISTICS AND CROSSLINK DENSITY OF NBR/SiO₂/IL COMPOSITES

Because the crosslinking of rubber is a vital step in obtaining a cured rubber matrix, so at very beginning the effect of ionic liquids on the curing kinetics and crosslink density was discussed.

With increasing time, sulfur curing of the rubber occurs, and the torque values (M_H , ΔM) increase. Silica filler clearly affected the curing characteristics. The shape of the rheometer curve of a silica-reinforced compound differs significantly from that of a non-reinforced compound, as is shown in Figure 6.1. The high value of the specific surface area of the silica in NBR/SiO₂ resulted in a higher viscosity and stiffness, which is reflected in much higher torque values (M_H , ΔM) than those of NBR samples (Table 6.1). The application of silica extended the curing time (t_{90}) and scorch time (t_2) and decreased the crosslink density of NBR/SiO₂ ($5.4 \times 10^{-5} \text{ mol} \cdot \text{cm}^{-3}$) composites compared to unfilled NBR ($5.9 \times 10^{-5} \text{ mol} \cdot \text{cm}^{-3}$). It can be assumed that the sulfur crosslinking system was partially adsorbed onto the outer surface of the silica, which resulted in a slower curing process and lower curing efficiency²⁹².

In further investigation, the presence of some ILs in the rubber composites was found to considerably affect the curing kinetics and crosslink density.

²⁹² A. Kosmalska, M. Zaborski, J. Sokołowska, Adsorption of curatives and activity of silica toward elastomers, *Macromol. Symp.* 2003, **194**, 269–276.

CHAPTER 6 IMPACT OF IMIDAZOLIUM IONIC LIQUIDS ON THE PROPERTIES OF NITRILE RUBBER COMPOSITES

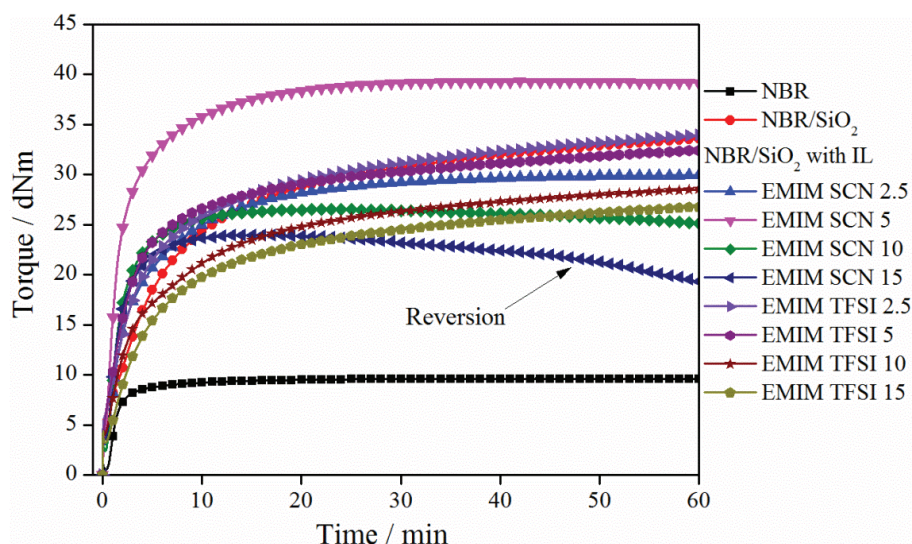


FIGURE 6.1 Rheographs of NBR/SiO₂/IL composites.

An analysis of the influence of thiocyanate (SCN) and bis(trifluoromethylsulfonyl) imide (TFSI) anions on the curing behavior revealed significant differences. Figure 6.1 shows the curing rheographs of NBR/SiO₂ composites that contain EMIM SCN and EMIM TFSI ILs at 0, 2.5, 5, 10 and 15 phr loadings. The results imply that the curing process is much faster when EMIM SCN IL is incorporated. Higher quantities of this imidazolium salt shorten the optimal vulcanization time, which can also be observed by increasing the curing rate index (CRI). The optimal curing time (t_{90}) of composites that contain 2.5 phr EMIM SCN was 15 min, which is approximately 15 min shorter than for those without IL. The incorporation of 5 phr EMIM SCN results in the highest stiffness of the rubber mix and increased the torques (M_H and ΔM), which are related to higher crosslink formation in the sample. Further addition (10 phr, 15 phr) led to lower values of these parameters. In NBR/SiO₂, an increase in the EMIM SCN content up to 15 phr leads to crosslink disappearance (reversion). Reversion, which is usually undesirable, is a thermally driven process by which the vulcanized rubber reverts back to the gum state and results in the deterioration of mechanical properties.

Applying EMIM TFSI ionic liquid at 2.5 phr and 5 phr resulted in shorter vulcanization times and scorch times of the rubber compounds compared to the neat sample (NBR/SiO₂), while the torque values (M_H , ΔM) showed only slight changes. Nevertheless, the accelerating effect of TFSI anions on the curing process was weak in comparison to EMIM SCN imidazolium salt. It is interesting that the process is faster in the presence of hydrophilic EMIM SCN than with hydrophobic EMIM TFSI. Previous studies from the literature have reported that some ILs act as accelerators by catalyzing the interface crosslinking reactions and improving the dispersion of zinc oxide. In these studies, the type

CHAPTER 6 IMPACT OF IMIDAZOLIUM IONIC LIQUIDS ON THE PROPERTIES OF NITRILE RUBBER COMPOSITES

of anion was found to have a strong influence on the curing reactions, whereas the length of the alkyl chains in the IL salts has a less significant impact on this process^{293, 240}.

TABLE 6.1 Curing characteristics and crosslink densities of NBR/SiO₂/ILs composites.

NBR composites	IL	M _H	ΔM	t ₂	t ₉₀	CRI	v _T * 10 ⁻⁵
	[phr]	[dNm]	[dNm]	[min]	[min]	[min ⁻¹]	[mol·cm ⁻³]
-		9.6	9.0	0.7	6.5	17.24	5.9±0.3
SiO ₂	-	31.6	27.6	0.8	29.4	3.50	5.4±0.2
SiO ₂ EMIM SCN	2.5	30.2	27.8	0.6	15.5	6.67	6.6±0.3
SiO ₂ EMIM SCN	5	39.3	37.0	0.6	9.6	11.11	7.1±0.3
SiO ₂ EMIM SCN	10	26.5	24.1	0.5	6.0	18.18	6.4±0.4
SiO ₂ EMIM SCN	15	24.0	22.2	0.5	5.1	21.74	6.3±0.3
SiO ₂ EMIM TFSI	2.5	31.1	27.8	0.6	25.4	4.03	5.9±0.2
SiO ₂ EMIM TFSI	5	32.5	29.1	0.6	22.8	4.51	6.0±0.3
SiO ₂ EMIM TFSI	10	28.6	25.3	0.7	26.0	3.95	5.7±0.3
SiO ₂ EMIM TFSI	15	26.8	23.6	0.9	26.8	3.86	5.3±0.4
SiO ₂ BMIM TFSI	2.5	30.8	27.2	0.6	26.0	3.94	5.6±0.4
SiO ₂ BMIM TFSI	5	30.9	27.3	0.6	26.1	3.92	5.7±0.3
SiO ₂ BMIM TFSI	10	27.4	23.9	0.6	27.2	3.80	5.5±0.3
SiO ₂ BMIM TFSI	15	25.5	22.4	0.8	30.5	3.37	5.1±0.2
SiO ₂ HMIM TFSI	2.5	30.0	26.7	0.6	27.2	3.80	5.5±0.3
SiO ₂ HMIM TFSI	5	29.7	26.0	0.6	28.6	3.60	5.4±0.3
SiO ₂ HMIM TFSI	10	26.0	23.1	0.6	30.2	3.38	5.2±0.4
SiO ₂ HMIM TFSI	15	24.3	22.0	0.7	31.7	3.23	5.0±0.2
SiO ₂ AMIM TFSI	2.5	30.8	27.1	0.7	29.2	3.51	5.6±0.3
SiO ₂ AMIM TFSI	5	30.0	26.5	0.7	28.3	3.62	5.6±0.3
SiO ₂ AMIM TFSI	10	26.9	23.8	0.8	30.6	3.36	5.3±0.2
SiO ₂ AMIM TFSI	15	26.0	23.4	0.8	31.2	3.29	5.1±0.3

Thiocyanate SCN anions appear to support the activation of the crosslinking reaction in sulfur-based systems. The ability of EMIM SCN to reduce the optimal vulcanization time (t₉₀) of NBR/SiO₂ composites demonstrates that this type of IL can act as an accelerator and catalyze curing reactions in these systems. Structurally, commercial accelerators contain a common functionality, N=C-S²⁹⁴. The reason for this behavior may be the chemical structure of the SCN anion, which contains sulfur and can function as both an accelerator and a sulfur-donor. In addition, ILs can play a role as a shielding agent and protect against adsorption of the sulfur crosslinking system onto the silica surface.

²⁹³ M. Maciejewska, F. Walkiewicz, M. Zaborski, Novel ionic liquids as accelerators for the sulfur vulcanization of butadiene–styrene elastomer composites, *Ind. Eng. Chem. Res.* 2013, **52**, 8410–8415.

²⁹⁴ W. Hofmann (1994), *Rubber Technology Handbook*, New York, Hanser Publishers.

CHAPTER 6 IMPACT OF IMIDAZOLIUM IONIC LIQUIDS ON THE PROPERTIES OF NITRILE RUBBER COMPOSITES

Variations of the alkyl chain length and the nature of the counterions also influenced the curing characteristics of NBR/SiO₂/IL composites. The application of ILs with ethyl groups attached to the imidazolium ring at low concentrations (2.5 phr, 5 phr) reduced the scorch and curing times and accelerated the curing process. For the ILs with longer alkyl chains (1-butyl-3-methylimidazolium bis(trifluoromethanesulfonate)imide (BMIM TFSI), 1-hexyl-3-methylimidazolium bis(trifluoromethanesulfonate)imide (HMIM TFSI) and (1-allyl-3-methylimidazolium bis(trifluoromethanesulfonate)imide (AMIM TFSI)), the accelerating effect on the curing time was less pronounced than for EMIM TFSI for IL concentrations of 2.5 phr or 5 phr in the rubber composites.

The mobility of the BMIM TFSI and HMIM TFSI in the polymer matrix was most likely reduced by the longer alkyl chains of the cations, which explains their lower activity during the curing process. Increasing the quantity of the EMIM TFSI IL (for 10 or 15 phr) in the composites decreased the torque values (M_H , ΔM), which can be ascribed to the plasticizing effect of imidazolium salt. A similar tendency was exhibited in the composites that contained BMIM TFSI, HMIM TFSI, AMIM TFSI and EMIM SCN ILs.

The crosslink densities of the NBR/SiO₂ and the filled ionic liquid composites are shown in Table 6.1. As previously mentioned, some of the ionic liquids may affect the sulfur crosslinking system and therefore the final crosslink density. This effect was found in samples that contain IL with thiocyanate anions, which exhibited the highest crosslink density. This trend is consistent with the rheometric data (high torque) and confirmed that EMIM SCN had the highest activity in the curing process, which increased its efficiency. The equilibrium swelling method reveals that the addition of 5 phr EMIM SCN increased the number of crosslinks to $7.1 \times 10^{-5} \text{ mol} \cdot \text{cm}^{-3}$ in the NBR/SiO₂/IL sample, while the crosslink density of the neat material is $5.5 \times 10^{-5} \text{ mol} \cdot \text{cm}^{-3}$. Generally, the crosslink density was also found to decrease with increasing EMIM SCN ionic liquid loading, which suggests that a higher IL content can hinder the formation of the polymer network. In contrast to hydrophilic ILs, a very slight effect of the TFSI-based ILs on crosslink network formation was observed. These investigations confirmed previous results of the decisive influence of the anion type in imidazolium ILs on the curing kinetics and crosslink formation in rubber composites.

6.2 TENSILE PROPERTIES OF NBR/SiO₂/IL COMPOSITES

The effects of ILs on the physical properties of NBR composites are shown in Table 6.2. The incorporation of 2.5 phr and 5 phr hydrophilic imidazolium salt EMIM SCN in the polymer matrix significantly increased the stiffness of the composites, which is reflected in the higher stress at 300 % elongation (SE_{300}). This parameter is related to the crosslink density of the composites and confirmed the previous results from swelling experiments and rheometric studies. The improvement in silica dispersion can also be attributed to the higher stiffnesses of these samples. Generally, the tensile strength and SE_{300} modulus of the NBR composites increased when 2.5 phr or 5 phr of EMIM SCN was added and decreased upon further addition of EMIM SCN. The elongation at break was reduced in all of the EMIM SCN-based composites, most likely due to the increase in crosslink density. In contrast to EMIM SCN-based materials, the NBR composites exhibit good mechanical properties even at high quantities of hydrophobic ILs. Compared to the reference sample, the incorporation of EMIM TFSI ions leads to an increase in the E_b parameter, which is related to the higher elasticity and flexibility of the rubber materials. Similar behaviors were exhibited by all of the composites that contained TFSI-based ILs. This observation shows that ILs with TFSI anions act as plasticizing agents, especially at higher proportions. The best mechanical properties were obtained for 2.5 phr and 5 phr concentrations of this salt. The tensile strength of the NBR sample that contained hydrophobic EMIM TFSI was higher than that of the other composites. At a given strain, an increase in stress is observed when 5 phr EMIM TFSI is added (23.8 MPa). Moreover, the TS increased to 20.7 MPa in the NBR/SiO₂/AMIM TFSI 5 composite, the NBR/SiO₂/BMIM TFSI 5 samples (up to 22.8 MPa) and the NBR/SiO₂/HMIM TFSI 5 samples (up to 22.5 MPa) compared to the neat NBR/SiO₂ (18.1 MPa). The improvement of the tensile properties of the composites may be attributed to the reduction of the silica agglomerates and the reinforcement of filler-filler or rubber-filler interactions in the presence of imidazolium salts. The addition of hydrophobic imidazolium salts made the NBR/SiO₂/IL composites less stiff, as was evident from the higher values of elongation at break and the changes in the E_{300} parameter. The modulus of the NBR/SiO₂/IL composites at 300 % elongation decreased with increasing quantity of IL in the investigated samples.

As in the rheometric study, the mechanical data also show a dependence between the length of the alkyl chains and the plasticizing effect of NBR composites. The highest E_b value of 820 % was found for a composite that contained 15 phr IL with a hexyl group

CHAPTER 6 IMPACT OF IMIDAZOLIUM IONIC LIQUIDS ON THE PROPERTIES OF NITRILE RUBBER COMPOSITES

(HMIM TFSI), which is consistent with the low glass transition obtained for this sample. This result agree with the fact that ILs can act as plasticizers and affect the physical properties of the composites. The plasticizing effect of ILs on the NBR composites has been analyzed by dynamic mechanical analysis (DMA) and differential scanning calorimetry (DSC) and is described in the next section.

TABLE 6.2 Mechanical properties of NBR/SiO₂/IL composites.

NBR composites	IL [phr]	SE ₃₀₀ [MPa]	TS [MPa]	Eb [%]
-	-	2.2±0.1	4.0±0.9	450±14
SiO ₂	-	3.9±0.2	18.1±1.5	650±18
SiO ₂ EMIM SCN	2.5	6.5±0.2	20.7±1.2	496±14
SiO ₂ EMIM SCN	5	7.2±0.3	19.1±1.4	464±15
SiO ₂ EMIM SCN	10	5.4±0.2	17.7±1.1	540±15
SiO ₂ EMIM SCN	15	4.2±0.1	14.6±1.0	555±20
SiO ₂ EMIM TFSI	2.5	4.0±0.2	22.3±1.3	677±15
SiO ₂ EMIM TFSI	5	4.1±0.3	23.7±1.7	698±20
SiO ₂ EMIM TFSI	10	3.5±0.2	21.8±1.1	706 ±21
SiO ₂ EMIM TFSI	15	3.3±0.1	20.9±1.2	715±18
SiO ₂ BMIM TFSI	2.5	3.9±0.3	21.3±1.1	680±20
SiO ₂ BMIM TFSI	5	3.8±0.2	22.8±1.6	700±19
SiO ₂ BMIM TFSI	10	3.4±0.2	21.9±1.6	751±21
SiO ₂ BMIM TFSI	15	3.3±0.1	19.9 ±2.0	755±24
SiO ₂ HMIM TFSI	2.5	4.1±0.2	21.2±1.1	673±15
SiO ₂ HMIM TFSI	5	3.7±0.2	22.5 ±2.1	685 ±18
SiO ₂ HMIM TFSI	10	3.2±0.2	18.9± 1.7	711± 19
SiO ₂ HMIM TFSI	15	2.7±0.1	18.2 ±1.9	820± 23
SiO ₂ AMIM TFSI	2.5	4.1±0.2	20.4±1.4	662±16
SiO ₂ AMIM TFSI	5	4.0±0.3	20.7±1.3	695±14
SiO ₂ AMIM TFSI	10	3.2±0.1	19.4±1.6	683±17
SiO ₂ AMIM TFSI	15	2.7±0.2	18.9±1.3	734±18

6.3 DMA AND GLASS TRANSITION TEMPERATURE (T_g) OF NBR/SiO₂/IL COMPOSITES

The glass transition temperatures (T_g) values of NBR/SiO₂/ILs composites were studied using dynamic mechanical analysis (DMA) and differential scanning calorimetry (DSC) techniques, and the results are shown in Table 6.3. The T_g values determined by DSC are always lower than the values of T_g that are based on tanδ (DMA). DMA and DSC

CHAPTER 6 IMPACT OF IMIDAZOLIUM IONIC LIQUIDS ON THE PROPERTIES OF NITRILE RUBBER COMPOSITES

identified only one T_g for each sample, which suggests that no phase separation occurred in the studied composite²⁹⁵.

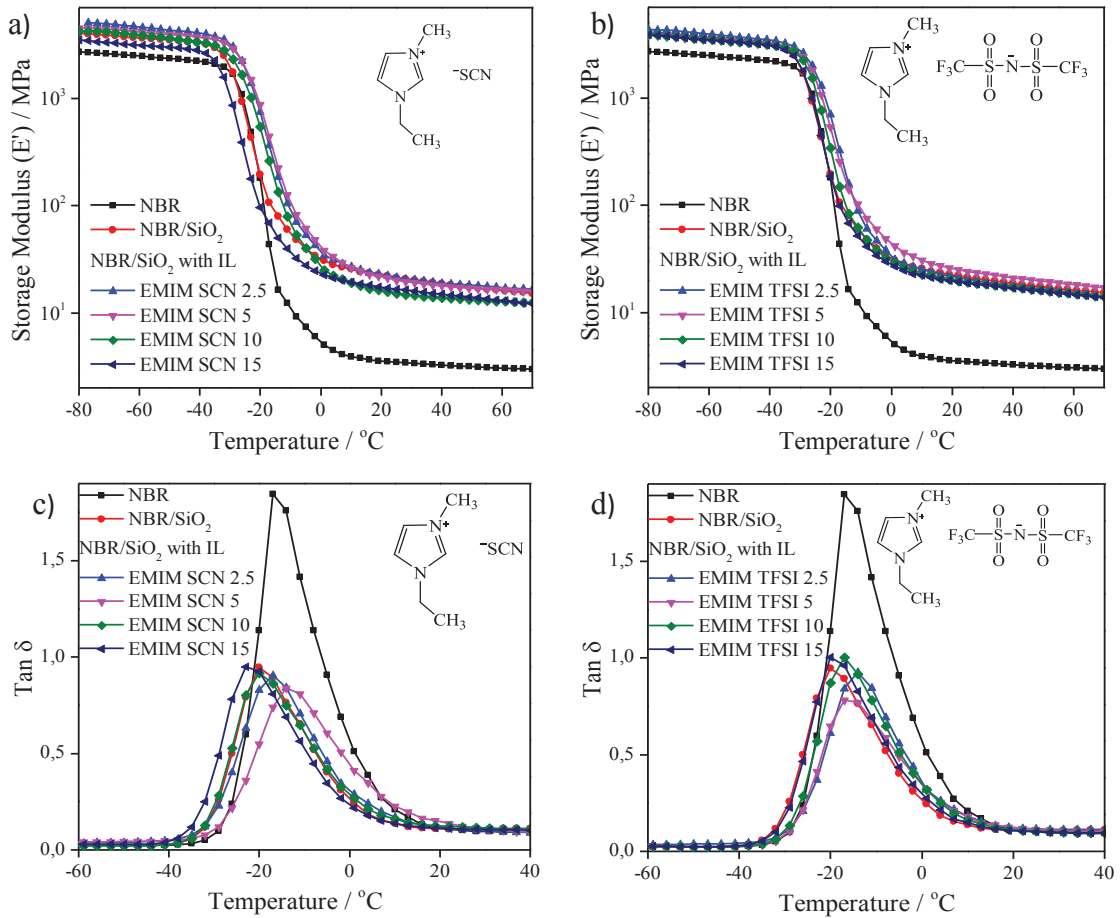


FIGURE 6.2 Temperature dependence of the storage modulus E' (a, b) and the loss tangent $\tan\delta$ (c, d) values at 10 Hz for the NBR, NBR/SiO₂ and NBR/SiO₂ composites with differing IL mass ratios.

Two ILs, hydrophilic EMIM SCN and hydrophobic EMIM TFSI, were selected to demonstrate the effects of anions and their increasing concentrations from 2.5 to 15 phr on the mechanical properties of NBR composites at small deformations. Figure 6.2 shows the temperature dependence of the storage modulus E' (a, b) and the decrease in the $\tan\delta$ (c, d) values for NBR, NBR/SiO₂ and NBR/SiO₂/IL composites with different IL ratios. As shown in Figure 6.2 (a-d), the composite that was filled with silica NBR/SiO₂ showed an increase in E' in the plateau region and a reduction of the $\tan\delta$ peak height in contrast to NBR, which is attributed to the hydrodynamic effect as well as filler–filler and rubber–filler interactions. After the addition of EMIM SCN IL (2.5 and 5 phr), the maximum decrease in the tangent shifted towards higher temperatures, and the peak $\tan\delta$ decreased in

²⁹⁵ R. J. Seyler (1994), Assignment of the glass transition, Philadelphia, American Society for testing and materials, p. 239–252.

**CHAPTER 6 IMPACT OF IMIDAZOLIUM IONIC LIQUIDS ON THE PROPERTIES
OF NITRILE RUBBER COMPOSITES**

comparison to the reference sample. Moreover, E' increased across the entire range of temperatures from the glassy to rubbery regions (Table 6.3). These results can be explained by stronger filler-filler or filler-rubber interactions as well as a higher crosslink density of the NBR composites in the presence of imidazolium salt.

The most significant increase in E' was found in the NBR composite that contained 5 phr of hydrophobic EMIM TFSI IL. The increase in E' to 24.3 MPa in the rubbery region for the same filler loading can be ascribed to the reinforcing effect of EMIM TFSI IL in the rubber composite. The T_g values of the NBR/SiO₂/EMIM TFSI 2.5 and 5 phr composites were similar to those of the reference sample. Further additions of both ILs resulted in slight shifts of the T_g maxima to lower temperatures, which confirmed that ILs act as plasticizing agents.

Generally, increasing IL contents in all of the NBR/SiO₂ composites led to reductions in T_g , which were accompanied by decreases in the mechanical properties as a result of the plasticizing effect (Table 6.3). For composites filled with 15 phr IL, the storage modulus in the rubbery region decreased due to the softening of the samples and weaker filler networking or filler-rubber interactions at the interface of the rubber matrix. These results are consistent with the mechanical property data at large deformations (from stress-strain measurements) that were discussed previously. Increases in the proportion of IL for NBR composites that contain BMIM TFSI and AMIM TFSI up to 15 phr resulted in decreases in the T_g values of the NBR/SiO₂/IL to -32 °C (DSC).

TABLE 6.3 Glass transition temperatures T_g and dynamic mechanical properties of NBR/SiO₂/IL composites at a vibrational frequency of 10 Hz.

NBR composites	IL [phr]	T_g DSC [°C]	tan δ		E' 25 °C [MPa]	E' 40 °C [MPa]
			T_g [°C]	Peak Value		
-	-	-28	-15.0	1.89	3.5	3.2
SiO ₂	-	-30	-16.2	0.94	21.0	18.6
SiO ₂ EMIM SCN	2.5	-30	-13.8	0.91	22.7	19.0
SiO ₂ EMIM SCN	5	-30	-13.1	0.85	20.1	17.9
SiO ₂ EMIM SCN	10	-31	-16.7	0.91	17.5	15.8
SiO ₂ EMIM SCN	15	-32	-17.0	0.92	16.3	14.8
SiO ₂ EMIM TFSI	2.5	-30	-15.5	0.93	22.0	18.1
SiO ₂ EMIM TFSI	5	-30	-15.7	0.83	24.3	21.1
SiO ₂ EMIM TFSI	10	-30	-17.0	0.97	19.4	17.1
SiO ₂ EMIM TFSI	15	-30	-17.9	1.01	18.7	16.6
SiO ₂ BMIM TFSI	15	-32	-18.8	0.94	17.8	15.8
SiO ₂ HMIM TFSI	15	-33	-19.8	0.97	17.4	15.9
SiO ₂ AMIM TFSI	15	-32	-18.7	0.98	16.6	14.9

CHAPTER 6 IMPACT OF IMIDAZOLIUM IONIC LIQUIDS ON THE PROPERTIES OF NITRILE RUBBER COMPOSITES

The T_g of NBR/SiO₂ composites diminish also as the length of the pendant alkyl chain in the IL cation increased, changing from 1-ethyl-3-methylimidazolium to 1-hexyl-3-methylimidazolium. The most significant plasticizing effect was noted for the NBR/SiO₂ composite filled with 15 phr HMIM TFSI, as the T_g was varied from -30 °C to -33 °C (DSC). Moreover, the lower modulus in the glassy and rubbery region for this sample correspond with the high value of elongation at break in tensile properties.

Similar behavior of TFSI-based ionic liquid in different elastomers was already reported by Subramaniam^{225, 234} Likozar²²⁶ or Marwanta²²³. The plasticizing effect of the ionic liquids was also investigated by Scott²²⁸, who employed 1-ethyl-3-methylimidazolium tetrafluoroborate as a plasticizer for the polymer and reported that ILs are better than conventional plasticizers. Nevertheless, there is no information in the literature about the impact of this type of IL on the rubber composites in this study.

6.4 MORPHOLOGY ANALYSIS OF NBR/SiO₂/IL COMPOSITES

Filler dispersion is an important factor that influences the properties of filled rubber composites. An important application of silica is its use as a filler in rubber matrix for reinforcement. NBR contains rubber chain nitrile groups (-CN) that are polar, which results in better interactions between the silanol groups of the silica and the NBR. Nevertheless, the hydrophilic nature of silica makes their incorporation and homogeneous dispersion in hydrophobic rubber materials difficult. Furthermore, particles with high surface energies more easily agglomerate as the size of the particles decreases.

The silanol groups that reside on the silica surfaces form hydrogen bonds and also lead to the formation of aggregates and agglomerates. Even a small number of agglomerates can lead to stress concentrations and to significant decreases in the tensile properties of polymeric materials. This problem can be overcome by the use of different dispersion agents, including ILs, to reduce the agglomerate size and facilitate the homogeneous distribution of silica particles in the rubber matrix^{296, 297}.

In this study, the morphologies of NBR/SiO₂/IL composites were investigated using scanning electron microscopy (SEM). Images were taken from several places on the composites, and the most informative are presented in this chapter.

²⁹⁶ Y. D. Lei, Z. Tang, L. Zhu, B. Guo, Demin Jia Functional thiol ionic liquids as novel interfacial modifiers in SBR/HNTs composites, *Polymer* 2011, **52**, 1337–1344.

²⁹⁷ K.-J. Kim, J. L. White, Silica surface modification using different aliphatic chain length silane coupling agents and their effects on silica agglomerate size and processability, *Compos. Interf.* 2002, **9**, 541–556.

CHAPTER 6 IMPACT OF IMIDAZOLIUM IONIC LIQUIDS ON THE PROPERTIES OF NITRILE RUBBER COMPOSITES

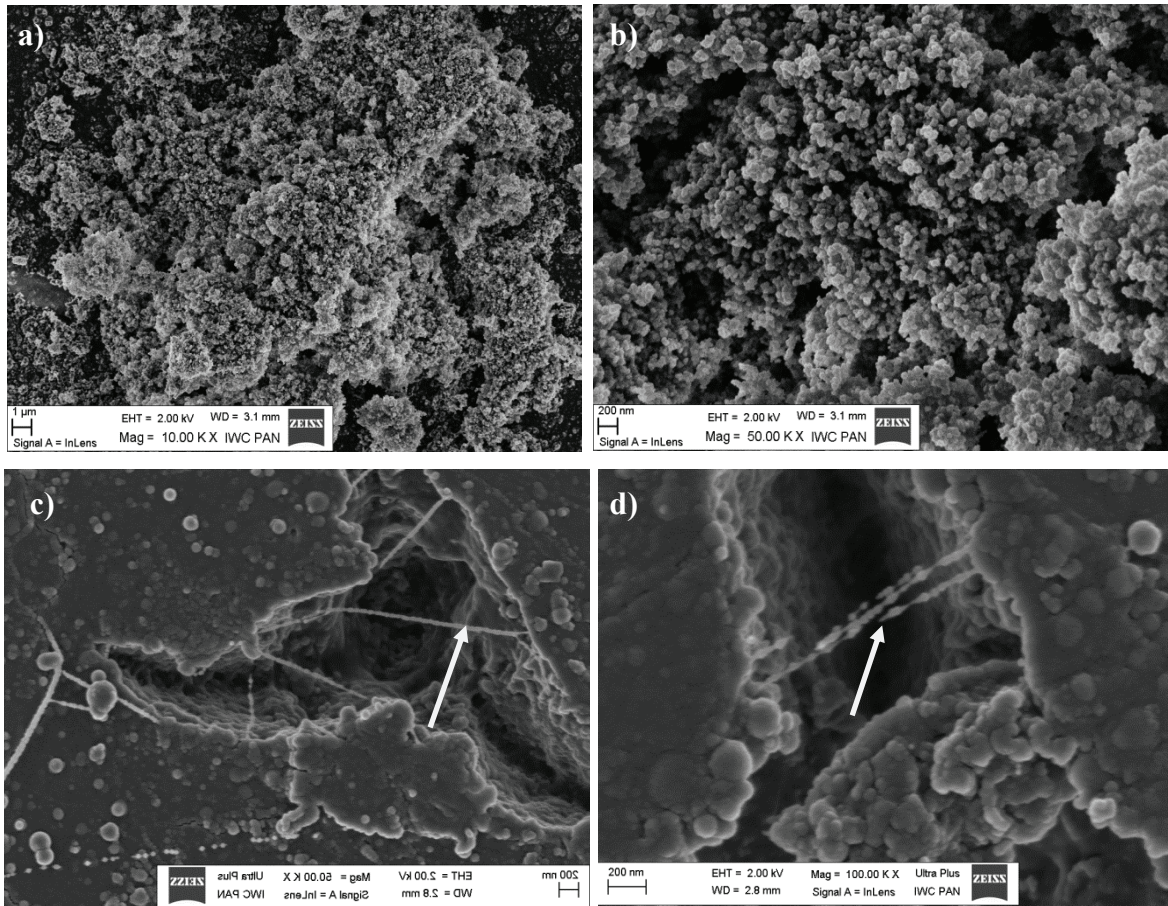


FIGURE 6.3 SEM micrographs of silica Aerosil 380 powder for different magnifications (a, b), filler network structure in NBR/SiO₂/EMIM TFSI 5 composite (c, d).

Microscopic images of representative fracture surfaces of the NBR/SiO₂/IL were made by different detectors, including InLens and ESB. While the InLens detector provides general morphological information, the ESB detector examines the composition contrasts and emphasizes edge effects, which allows for accurate observation of the behavior of the filler in the polymer matrix. Figure 6.3 (a, b) presents microscopic images of agglomerates of the Aerosil 380 filler, which is characterized by spherical particles and a high specific surface area (approximately 380 m²·g⁻¹). The pictures of the reference composite NBR/SiO₂ show that the dimensions of many of the agglomerates are greater than 3 μm (Fig. 6.4 a, b, c, d), whereas the composite that contains 5 phr of hydrophobic EMIM TFSI (Fig. 6.4 e, f, g, h) contains agglomerates even less than 1 μm in size. The silica agglomerates in the NBR/SiO₂ compound are larger than those in the compounds that contain TFSI-based ILs.

CHAPTER 6 IMPACT OF IMIDAZOLIUM IONIC LIQUIDS ON THE PROPERTIES OF NITRILE RUBBER COMPOSITES

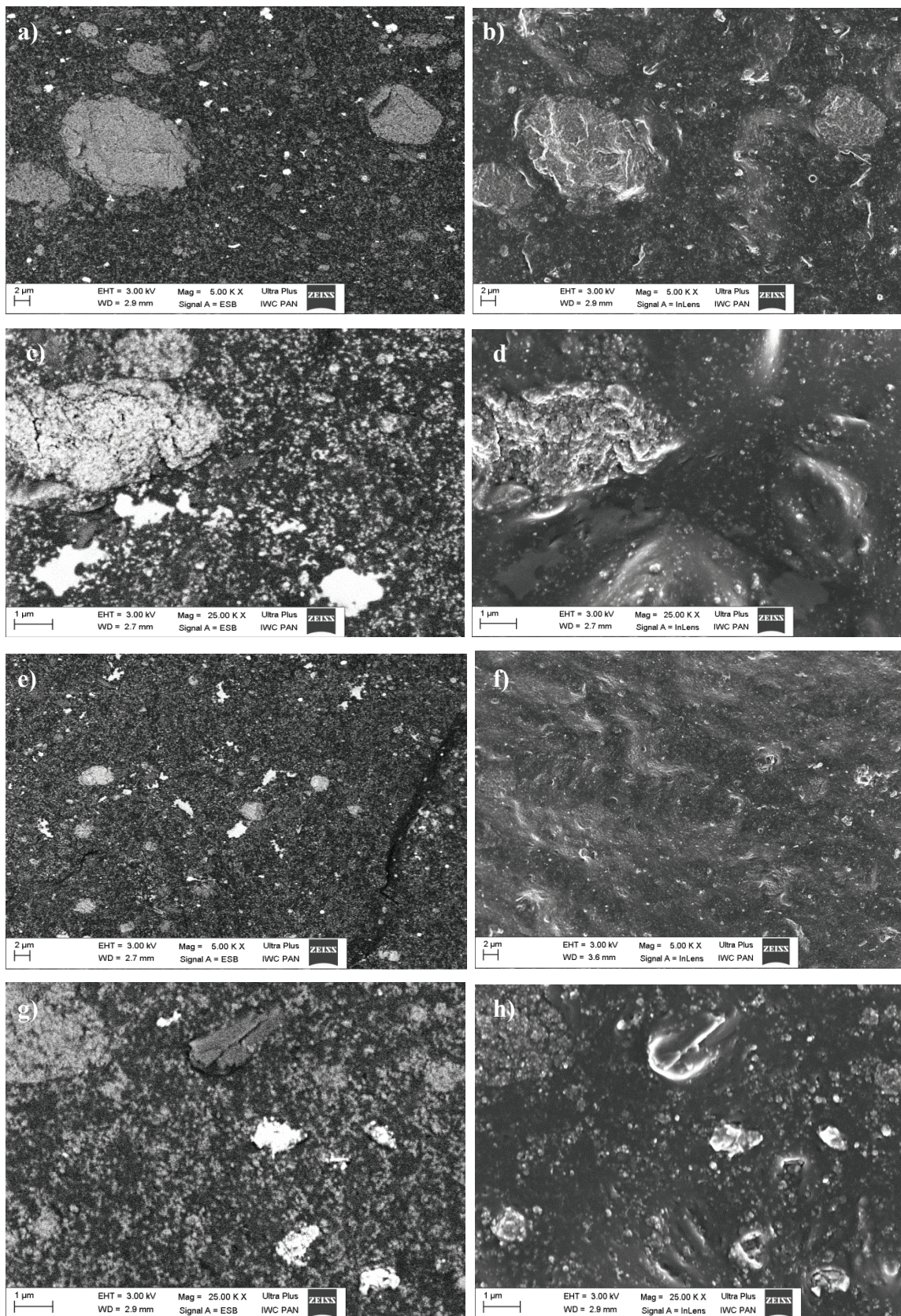


FIGURE 6.4 SEM micrographs of NBR/SiO₂: ESB (a, c), InLens (b, d), NBR/SiO₂/EMIM TFSI 5: ESB (e, g), InLens (f, h).

CHAPTER 6 IMPACT OF IMIDAZOLIUM IONIC LIQUIDS ON THE PROPERTIES OF NITRILE RUBBER COMPOSITES

The addition of hydrophobic EMIM TFSI ILs reduced the size of the silica agglomerates and facilitated their homogeneous distribution in the NBR/SiO₂ composites, which can clearly be seen with higher quantities of IL (10 phr or 15 phr) due to the greater distance between the particles (Fig. 6.5 a, b). The SEM pictures show that all of the hydrophobic ILs improved the silica dispersion, notably at 10 and 15 phr loadings. Figure 6.3 (c, d) shows part of the filler network structure in the NBR/SiO₂/EMIM TFSI 5 composite. The presence of IL decreases the tendency of silica to agglomerate and therefore likely affects the filler networking or the filler-rubber interactions. Such behavior of ILs may explain the better mechanical properties of NBR/SiO₂ composites that contain 2.5 phr and 5 phr ILs with TFSI anions. Although the dispersion of silica improved with increases in the proportion of EMIM TFSI (10 phr or 15 phr), there was no corresponding improvement in the mechanical properties of the composite.

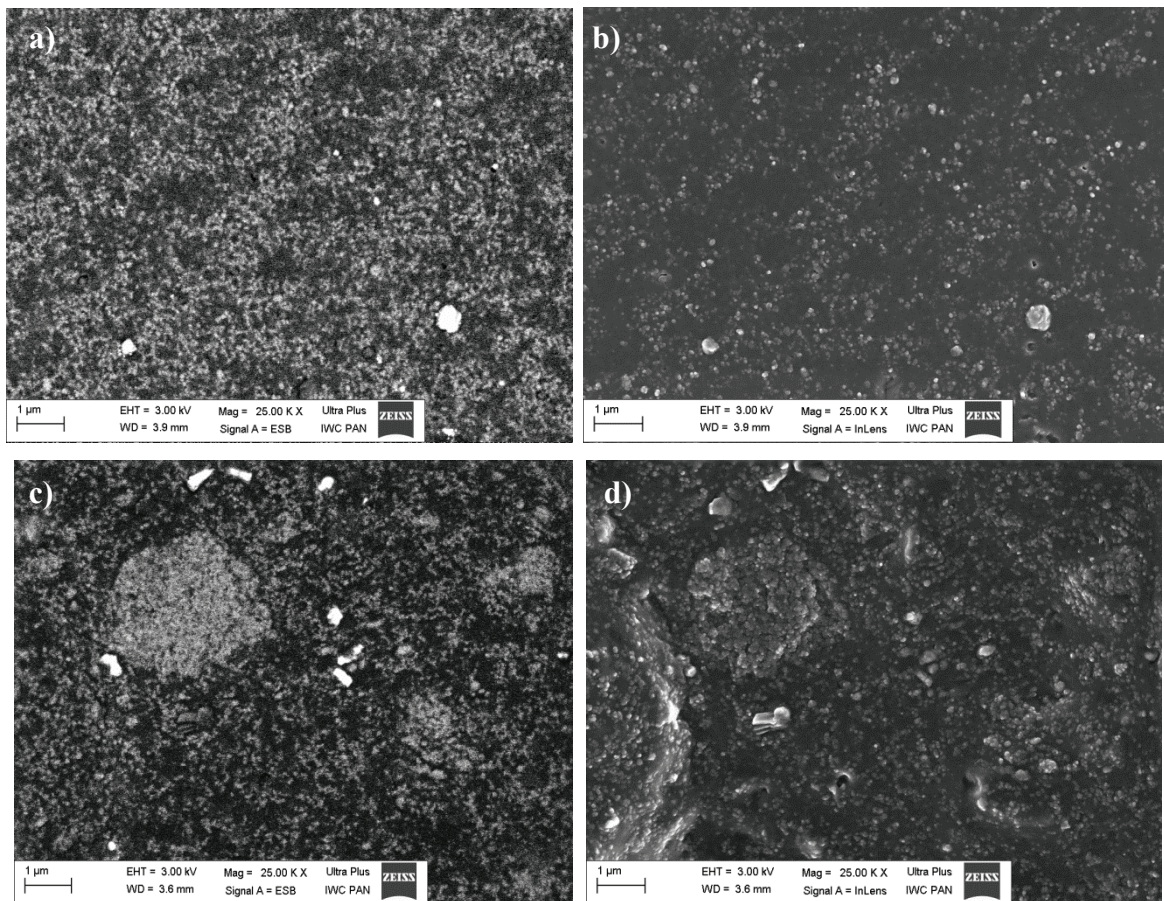


FIGURE 6.5 SEM micrographs of NBR/SiO₂/EMIM TFSI 15: ESB (a), InLens (b), NBR/SiO₂/EMIM SCN 15: ESB (c), InLens (d).

CHAPTER 6 IMPACT OF IMIDAZOLIUM IONIC LIQUIDS ON THE PROPERTIES OF NITRILE RUBBER COMPOSITES

Hydrophobic ILs appear to facilitate the incorporation and dispersion of silica filler in NBR rubber compounds but diminish its reinforcement capacity as measured by the bound rubber and stress-strain analysis. The data suggest that higher concentrations of imidazolium salts not only support filler dispersion by reducing silica agglomeration but also reduce the reinforcement capacity by weakening the filler-filler interactions or adhering between the filler and rubber. This effect is related to the fact that in the studied NBR system, greater amounts of ILs with TFSI anions (10 phr and 15 phr) act as plasticizers, which can also be observed by the variations in the T_g results. It is worth noting that Marwanta²²³ reported the Raman study of NBR/EIMM TFSI composites and detected interactions between the TFSI anions and the $-CN$ group, which may be responsible for the better compatibility of this type of IL with the polar matrix and the weaker filler-rubber interaction in composites that contain 10 phr and 15 phr of IL with TFSI anions.

The SEM micrographs showed that the dispersion of silica in the presence of hydrophilic EMIM SCN was better than the NBR/SiO₂ sample (especially for 10 phr and 15 phr of EMIM SCN IL; Figure 6.5 c, d). As was described previously, the tensile properties of the NBR composites increase slightly with EMIM SCN IL content until reaching a critical ratio (5 phr), after which deterioration of the mechanical properties occurs. This clearly demonstrates that EMIM SCN also acts as a plasticizing agent at higher concentrations. Nevertheless, the silica agglomerates in the composites with EMIM SCN IL are larger than are those in the compounds that contain TFSI-based ILs. This observation may be related to the hydrophilic nature of SCN anions and their lower compatibility with the hydrophobic rubber matrix.

6.5 IONIC CONDUCTIVITY OF NBR/SiO₂/IL COMPOSITES

Recently, ILs have been recognized as convenient sources of ions for some polymer materials due to their low T_g ²⁹⁸. ILs are generally highly dissociated, and there is no need to design strong ion-dipole interactions with polymer matrices to induce salt dissociation to enhance ion conduction. This observation suggests that some ILs are potential additives to improve the ionic conductivity of many polymers as long as they show moderate affinity toward each other.

²⁹⁸ M. Armand, F. Endres, D. R. MacFarlane, H. Ohno, B. Scrosati, Ionic-liquid materials for the electrochemical challenges of the future, *Nat. Mater.* 2009, **8**, 621–629.

CHAPTER 6 IMPACT OF IMIDAZOLIUM IONIC LIQUIDS ON THE PROPERTIES OF NITRILE RUBBER COMPOSITES

Because ILs are composed of only ions, they have very high ionic conductivities; the hydrophilic EMIM SCN and the hydrophobic EMIM TFSI have conductivities of $27 \text{ mS}\cdot\text{cm}^{-1}$ and $8.6 \text{ mS}\cdot\text{cm}^{-1}$ (25°C), respectively. The use of hydrophobic TFSI-based ILs more effectively enhances the ionic conductivity of NBR/SiO₂ composites than hydrophilic ionic liquids with SCN anions. The effect of IL concentration on the conductivity σ' of the NBR composites is shown in Figures 6.6 and 6.7.

The σ' values of the NBR/SiO₂ composites increased from $3.6\cdot 10^{-10} \text{ S}\cdot\text{cm}^{-1}$ to $1.8\cdot 10^{-9} \text{ S}\cdot\text{cm}^{-1}$ and $3.4\cdot 10^{-9} \text{ S}\cdot\text{cm}^{-1}$ in the presence of 2.5 phr and 5 phr EMIM SCN, respectively, whereas samples that contain EMIM TFSI salt exhibited conductivities of $6.3\cdot 10^{-9} \text{ S}\cdot\text{cm}^{-1}$ (2.5 phr) and $1.3\cdot 10^{-8} \text{ S}\cdot\text{cm}^{-1}$ (5 phr), respectively, at the same IL contents. This phenomenon may be due to the active participation of the SCN anions in the crosslinking process or the lower compatibility of this IL with the hydrophobic polymer matrix.

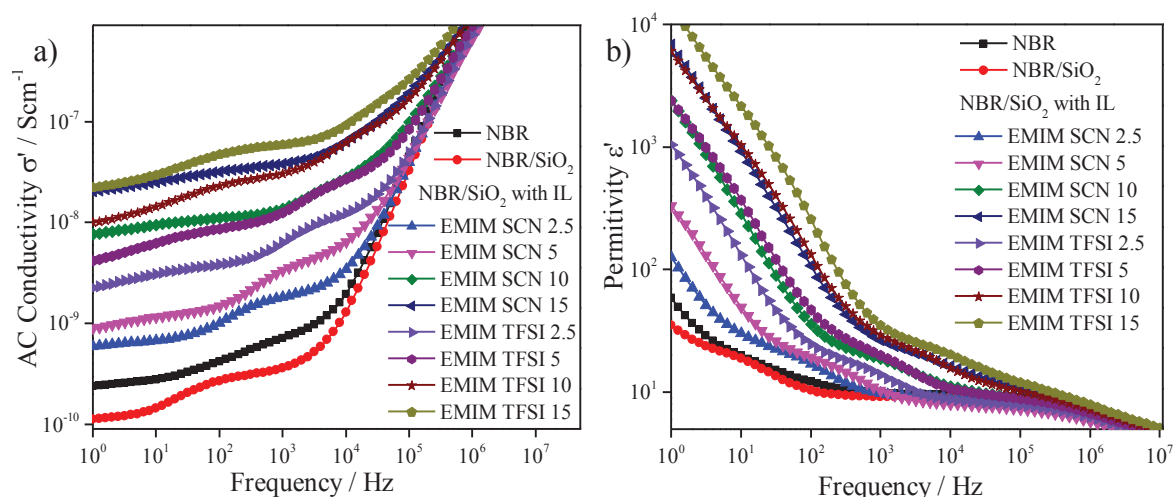


FIGURE 6.6 Dependence of AC conductivity σ' (a) and permittivity ϵ' (b) of NBR composites on differing IL mass ratios at 25°C .

With the addition of 10 phr of EMIM SCN imidazolium salt, the σ' of the composites raised up to $1.4\cdot 10^{-8} \text{ S}\cdot\text{cm}^{-1}$. Further increases in the levels of the hydrophobic ILs to 15 phr had a less significant impact on σ' than was expected. These results suggest that the number of ions is not the only factor that controls σ' . A decrease in T_g has been reported to result in better ion transport and higher ionic conductivities of polymer materials²⁹⁹. In the studied samples, the change in T_g was most prominent for ILs with a long side chain (HMIM TFSI), and the ionic conductivities of the NBR composites were the best in this salt at each concentration. It appears that the higher ionic conductivity can be attributed to

²⁹⁹ S. Tabata, T. Hirakimoto, H. Tokuda, M. Susan, M. Watanabe, Effects of novel boric acid esters on ion transport properties of lithium salts in nonaqueous electrolyte solutions and polymer electrolytes, *J. Phys. Chem. B* 2004,108, 19518–19526.

CHAPTER 6 IMPACT OF IMIDAZOLIUM IONIC LIQUIDS ON THE PROPERTIES OF NITRILE RUBBER COMPOSITES

the plasticizing effect of the bulky HMIM TFSI IL; however, due to the minor change in T_g , only a slight increase can be observed. Figure 6.6 shows the ionic conductivity and permittivity values of the NBR/SiO₂/IL composites relative to the neat composites as a function of frequency.

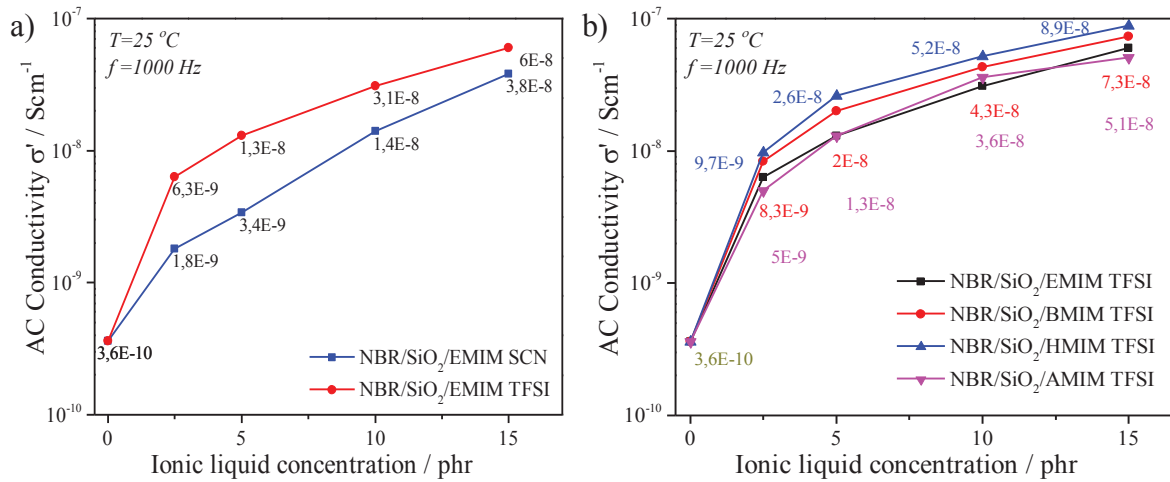


FIGURE 6.7 Ionic conductivity σ' in function of IL amount in NBR/SiO₂ composite effect of anions (a) and cations (b) of imidazolium ILs.

Generally, the conductivity measurements of the composites, especially those loaded with silica filler, show three characteristic spectral regions (Fig. 6.6 a). At high frequencies (10 kHz – 10 Hz), an increase in σ' is observed due to local charge fluctuations that correspond to a capacitive response of the material. This effect occurs because the hopping time of the charge carriers is much longer than the experimental time-scale.

In the frequency range between ~ 100 Hz and 10 kHz, a quasi-plateau develops that corresponds to the long-range diffusion of the charge carriers that correspond, by extrapolation to lower frequencies, to the value of the DC conductivity. The transition between this plateau and the increase in σ' observed in the high-frequency range is marked by a characteristic frequency f_e that corresponds to the hopping time of the charge carriers $\tau_e = 1/2\pi f_e$. The addition of the IL increases the characteristic frequency f_e , which is probably related to the enhanced mobility of the charge carriers due to plasticizing effects. At the same time, the DC conductivity increases with increasing concentrations of the IL in the material. A slight decrease in σ' occurs in the low-frequency region (1 Hz – 100 Hz), most likely due to the electrode polarization that is caused by a blocking effect of the charge carriers in the vicinity of the electrodes.

As shown in Figure 6.6 b, the permittivity ϵ' of rubber materials decreases rapidly with increasing frequency at 25 °C at frequencies between 10 and 10⁵ Hz, which is attributed to

CHAPTER 6 IMPACT OF IMIDAZOLIUM IONIC LIQUIDS ON THE PROPERTIES OF NITRILE RUBBER COMPOSITES

the mobile ions; this effect is particularly evident at higher IL concentrations of 15 phr and is not observed in the pure NBR and NBR/SiO₂ composites. A constant value of the permittivity ϵ' was obtained at frequencies higher than 10⁶ Hz.

6.6 EFFECT OF WEATHERING ON THE TENSILE PROPERTIES AND CROSSLINK DENSITY

Before aging, the NBR/SiO₂/AMIM TFSI and NBR/SiO₂/EMIM TFSI samples exhibited higher strain and elasticity than the NBR/SiO₂/EMIM SCN and neat NBR/SiO₂ composites. In samples that contain EMIM TFSI and AMIM TFSI, the strains at break was were approximately 699 % and 695 % before aging. The mechanical behavior of these materials was different after 24 h of aging, with lower elongations at of approximately 25 % and 26 % for EMIM TFSI and AMIM TFSI, respectively.

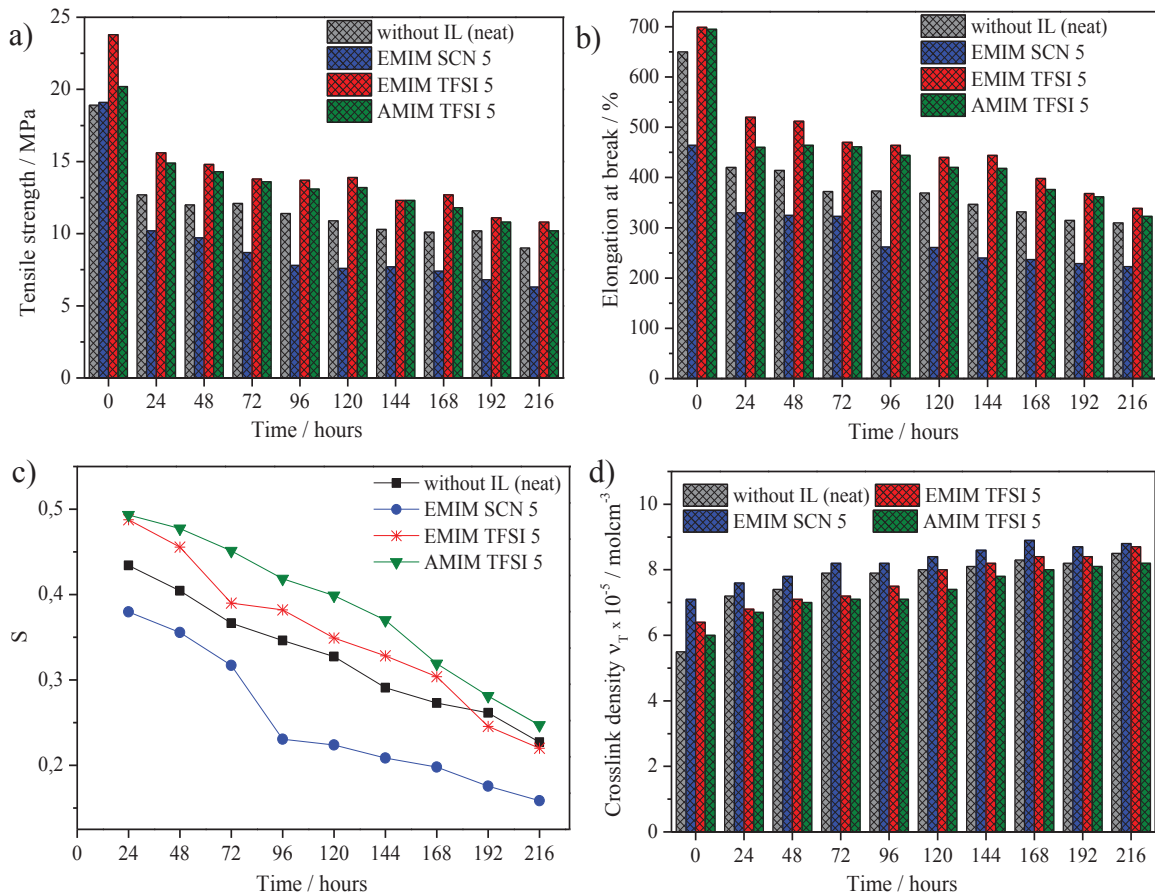


FIGURE 6.8 Tensile strength (a), elongation at break (b), aging coefficient S (c) and crosslink density v_T (d) as a function of the aging time of the NBR composites.

**CHAPTER 6 IMPACT OF IMIDAZOLIUM IONIC LIQUIDS ON THE PROPERTIES
OF NITRILE RUBBER COMPOSITES**

TABLE 6.4 The results of the tensile properties as a function of the aging time.

NBR composites	Time* [hours]	SE ₁₀₀ [MPa]	SE ₂₀₀ [MPa]	SE ₃₀₀ [MPa]	TS [MPa]	Eb [%]	H [°Sh]
neat	-	2.2±0.1	3.3±0.1	4.0±0.3	18.9±1.6	650±16	76
neat	24	2.6±0.2	5.1±0.2	6.5±0.3	12.0±2.0	420±10	79
neat	48	3.4±0.2	5.3±0.1	7.8±0.3	11.2±1.1	414±8	81
neat	72	3.1±0.1	5.4±0.2	8.8±0.4	12.1±1.4	372±11	82
neat	96	3.4±0.2	5.5±0.3	8.7±0.3	11.4±1.2	373±12	81
neat	120	3.4±0.3	5.9±0.3	9.8±0.4	10.9±1.2	369±7	82
neat	144	4.1±0.2	7.2±0.2	11.3±0.	10.3±1.0	347±9	82
neat	168	4.3±0.2	7.3±0.3	11.0±0.	10.1±0.9	332±10	82
neat	192	4.4±0.3	7.1±0.3	10.8±0.	10.2±2.0	315±11	83
neat	216	4.5±0.3	7.2±0.3	10.7±0.	9.0±1.2	310±9	83
EMIM SCN	-	3.0±0.1	5.4±0.2	7.2±0.2	19.1±1.7	464±13	77
EMIM SCN	24	3.3±0.2	5.1±0.2	7.5±0.3	10.2±2.0	330±5	78
EMIM SCN	48	3.5±0.2	4.7±0.3	7.3±0.2	9.7±1.1	325±7	80
EMIM SCN	72	3.5±0.2	5.4±0.1	8.1±0.3	8.7±0.9	323±14	82
EMIM SCN	96	3.7±0.1	5.6±0.2	-	7.8±0.8	262±9	82
EMIM SCN	120	3.8±0.1	5.9±0.4	-	7.6±0.7	261±8	83
EMIM SCN	144	4.4±0.2	6.5±0.2	-	7.7±1.0	240±7	83
EMIM SCN	168	4.7±0.2	7.4±0.3	-	7.4±1.2	237±6	82
EMIM SCN	192	4.6±0.3	7.5±0.4	-	6.8±2.0	229±6	80
EMIM SCN	216	4.6±0.2	7.4±0.3	-	6.3±1.1	223±5	79
EMIM TFSI	-	2.8±2.0	3.5±0.1	4.1±0.3	23.7±2.0	698±15	73
EMIM TFSI	24	3.2±2.0	4.2±0.3	6.0±0.3	15.6±2.2	520±12	75
EMIM TFSI	48	3.4±0.3	4.3±0.2	7.4±0.2	14.8±2.1	512±13	77
EMIM TFSI	72	3.5±0.1	4.1±0.1	5.5±0.1	13.8±2.0	470±14	80
EMIM TFSI	96	3.7±0.2	5.3±0.3	7.4±0.2	13.7±1.3	464±11	80
EMIM TFSI	120	3.6±0.2	5.3±0.1	7.6±0.1	13.9±1.0	440±12	80
EMIM TFSI	144	4.2±0.1	5.6±0.2	8.9±0.3	12.3±1.3	444±13	81
EMIM TFSI	168	4.1±0.2	6.1±0.2	8.4±0.3	12.7±0.9	398±10	83
EMIM TFSI	192	4.3±2.0	6.5±0.3	9.2±0.2	11.1±1.1	368±11	82
EMIM TFSI	216	4.3±0.3	6.8±0.3	9.8±0.4	10.8±0.8	339±7	83
AMIM TFSI	-	2.9±0.1	3.4±0.2	4.0±0.2	20.2±1.4	695±14	73
AMIM TFSI	24	3.3±0.2	4.4±0.3	5.4±0.3	15.1±1.6	460±9	75
AMIM TFSI	48	3.1±0.3	4.1±0.2	5.7±0.3	14.3±1.3	464±13	78
AMIM TFSI	72	3.4±0.1	4.9±0.3	6.8±0.2	13.6±1.1	461±10	80
AMIM TFSI	96	3.4±0.1	5.1±0.2	7.6±0.3	13.1±1.2	444±9	81
AMIM TFSI	120	3.5±0.2	4.9±0.1	7.0±0.2	13.2±1.0	420±8	80
AMIM TFSI	144	3.5±0.3	5.7±0.3	7.8±0.3	12.3±1.3	418±10	80
AMIM TFSI	168	3.7±0.2	5.6±0.2	8.3±0.3	11.8±1.1	376±13	81
AMIM TFSI	192	4.0±0.2	5.8.9±0	9.2±0.1	10.8±0.8	362±13	82
AMIM TFSI	216	4.1±0.3	6.0±0.3	9.0±0.3	10.2±1.2	323±9	81

*Weathering time

CHAPTER 6 IMPACT OF IMIDAZOLIUM IONIC LIQUIDS ON THE PROPERTIES OF NITRILE RUBBER COMPOSITES

The decrease in the elongation at break was most pronounced for the neat NBR/SiO₂ and reached approximately 35 %. The low elasticity of the NBR/SiO₂ and NBR/SiO₂/IL composites was most likely due to the large increase in the composite crosslink density during the aging process (Fig. 6.8 d). The results shown in Figure 6.8 (a, b, c) show that the mechanical properties were retained better in the composites that used EMIM TFSI and AMIM TFSI (higher S) as opposed to NBR/SiO₂ and NBR/SiO₂/EMIM SCN. Figure 6.8 (a, b) shows the changes in the tensile strength TS and elongation at break of the composites during the aging process. The TS decreases rapidly in NBR/SiO₂ and NBR/SiO₂/EMIM SCN with an increase in the exposure time. However, the decreases in the tensile properties of samples with EMIM TFSI and AMIM TFSI were not as rapid as was observed in the NBR/SiO₂ and NBR/SiO₂/EMIM SCN composites.

This effect is most likely due to the lower tendency for crosslink formation in the presence of the hydrophobic ILs in NBR composites during outdoor exposure. The EMIM SCN showed high crosslinking activity during the aging process, which increased the brittleness of the samples and caused faster degradation of the polymer. The effect of aging time on the tensile modulus (stress at 100 %, 200 % and 300 % elongation) of the NBR/SiO₂ and NBR/SiO₂/IL composites is shown in Table 6.4. The modulus are related to the stiffness and cross-linking density (Fig. 6.8 d) of the rubber compounds. The stress modulus of the compounds increased with increasing aging time; this increase was especially pronounced in the NBR/SiO₂ and NBR/SiO₂/EMIM SCN composites. The crosslinked network in the studied materials during aging caused an increase in the stiffness of the composites. As a result, the materials become more brittle, lose flexibility, and their surfaces crack, which results in a decrease in the mechanical strength of the samples.

Furthermore, a decrease in the stress of NBR/SiO₂/EMIM SCN at 300 % elongation was observed when the irradiation lasted for more than 96 h. These changes were directly associated with changes in the original crosslinked structure; i.e., main chain scission and crosslinking³⁰⁰. The formation of photo products and the crosslink densities increased in all of the samples during the studied aging time. The crosslink density was found to be the highest in the NBR/SiO₂/EMIM SCN composite. It appears that this IL most likely acts as an accelerator for the formation of crosslinks in NBR sulfur-based systems during aging. The hardness values of the unaged and aged composites are shown in Table 6.4. With

³⁰⁰ S. Thiruvarudchelvan, The potential role of flexible tools in metal forming, *J. Mater. Process. Technol.* 1993, **39**, 55–61.

CHAPTER 6 IMPACT OF IMIDAZOLIUM IONIC LIQUIDS ON THE PROPERTIES OF NITRILE RUBBER COMPOSITES

increasing aging time, the hardness increased in all of the studied composites, which is correlated with increased brittleness of the samples due to the increased crosslink density. The lowest values of hardness during weathering were obtained in NBR/SiO₂/AMIM TFSI, which is consistent with its lowest crosslink density. In all of the composites, the difference between the mechanical responses of the unaged and aged materials is most likely due to the formation of an oxidative layer during thermal and photo aging. The hardening at the surface during irradiation is linked to the formation of a crosslinked network, and the oxidized products hinder the mobility of the macromolecules. These constraints at the surface of the material indicate the formation of cracks during elongation, which lead to a lower strain at break compared to the unaged material.

6.7 DMA AND IONIC CONDUCTIVITY AFTER WEATHERING

During the outdoor exposure of rubber, the formation of three-dimensional networks by means of crosslinks leads to a decrease in the maximum loss factor ($\tan\delta$). Studies from the literature have reported that during aging, some variations in T_g of the elastomer composites can be related to crosslinking or chain scission^{301, 251}.

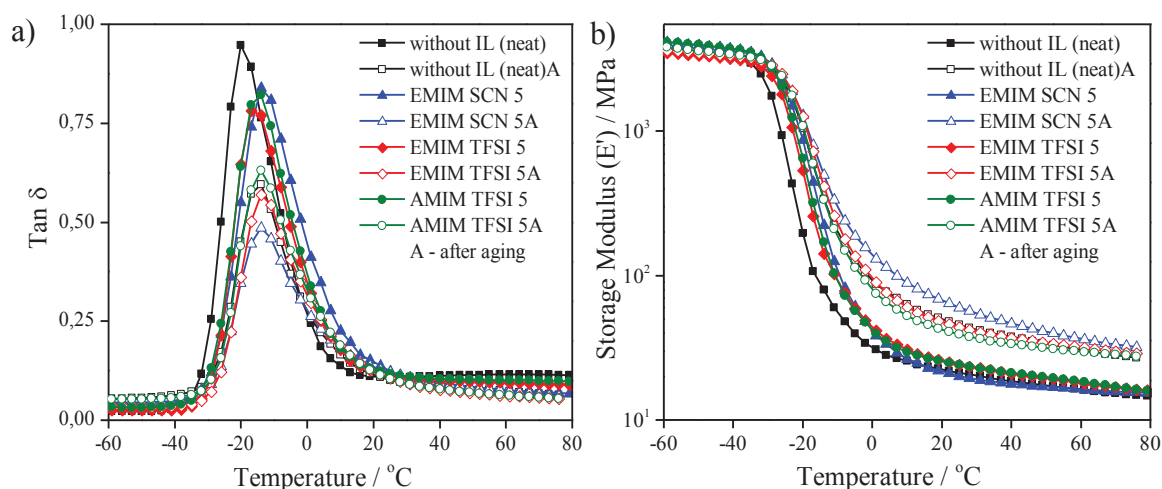


FIGURE 6.9 Temperature dependence of the loss tangent $\tan\delta$ (a) and the storage modulus E' (b) values at 10 Hz for the NBR/SiO₂/IL composites before and after aging for 216 h.

This observation can explain the slight changes in the T_g values of NBR composites after aging, as was observed from the DMA. Figure 6.9 (a, b) and Table 6.5 show the $\tan\delta$ values and the storage modulus of the studied materials before and after 216 h of irradiation. Decreases in $\tan\delta$ were observed in NBR/SiO₂ and NBR/SiO₂/IL after 216 hours of

³⁰¹ G. Mertz, F. Hassouna, P. Leclère, A. Dahoun, V. Toniazzo, D. Ruch, Correlation between (nano)-mechanical and chemical changes occurring during photo-oxidation of filled vulcanised styrene butadiene rubber (SBR), *Polym. Degrad. Stab.* 2012, **97**, 2195–2201.

CHAPTER 6 IMPACT OF IMIDAZOLIUM IONIC LIQUIDS ON THE PROPERTIES OF NITRILE RUBBER COMPOSITES

weather aging, which suggests variations in the visco-elastic properties during outdoor aging of NBR-based materials. The smallest changes after 216 h of exposure occurred in the NBR/SiO₂/AMIM TFSI composite; the tanδ values changed from 0.85 to 0.63. The effects of ILs on tanδ of the unaged samples were discussed in a previous section (6.3).

After 216 h of irradiation, we observed increases in E' and decreases in tanδ in all of the aged samples compared to their unaged counterparts, which were mainly due to the increasing crosslinking density. A significant increase in the E' was observed for NBR/SiO₂/EMIM SCN (60.3 MPa at room temperature), whereas E' reached 45.6 MPa in NBR/SiO₂ under the same temperature conditions. However, the increase in the E' value of composites that contain AMIM TFSI (38 % at room temperature) and EMIM TFSI (45 % at room temperature) was less than in the NBR/SiO₂ sample (54 % at room temperature).

TABLE 6.5 DMA properties of the NBR composites after 216 h of aging.

NBR composites	Time * [hours]	E' [MPa]		tanδ	
		25 °C	40 °C	Peak Value	T _g [°C]
neat	-	21.3	18.6	0.95	-16.2
neat	216	45.6	37.6	0.60	-15.1
EMIM SCN	-	20.1	17.9	0.85	-13.1
EMIM SCN	216	60.3	46.9	0.57	-14.2
EMIM TFSI	-	24.3	21.1	0.83	-15.6
EMIM TFSI	216	43.8	37.0	0.48	-14.0
AMIM TFSI	-	24.1	21.2	0.85	-15.4
AMIM TFSI	216	39.1	33.7	0.63	-14.3

*Weathering time

Table 6.6 shows the AC conductivities of the studied samples before and after aging. The σ' values of unaged NBR/SiO₂ and NBR/SiO₂/EMIM SCN were 3.6×10⁻¹⁰ S·cm⁻¹ and 1.8×10⁻⁹ S·cm⁻¹, respectively, whereas both of the composites that contained TFSI anions, NBR/SiO₂/EMIM TFSI and NBR/SiO₂/AMIM TFSI, had σ' values of 1.3×10⁻⁸ S·cm⁻¹. However, after 216 h of exposure, the conductivities of the neat NBR/SiO₂ and TFSI-based IL compounds decreased. This observation may be related to the changes in the polymer structure during aging. In contrast to the samples discussed previously, the conductivity of NBR/SiO₂/EMIM SCN increased slightly to 1.1×10⁻⁸ S·cm⁻¹. This behavior can most likely be ascribed to the hydrophilic nature of this imidazolium salt.

Due to factors such as temperature and light, the IL most likely leaked onto the surface of the composite, which increased its conductivity after aging. This phenomenon was not

CHAPTER 6 IMPACT OF IMIDAZOLIUM IONIC LIQUIDS ON THE PROPERTIES OF NITRILE RUBBER COMPOSITES

observed in the composites that were filled with hydrophobic ILs that contained TFSI anions. Better stability of NBR composites may be provided by the compatibility of hydrophobic ILs with a hydrophobic polymer matrix and the interaction of the TFSI anions with the functional groups of the polymer –CN, as was described previously.

TABLE 6.6. Ionic conductivity σ' after 216 h weathering for the NBR composites.

NBR composites	Time * [hours]	σ' [S·cm ⁻¹], 1 kHz, 25 °C
neat	-	3.6×10^{-10}
neat	216	9.7×10^{-11}
EMIM SCN	-	1.8×10^{-9}
EMIM SCN	216	1.1×10^{-8}
EMIM TFSI	-	1.3×10^{-8}
EMIM TFSI	216	4.6×10^{-9}
AMIM TFSI	-	1.3×10^{-8}
AMIM TFSI	216	8.8×10^{-9}

*Weathering time

Das ²³⁵ studied the coupling activity of 1-allyl-3-methylimidazolium chloride between diene elastomers and multi-walled carbon nanotubes and concluded that the double bond that is present in 1-allyl-3-methylimidazolium chloride molecules was chemically linked to the double bond of the diene rubber molecules by sulfur bridges, which provided superior mechanical and electrical properties. In our investigation, AMIM TFSI has a double bond that is attached to the imidazolium cation ring, which can exhibit similar behavior in NBR and improve the IL stability of the polymer matrix.

6.8 SURFACE STUDY AFTER WEATHERING

Colorimetric studies of the CIE L*a*b* system provided information on the color characteristics of the composites after the weather test (Fig. 6.10). The coefficient ΔE defines the extent to which the color of the samples changed during the 216 h of exposure. The obtained data indicate that the colors of all of the studied samples, changed after 24 h of irradiation. ILs with TFSI anions appear to not significantly influence the surface color of the composites during irradiation; the values of the ΔE coefficients in these samples were similar to those of the neat sample. The obtained data indicate that the color of all of the studied samples, especially that of the NBR/SiO₂/EMIM SCN composite, changed after 24 h of irradiation. The significant change in color of this sample can be explained by the weak light stability of the EMIM SCN IL. EMIM SCN salt is often yellow or orange in

CHAPTER 6 IMPACT OF IMIDAZOLIUM IONIC LIQUIDS ON THE PROPERTIES OF NITRILE RUBBER COMPOSITES

color and darkens with extended exposure to sunlight. The thiocyanate ion is known to dimerize to thiocyanogen (SCN)₂ under chemically or electrochemically oxidative conditions in melt and then polymerize to polythiocyanogen (SCN)_x. Both thiocyanogen and polythiocyanogen are known to be photoactive²⁰⁶.

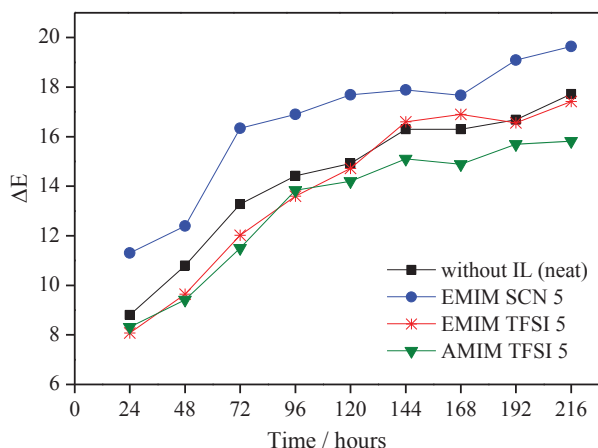


FIGURE 6.10 Color difference (ΔE) of the NBR/SiO₂/IL after weather aging.

The micro-morphology and microstructures of the composites were investigated by SEM. Figure 6.11 shows SEM photos of the NBR/SiO₂ and NBR/SiO₂/AMIM TFSI composites before and after 216 h of weathering. The vulcanizates before aging (6.11 a, d) are characterized by smooth surfaces and uniform structures. A series of cracks of varying sizes appeared on the composite surfaces after aging (6.11 a, d) due to the rupture of the macromolecular network structure on the nitrile rubber surface or molecular chain crosslinking or degradation, which formed surface defects. In the case of NBR/SiO₂, significant changes in the surface morphology were observed after aging; the cracks are prominent as a result of the surface oxidation. It is worth noting that the images were taken from different areas of the composites. The SEM images of NBR/SiO₂/AMIM TFSI also showed surface defects, but they were not as significant as those in the NBR/SiO₂. To confirm the post-aging chemical changes of the composites, they were analyzed using ATR-FTIR spectroscopy. After 24 h of aging, the changes in the analyzed spectra of the rubber/IL composites were slightly lower than those in the spectrum of NBR/SiO₂. Nevertheless, the differences between the composites that were aged for more than 24 h were found to be marginal.

CHAPTER 6 IMPACT OF IMIDAZOLIUM IONIC LIQUIDS ON THE PROPERTIES OF NITRILE RUBBER COMPOSITES

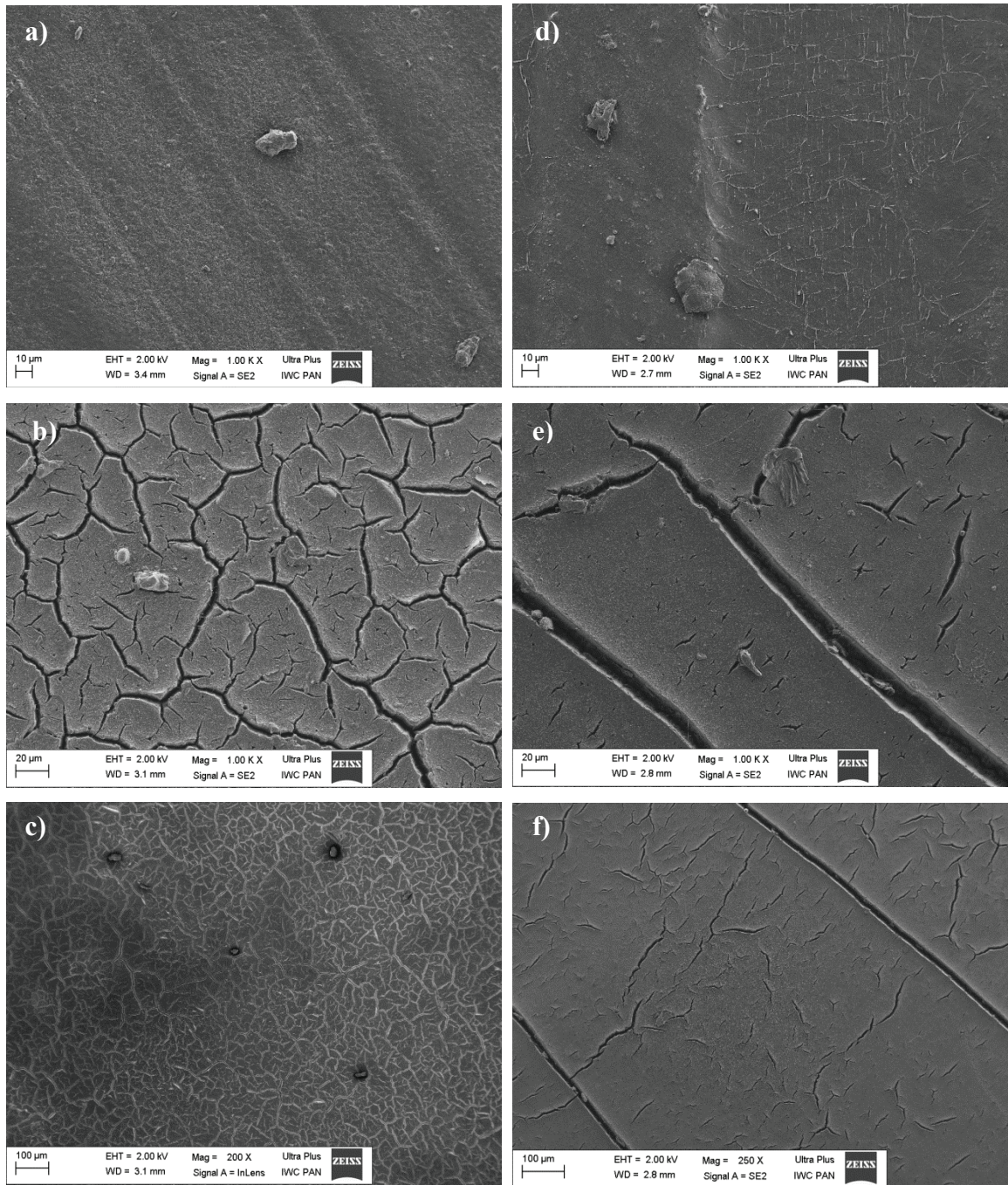


FIGURE 6.11 SEM micrographs of (a) NBR/SiO₂ before aging, (b, c) NBR/SiO₂ after 216 h aging, (d) NBR/SiO₂/AMIM TFSI before aging, (e, f) NBR/SiO₂/AMIM TFSI after 216 aging.

6.6 CONCLUSIONS

These investigations considered the effects of multifunctional additives, such as hydrophilic and hydrophobic imidazolium ILs, on the curing kinetics, crosslink density, mechano-dynamic, morphological and ionic conductivity properties of NBR/SiO₂ composites. The hydrophilic IL with SCN anions was found to be an accelerator in the sulfur vulcanization of NBR rubber composites. The incorporation of this type of IL

CHAPTER 6 IMPACT OF IMIDAZOLIUM IONIC LIQUIDS ON THE PROPERTIES OF NITRILE RUBBER COMPOSITES

resulted in considerably shorter curing times and higher crosslink densities. However, the potential applications of SCN-based ILs are limited by concentration because the use of more than 10 phr in NBR composites led to reversion during the curing process and deterioration of the mechanical properties. TFSI-based ILs had a minor effect on the curing process that depended mainly on the length of the alkyl chains that are attached to the imidazolium ring in the IL molecule.

DMA and DSC provided only one glass transition temperature T_g for each sample, which suggests that no phase separation occurred in the studied composites. The T_g values of the NBR/SiO₂ composites decreased as the concentrations of hydrophilic and hydrophobic ILs increased. Moreover, the alkyl chain length was found to slightly affect the plasticizing effect and therefore the σ' ionic conductivity of the polymers. An increase in the IL content of the NBR/SiO₂ composite resulted in a decrease in T_g , which was accompanied by a slight increase in ion conductivity, especially in NBR/SiO₂/HMIM TFSI 15. Nevertheless, EMIM SCN IL was not as effective at improving the ionic conductivity as TFSI-based imidazolium salts, in which the addition of 5 phr of hydrophobic ILs increased the conductivity by two orders of magnitude. The weaker filler-filler interaction and decrease in silica agglomerate size in the NBR composites that contain 2.5-5 phr TFSI-based imidazolium ILs were the most likely reasons for the enhancement of the NBR/SiO₂/IL tensile properties. The application of hydrophobic ILs at higher contents (10 phr and 15 phr) caused a plasticizing effect that was accompanied by losses of mechanical strength.

Weathering experiments provided information about the influence of selected ILs on the properties of NBR composites under adverse outdoor conditions. The studied hydrophilic EMIM SCN strongly contributed to faster degradation of the polymer, whereas NBR/SiO₂ composites that contain EMIM TFSI and AMIM TFSI aging slower than the reference sample.

The results of the performance studies indicate that the addition of hydrophobic TFSI-based imidazolium ILs in quantities of 2.5-5 phr most effectively improved the mechanical properties and σ' of the NBR/SiO₂ composites and has positive effects on the rubber matrix during outdoor exposure.

CHAPTER 7
GENERAL CONCLUSIONS

This research examined the effects of solvent dyes and pigments on the durability of ethylene-norbornene (EN) and acrylonitrile-butadiene rubber (NBR) composites that were exposed to weathering conditions with UV irradiation and the full solar spectrum. The analysis of the properties of EN during UV aging showed that all of the studied dyes (except Solvent Red) retard the degradation of EN composites. The best improvement in durability was found in the samples that contained anthraquinone solvent dyes with strong electron-donating substituents, such as Solvent Blue 97, Solvent Blue 104, Solvent Blue, Solvent Green 28 and Solvent Yellow 93. This protective effect of solvent dyes appears to be related to not only light absorption but also their activity toward free radicals, as determined by the ABTS method. The investigated stabilizers, including Tinuvin 234, Chimassorb 81, Tinuvin 1577 and Chimassorb 994, extended the lifetime of EN composites under UV irradiation of 343 nm and more effectively protected the composites than the solvent dyes. The number of dye particles did not have a significant impact on the final result of aging in the composites. The exception was the EN/S. Yellow 93 composite, which demonstrated less protection of the material with a dye concentration of 3.5×10^{-4} because S. Yellow 93 has a lower molecular weight than the other studied dyes.

The results of weathering in the full solar spectrum exhibited a similar trend to the UV aging study. However, the protection efficiencies of solvent dyes in EN composites under exposure to the full solar spectrum were much greater than those of most of the investigated stabilizers. The application of anthraquinone dyes with strong electron-donating substituents significantly prolonged the lifetimes of EN composites during the aging process. The addition of stabilizers into EN did not ensure good protection of EN composites in solar conditions, as it did under UV exposure (except for HALS). This effect could be related to the greater ability of anthraquinone dyes to protect EN composites under weathering conditions with full sun exposure than commercial absorbers. On the other hand, this type of stabilizer cannot provide sufficient protection under this set of aging conditions. These results demonstrate that the presence of anthraquinone solvent dye can play two roles in EN composites; it may provide intense colors at low concentrations and provide better protection against unfavorable outdoor conditions than some commercial stabilizers.

The accelerated UV aging test showed that all of the investigated pigments improved the durability of EN and that phthalocyanine blue provided the best in this regards. The

results indicated that pigments provided good protection of EN composites in bulk but allowed significant deterioration of their surfaces.

Further investigations demonstrated that solvent dyes with strong electron-donating substituents improved the durability of EN composites better than most of the studied pigments and provided better surface protection. Nevertheless, the loss of color in solvent dyes was associated with sample degradation, while the color of EN/pigment composites remained nearly unchanged despite substantial sample degradation. A synergistic effect was observed between the dispersed pigments and the molecular solution of dyes in EN composites during UV exposure. The addition of dye and pigment mixtures to EN composites resulted in materials with better resistance to UV exposure than those with pigments at the same concentration.

The research also focused on the behavior of NBR composites that contain solvent dyes under UV exposure and showed that solvent dyes provide no protective effect in NBR materials. In contrast, the investigated pigments improved the durability of NBR composites better than most of the applied stabilizers (Tinuvin 234, Chimassorb 81 and Tinuvin 1577). Of the pigments, the best protection against UV aging was provided by NBR composites that contained phthalocyanine blue (P. Blue 15:1) and green (P. Green 7), and the Chimassorb 994 stabilizer was most effective. However, the surfaces of the studied NBR/SiO₂/ pigments showed more defects, cracks and corrosion after 120 h of UV aging than the surfaces of the reference and NBR/Chimassorb 994 samples. This investigation confirmed the results from ethylene-norbornene studies that pigments provide effective protection of polymer composites in bulk, but they contribute to faster surface degradation under UV irradiation. Finally, to produce colored NBR composites with enhanced aging resistance, a better alternative is to use pigments as colorants rather than this type of solvent dye.

The next part of this study estimated the effects of multifunctional additives, such as hydrophilic and hydrophobic ILs, on the properties of NBR composites, including their behavior during aging. Hydrophilic ILs had different impacts on the curing kinetics, crosslinks density, mechano-dynamics, morphology and ionic conductivity of NBR/SiO₂ composites in comparison to hydrophobic imidazolium salts. Hydrophilic ILs with SCN anions were found to be accelerators in the sulfur vulcanization of NBR composites, which considerably shortens the curing time and increases the crosslink density in these samples. However, the potential applications of SCN-based ILs are limited by concentration because

the use of more than 10 phr in NBR composites led to reversion during the curing process and the deterioration of the mechanical properties. TFSI-based ILs had only minor effects on the curing process, which depended on the length of the alkyl chains attached to the imidazolium ring in the IL molecule. The TFSI-based ILs were much more effective at improving σ' than the hydrophilic EMIM SCN, as the addition of 5 phr of hydrophobic ILs increased the conductivity of the NBR by two orders of magnitude.

Weathering experiments provided information about the influence of selected ILs on the properties of NBR composites under adverse outdoor conditions. The studied hydrophilic EMIM SCN was found to contribute to faster degradation of the polymer, whereas NBR/SiO₂ composites that contained EMIM TFSI and AMIM TFSI aged more slowly than the reference sample.

Based on the performance studies demonstrated that the addition of hydrophobic TFSI-based imidazolium ILs in quantities of 2.5-5 phr resulted in NBR/SiO₂ composites with improved mechanical properties and ionic conductivities as well as better retention against aging.

SUMMARY

This study demonstrated the effects of several polymer additives on the aging properties of elastomer composites. Solvent dyes, high-performance pigments and conductive ILs were employed as additives to obtain elastomer composites that were characterized by enhanced weather aging resistance and good mechanical properties.

In the first part of the investigation, selected solvent dyes, most of which contained anthraquinone chromophores and high performance pigments, that exhibited high light and temperature resistance were applied to ethylene-norbornene (EN) cyclic olefin and acrylonitrile butadiene rubber (NBR) and then subjected to aging process. The aging tests demonstrated that the best protection of EN composites against different weathering conditions (UV irradiation and the full solar spectrum) was provided by anthraquinone dyes with strong electron-donating substituents. The results were compared with the properties of samples that contain commercial stabilizers that are commonly used in polymer technology. Analyses of the mechanical properties (DMA and tensile tests) as well as surface analysis (FTIR, XPS, SEM) of EN composites confirmed that solvent dyes with strong electron substituents provided better protection against aging in the full solar spectrum than most of the investigated commercial stabilizers. Moreover, the application of dye and pigment mixtures in EN composites was found to enhance their resistance to UV exposure more effectively than pigments at the same concentration. The durability of NBR composites was increased by the addition of pigments to the polymers, whereas this effect was not observed in samples with solvent dyes. The next part of the thesis focused on the impact of hydrophilic and hydrophobic imidazolium ions on NBR. The influences of thiocyanate, (SCN) and bis(trifluoromethylsulfonyl)imide, (TFSI) anions and the length of the alkyl chain (from ethyl to hexyl) of imidazolium ionic liquids (ILs) on the curing kinetics, mechanical, morphological, ionic conductivity and weathering properties of nitrile rubber composites were investigated. A hydrophilic IL with SCN anions was found to accelerate the sulfur vulcanization of NBR rubber composites, which resulted in a considerably shorter curing time and increased crosslink density. Nevertheless, the hydrophilic IL was not as effective at improving the ionic conductivity as hydrophobic TFSI-based imidazolium salts, in which the addition of 5 phr of this IL increased the conductivity by two orders of magnitude. The results demonstrate that the addition of hydrophobic TFSI-based imidazolium ILs in quantities of 2.5-5 phr most effectively improved the mechanical properties and ionic conductivities of the NBR composites and had positive effects on the rubber matrix during outdoor exposure.

PUBLICATIONS AND PATENTS

BOOK CHAPERS

1. A. Marzec, M. Zaborski, *Krzemionka jako napelniaz elastomerów*, Na Pograniczu Chemii i Biologii, Poznań 2009, 978-83-232-2114-2.
2. A. Marzec, M. Zaborski, *Wpływ pigmentów kompozytowych zawierających cieczy jonowe na właściwości kauczuku butadienowo-akrylonitrylowego (NBR)*, Na Pograniczu Chemii i Biologii, Poznań 2010, 978-83-232-2254-5.
3. A. Marzec, M. Lipińska, J. Sokołowska, M. Zaborski, *Properties of silicone rubber with pigment-modified silicas*, Modern Polymeric Materials for Environmental Applications, Kraków 2010, 978-83-930641-1-3.
4. A. Marzec, M. Zaborski, *Pigment and dye modified fillers as elastomeric additives*, Advanced Elastomers Technology, Properties and Applications, Croatia 2012, 978-953-51-0739-2.

PUBLICATIONS

1. A. Marzec, M. Lipińska, J. Sokołowska, M. Zaborski, Krzemionki modyfikowane pigmentem jako napelniaz kompozytów elastomerowych, *Przemysł Chemiczny* 2010, **89**, 1475–1478.
2. A. Marzec, M. Zaborski, Wpływ wybranych barwników na właściwości antystarzeniowe kauczuku butadienowo-akrylonitrylowego, *Przemysł Chemiczny* 2011, **90**, 1083–1087.
3. A. Marzec, M. Zaborski, Wpływ pigmentu tiazynowego na właściwości przeciwstarzeniowe kompozytów kauczuku butadienowo-akrylonitrylowego, *Przemysł Chemiczny* 2012, **91**, 879–882.
4. A. Marzec, M. Zaborski, Właściwości kauczuku butadienowo-akrylonitrylowego zawierającego imidazoliowe cieczy jonowe, *Przemysł Chemiczny* 2012, **91**, 875–878.
5. A. Laskowska, A. Marzec, G. Boiteux, M. Zaborski, O. Gain, A. Serghei, Effect of imidazolium ionic liquid type of nitrile rubber composites, *Polymer International* 2013, **62**, 1575–1582.
6. A. Marzec, A. Laskowska, G. Boiteux, M. Zaborski, O. Gain, A. Serghei, The impact of imidazolium ionic liquids on the properties of nitrile rubber composites, *European Polymer Journal* 2014, **53**, 139–146.
7. A. Laskowska, A. Marzec, G. Boiteux, M. Zaborski, Reinforcement of carboxylated acrylonitrile-butadiene rubber (XNBR) with graphene nanoplatelets with varying surface area, 2014 *Journal of Polymer Engineering* DOI: 10.1515/polyeng-2013-0149.
8. A. Laskowska, M. Zaborski, G. Boiteux, O. Gain, A. Marzec, W. Maniukiewicz, Ionic elastomers based on carboxylated nitrile rubber (XNBR) and magnesium aluminum layered double hydroxide (hydrotalcite), *Express Polymer Letters* 2014, **8**, 374–386.

9. A. Laskowska, A. Marzec, G. Boiteux, M. Zaborski, O. Gain, A. Serghei, Properties of carboxylated nitrile rubber/hydrotalcite composites containing imidazolium ionic liquids, *Macromolecular Symposia* 2014, **341**, 7–17.
10. A. Marzec, A. Laskowska, G. Boiteux, M. Zaborski, O. Gain, A. Serghei, Investigations of nitrile rubber composites containing imidazolium ionic liquids, *Macromolecular Symposia* 2014, **341**, 18–25.
11. A. Laskowska, A. Marzec, G. Boiteux, M. Zaborski, O. Gain, A. Serghei, Improved ionic conductivity of carboxylated nitrile rubber/LDH composites by adding imidazolium bis(trifluoromethylsulfonyl)imide ionic liquids, *Macromolecular Symposia* 2014, **342**, 35–46.
12. A. Marzec, A. Laskowska, G. Boiteux, M. Zaborski, O. Gain, A. Serghei, Study on weather aging of nitrile rubber composites containing imidazolium ionic liquids, *Macromolecular Symposia* 2014, **342**, 25–34.
13. A. Laskowska, M. Zaborski, G. Boiteux, O. Gain, A. Marzec, W. Maniukiewicz, Effects of unmodified layered double hydroxides MgAl-LDHs with various structures on the properties of filled carboxylated acrylonitrile-butadiene rubber XNBR, *European Polymer Journal* 2014, DOI: 10.1016/j.eurpolymj.2014.09.013.

PATENTS

1. Marzec A. Zaborski M., Boruszczak Z., Laskowska A., „Kompozycja elastomerowa przeznaczona do produkcji materiałów o podwyższonej odporności na starzenie klimatyczne”, eng. „Elastomer composition intended for rubber products with increased resistance to climatic aging”. Date of grant of a patent: 15.05.2012 P. 212508.

PATENT APPLICATION

1. A. Marzec, M. Zaborski, Z. Boruszczak, A. Laskowska, „Kompozycja elastomerowa przeznaczona do produkcji materiałów o podwyższonej odporności na starzenie klimatyczne i UV”, eng. „Elastomer composition intended for rubber products with increased resistance to climatic aging and UV aging”. Date of notification: 12.05.2014 P. 408194.
2. A. Laskowska, M. Zaborski, A. Marzec, „Kompozycja elastomerowa przeznaczona na wyroby gumowe wykazujące właściwości termochromowe”, eng. “Elastomer composition intended for rubber products exhibiting thermochromic properties”. Date of notification: 12.06.2014 P. 408535.

TABLE 1 Modulus at 300 % elongation, tensile strength and elongation at break as a function of the UV and solar aging time of EN composites that contain dyes (0.2 phr).

Sample	weathering with UV irradiation ($\lambda = 343$ nm)				weathering with the full solar spectrum ($\lambda = 280-3000$ nm)			
	Aging time	SE ₃₀₀ [MPa]	TS [MPa]	Eb [%]	Aging time	SE ₃₀₀ [MPa]	TS [MPa]	Eb [%]
EN (Topaz)	-	8.8±1.2	38.7±2.6	478±11	-	8.8±2.1	38.7±2.0	478±14
	400h	9.7±1.1	10.0±2.5	426±13	350h	9.4±2.0	24.6±1.3	394±15
	800h	-	7.4±1.9	22±6	700 h	10.0±2.2	16.2±1.2	331±7
	1200h	-	7.5±1.1	20±2	1050h	10.2±3.1	10.2±1.1	258±9
	1600 h	-	7.3±0.8	18±4	1400 h	-	8.1±0.9	216±7
Solvent Blue 97	-	8.9±1.4	40.1±1.1	482±16	-	8.9±1.3	40.1±0.9	482±10
	400h	9.0±1.2	37.0±1.7	474±15	350h	9.2±2.1	41.0±1.2	483±16
	800h	9.9±2.0	36.7±2.1	432±12	700 h	9.4±1.1	39.5±1.1	481±12
	1200h	10.5±1.1	37.3±1.1	405±10	1050h	9.8±2	38.0±1.5	480±14
	1600 h	10.3±1.2	25.3±1.9	336±8	1400 h	10.9	36.2±1.4	484±8
Solvent Blue 104	-	9.0±1.4	39.4±1.5	463±13	-	9.0±0.9	39.4±1.7	463±10
	400h	9.6±2.2	36.3±1.1	459±12	350h	9.2±1.3	40.2±1.2	460±11
	800h	10.7±2.0	32.6±1.5	437±13	700 h	9.6±1.1	39.9±1.3	446±12
	1200h	10.7±3.1	29±1.1	430±11	1050h	9.6±2.2	35.2±1.6	412±15
	1600 h	10.5±1.7	27.6±2.7	331±12	1400 h	10.0±2.1	23.6±1.2	445±11
Solvent Blue 35	-	9.0±1.1	39.2±1.6	448±14	-	9.0±1.7	39.2±1.5	468±13
	400h	9.4±2.4	39.2±3.1	468±9	350h	9.1±1.2	39.8±1.7	449±16
	800h	9.7±1.9	40.1±1.1	460±17	700 h	9.6±1.5	37.9±1.3	449±15
	1200h	10.0±2	37.9±2.4	457±13	1050h	9.5±2.0	38.7±1.6	460±12
	1600 h	10.3±1.8	38.1±2.0	448±11	1400 h	9.7±1.1	32.8±1.1	460±9
Solvent Green 28	-	9.5±2.1	41.3±3.1	474±13	-	9.5±2	41.3±1.7	474±13
	400h	9.9±2.3	39.6±2.6	472±16	350h	9.6±1.1	39.9±1.2	475±12
	800h	9.7±1.2	34.9±1.5	456±22	700 h	9.7±2	39.1±1.3	479±13
	1200h	10.5±1.6	34.2±2.3	449±18	1050h	9.9±1.8	35.4±0.9	470±16
	1600 h	10.6±1.3	24.8±1.1	418±13	1400 h	9.8±2	31.0±1.0	476±10
Solvent Red	-	9.2±2.2	37.7±1.1	439±9	-	9.2±2	37.7±2.1	439±15
	400h	9.6±2.1	9.0±1.1	323±14	350h	9.4±1.1	24.3±1.0	378±12
	800h	-	10.9±1.3	39±13	700 h	9.9±3	9.0±1.7	323±7
	1200h	-	10.3±2.1	37±10	1050h	-	9.0±1.7	8.7±1.7
	1600 h	-	8.7±2.4	23±19	1400 h	-	-	-
Solvent Red 207	-	9.3±2	40.0±3.1	458±17	-	9.3±1.1	40.0±1.5	458±11
	400h	9.7±1.1	36.3±1.1	436±8	350h	9.3±1.3	29.6±1.6	451±13
	800h	9.9±1.6	24±1.8	402±10	700 h	9.4±1.1	19.5±1.3	448±10
	1200h	9.8±1.2	19.8±1.5	380±15	1050h	9.7±2.0	15±1.8	432±14
	1600 h	10.6±1.8	16.9±2.2	330±18	1400 h	10.8±1.1	6.8±1.1	326±12

TABLE 2 Modulus at 300 % elongation, tensile strength and elongation at break as a function of the UV and solar aging time of EN composites that contain dyes (0.2 phr).

Sample	weathering with UV irradiation ($\lambda = 343$ nm)				weathering with the full solar spectrum ($\lambda = 280-3000$ nm)			
	Aging time	SE ₃₀₀ [MPa]	TS [MPa]	Eb [%]	Aging time	SE ₃₀₀ [MPa]	TS [MPa]	Eb [%]
Solvent Red 149	-	8.9±0.7	42.7±2.1	480±11	-	9.1±2	42.7±2.3	480±11
	400h	9.4±1.1	38.3±1.9	478±10	350h	9.2±0.8	31.1±1.3	421±16
	800h	9.6±1.5	39.3±3.2	454±16	700 h	9.7±1.1	18.4±1.7	399±12
	1200h	10.3±2.0	30.8±3.0	400±12	1050h	10.4±0.9	9.3±2	28.7±1.7
	1600 h	-	9.1±1.2	29±15	1400 h	-	-	-
Solvent Red 52	-	9.0±1.1	37.8±2.7	466±12	-	9.0±0.7	37.8±1.9	466±13
	400h	9.4±1.4	37.7±1.5	451±14	350h	9.2±1.0	34.1±1.2	453±11
	800h	10.4±2.2	35.3±2.1	422±11	700 h	9.4±1.4	29.5±1.2	456±10
	1200h	9.8±1.7	27.7±1.7	421±16	1050h	9.9±1.1	19.4±1.2	413±11
	1600 h	9.8±1.3	12.2±2.1	346±9	1400 h	10.2±1.2	14.2±1.2	336±7
Solvent Yellow 98	-	9.4±0.8	40.3±2.8	463±14	-	9.4±2.1	40.3±2.1	463±12
	400h	10.0±1.1	31.2±2.5	452±12	350h	9.4±1.0	33.4±1.7	452±8
	800h	-	10.5±2.1	224±10	700 h	9.7±1.3	20.5±1.5	458±10
	1200h	-	10.1±1.6	38±7	1050h	-	11.1±1.1	412±11
	1600 h	-	9±2.1	28±4	1400 h	-	8.7±1.4	348±10
Solvent Yellow 163	-	9.1±1.6	42.1±2.8	471±16	-	9.1±0.8	42.1±1.9	471±9
	400h	9.8±1.2	39.8±2.1	446±13	350h	9.2±1.3	37.2±1.8	469±10
	800h	10.4±2.0	20.1±1.9	437±11	700 h	9.7±1.3	31.5±1.7	450±12
	1200h	10.8±2.1	21.6±2.1	393±12	1050h	10.0±2	17.9±1.1	429±9
	1600 h	10.4±1.5	19.8±1.7	385±10	1400 h	10.5±1	9.8±1.3	406±11
Solvent Green 5	-	9.3±0.8	39.9±2.1	472±13	-	9.3±1.4	39.9±2.1	472±11
	400h	10.0±1.0	38.8±2.5	467±16	350h	9.4±2.1	36.1±2.2	470±14
	800h	10.3±1.8	39.4±2.1	448±13	700 h	9.7±1.2	33.1±1.4	476±12
	1200h	10.4±2.1	10.4±1.4	300±15	1050h	9.6±1.1	27.5±1.5	468±15
	1600 h	-	8.9±1.2	31±7	1400 h	10.2±1.1	22.2±1.1	464±12
Solvent Yellow 93	-	9.8±0.9	39.2±1.8	471±13	-	9.1±2.2	39.2±1.3	471±8
	400h	9.0±1.2	39.7±2.1	462±9	350h	9.0±2.1	39.8±1.6	449±12
	800h	9.6±2.2	36.6±2.7	447±14	700 h	9.3±1.3	37.9±2.1	449±10
	1200h	10.1±1.1	30.4±1.9	434±10	1050h	9.4±1.4	38.7±2.3	450±17
	1600 h	10.1±1.2	29.2±2.1	412±12	1400 h	9.7±1.0	33.8±1.2	466±16

TABLE 3 Modulus at 300 % elongation, tensile strength and elongation at break as a function of the UV and solar aging time of EN composites that contain stabilizers (0.2 phr).

Sample	weathering with UV irradiation ($\lambda = 343$ nm)				weathering with the full solar spectrum ($\lambda = 280-3000$ nm)			
	Aging time	SE ₃₀₀ [MPa]	TS [MPa]	Eb [%]	Aging time	SE ₃₀₀ [MPa]	TS [MPa]	Eb [%]
Tinuvin 234	-	9.2±1.3	39.5±2.1	477±13	-	9.2±1.0	39.5±1.9	477±14
	400h	9.0±1.1	36.3±2.0	471±11	350h	9.6±1.1	35±1.8	450±14
	800h	9.8±1.2	35±1.9	457±15	700 h	9.9±1.1	27.0±1.2	432±12
	1200h	9.8±1.3	31±2.0	422±14	1050h	10±1.5	16.7±1.6	408±14
	1600 h	11.0±2.0	29±2.1	397±9	1400 h	10.4±1.8	14.9±1.6	328±12
Chimassorb 81	-	9.3±1.1	41.6±1.8	471±14	-	9.3±1.1	41.6±1.9	471±15
	400h	10.2±1.0	38.9±2.0	461±16	350h	10.1±1.5	34.9±1.6	468±14
	800h	10.6±1.2	31.3±1.7	438±13	700 h	10.5±1.3	26.1±1.7	460±1.7
	1200h	10.5±2.1	30±2.1	423±14	1050h	10.8±1.2	20.9±2.0	452±14
	1600 h	10.7±1.9	29.4±2.0	398±11	1400 h	10.6±2.1	17.0±1.4	445±1.7
Tinuvin 1577	-	9.3±1.0	40.1±2.2	482±14	-	9.6±1.3	40.1±2.2	482±10
	400h	9.5±0.9	39.1±1.9	470±15	350h	9.8±1.1	37.3±2.0	463±14
	800h	10.4±1.2	36.5±1.8	465±110	700 h	10.3±1.5	34.5±1.7	452±12
	1200h	10.8±1.7	35.7±1.7	468±14	1050h	10.8±1.7	29.9±1.5	450±14
	1600 h	10.1±1.8	29.9±1.5	446±9	1400 h	10.9±1.9	25.9±1.4	448±13
Chimassorb 944	-	9.7±1.2	40.1±2.2	475±14	-	9.7±1.3	40.1±2.0	475±11
	400h	9.8±1.9	37.8±1.9	474±11	350h	9.7±1.2	41.1±1.9	473±14
	800h	9.9±1.4	36.8±2.0	468±10	700 h	9.7±1.5	38.8±1.2	466±9
	1200h	10.4±1.6	32.8±1.6	455±14	1050h	10.1±1.8	37.5±1.6	450±14
	1600 h	10.3±2.0	30.1±1.2	452±12	1400 h	10.5±1.8	35.0±1.3	456±7

TABLE 4 Tensile strength and elongation at break as a function of the UV time of EN composites that contain dyes and pigments (0.2 phr).

Aging time	Pigments			Mixture solvent dye (0.1 phr) and pigment (0.1 phr)		
	Sample	TS [MPa]	Eb [%]	Sample	TS [MPa]	Eb [%]
-	<i>trans</i> -indigothiazine	39.9±2.1	477±17	P. Blue 15:1/ S.Blue 97	40±2.5	477±19
400h		31.4±2.2	437±18		41±2.2	463±15
800h		16.7±1.1	397±13		39.5±2.0	457±13
1200h		10.2±1.3	325±12		36.5±2.1	432±15
1600 h		8.7±1.1	37±4		29.2±1.6	430±14
-	P. Blue 15:1	39.3±2.2	479±13	P.Green 7 / S.Green 28	39.2±1.4	468±10
400h		37.7±2.7	468±12		36.7±2.3	459±12
800h		38.1±1.9	453±16		37.8±2.3	440±16
1200h		34.7±2.4	431±13		30.9±2.5	433±12
1600 h		32.3±2.1	413±11		20.3±1.7	357±10
-	P. Green 7	40.4±2.6	478±14	P. Yellow 173/ S.Yellow 93	39.1±2.5	475±16
400h		41.4±2.7	462±17		36.6±2.2	449±13
800h		38.7±2.4	448±14		35.8±2.3	436±12
1200h		17.3±1.8	417±11		34.6±2.5	420±10
1600 h		5.7±10.9	37±5		26.6±1.8	393±9
-	P. Yellow 173	40.2±2.9	484±17	P. Yellow 173/ S.Yellow 98	40.7±2.6	469±11
400h		38.3±2.7	452±14		38.6±2.5	437±13
800h		36.4±2.6	448±14		37.5±2.1	416±15
1200h		30.6±2.5	397±13		33.6±1.9	408±12
1600 h		8.1±1.8	207±11		12±1.2	297±10